NASA CONTRACTOR REPORT

NASA CR-2301

NASA CR-2301

PREDICTION OF OVERALL AND BLADE-ELEMENT PERFORMANCE FOR AXIAL-FLOW PUMP CONFIGURATIONS

by George K. Serovy, Patrick Kavanagh, Theodore H. Okiishi, and Max J. Miller

Prepared by
IOWA STATE UNIVERSITY OF SCIENCE AND TECHNOLOGY
Ames, Iowa 50010
for Lewis Research Center

NATIONAL AERONAUTICS AND SPACE ADMINISTRATION • WASHINGTON, D. C. • AUGUST 1973

2301

1. Report No.	2. Government Accession No.	3. Recipient's Catalog No.
NASA CR-2301		

4. Title and Subtitle	5. Report Date
PREDICTION OF OVERALL AND BLADE-ELEMENT PERFORMANCE FOR AXIAL-FLOW PUMP CONFIGURATIONS	August 1973
	6. Performing Organization Code
7. Author(s) George K. Serovy, Patrick Kavanagh, Theodore H. Okiishi, and Max J. Miller	8. Performing Organization Report No. ISU-ERI-AMES-72322
	10. Work Unit No.
9. Performing Organization Name and Address Iowa State University of Science and Technology Ames, Iowa 50010	11. Contract or Grant No. NGL 16-002-005
	13. Type of Report and Period Covered Contractor Report
12. Sponsoring Agency Name and Address National Aeronautics and Space Administration Washington, D.C. 20546	14. Sponsoring Agency Code

15. Supplementary Notes

Project Manager, Werner R. Britsch, Fluid System Components Division, NASA Lewis Research Center, Cleveland, Ohio

16. Abstract

A method and a digital computer program for prediction of the distributions of fluid velocity and properties in axial-flow pump configurations are described and evaluated. The method uses the blade-element flow model and an iterative numerical solution of the radial equilibrium and continuity conditions. Correlated experimental results are used to generate alternative methods for estimating blade-element turning and loss characteristics. Detailed descriptions of the computer program are included, with example input and typical computed results.

17. Key Words (Suggested by Author(s))	18. Distribution Statement
Axial-flow pumps Blade-element method Performance prediction Radial equilibrium	Unclassified - unlimited

19. Security Classif. (of this report)	20. Security Classif. (of this page)	21. No. of Pages	22. Price*
Unclassified	Unclassified	248	$3.00

* For sale by the National Technical Information Service, Springfield, Virginia 22151

TABLE OF CONTENTS

SUMMARY

This report describes a method and a digital computer program for prediction of the distributions of fluid velocity and properties in axial-flow pump configurations. A mathematical model of the flow is developed for calculation planes in which the flow is assumed to be steady and axisymmetric. Flow patterns in these planes are determined by an iterative numerical procedure. The calculation planes are located at the configuration entrance and exit, and between blade rows. Correlated results of pump configuration experiments are used to generate alternative methods for estimating the turning and loss characteristics of the blade elements intersected by approximate steam surfaces.

Detailed descriptions of program logic and use are followed by example input and output data sets, plus typical computed results. Strengths and weaknesses of the method are outlined. In general, it is found that the flow model and computational procedures are satisfactory. The results are useful for both qualitative and quantitative purposes. Limitations are related to the quality of the empirical estimation of blade section performance. These limitations are characteristic of all axial-flow compressor and pump performance prediction systems described in the literature to date.

INTRODUCTION

This report reviews an extended study of the problem of prediction of distributions of fluid velocity and properties in axial-flow pump configurations. This study was begun in 1960 as one response to the need for fundamental improvement in performance levels and reliability of turbopumps for liquid-propellent rocket systems and has been carried on in cooperation with the research staff of the NASA Lewis Research Center. Principal objectives were to select a satisfactory flow model and a logical sequence of steps for computation of the required flow patterns, and to incorporate these steps into an efficient digital computer program. In addition, necessary correlations of experimental information were to be developed to support the program.

In the first part of the report, the scope of the project is outlined and compared with related investigations in the fluid mechanics of turbomachinery. The second portion is a detailed description of a method and computer program for axial-flow pump performance prediction. The method and program are based on numerical solution of equations representing a model of the real flow in an axial-flow turbomachine. The third part reviews the results of utilization of the program for typical axial-flow pump geometries.

Computed results are compared with experimental measurements from NASA research involving water tunnel tests of these geometries. These comparisons are useful in defining areas in which the performance prediction method is successful and valid. It is also possible to identify characteristics of the method which are not satisfactory at present.

The performance prediction problem for turbomachinery, as it is defined in this report, is one of the most difficult unsolved problems in applied fluid mechanics. It is, therefore, a primary objective of this review to provide a foundation for future studies in performance prediction and related areas.

PERFORMANCE PREDICTION FOR AXIAL-FLOW TURBOMACHINERY

Two fundamental problems occur in selection of a geometrical configuration for a turbomachine. The first is the design or indirect problem and is concerned with the determination of a satisfactory passage and blading configuration. For this problem, the given information includes the nature and characteristics of the working fluid, the fluid properties at the entrance to the turbomachine for the design operating point of the system, the flow rate and a required change in one or more fluid properties between the entrance and exit. In addition, there may be other initial requirements or limits, related to rotational speed, size, efficiency, and other operating characteristics of the machine.

After a possible design point configuration is determined, it is essential to consider what will happen to the performance of the configuration when it is operated at flow rates or rotational speeds, or with entering fluid conditions other than those used as design point values. This second problem, called the analysis or direct problem, can be, for reasons which will be made evident in the report, considerably more difficult than the design problem. The level of difficulty is, however, substantially dependent on the nature of the information to be provided by the solution. Some of the methods which have been proposed will be reviewed briefly in the following paragraphs to indicate clearly their character.

Performance Prediction Systems Background

Although this section considers some work related to the most general forms of solution of the analysis problem, primary emphasis is on turbomachines in which energy is transferred from the rotor to the working fluid and in which the result is an increase in the fluid pressure or head, that is to compressor and pump configuration analysis. In addition, because of the objectives of the current program, detailed consideration is restricted to work applicable to the class of turbomachines (axial-flow) in which the main flow is essentially parallel to the rotational axis. Within these limits, there is a considerable volume of information available on methods for solution of the analysis problem. These methods may best be classified by reference to the scope and nature of the results obtained.

One category of performance prediction systems produces only overall performance characteristics. This class is exemplified by references 1-4 and its use is discussed by Robbins and Dugan in reference 5. Ordinarily, these methods are based on one-dimensional (e.g. mean radius) calculations, on "stacking" of the estimated performance curves for individual stages, or on assumed analogous behavior between the configuration of unknown performance and previously-tested configurations. Such methods are useful for component-matching and systems studies, and to a limited extent can be used for locating mismatches between stages in multistage compressors and pumps.

A second and far more difficult type of performance prediction method is based on computation of the fluid velocity and properties at selected points in the flow path of the turbomachine. A mathematical model of the flow is developed and solution of the resulting equations permits determination of flow patterns in the turbomachine and, by appropriate averaging techniques, the overall performance characteristics. The solutions are iterative and, for all practical cases, are feasible only if accomplished using a large-scale digital computer.

The significance of such methods can readily be understood. If the local velocity and properties could be calculated with some accuracy at desired points in a proposed configuration, alternate geometry choices could be evaluated during the design process without experimentation. Furthermore, the availability of both overall performance and detailed velocity distributions for off-design operating conditions would contribute substantially to reducing required design and development time for the system in which the turbomachine is a component.

The performance prediction method described in this report is of the second type and all subsequent uses of the term "performance-prediction method" herein refer to methods of this type. As background information for the work discussed, it is appropriate to review some of the related prior studies.

Some of the earliest reported work on the analysis problem was done by Serovy (refs. 6 and 7) and by Swan (refs. 8 and 9) for axial-flow compressor configurations. Both investigations were based on a finite-difference solution of the nonisentropic radial equilibrium and continuity conditions at stations between blade rows. The steady, axisymmetric model of the flow used has been described and justified thoroughly in references 10, 11 and 12. In each method, correlations of experimental data were developed and used for predicting the radial distribution of the fluid turning angle and of the total-pressure loss for each blade row. Trial solutions were presented for single-stage geometries, and comparison with experimental data was not good. Principal discrepancies appeared to be the result of inadequate data correlations for flow angle and loss. Nevertheless, the two studies demonstrated the feasibility of numerical solution systems in generating both detailed flow passage distributions and overall compressor performance.

Jansen and Moffatt (ref. 13) used a similar approach in developing a program for computation of multistage axial-flow compressor performance.

The steady, axisymmetric model was again used as formulated by Novak (ref. 14), and this formulation included improved schemes for iterative location of the axisymmetric stream surfaces and for computation of local values of stream surface slope and curvature. Example solutions for two multistage compressor configurations were, as in the earlier investigations, less than satisfactory. It is likely that experimental data correlations and computed annulus wall boundary layer displacement thicknesses were responsible for much of the observed difficulty.

Davis (refs. 15 and 16) has described a program and data correlations for compressor analysis and design problem solutions. This program was primarily based on the flow model of Novak (ref. 14), combined with correlations available from earlier studies. Davis provides extensive flow diagrams and descriptions of program logic, together with explicit definition of the correlation equations used. Creveling and Carmody (ref. 17) also have developed an analysis program for multistage axial-flow compressors. Again, the documentation of the program is reasonably complete for both data correlations and the flow model.

More recently Daneshyar (ref. 18) and Grahl (refs. 19 and 20) used flow models similar to Novak (ref. 14) and their own data correlations to predict compressor performance. Daneshyar discusses in somewhat more detail than any earlier work, the numerical problems which are encountered in flow passage solutions. This useful discussion is supplemented by papers of Marsh (ref. 21) and Wilkinson (ref. 22), who give a good deal of insight into some of these numerical difficulties. These stability, convergence, and loss-of-solution problems are important, and this will be made evident in the discussion of the current analysis program development.

All of the preceding referenced work is concerned with analysis for axial-flow-compressor geometries. The methods are also similar in that they assume a steady, axisymmetric flow. All reported calculations are at stations located in the axial spaces between blade rows. The basic flow model is, therefore, that identified as the blade-element model and described in reference 10. Fundamental differences in strategy exist between these methods in the numerical solution techniques applied, including the means for estimating local values of stream surface position, slope and curvature. It is clear, even in those instances where program documentation is not included, that program logic is not similar in the various systems. Finally, there is evidence in all cases that the experimental data correlations required are a major source of program trouble. Because these correlations, which permit calculation of blade row relative exit flow angle and blade row relative total-pressure loss as a function of spanwise location, are present in every method, they may be isolated as a possible source of difficulty in the work reported herein.

A somewhat different means for formulation of the analysis problem for axial flow turbomachines has been proposed and used by Marsh, Gregory-Smith and others (refs.23 and 24). The matrix through-flow method has been reasonably well documented, but unfortunately has not been tested by application to an adequate number of realistic flow situations. It does not avoid the requirement for input of key empirical data correlations and in example solutions currently available, does not appear to offer a clear improvement in any area of performance calculation.

Additional examples of related research on turbomachine analysis are contained in references 25 to 28. A procedure and computer program for axial-flow turbine analysis is described in reference 25. Another is discussed Renaudin and Somm (ref. 26). A novel method for avoiding solution convergence problems is used in reference 26, which should be applicable to other turbomachine cases. Novak et al. (ref. 27) have attempted adaptation of the earlier system reported in reference 13 to the estimation of effects of inlet flow distortion on axial-flow compressor performance. Ribaut (ref. 28) has outlined a system for a very general analysis of the through-flow field, but unfortunately, the problems of application appear to be substantial.

The analysis system described in this report differs essentially from earlier efforts in a few areas. First, the blade-element model is applied to axial-flow-pump analysis. As a result, it avoids problems that derive from changes in fluid density and from the loss phenomena associated with shock waves where acoustic velocity levels are reached or exceeded in compressor blade passages. Second, the influences of stream surface slope and curvature on the radial distribution of velocity are omitted. Third, a program logic is used that is believed to be somewhat unique and very efficient. Finally, some new ideas in data correlation are developed, which can only be proven by comprehensive application and testing. In every area, it is the intent of the report to disclose the reasoning leading to choices among alternate options and to expose the segments of the program that presented the greatest difficulty.

Problem Analysis For Axial-Flow Pump Configurations

Figure 1 is a typical plot of the experimental performance of an axial-flow pump stage. The data points were obtained by measuring fluid properties and velocities at the pump inlet and downstream from the stage at stations as shown in figure 2. Operating at constant rotational speed, while controlling the flow by means of a downstream throttle, data sets were measured at specified volume flow rates. The actual points plotted were obtained by averaging the radial distributions of measured properties. Corresponding to each data point on figure 1 are radial distributions of various flow parameters and reduced data such as those shown in figure 3.

Because most system analysis and design evaluation requirements are based on the use of curves such as those in figures 1 and 3, it is logical to make generation of such curves a major goal in a performance prediction method. It is less apparent, but equally important to note that the mode of operation and data acquisition for the pump is based on the assumption of certain characteristics of the flow that are in keeping with the nature of the flow model described in the following paragraphs. These considerations have an important influence on the development of procedures and logic.

Flow Model

The analysis method described here is directed toward the problem of prediction of the flow patterns in axial-flow pump configurations. In proceeding toward this objective, a number of decisions were made which called for the use of parameters or techniques drawn from established axial-flow compressor and pump technology. Wherever possible, attention will be called to these decisions and to the limitations which they might place on the method.

All calculations are made in planes perpendicular to the rotational axis of the configuration. These planes must be located in the axial spaces between blade rows and are analogous to measuring stations shown in figure 2. Aside from the computational convenience resulting from use of such stations, the computed velocities and properties may readily be checked against experimentally measured data obtained from the radial survey probes. The local flow in all of these calculation planes is assumed to be steady and axisymmetric. Again, this is consistent with data acquisition methods, in which most rotor data have been taken using steady-state instrumentation located at a limited number of circumferential positions. Behind stationary blade rows, circumferential property surveys have typically been made at constant radius values and averages have been taken at each radius to compute velocity diagram quantities for that radius. The result for rotor and stator measuring planes is a series of local velocity diagrams for selected radial positions.

A coordinate system which is consistent with typical data acquisition is used for the analysis program. The system is a cylindrical type with r, θ, and z coordinates. The z axis is coincident with the rotational axis of the pump and is positive in the direction of inlet flow. Local velocity diagrams for all calculation planes follow the sign convention shown in figure 4. The reason for omission of the radial component of velocity will be given later.

The flow through all blade rows is assumed to follow stream surfaces of revolutions which are fixed by the flow continuity condition at the calculation planes upstream and downstream from the blade row. No attempt is made in the performance prediction method to trace the assumed stream surface within the blade row. For calculation purposes, these surface of revolution may be thought of as shown in figure 5. These surfaces intersect the blades to form a cascade of blade sections. A "cascade plane" view of the intersection surface, as seen by an observer looking along a radial line, is the basis for estimation of changes in flow angle and total pressure through each blade row (ref. 29). Figure 6 represents such a cascade plane projection and defines a number of blade section geometry and cascade flow parameters.

For the calculation system, radial components of local velocity in all calculation planes are assumed to be negligible. At the same time, all stream surface slope and curvature effects are eliminated in establishing the equations governing the flow. This aspect of the flow model differs from the treatment of flows in most axial-flow compressor analysis systems, in which stream surface slope and curvature influences may be significant factors. In the current study, examination of experimental data from a large number of axial-flow pump geometries showed that stream surfaces for a range of flow conditions were very nearly cylindrical, with near-zero radial velocity components.

For all calculations, local effects of fluid shear stress are neglected in setting up the equations representing the flow model. This does not mean that the cumulative effects of shear stresses do not affect the local flow, because upstream total-pressure losses are accounted for in determining the flow patterns in each calculation plane. This is an important distinction, because it will become evident that the accumulated losses in total pressure which occur on the assumed stream surfaces are among the most significant factors in influencing velocity distributions.

The equations representing the flow are all formulated for a fluid with a constant density. Nowhere in the analysis system is provision made for two-phase flow or for effects of cavitation.

For a steady, axisymmetric flow neglecting local fluid shear stress terms, the radial component of the differential equation of motion is

$$g \frac{\partial h}{\partial r} = \frac{V_\theta^2}{r} - V_r \frac{\partial V_r}{\partial r} - V_z \frac{\partial V_r}{\partial z} . \tag{1}$$

For constant-density fluid flows, a historically significant parameter has been the local total head defined as

$$H = h + \frac{V^2}{2g} . \tag{2}$$

Differentiating equation (2) with respect to radius and substituting in equation (1), gives

$$g \frac{\partial H}{\partial r} = \frac{V_\theta^2}{r} + V_\theta \frac{\partial V_\theta}{\partial r} + V_z \frac{\partial V_z}{\partial r} - V_z \frac{\partial V_r}{\partial z} . \tag{3}$$

This is the radial equilibrium condition and is the equation used to determine the radial variation of axial velocity component in each calculation plane. The last term is omitted as a result of the assumption of negligible radial components of velocity.

In each calculation plane, the flow must also be consistent with the designated pump entrance flow rate. For an axisymmetric flow of a constant-density fluid, the flow rate equation in integral form is

$$q = 2\pi \int_{r_{hub}}^{r_{tip}} V_z \, r dr \; . \tag{4}$$

For flow through a rotating blade row, in which energy is added to the fluid, the change in total head along a stream surface between entrance and exit calculation planes is

$$H_2 = H_1 + U_2 V_{\theta,2} - U_1 V_{\theta,1} - H_{loss} \; . \tag{5}$$

For a stationary blade row, in which no energy transfer occurs, the corresponding equation is

$$H_2 = H_1 - H_{loss} \; . \tag{6}$$

These equations, together with equations defining the various passage and cascade flow parameters, are those which represent the flow in the calculation planes for the axial-flow pump analysis system. In the following section, these equations will be written in finite difference form as they have been programmed for digital computer solution.

With the exception of the assumptions concerned with radial velocity components and stream surface shape effects, the flow model proposed is essentially the same as that presented in reference 10 and used in numerous axial-flow compressor design and analysis situations. The equations presented are particularly adapted to the study of constant-density fluid flows. It should also be noted that no arbitrary factors are defined to account for passage wall effects. Specifically, no boundary-layer blockage factor enters the continuity condition. This point should be recalled in connection with comparison and interpretation of experimental and computed results as presented in later sections of this paper.

Computing Sequence

As described in the following section, the performance analysis program computes fluid velocities and properties for discrete values of inlet flow rate at a constant pump rotational speed for fixed and specified passage and blade row geometries. Beginning at a base flow rate, the program marches up and/or down in flow rate in much the same way the pump configuration would be experimentally evaluated. Results available to the user include those which would be most significant in design evaluation.

Numerical Solution of Governing Equations

The simple radial equilibrium equation for determination of the radial distribution of axial velocity V_z in the leaving flow from a blade row is given in equation (3). Solution of this equation for arbitrary blade row geometry and operating conditions has to be performed numerically in conjunction with requirements of the continuity equation and empirical approximations for head losses and leaving flow angle deviation in the flow. The development of a finite difference approximation to equation (3) for the numerical solution is given below.

Consider the meridional section through a blade row as shown in figure 5. A finite number of finitely spaced streamlines given by the traces of the axisymmetric stream surfaces in the meridional plane are used; intersections of these stream surfaces in the blades are the blade elements defined by the flow through the blade row. The computing stations just upstream and downstream of the blade row are constant z-planes identified as i and i + 1, respectively. As seen in figure 5, two adjacent streamlines in the analysis are called streamlines j and j + 1, with the streamline j = 1 the hub streamline, and $j = j_{lim}$ the tip or outer casing streamline.

The flow conditions satisfying radial equilibrium and continuity at the upstream axial station i are known. To be determined, of course, is the radial equilibrium and continuity solution for the flow leaving the blade row at station i + 1, and the radial positions there of the streamlines used in the solution.

The finite difference approximation to equation (3) is obtained by integration of the equation between streamlines j and j + 1 at axial station i + 1. Note again that the final term in equation (3) is omitted because of the assumption of negligible radial velocities. Thus,

$$\int_{V_{z\,i+1,j}}^{V_{z\,i+1,j+1}} V_z dV_z = g \int_{H_{i+1,j}}^{H_{i+1,j+1}} dH - \int_{r_{i+1,j}}^{r_{i+1,j+1}} \frac{V_\theta^2}{r} dr - \int_{V_{\theta\,i+1,j}}^{V_{\theta\,i+1,j+1}} V_\theta dV_\theta \qquad (7)$$

or

$$\frac{V^2_{z\ i+1,j+1} - V^2_{z\ i+1,j}}{2} = g(H_{i+1,j+1} - H_{i+1,j}) - \frac{1}{2}\left(\frac{V^2_{\theta\ i+1,j+1}}{r_{i+1,j+1}} + \frac{V^2_{\theta\ i+1,j}}{r_{i+1,j}}\right)(r_{i+1,j+1} - r_{i+1,j}) - \frac{1}{2}\left(V^2_{\theta\ i+1,j+1} - V^2_{\theta\ i+1,j}\right) \quad (8)$$

Solving this equation for the velocity $V_{z\ i+1,\ j+1}$ in terms of the known velocity $V_{z\ i+1,j}$ on the adjacent streamline and remaining variables yet to be determined, we obtain,

$$V^2_{z\ i+1,j+1} = V^2_{z\ i+1,j} + 2g(H_{i+1,j+1} - H_{i+1,j}) - \left(\frac{V^2_{\theta\ i+1,j+1}}{r_{i+1,j+1}} + \frac{V^2_{\theta\ i+1,j}}{r_{i+1,j}}\right)(r_{i+1,j+1} - r_{i+1,j}) - (V^2_{\theta\ i+1,j+1} - V^2_{\theta\ i+1,j}) \quad (9)$$

The head difference term in equation (9) can be written in terms of the ideal head rise and head loss for the (j+1)th streamline or blade element as,

$$H_{i+1,j+1} - H_{i+1,j} = H_{i,j+1} + (\Delta H_{ideal})_{j+1} - H_{loss,j+1} - H_{i+1,j}\ . \quad (10)$$

This, with substitution of the ideal head rise from equation (5), along with the velocity triangle relation

$$V_{\theta\ i+1,j+1} = U_{i+1,j+1} - V_{z\ i+1,j+1} \tan \beta'_{i+1,j+1} \quad (11)$$

for the leaving whirl velocity component, becomes

$$H_{i+1,j+1} - H_{i+1,j} = H_{i,j+1} + \frac{1}{g}\Big[U_{i+1,j+1}\,(U_{i+1,j+1} - V_{z\ i+1,j+1}\tan\beta'_{i+1,j+1}) - U_{i,j+1}V_{\theta\ i,j+1}\Big] - H_{loss,j+1} - H_{i+1,j}\ . \tag{12}$$

Finally, with substitution of equations (11) and (12) into equation (9) it is readily apparent that the unknown velocity $V_{z\ i+1,j+1}$ is reintroduced on the right-hand side of the equation. With further extensive but straight-forward rearrangement of the equation, the following quadratic equation for $V_{z\ i+1,j+1}$ results:

$$AV^2_{z\ i+1,j+1} + BV_{z\ i+1,j+1} + C = 0 \tag{13}$$

where

$$A = 1 + \tan^2\beta'_{i+1,j+1}\left[1 + \left(\frac{r_{i+1,j+1} - r_{i+1,j}}{r_{i+1,j+1}}\right)\right], \tag{14}$$

$$B = -2U_{i+1,j+1}\tan\beta'_{i+1,j+1}\left(\frac{r_{i+1,j+1} - r_{i+1,j}}{r_{i+1,j+1}}\right), \tag{15}$$

$$C = -V^2_{z\ i+1,j} - 2g(H_{i,j+1} - H_{i+1,j} - H_{loss,j+1}) + 2U_{i,j+1}V_{\theta\ i,j+1} - U^2_{i+1,j+1}\left(\frac{r_{i+1,j}}{r_{i+1,j+1}}\right) + V^2_{\theta\ i+1,j}\left(\frac{r_{i+1,j+1}}{r_{i+1,j}} - 2\right)\ . \tag{16}$$

Solution of equation (13) is iterative due to the fact that $V_{z\ i+1,j+1}$ is dependent on the leaving streamline radial positions, the blade element head loss and flow deviation, and on the leaving flow total head $H_{i+1,j}$ and velocity components $V_{z\ i+1,j}$, $V_{\theta\ i+1,j}$ on the adjacent streamlines as well. A plot of the left-hand side of equation (13) as a function of $V_{z\ i+1,j+1}$ is a parabola; the correct root of equation (13) is at the intersection of the parabola with the V_z axis yielding the greatest V_z. The iteration process to obtain the V_z distribution leaving a blade row continually revises the coefficients in equation (13) for any one streamline, and hence the solution, until convergence is obtained. In the case of divergent iterations, the parabola is altered and readjusted until an intersection of the parabola (for the streamline) with the V_z axis fails to exist.

Initialization of head losses at zero and streamline radii at constant radial increments are therefore used at an initial flow rate assignment. Also, the axial velocity component at a starting or base streamline in the leaving flow ($V_{z\ i+1,jbase}$) is assumed for the initial flow rate. With this starting information, deviation angle can be calculated in order to determine relative leaving flow angle $\beta'_{i+1,j+1}$, and leaving flow total head and whirl velocity on the adjacent streamline. This incremental procedure is followed to solve for the blade element radial distribution of axial velocity, working adjacent streamline to the next, from the base streamline outward to the outer casing and inward to the hub.

With the $V_{z\ i+1}$ distribution known, the continuity requirements from the assigned flow rate can be checked to revise the base streamline velocity and iterate as necessary. This is done using simple quadrature across the annulus to obtain a measure of the flow rate according to

$$Q_{i+1,j_{lim}} = \sum_{j=1}^{j_{lim}-1} (V_{z\ i+1,j+1} + V_{z\ i+1,j})(r^2_{i+1,j+1} - r^2_{i+1,j}) \ . \tag{17}$$

Upon convergence of the base streamline axial velocity value, radial positions of the leaving streamlines are determined according to continuity and the entering streamline radii; the leaving radii are revised and iterated on until convergence is obtained. Finally, exterior to the radial equilibrium and continuity iterations, head losses are estimated on the basis of the determined flow. This procedure for solution is followed, of course, at the exit axial station for each blade row through the pump, with the determined leaving flow for a blade row becoming the known inlet flow for the following blade row. (Details of the radial equilibrium and continuity solution are given in the later discussion of subroutine RADEQC of the pump performance computer program. The basis of blade element head loss and deviation angle calculations is in the following section.)

As will be illustrated in the RESULTS section, the method for predicting axial-flow pump off-design performance proposed in this report can only be as successful as the blade-element total pressure loss and deviation angle estimation procedures required. The simplifications that led to the tractable mathematical formulation of the axial-flow pump off-design analysis problem must eventually be compensated for via realistic loss and deviation angle prediction.

To date, totally satisfactory general means for obtaining axial-flow pump or compressor losses and deviation angles, even in terms of empirical correlations, are not to be found in the literature. Several options for loss and for deviation angle prediction in pumps have been made available with the present computer program. The background associated with each technique is described in the following paragraphs. Stationary plane cascade results are discussed first followed by an explanation of how these results were extended to apply to three-dimensional pump flow.

Because of the short time available for developing general three-dimensional pump flow blade-element loss and deviation angle calculation procedures, an empirical approach using reasonably orthodox ideas was pursued. Realizing that completely satisfactory loss and deviation angle estimation procedures would probably not result from empiricism, the goal established was to seek procedures that represented improvement over use of Carter's rule for deviation angle estimation and two-dimensional cascade data for loss calculation. Correlations are based on axial-flow pump rotor blade-element loss and deviation angle data. For stationary blade rows, pump configuration data were not available in sufficient quantity to permit correlation studies.

Stationary Plane Cascade Flow

In view of the widespread use of the blade-element method, it is not surprising to find that most current loss and deviation angle prediction methods are traceable to stationary two-dimensional cascade flow ideas. In many instances, more or less empirical "correction factors" have been used to make two-dimensional methods applicable to turbomachinery flows. Thus it seems appropriate to discuss briefly some of the two-dimensional cascade loss and deviation angle research relevant to the options available with the present performance prediction method.

Loss prediction. – As fluid flows over the suction and pressure surfaces of an airfoil representing a cross-section of a turbomachine blade, boundary layers develop on these surfaces and meet at the trailing edge to produce a wake. Consequently, a decrease or "loss" of relative total pressure is suffered by the fluid as it flows past the airfoil. Depending mainly on the surface pressure gradients involved, large or small wakes and consequent losses may occur. Large losses are generally related to boundary layer separation on either the airfoil suction or pressure surface.

Results of the two-dimensional cascade loss-related research conducted by S. Lieblein and co-workers (refs. 30 to 34) in the 1950's remain influential today. Three data correlating parameters, namely, diffusion factor, blade-wake momentum thickness to chord ratio, and equivalent diffusion ratio that evolved from this work form the basis for many current axial-flow turbomachine loss prediction techniques.

Diffusion factor: Chronologically, the diffusion factor was developed first (ref. 30). It was mainly intended and developed as a limiting-blade-loading or separation criterion for design point operation that could be easily calculated from blade row inlet and outlet velocity diagram values. The Buri shape factor (ref. 35),

$$\Gamma = \frac{\theta}{U}\frac{dU}{dx}\left(\frac{U\theta}{\nu}\right)^n , \tag{18}$$

was selected as the fundamental basis for the diffusion factor. Application of the Buri shape factor to the blade suction-surface velocity distribution of a blade element operating at minimum loss in a two-dimensional cascade led to the derivation of the diffusion factor or parameter

$$D = 1 - \frac{V_2}{V_1} + \frac{\Delta V_\theta}{a\sigma V_1} + b \tag{19}$$

where a is empirically determined to be equal to 2.0 and b is considered to be negligibly small. This diffusion factor was used with data for NACA 65-series compressor blade sections in two-dimensional low speed cascade and found to be satisfactory in terms of defining a limiting value of diffusion. The diffusion factor was also applied to selected conventional (65-series and circular-arc blade section) single stage compressor rotor and stator data. No significant variation of minimum (design) loss coefficient with diffusion factor was noted for the hub and mean radius regions of the rotors and the hub, mean and tip regions of the stators over the range of data considered. A marked and practically linear variation of minimum (design) and even off-design (positive incidence) loss coefficient with diffusion factor was noted for the tip region data of the rotors for a relative inlet Mach number less than 0.75.

Momentum thickness to chord ratio: Further developments by Lieblein and co-workers (ref. 32) appeared to be motivated by the idea that low-speed two-dimensional cascade losses are mainly attributable to the blade suction and pressure surface boundary layers. It was pointed out by Lieblein (ref. 36) that according to the results of references 32, 37, and 38, the contribution of conventional blade trailing-edge thickness to the total loss is not generally large for compressor sections. He also observed, on the basis of the data of references 37 and 39, the effect of blade thickness is small for conventional cascade configurations. The approach to developing a viable loss prediction method consisted of developing a relationship between loss and blade wake characteristics and then identifying parameters that significantly influence these wake characteristics. The following relationship between total-pressure loss coefficient and blade wake characteristics was developed (ref. 32) for the outlet measuring plane (up to 1.5 chord lengths downstream of the blade trailing edge) of a constant density flow two-dimensional cascade of compressor blades:

$$\bar{\omega} = 2\left(\frac{\theta}{c}\right)\frac{\sigma}{\cos \beta_2}\left(\frac{\cos \beta_1}{\cos \beta_2}\right)^2 \frac{\dfrac{2H_2}{3H_2 - 1}}{\left[1 - \dfrac{\theta}{c}\dfrac{\sigma H_2}{\cos \beta_2}\right]^3} \tag{20}$$

The important assumptions associated with this equation are that

1. the cascade outlet flow can be divided into a wake region where total pressure varies and a free stream region where total pressure remains constant,

2. the inlet flow is uniform across the blade spacing,

3. the outlet static pressure and flow angle are constant across the entire blade spacing,

4. the outlet free-stream total pressure is equal to the inlet total pressure.

The term involving shape factor

$$\frac{\dfrac{2H_2}{3H_2 - 1}}{\left[1 - \left(\dfrac{\theta}{c}\right)\dfrac{\sigma H_2}{\cos \beta_2}\right]^3}$$

was judged to be essentially equal to 1.0 for conventional unstalled configurations. The parameters primarily influencing the boundary layer growth and subsequent losses on low speed cascade blade sections were identified (ref. 36) as a) blade surface velocity gradients, b) blade-chord Reynolds number, and c) the free-stream turbulence level.

Considering the suction surface boundary layer and thus the suction surface velocity distribution as being the major contributor to wake momentum thickness and consequently loss, Lieblein (ref. 36) successfully correlated some two-dimensional cascade minimum-loss data with (θ/c) and D. Recalling that the shape factor term in the relationship between loss coefficient and wake characteristics is secondary, it was also determined that approximate values of θ/c calculated from

$$\frac{\bar{\omega} \cos \beta_2}{2\sigma} \left(\frac{\cos \beta_2}{\cos \beta_1}\right)^2$$

and

$$\frac{\bar{\omega} \cos \beta_2}{2\sigma}$$

resulted in strong correlation of the cascade minimum loss data of reference 40.

Equivalent diffusion ratio: Subsequently, Lieblein (refs. 33 and 34) showed that two-dimensional cascade data for minimum-loss incidence angle, as well as incidence angles greater than the minimum loss value, could be generally correlated with θ/c and $V_{max,s}/V_{2,freestream}$ as correlating parameters. Since the diffusion ratio, $V_{max,s}/V_{2,freestream}$ is difficult to evaluate for turbomachine flow, an equivalent diffusion ratio, that could be calculated in terms of blade row inlet and outlet characteristics, was sought. The following semi-empirical relationship was developed for two-dimensional cascade flow:

$$DEQ = \frac{\cos \beta_2}{\cos \beta_1} \left[C_1 + C_2 (i - i^*)^{C_3} + C_4(C.P.)\right] \tag{21}$$

where

$$C.P. = \frac{\Gamma}{cV_1} \cos \beta_1,$$

$$C_1 = 1.12,$$

$$C_2 = 0.0117 \text{ for NACA } 65(A_{10}) \text{ blades,}$$

$$= 0.007 \text{ for C.4 circular-arc blade,}$$

$C_3 = 1.43,$

$C_4 = 0.61,$

and

$i^* =$ minimum loss incidence angle.

Reynolds number effect: As shown by Lieblein in reference 36, laminar boundary layer separation associated with low Reynolds number flow significantly affects the blade element losses involved. At low Reynolds number, turbulence level markedly influences the laminar boundary layer and thus loss. As Reynolds number increases, the extent of laminar boundary layer separation decreases and the influence of Reynolds number and turbulence level on loss diminishes. Schlicting and Das (ref. 41) suggest that "low" Reynolds numbers are of order 10^5, while "high" Reynolds numbers are of order 10^6. The evidence presented by Lieblein (ref. 36) supports these numbers. Because the NASA axial-flow pump data used for determining loss correlations involved minimum blade-chord Reynolds number of the order of 10^6, Reynolds number and turbulence effects on loss were not considered further during the present study.

Deviation angle prediction. - The average flow angle of the fluid leaving a cascade of identical blades differs from the blade outlet angle by an amount defined as the deviation angle. Cascade geometrical and flow parameters thought to influence stationary plane cascade deviation angles are as follows:

blade setting angle,
solidity,
profile shape,
total camber,
maximum blade thickness,
thickness and camber distribution,
trailing-edge thickness,
surface finish,
incidence angle,
axial velocity ratio,
inlet velocity level (Mach number),
Reynolds number,
turbulence level,
unsteadiness, and
cavitation.

Two-dimensional geometric parameters: Two-dimensional cascade results, and to a lesser extent potential flow theory, have been used to establish the values of deviation angle for various two-dimensional cascade geometries. The plausibility of the dependence of deviation angle in two-dimensional flow on geometric parameters can be established by considering the cascades drawn in figure 7. The cascades in figure 7a each have the same chord length, solidity and camber, but the cascade on the right has a higher blade setting angle than the other cascade, and hence has a significantly shorter length of passage bounded on both sides by blade surfaces. Thus, for a fixed incidence angle, increasing blade setting angle tends to decrease guidance of the flow and hence tends to increase deviation angle. Decreasing solidity, σ, also tends to decrease guidance of the flow and increase deviation angle as seen by the difference in channel length of the two cascades in figure 7b. Although it is not so graphically obvious (figure 7c) deviation angle does increase with increasing camber, and according to Lieblein (ref. 36) the relationship between deviation angle and camber is linear for potential flow.

One frequently-used deviation angle prediction equation, Carter's rule (ref. 42) reflects these ideas as

$$\delta = \frac{m_c \phi^o}{\sigma^{1/2}} \qquad (22)$$

where m_c is a function of blade setting angle and the position of maximum camber. Curves of m_c as a function of blade setting angle that are based on theory and experimental data are given by Carter and Hughes (ref. 43) for circular arc and parabolic arc (maximum camber at 40% of the chord from the leading edge) camberline blades. Howell (ref. 44) ascribed to Constant (ref. 45) an early version of equation (22) in which $m_c = 0.26$ was used. Equation (22) applies specifically to the "nominal" incidence angle which Howell (ref. 44) defines as the incidence angle for which the turning angle, (ϵ), is equal to 0.8 of the turning angle at which the loss is twice the minimum value, however, it is frequently applied throughout the low-loss incidence angle range under the assumption that deviation angle does not change appreciably with incidence angle in the low-loss range.

Lieblein's method: A deviation angle prediction method, which includes more geometric parameters, was presented by Lieblein (ref. 36). The method was based on two-dimensional cascade data for NACA 65-series compressor blades which were presented by Emery et al. (ref. 40). Correlations were made for performance at a reference incidence angle (i_{ref}) defined to be midway between the incidence angle at which the total pressure loss across the cascade was equal to twice the minimum-loss value (see figure 8). At the reference incidence angle, i_{ref}, deviation angle is expressed as

$$\delta = \delta_o + m\phi^o \qquad (23)$$

where δ_o is the reference deviation angle for zero camber, ϕ^o is camber, and m is the slope of the deviation angle function with camber. Curves are presented by Lieblein (ref. 36), giving the slope factor m as a function of inlet air angle and solidity for circular-arc-mean-line blades. Inlet air angle was used instead of blade setting angle because the cascade date of Emery et al. (ref. 40) were obtained at a constant inlet air angle rather than a constant blade setting angle. The zero-camber deviation angle is given by Lieblein (ref. 36) as

$$\delta_o = \left(K_\delta\right)_{sh}\left(K_\delta\right)_t\left(\delta_o\right)_{10} \tag{24}$$

where $(\delta_o)_{10}$ represents the zero-camber deviation angle for a 10% thick NACA 65-series distribution, $(K_\delta)_{sh}$ is a correction for blade shapes with thickness distributions different from the 65-series, and $(K_\delta)_t$ is a correction for maximum blade thickness other than 10% of the chord. Empirical curves are given for $(\delta_o)_{10}$ as a function of inlet air angle and solidity and for $(K_\delta)_t$ as a function of maximum thickness ratio, t_{max}/c. A value of 1.1 for $(K_\delta)_{sh}$ is recommended for C-series circular-arc blades and 0.7 for double-circular-arc blades. Both of these values were based on limited data. Plots of deviation angle versus camber, comparing values from equation (23) with cascade data of Emery et al. (ref. 40), are given by Lieblein (ref. 36). Equation (24) approximates the data quite well. However, at high cambers where D-factors exceed 0.62, the experimental data tend to fall above the predicted values. Blade sections operating at D-factors greater than 0.62 evidently have blade surface boundary layers thick enough at i_{ref} to cause the flow to differ significantly from the potential flow for which a linear relation between deviation angle and camber angle is predicted. A quantitative evaluation of deviation angle as a function of camber for D-factors greater than 0.62 is currently lacking.

Both methods previously described assumed the incidence angle to be fixed at some "design" value. In the following paragraphs, methods to predict the deviation angle at "off-design" values of incidence angle are reviewed.

Incidence angle effects: The deviation angle of a plane cascade is a function of the incidence angle in addition to blade geometry. A typical curve of deviation angle as a function of incidence angle for a cascade with a fixed inlet flow angle is shown in figure 9. The deviation angle curve can be roughly divided into two parts, one corresponding to the so-called low-loss incidence angle interval and the other corresponding to incidence angles outside the low-loss interval. When the incidence angle is in the low-loss interval, the blade surface boundary layers are probably quite thin, so that the flow closely approximates potential flow. Therefore, in the low-loss region, the functional relationship between deviation angle and incidence angle for a two-dimensional cascade is quite similar to the relationship for potential flow. Lieblein (ref. 46) concluded, based on calculations using the potential flat plate flow theory of Weinig (ref. 47), that $\left(\frac{d\delta}{di}\right)_{ref}$ is positive for potential flow and that it is a function of solidity and blade chord angle. Smith (ref. 48), in a discussion of reference 46, indicated that $\left(\frac{d\delta}{di}\right)_{ref}$ is also a strong function of camber.

Using the low-speed cascade data for 65-(A_{10})10 blades of reference 40, Lieblein developed an empirical method to estimate the variation of deviation angle in the low-loss incidence interval. He assumed that since operation could be considered to be in the low-loss region for only a small incidence angle interval, the following linear function could be used to compute deviation angle:

$$\delta = \delta_{ref} + \left(i - i_{ref}\right)\left(\frac{d\delta}{di}\right)_{ref} \tag{25}$$

where δ_{ref} and $\left(\frac{d\delta}{di}\right)_{ref}$ are determined at $i = i_{ref}$. Lieblein presented a family of curves from which values of $\left(\frac{d\delta}{di}\right)_{ref}$ may be obtained for solidities ranging from 0 to 1.8, and for inlet air angles ranging from 0 to 70°. These correlations are also presented in reference 36.

Because the 65-Series cascade data (ref. 40) were obtained with inlet air angle fixed, the $\left(\frac{d\delta}{di}\right)_{ref}$ obtained from Lieblein's curves is applicable to a constant inlet air angle cascade, while, as Smith (ref. 48) pointed out, in practical applications the blade setting angle, γ, is fixed and the inlet air angle varies. Smith (ref. 48) developed relations to obtain $\left(\frac{d\delta}{di}\right)_{ref}$ applicable to fixed-γ blade rows from Lieblein's correlations and gave a numerical example in which the fixed-γ derivative was larger than the fixed-β_1 derivative by a factor of three for NACA 65-(12)10 blades with $\sigma = 1.0$ and $\beta_1 = 60°$. Figure 10 shows the variation of deviation angle with incidence angle from reference 40 for the NACA 65-(12)10 blades of Smith's (ref. 48) example at a constant inlet air angle, $\beta_1 = 60°$. Date from reference 40 were crossplotted to obtain a second curve shown in figure 10 for the same blades with a constant stagger angle of 47.6°, which is the stagger angle of a cascade of NACA 65-(12)10 blades with $\beta_1 = 60°$, $\sigma = 1.0$, and $i = i_{ref}$ computed using the correlations of reference 46. Graphically determined values of $\left(\frac{d\delta}{di}\right)_{ref}$ are compared with values from Lieblein's (ref. 46) correlation and Smith (ref. 48) calculation. Based on the differences in this example, it appears that the fixed-γ derivative should be used in preference to fixed-β_1 derivatives in analysis applications when computing the change of deviation angle for a change of incidence angle in the low-loss incidence angle interval. Smith (ref. 48) also pointed out that because the fixed-γ derivative was strongly dependent on camber, the fixed-β_1 derivative should be also.

Howell (ref. 49) presented a single curve for $(\delta - \delta_{nom})/\varepsilon_{nom}$ as a function of $(i - i_{nom})/\varepsilon_{nom}$ where the nominal conditions occur at 0.8 of the turning angle at which the loss is twice the minimum value.

Apparently no method (empirical or analytical) has been published as yet to predict the functional relation between deviation angle and incidence angle outside the low-loss incidence angle interval, even for a plane two-dimensional cascade flow.

Axial velocity ratio effects: It is well known that the deviation angle in a rectilinear or plane cascade depends on the ratio of the leaving to the entering axial velocities (AVR). Katzoff et al. (ref. 50) among others reported the phenomenon in 1947. Because of this effect, discrepancies exist between deviation angle data measured under two-dimensional conditions in cascades with side and end wall suction and data measured in similar cascades with solid walls. The leaving axial velocity in a solid wall cascade is usually higher because of the general increase of boundary layer thickness and particularly because of regions of separation in the corner where the blade suction surface intersects the side wall. These regions of separation reduce the effective flow area, which raises the general level of axial velocity leaving the blade row. Elimination of these regions of separation and establishment of a constant axial velocity through the cascade can be accomplished by continuous boundary-layer removal through porous walls, as described in Erwin and Emery (ref. 51). A constant axial velocity is a consequence of continuity for the two-dimensional flow of an incompressible fluid.

The changes in flow through a cascade as axial velocity ratio changes may be described by considering the accompanying change in pressure distribution. If the losses are assumed constant for a small change in AVR, then the static pressure rise across a blade in a cascade decreases (increases) as AVR increases (decreases), assuming incompressible flow. The resulting change in pressure distribution is illustrated in figure 11. In general, the airfoil circulation may also be expected to change as AVR varies. The magnitude of the change in circulation has a direct effect on the change in deviation angle. Evaluating circulation using the path EFGH of figure 12, assuming $s_1 = s_2$, yields the result

$$\Gamma = s\left(V_{\theta,1} - V_{\theta,2}\right) . \tag{26}$$

From the velocity diagrams in figure 12 it is apparent that the deviation angle will decrease as AVR increases, if circulation increases (i.e. $V_{\theta,2}$ decreases) or decreases less than an amount that allows $V_{\theta,2}$ to increase by more than d units. Similarly if circulation decreases or increases less than a critical amount, deviation angle will increase as AVR decreases. In fact, available experimental results (refs. 50 to 53) indicate that deviation angle does decrease with increasing AVR and increases with decreasing AVR, although the data of reference 51 indicate that circulation decreases slightly as AVR increases. A reasonably complete summary of empirical, semi-empirical and potential flow methods for calculating axial velocity ratio effects is presented in reference 54.

Thickness and camber distribution: Factors are presented in reference 36 which compensate for the differing thickness distributions of 65-series, C-series circular-arc, and double-circular-arc blades. Though this correction is rather small, the data of reference 55 (e.g., figure 57 of that reference) indicate that camber distribution may have significant effects on deviation angle, at least at off-design incidence angles. For double-circular-arc blade sections, however, predicting this effect does not seem especially important.

Trailing-edge thickness effect: Minor geometric parameters, such as trailing-edge thickness, apparently have negligible effect on deviation angle for normally specified values (refs. 37, 55 and 56).

Miscellaneous effects: The effect of fluctuation of circulation and other unsteady flows on deviation angle is unknown. Cavitation and Mach number effects are listed for completeness, but are beyond the intended scope of the present method and will not be considered further. Surface finish, turbulence level and Reynolds number did not significantly affect the pump data available for correlation and hence were not considered in detail.

Extension of Stationary Plane Cascade Methods and Results to Pump Rotor Flow

If the previously mentioned two-dimensional cascade loss and deviation angle prediction methods are to be extended to serve usefully in axial-flow pump design and analysis, the significant differences existing between stationary cascade and axial-flow pump flows need to be identified and considered. Many of the complicated features of pump flow are inherently absent in the cascade environment. Whereas the flow through a typical axial-flow pump blade row is three-dimensional and unsteady, the flow through plane cascades is mainly steady and two-dimensional. The three-dimensionality and unsteadiness associated with typical pump flow stem mainly from blade divergence and twist and rotor relative motion with respect to the fluid and stationary annulus walls and blades, features usually not found in plane cascades. At constant speed, a typical pump rotor blade section operates with unchanging blade setting angle as incidence changes with flow rate. Most plane cascades have been operated with incidence variation accomplished by changing cascade blade setting angle while maintaining constant relative inlet angle. In a large portion of the plane cascade work, end wall boundary layer effects on the resulting flow were minimized by fluid removal. The flow through an axial-flow pump blade row on the other hand is appreciably influenced by end wall boundary layers.

Within the time available for developing loss and deviation angle prediction methods, it was decided that axial-flow pump experimental data correlation would be most practical and therefore should be pursued. Available for this purpose was a substantial amount of axial-flow pump rotor experimental data obtained at the NASA Lewis Research Center (ref. 57). Pertinent information related to these rotors is given in Table I. To minimize analysis time and cost, five rotor configurations were selected as representative of the range of geometry and design variables present in the twelve rotor configurations for which data were initially available. The five selected, indicated by asterisks in Table I, were used exclusively to obtain the correlations explained below. Configurations 07 and 09 differ only in the number of blades and the chord length. The hydrodynamic design is identical for configurations 5, 6, 8, 9 and 10, but configurations 5 and 6 have 9-in. diameters while configurations 8, 9, and 10 have 5-in. diameters. The only other differences among these five configurations are the tip clearance values. Configurations 13 and 16 have the same blade angles but different blade section profiles. The double-circular-arc profile of configuration 13 is the more conventional profile and thus configuration 13 was chosen instead of configuration 16. Configuration 15 data were reserved to "test" the resultant correlations. Although the two-parameter correlation philosophy served well in working with plane cascade data, the minimum number of axial-flow pump data correlation parameters necessary was felt to be three. An explanation of the development of the various parameters associated with the three-parameter loss and deviation angle correlation options available with the present off-design analysis computer program follows.

Loss prediction. – Swan (refs. 8 and 9) claimed reasonable success in correlating axial-flow compressor blade-element profile and secondary losses using Lieblein's DEQ (modified slightly for use with compressor rotor flow) and θ/c as calculated from $\frac{\theta}{c} = \frac{\overline{\omega} \cos \beta_2}{2\sigma}$ as correlating parameters. Additionally, spanwise location was used as a third correlating parameter for minimum-loss data and inlet relative Mach number was used as the third correlating parameter for off-minimum-loss data. In view of this fact, it was felt that appropriately modified versions of Lieblein's DEQ and θ/c relationships, plus at least one other independent correlating parameter, might serve as the base for an axial-flow pump blade-element data correlation method. The modification of DEQ for use with pump rotor and stator flows is outlined in Appendix A. The results are:

$$DEQ_r = \frac{V_{z,1}}{V_{z,2}} \frac{\cos \beta_2'}{\cos \beta_1'} \left\{ C_1 + C_2 \left(i - i_{ref}\right)^{C_3} \right.$$

$$\left. + C_4 \frac{\cos^2 \beta_1'}{\sigma_1 V_{z,1}} \left[\frac{r_1}{r_2} V_{\theta,1}' - V_{\theta,2}' \right] \right\} \tag{27}$$

and

$$DEQ_s = \frac{V_{z,1}}{V_{z,2}} \frac{\cos \beta_2}{\cos \beta_1} \left\{ C_1 + C_2 \left(i - i_{ref}\right)^{C_3} \right.$$

$$\left. + \frac{C_4 \cos^2 \beta_1}{\sigma_2 V_{z,1}} \left[V_{\theta,2} - \frac{r_1}{r_2} V_{\theta,1} \right] \right\} . \tag{28}$$

Several parameters related to Lieblein's (θ/c) parameter for plane cascades were identified as possible candidates for use with the axial-flow pump data. These were:

$$\left(\frac{\theta}{c}\right)_A = \frac{\overline{\omega} \cos \beta_2'}{2\sigma} , \tag{29}$$

$$\left(\frac{\theta}{c}\right)_B = \frac{\overline{\omega} \cos \beta_2'}{2\sigma} \left(\frac{\cos^2 \beta'_2}{\cos^2 \beta_1'}\right) \left(\frac{V_{z,1}}{V_{z,2}}\right)^3 \left(\frac{3H_2 - 1}{2H_2}\right) , \tag{30}$$

$$\left(\frac{\theta}{c}\right)_C = \frac{\overline{\omega} \cos \beta_2'}{2\sigma} \left(\frac{V_1'}{V_2'}\right)^2 , \tag{31}$$

$$\left(\frac{\theta}{c}\right)_D = \frac{\overline{\omega} \cos \beta_2'}{2\sigma} \left(\frac{\cos \beta_2'}{\cos \beta_1'}\right)^2 , \tag{32}$$

$$\left(\frac{\theta}{c}\right)_E = \frac{\overline{\omega} \cos \beta_2'}{\left(\frac{P_1' - p_2}{P_1' - p_1}\right) \sigma \left(\frac{4H_2}{3H_2 - 1}\right) + \overline{\omega} \sigma H_2} . \tag{33}$$

Note that $(\theta/c)_A$ and $(\theta/c)_D$ are abbreviated forms of Lieblein's relationship for θ/c for plane cascade flow that was shown earlier (equation 20) to be suitable for correlating plane cascade minimum loss data (ref. 36). Derivations of $(\theta/c)_B$ and $(\theta/c)_C$ have been included in Appendix B. The derivation of $(\theta/c)_E$ is given in reference 58.

A "blade-loading" parameter used extensively in compressor design and sometimes for correlating compressor off-design loss data is the D-factor modified for 3-dimensional flow, as shown in Appendix C:

$$D_r = 1 - \frac{V_2'}{V_1'} + \frac{r_1 V_{\theta,1}' - r_2 V_{\theta,2}'}{\sigma_{av}\left(r_1+r_2\right)V_1'} \tag{34}$$

$$D_s = 1 - \frac{V_2}{V_1} + \frac{r_2 V_{\theta,2} - r_1 V_{\theta,1}}{\sigma_{av}\left(r_1+r_2\right)V_1} \ . \tag{35}$$

In order to "test" the various relationships for blade wake momentum thickness parameter for suitability as experimental data correlators, each was used with the pump data provided by NASA. DEQ and D as expressed by equations (27-28) and (34-35), respectively, provided an indication of blade loading level. In order to ascertain possible effects associated with spanwise location that are not strongly reflected in the expression for wake momentum thickness and loading, suitability tests were performed on data from similar spanwise locations only. As indicated in figures 13, $(\theta/c)_A$ and $(\theta/c)_E$ appeared to be about equally more suitable than the other θ/c relationships as experimental data correlators. Similar trends were indicated when D-factor was used as the abscissa variable. Neither $(\theta/c)_A$ or $(\theta/c)_E$ seemed to be entirely satisfactory. Nevertheless, since $(\theta/c)_A$ is the simpler relationship, it was selected as the wake momentum thickness parameter to use in constructing the three-parameter loss tables involving $(\theta/c)_A$, spanwise location and DEQ or D. The tables are represented graphically in figures 14 and 15. The curves shown are indicative of the trends demonstrated by the NASA axial-flow pump rotor data in figures 16 and 17.

In order to ascertain the worth of the three-parameter loss tables mentioned above, with respect to a two-dimensional cascade data related method for calculating losses, an option involving equations (27) or (28) for DEQ, equations (20) for loss coefficient and the two-dimensional cascade loss data indicated in figure 18 was made available.

Deviation angle prediction. — In addition to those items influencing deviation angle previously discussed in the Stationary Plane Cascade Section, the following can be identified for the three-dimensional flow through a typical axial-flow pump rotor:

corner stall,
tip clearance,
annulus wall boundary layers,
radial gradients of circulation,
radial flow of blade boundary layer fluid,
blade row interaction parameters, and
blade sweep and dihedral angles.

Corner stall and tip clearance flow, while important locally, probably directly affect the deviation angle for only a small percentage of the total span. For this reason, and because data are lacking for empirical correlations, the influence of corner stall and tip clearance flow was not directly accounted for in the present correlation.

Presence of annulus wall boundary layers in the flow approaching a blade row tends to result in local overturning or decreased deviation angles. This phenomenon has been discussed for the simpler case of curved channels in reference 59 and for two-dimensional cascades in reference 60. It is also included in the more general analysis of reference 61. However, in all cases, the flow model is highly idealized, and the theory does not appear to be directly applicable to real flows where skewed boundary layers and tip clearance flows exert significant influence on flow patterns. In any case, the percentage of fluid involved is small and the errors involved in neglecting cascade secondary flow are not expected to be large (see data presented in reference 60).

The effects of radial gradients of circulation on deviation angle have been considered in reference 62 for inlet guide vanes and in a more general context by reference 61. A conclusive evaluation of this effect was not completed, but it may be worthwhile in the future to apply the analysis of reference 61 to a typical pump rotor for a quantitative indication of the magnitude of the effect.

Radial flow of boundary layer fluid may have both a direct and indirect influence on deviation angle. Deviation angle would be directly affected when radial movement of the boundary layer either triggers or retards flow separation from a particular blade section. Indirect effects could result from the axial velocity ratios required to satisfy radial equilibrium for a flow with loss profiles that include effects of low momentum fluid moving radially in the wake behind the blade. In both cases, the movement of boundary layer material could be expected to be reflected in the downstream axial velocity profile. This suggests that an empirical correlation based on three-dimensional data, which accounts for axial velocity ratio effects, might also partially account for the effect of radial boundary layer flows.

yields a quadratic equation in $V'_{2,c}$. The corrected diagram can then be computed from the appropriate root $V'_{2,c}$, U_2, and $V_{z,1}$. The expectation was that δ_c from either of the iterative approaches would more closely approximate the measured deviation angle than a value computed directly from Carter's rule using the actual blade section camber. However, the comparison of results in figure 22 shows that the corrected deviation angles are generally smaller than the deviation angles from Carter's rule which are in turn much too small over most of the blade span for the high loaded rotors in figures 22b and 22c. These results are typical for all the rotor configurations and for other flows. Based on these results these correlation approaches are also discarded.

An approach similar to the iterative, constant circulation one discussed above with a variable exponent on the camber term in the function used to compute δ_c, namely

$$\delta_c = m\left(\phi_c^o\right)^b / \sigma^{1/2} , \tag{43}$$

was tried next. In this case, the exponent was chosen so that

$$\delta_c = \delta_{exp} . \tag{44}$$

Values of b computed at all radial positions for operation at reference incidence angle are given in figure 23. The exponents show a consistent trend except at the hub and tip for configuration 02. This configuration is a low hub-tip ratio, lightly loaded rotor intended to typify a transition rotor, located between a lightly loaded inducer and high loaded main stages. With the subsequent development of higher loaded inducers (ref. 65), this type of rotor is not likely to appear in a multistage pump. Therefore, the fact that the exponents from configuration 02 fall outside the band in figure 23 is not considered a major deficiency in the method, although it indicates a lack of generality.

As another approach, the method just described was simplified by using the actual blade camber instead of a corrected camber in the functions for δ_c:

$$\delta_c = m\left(\phi^o\right)^b / \sigma^{1/2} . \tag{45}$$

The exponent was again chosen so that the following expression was obtained:

$$\delta_c = \delta_{exp} . \tag{46}$$

The resulting exponents are shown as a function of percent passage height in figure 24. The band of data is about the same width as that in figure 23, except at the tip section where the exponent for configuration 07 shows more scatter. This was considered the most promising approach for predicting deviation angles at reference incidence angle operation. A preliminary check on the method was made by calculating deviation angles for the five configurations using equation (45), where b was obtained as the mean line of the band in figure 24. The results are given in Table II. Excluding configuration 02, the deviation angles, δ_c, computed from equation (45) are within $\pm$ 2.6° of the measured angles, which is a significant improvement over Carter's rule. Note that because the camber of configuration 07 is small at the 10% station, the large scatter in the exponent (figure 24) resulted in only a 1.3° discrepancy in deviation angle. However, this is still a large percentage of the relative turning angle.

Incidence angle: Prior efforts to predict deviation angles at off-reference incidence angles are mainly represented by Lieblein's correlations (ref. 36) of two-dimensional low-speed air cascade results. In this correlation, values of $d\delta/di$ are presented as a function of solidity and inlet flow angle. The $d\delta/di$ is always positive and only applies to incidence angles near i_{ref}. However, in the analysis problem it is necessary to predict deviation angles over the entire range of operation and not just near i_{ref}. Furthermore, as illustrated by data in figure 25, the slope $d\delta/di$ is not always positive for pump rotor blade sections even at i_{ref}. The incidence angle corrections of reference 36 are clearly inadequate and the characteristics of data in figure 25 preclude any possibility of a simple functional relationship of the form

$$\delta - \delta_{ref} = f\left(i - i_{ref}\right) . \tag{47}$$

The method involving equations (43) and (44) described earlier was also applied at off-reference conditions to obtain values of camber exponent b. The results are shown in figure 26 for five spanwise positions. If configuration 02 data are excluded, a consistent trend is exhibited near the tip and hub but considerable scatter exists in the midspan data at low incidence angles.

Very similar results were obtained when the camber exponent was computed using the actual camber equation (equation 45). These results are presented in figure 27. At the tip section the exponents for configuration 07 fall above the others, which is consistent with results in the previous section. In spite of the greater scatter in figure 27 as compared to figure 26, the simplicity of using actual blade camber instead of an equivalent camber obtained by an iterative calculation suggests its use. Lines fitted through the data of figure 27 are shown in figure 28. These variations of the exponent b and the relationship expressed by equation (45) together form a method for calculating deviation angles that is available as a program option.

Reference incidence angle. — Associated with the loading parameter, DEQ, and the three-parameter off-design deviation angle correlation method involving the camber exponent b, i - i_{ref} and spanwise location (fraction of passage height from the tip), is a reference incidence angle, i_{ref}. Two possible reference incidence angles were considered: (1) a reference incidence angle based on the experimental rotor data for a given blade element; and (2) the reference incidence angle which would be predicted for the given geometry using the two-dimensional cascade correlations of reference 36. Basing the reference angle on the experimental rotor data seems attractive at first, but is not possible because of the complicated nature of flow in rotors. For example, the loss coefficients measured for blade elements at 50, 70 and 90% of passage height from the tip often are very low and change very little over the entire test incidence angle interval, making it impossible to determine a reference angle as defined in reference 36. Typical examples of flat loss-coefficient distributions for these blade elements are shown in figure 29. Sometimes the loss coefficients increase or decrease as a function of incidence angle with no minimum value defined, as illustrated in figure 30. In either case, the reference incidence angle cannot be defined as in reference 36. Even in the few cases where the experimental loss coefficient curves allow the reference incidence angle to be defined (figure 31), the incidence angle so obtained may be misleading because the loss indicated from measurements downstream of the rotor is probably a distorted indication of the loss generated by that element. It may be more or less than the actual loss generated by the flow around the blade section because of the migration of low momentum fluid along the blade and annulus surfaces (ref. 66). For these reasons a reference incidence angle based on the experimental rotor data was not used.

Instead, a reference incidence angle based on the correlations of reference 36 was chosen. These correlations were derived from cascade data obtained with fixed inlet flow angles, i.e., the incidence angle was varied by re-setting the blades, and hence the correlation incorporates inlet flow angle as a parameter rather than stagger angle. Since rotor blades have fixed setting and variable inlet relative flow angles, the correlations of reference 36 do not directly yield a single reference incidence angle for rotor blade elements. However, a unique reference angle can be obtained by an iterative procedure as follows (ref. 67):

1. an initial estimate of i_{ref} is made;
2. from the known blade angle and the estimated i_{ref}, a corresponding inlet relative flow angle is calculated;
3. using the calculated relative flow angle and the correlations of reference 36, a new value of i_{ref} is obtained and compared with the estimated value; and
4. if the calculated and estimated values of i_{ref} are different, the estimated value is revised and steps 2, 3, and 4 are repeated until convergence is obtained.

This procedure contains the implicit assumption that the same reference incidence angle would be measured in a constant blade setting angle cascade (γ = constant) and a constant inlet flow angle cascade [$\beta_1 = (i_{ref})_\beta + \alpha_1$, where α_1 is the inlet blade angle corresponding to γ = constant]. This assumption is not strictly correct as noted in reference 36 and illustrated by cross-plotted data (ref. 40) in figure 32. For this example, the reference incidence angle for a constant setting angle cascade is 1.2° less than for a constant inlet flow angle cascade. Applying the reference incidence angles obtained from reference 36 also involves the assumption that the reference incidence angle is not dependent on the axial velocity change across the cascade because the axial velocity ratio was about 1.0 for the data correlated in reference 36, while axial velocity ratios ranging from 0.55 to 1.40 were measured across the rotor blade sections. No attempt has been made to evaluate the possible change of reference incidence angle caused by the change in diffusion accompanying axial velocity ratio changes. While the assumptions involved were recognized, the i_{ref} obtained from reference 36 was considered to be the most consistent and best estimate available for the reference incidence angle.

Specific experimental data correlations. — A less general data correlation method for individual pump rotors was also determined. As mentioned previously the blade chord Reynolds numbers associated with the axial-flow pump experimental data were high enough to justify neglecting Reynolds number effects. It seems reasonable then to assume that the experimental data blade-element non-dimensional velocity diagrams (all velocities non-dimensionalized with tip speed), and therefore loss coefficients and deviation angle, will be mainly dependent on average flow coefficient in addition to spanwise location and blade row geometry. Based on this assumption, tables of experimentally determined loss coefficients and deviation angles as functions of exit streamline spanwise location (radius) and effective average inlet flow coefficient can be constructed for specific rotor configurations. In such loss and deviation angle correlations, appropriate effective inlet flow area to annulus area ratios as a function of flow rate are required. These ratios permit the calculation of effective average flow coefficients from theoretically computed ones determined in a radial equilibrium solution.

In all of the other loss correlation methods discussed, the resulting predicted loss is strongly dependent on the calculated exit flow conditions via the loading parameter D or DEQ. Inherent with the specific loss correlation method presently described is a weak relationship between predicted loss and calculated exit flow conditions via exit radius. This difference accounts partly for the solution stability associated with using the specific loss correlation method.

COMPUTER PROGRAM CAPABILITY AND UTILIZATION

As already outlined in the solution method, the performance prediction program is based on numerical solution for radial equilibrium and continuity requirements in the meridional flow at axial stations between blade rows in a given pump configuration. Blade-element head losses, deviation angles, and reference incidence angles are estimated, based on available correlated data tables. Simple radial equilibrium, accounting for streamline shift across a blade row but ignoring streamline slope and curvature at computing stations, is employed. Blade elements in a blade row defined by streamlines as determined in the solution are the basis for the computed blade-element performance.

Input to the program includes pump annulus and blade geometry, rotational speed, flow rate, and reference data tables for head loss and deviation angle calculations. Number of streamlines at which the numerical solution is made is also prescribed by the user. The geometry data describing the annulus inner and outer radii and blade element geometric parameters are inputed in tabular form for between blade-row stations. Flow rates are also given in the form of tables assigning radial distributions of flow velocity and total head at the inlet station to the pump. Using these input tables for the flow at the inlet station, the program computes flow rate and establishes streamlines which are followed in calculation of the flow solution through the blade rows. Extensive use is made of interpolation procedures in the program to obtain blade-element results from the various data tables. Both blade-element and mass-averaged rotor or stage performance is computed and outputed by the program.

Overall operation of the program for a given pump performance problem is formed in two nested iteration loops. These are a head loss iteration loop, and a radial equilibrium and continuity iteration loop nested within, both of which require initializations. Blade-element head losses are initialized zero prior to solution at the beginning flow rate for a given rpm, while a base streamline velocity is assigned an approximating average value corresponding to the beginning flow rate. The same basic calculation scheme is used for any blade row, rotating or stationary, for any given rotational speed and flow rate of the pump. However, the program input and calculations are arranged so that successive values of flow rate are computed along lines of constant rpm. (Beginning flow rate for a constant rpm line is generally high relative to the design flow, since loss of radial equilibrium solution may be encountered at lower assigned flow rates). In this process, the solution, including head loss distribution obtained at the preceding flow rate,is used as initialization of iterations at the next flow rate.

In the following sections, explanation of program input load preparation is given along with a detailed discussion of the program. Descriptions, including flow diagrams and glossaries, are given for the main program and each subroutine. A complete listing of the program and sample program loads and outputs are contained in Appendices D and E.

Input Load Description

In this section a working description of input load preparation is given to enable the program user to estimate off-design performance for arbitrary pump configurations and operating conditions.

Input is identified by card packets which carry an identification number (ID) in the first two columns of each card. The ID is read by the program as the data are loaded into the computer to check the ordering of input cards. If incorrect ordering is detected, an error message is printed and calculations terminated.

The card packets and their arrangement in particular card packet sets are described below. The numerous options that exist within an input data load are explained. Also sample data loads are presented for purposes of illustration.

Card packet sets. — Input is ordered in terms of six basic sets of card packets. These card packet sets, referred to for convenience by the initial card packet in each set, are as follows:

a) Card packet set 10 — limit specifications card for pump configuration

b) Card packet set 18 — head loss and deviation angle specifications per blade row of configuration

c) Card packet set 30 — geometry data per blade row of configuration

d) Card packet set 50 — assigned rotational speed (rpm) per blade row of configuration

e) Card packet set 70 — base streamline axial velocity initialization card corresponding to first flow rate

f) Card packet set 80 — assigned flow rate, inlet conditions, and axial station effective flow area factors

Card packet sets 18 for all the blade rows of the pump configuration are loaded before proceeding to packet sets 30. The same is true for packet sets 30, before proceeding to packet sets 50. Multiple rpm calculations are made by successively loading packet sets 50, each followed by packet sets 80 for the appropriate flow rates. Finally, multiple pump configurations may be loaded, each starting with packet set 10, followed by sets as described above.

Card packets:

ID	Card Col.	Format	Data Input
10	1,2	I2	identification number, ID
	3,4	I2	number of blade rows plus 1, ILIM
	5,6	I2	number of streamlines, JLIM; ≥ 3, ≤ 20
	7,8	I2	base streamline number, JBASE; ≥ 1, $\leq$ JLIM (but generally taken near mid-radius of the annulus)
	9-14	I6	problem run identification, IRUN
	15-20	F6.4	tolerance value for head loss iteration, THL (ratio of change in computed head loss to previously computed head loss)
18	1,2	I2	ID
	5,6	I2	blade row number
	7-13	F7.4	blade row reference radius, RSTAR, ft
19	1,2	I2	ID
	3,4	I2	blade row option for head loss calculation, IEXLOS
	5,6	I2	blade row option for deviation angle calculation, IEXDEV
20	1,2	I2	ID
	3,4	I2	number of elements in PHIBB array (packet 21) for blade row; ≥ 3, ≤ 20

ID	Card Col.	Format	Data Input
	5,6	I2	number of elements in XPB array (packet 22) for blade row; ≥ 3, ≤ 20
21	1,2	I2	ID
	3-7	F5.4	reference table of inlet flow coefficient for blade row, PHIBB
	⋮	⋮	
	68-72	F5.4	
22	1,2	I2	ID
	3-7	F5.4	reference table streamline radius at outlet of blade row, XPB, ft
	⋮	⋮	
	68-72	F5.4	
23	1,2	I2	ID
	3,4	I2	card identification (visual checking only)
	5-9	F5.4	reference table (for blade row) of head loss coefficient, OMEGBB, function of PHIBB, XPB
	⋮	⋮	
	70-74	F5.4	
24	1,2	I2	ID
	3,4	I2	card identification (visual checking only)
	5-9	F5.4	reference table (for blade row) of flow deviation angle, DEL2B deg., function of PHIBB, XPB
	⋮	⋮	
	70-74	F5.4	
25	1,2	I2	ID
	3,4	I2	number of elements in XDBB or DEQBB array (packet 26) for blade row; ≥ 3, ≤ 20
	5,6	I2	number of elements in RPBB array (packet 27) for blade row; ≥ 3, ≤ 7
26	1,2	I2	ID

ID	Card Col.	Format	Data Input
	3-8	F6.4	reference table of D-factor or equivalent D-factor, XDBB or DEQBB, for blade row
	⋮	⋮	
	69-74	F6.4	
27	1,2	I2	ID
	3-8	F6.4	reference table of fraction of passage height from outer casing, RPBB, for blade row
	⋮	⋮	
	69-74	F6.4	
28	1,2	I2	ID
	3-8	F6.4	reference table (for blade row) of wake momentum thickness/chord, THACBB, function of XDBB or DEQBB and RPBB
	⋮	⋮	
	69-74	F6.4	
30	1,2	I2	ID
	3,4	I2	blade row number
31	1,2	I2	ID
	3,4	I2	number of elements in geometry arrays (packet 32) for blade row
32	1,2	I2	ID
	3,4	I2	blade row identification (visual check only)
	5,6	I2	number of radial position, J
	7-13	F7.4	reference radius at blade row inlet, X, ft
	14-20	F7.4	blade element leading edge camberline tangent angle, ALFB, deg., function of X
	21-26	F7.4	reference angle radius at blade row exit, XP, ft
	27-33	F7.4	blade-element trailing edge camberline tangent angle, ALFPB, deg., function of XP
	34-40	F7.4	blade-element solidity, SGMAB, function of XP

ID	Card Col.	Format	Data Input
	41-47	F7.4	blade-element maximum thickness/chord, TMXCB, function of XP
	48-54	F7.4	blade-element reference incidence angle minus cascade rule incidence angle, FI2DB, deg., function of XP
	55-62	F7.4	blade-element wake form factor, FHB, function of XP
	63-69	F7.4	Shape correction factor, FKSHA, function of XP
50	1,2	I2	ID
	3-8	F6.4	blade row rotational speed, rpm
70	1,2	I2	ID
	3-8	F6.4	initializing base streamline axial velocity, ft/sec
80	1,2	I2	ID
	3-8	F6.4	flow rate calculation identification number, PHIRUN
81	1,2	I2	ID
	3,4	I2	number of elements per array (packet 82), ≥ 3, ≤ 20
82	1,2	I2	ID
	3-8	F6.4	reference radius at inlet station, X1, ft
	9-14	F6.4	fluid axial velocity at inlet station, VZB, ft/sec, function of X1
	15-20	F6.4	fluid whirl velocity at inlet station, VUB, ft/sec, function of X1
	21-26	F6.4	total head at inlet station, HB, ft, function of X1
	27-32	F6.4	reference radius at inlet station, X1, ft
	⋮	⋮	
	45-50	F6.4	total head at inlet station, HB, ft, function of X1

ID	Card Col.	Format	Data Input
	51-56	F6.4	reference radius at inlet station, X1, ft
	⋮	⋮	
	69-74	F6.4	total head at inlet station, HB, ft, function of X1
83	1,2	I2	ID
	3-8	F6.4	effective flow area/annulus area, ARFAC, per successive axial calculation station
	⋮	⋮	
	69-74	F6.4	

Blade rows are numbered sequentially through a pump configuration, starting with the first blade row as blade row 1. Axial stations are also numbered sequentially through the configuration, starting with the inlet station to the pump as station 1.

Card packets 20-24 (optional) constitute user supplied reference tables of head loss coefficient and flow deviation angle as a function of inlet flow coefficient and leaving streamline radius for the blade row. This is true also regarding packets 25-28, in which tables of wake momentum thickness/chord are inputed as functions of D-factor (or equivalent D-factor) and fraction of passage height from the outer casing. As many cards as necessary are used in packets 21-24 and 26-28 to fill out the specified arrays.

In packet 21, the reference flow coefficients given are to be consistent with flow coefficients based on blade speed computed by the program using the supplied reference radius in packet 18 and the given rotational speed. For a stationary blade row, the reference blade speed is based on the reference radius for the blade row and the rotational speed of the rotor of the pump. In the case of no rotor, reference blade speed is taken as unity, and reference radius is ignored.

Radius values given in packets 22, 27, 32, and 82 should range across the entire annulus at the axial station considered to include hub and casing locations.

User supplied blade-element geometry data in packet 32 are to conform with the sign convention previously noted. Wake form factor and blade section geometry correction factors are as presented in the section BLADE-ELEMENT LOSS AND DEVIATION ANGLE PREDICTION.

In packet 50, rotational speed - 1 indicates a new pump configuration follows immediately (starting with packet 10).

Packet 70 accompanies only the first flow rate to be calculated for a pump configuration.

Packet sets 80 for all assigned flow rates for a given rotational speed follow packet 50 (or 70). PHIRUN < 0 in packet 80 signals new rotational speed follows immediately (starting with packet 50). PHIRUN = 0 in packet 80 signals termination of calculations.

Calculation options for head loss and deviation angle. — A total of six program options are available for calculation of blade-element head losses. These options involve correlated wake momentum thickness parameter and diffusion factor or equivalent diffusion factor, and blade-element radial location; or they involve correlated loss and flow coefficients and radial location. Three options are available for deviation angle calculations. These involve Carter's rule, a camber exponent modification of Carter's rule, or correlated deviation angle with flow coefficient and blade element radial location.

The options are specified by the user per blade row of the pump configuration in terms of input values of IEXLOS and IEXDEV (card packet 19) as follows:

IEXLOS = 1 specifies that the user is supplying a reference table of loss coefficient as a function of flow coefficient and radial position (card packets 20-23) for basis of head loss calculations. Card packets 25-28 for head loss are omitted.

IEXLOS = 0 specifies that reference table of wake momentum thickness/chord as function of equivalent D-factor from the BLOCK DATA routine is used for basis of head loss calculation. Card packets 20-23 and 25-28 for head loss are omitted.

IEXLOS = - 1 specifies reference table of wake momentum thickness/chord as function of equivalent D-factor and fraction of passage height from outer casing from the BLOCK DATA routine is used for basis of head loss calculation. Card packets 20-23 and 25-28 for head loss are omitted.

IEXLOS = - 2 specifies reference table of wake momentum thickness/chord as function of D-factor and fraction of passage height from outer casing from the BLOCK DATA routine is used for basis of head loss calculation. Card packets 20-23 and 25-28 for head loss are omitted.

IEXLOS = - 3 specifies that the user is supplying a reference table of wake momentum thickness/chord as a function of equivalent D-factor and radial position (card packets 25-28) for basis of head loss calculations. Card packets 20-23 for head loss are omitted.

IEXLOS = - 4 specifies that the user is supplying a reference table of wake momentum thickness/chord as a function of D-factor and radial position (card packets 25-28) for basis of head calculations. Card packets 20-23 for head loss are omitted.

IEXDEV = 1 specifies that the user is supplying a reference table of flow deviation angle as a function of flow coefficient and radial position (card packets 20-22, 24) for deviation angle calculations.

IEXDEV = 0 specifies that Carter's deviation angle rule based on reference table from BLOCK DATA routine is used for basis of deviation angle calculations. Card packets 20-22, 24 for deviation angle calculation are omitted.

IEXDEV = - 1 specifies that reference table of deviation angle rule camber exponent as a function of incidence angle minus reference incidence and fraction of passage height from outer casing from BLOCK DATA routine is used for basis of deviation angle calculations. Card packets 20-22, 24 for deviation angle calculations are omitted.

Sample input loads. — Two sample input loads are given in Appendix E. Listings of the input card decks are shown, with the ID numbers in the first two card columns for identification. These two sample problems were run on the Iowa State University IBM 360 Model 65 computer Operating System Release 21. Running time, including input and output, was less than one minute for each problem. The program outputs for each are in Appendix E. Discussion of program output is given in the following section.

The first sample load is for a single stage composed of a rotor followed by a stator row. The annulus has constant hub and outer casing radii of 0.1500 and 0.3750 ft, respectively. The input load is set up to calculate performance for one rotational speed (3910 rpm) at two flow rates. As can be seen in packets 82, inlet data for each of the flow rates are given in terms of nine different radial positions across the annulus. Geometry data for the two blade rows are given in packets 32, each involving seven radial locations. No head loss or deviation angle calculation reference tables are inputed, since the IEXLOS and IEXDEV specifications in cards 19 show that reference tables from BLOCK DATA are to be used.

The second sample is for a single rotor blade row in a straight annulus with hub and outer casing radii of 0.2625 and 0.3750 ft, respectively. With this input, performance is to be computed for two rotational speeds. The first is 3620 rpm as indicated by the first 50 card, followed by the 70 card for base streamline velocity initialization and two 80 packet sets for the assigned flow rates at this speed. A third 80 card follows, carrying the value - 1 and signaling that a second rotational speed follows. This rpm value (2890) is shown on the second 50 card. One more flow rate is then indicated by the one 80 packet set. The final 80 card indicates termination of the calculations. The IEXLOS and IEXDEV head loss and deviation calculation options in card 19 for the second sample load are each indicated as 1. The corresponding user supplied reference tables are included in packets 20-24.

Program Output Description

Sample program outputs. – Sample output listings from the program are given in Appendix E. These were produced using the two input loads just described.

An output listing from the program begins with identification of the problem run, designated base streamline, and number of streamlines used in the solution. Data tables for reference incidence angle analysis (from BLOCK DATA routine) are printed out next. The additional data load to the problem is printed out at the starting flow rate for a rpm line on a blade row by blade row basis. This includes blade row rpm, reference radius, deviation angle and head loss calculation options specified, blade row geometry, and specified deviation angle and head loss reference data tables (these tables are printed whether obtained from input cards or from BLOCK DATA). Variables can be identified by referring to the glossaries contained in the program descriptions of subroutines INOUT or INPUT.

Output of computed results for a given flow rate begins with the listing of the inlet conditions. Flow rate identification (PHIRUN NO.) is based on the combined IRUN (card packet 10) and PHIRUN (card packet 80) numbers. Calculated flow rate and entering and leaving blade-element radial equilibrium results follow, blade row by blade row. Blade-element results are printed in order from the outer casing in toward the hub. Mass-averaged results for a rotor or for a stage, and blade row identification (I) follow the blade-element results.

Column heading identifications in the input are the following (refer also to LIST OF SYMBOLS).

BETA flow angle, β

BETAP relative flow angle, β'

CMBR camber angle, ϕ^{o}

DEV deviation angle, δ

EFFIC	efficiency, η
EQ D-FAC	equivalent D factor, D_{eq}
HD LOSS	head loss, H_{loss}
INCID	incidence angle, i
J	streamline or blade element number, j
LOSS DIFF	head loss relative difference, HLDP (see subroutine OUTPUT)
OMEGABAR	loss coefficient, $\bar{\omega}$
%PH F T	percentage passage height from tip
PHI1	flow coefficient, ϕ_1
PHI2	flow coefficient, ϕ_2
PSI	head coefficient, ψ
PHI I	ideal head coefficient, ψ_i
R/R(TIP)	radius ratio, r/r_t
R/RT(I)	radius ratio, r/r_t
REF INC	reference incidence, i_{ref}
STAG	blade setting angle, γ
STAT HD	static head, h
(THTA/C)	wake momentum thickness to chord ratio, $(\theta/c)_A$
TMAX/C	maximum thickness ratio, t_{max}/c
TOT HD	total head, H
V(REL)	relative velocity, V'
VU	velocity, V_θ
VZ	velocity, V_Z

In the first sample output given, the results are shown for a stage (a rotor, followed by a stator row) for one rpm and two flow rates.

Twenty streamlines were used in the solution, and as indicated by the IEXLOS and IEXDEV parameter values, reference data tables from BLOCK DATA were used in computing blade element head losses and deviation angles in the rotor and in the stator. The extrapolation warning messages given in the output are due to high stagger angle (> 70 deg.) in the rotor near the outer casing, and to high D_{eq} (> 2.2) toward the hub in the stator.

In the second example in Appendix E, the results are for a single rotor blade row. Two values of rpm were computed for, with two flow rates at the first rpm and one at the second. According to IEXLOS and IEXDEV, user supplied reference data tables for head loss and deviation angle calculations were read in from cards.

<u>Abnormal problem completions</u>. — The following error or warning messages may be produced by the program in the case of abnormal problem completion:

"Error in input data card order, MAIN program"

> An error has been detected by MAIN in checking ID on input cards. Problem is terminated. Refer to Section, Input Load Description to correct error.

"Error in input data card order, subroutine INPUT. ID = xx I = xx K = xx L = xx J = xx"

> An error has been detected in subroutine INPUT in checking ID. Current values of ID, I, K, L, J are printed out to help in correcting error. Problem is terminated.

"Error in input — xx must be greater than 2 for interpolation, I = xx, ID = xx"

> Number of elements in an input data table has been detected as too small. The table delimiter and values of I, ID are printed out. Problem is terminated.

"Warning — FIT1D called in xx — extrapolation of table xx"

> An extrapolation of a reference data table has occurred in FIT1D. The calling routine and table involved are identified. Problem calculation continues.

"Warning — FIT2D called in xx — extrapolation of table xx"

> An extrapolation of a reference data table has occurred in FIT2D. The calling routine and table involved are identified. Problem calculation continues.

"IREF at streamline xx required extrapolation of tables because BTP1 = xx deg"

Analysis in subroutine IREF required extrapolation of reference incidence angle data tables from BLOCK DATA. Relative entering flow angle BTP1 exceeds 75 deg. Problem calculation continues.

"ALF1 = 0 not allowed"

Entering blade tangent angle ALF1 has been computed as zero for a blade element in subroutine RADEQC. Problem calculation continues with next inputed flow rate.

"Radial equilibrium solution failed"

Negative radicand encountered in iterations for radial equilibrium solution in subroutine RADEQC. Head loss iterations prior to failure are repeated and results printed out. Problem calculation resumes with next inputed flow rate.

"Solution failure due to negative radicand during loss iteration"

Message following "Radial equilibrium solution failed". Failure encountered during head loss iteration as indicated.

"Solution for several loss iterations preceding failure are printed next"

Message following radial equilibrium solution failure.

"Solution for the loss iteration preceding failure is printed next"

Message following radial equilibrium solution failure.

"Loss solution not achieved in 40 iterations"

Convergence of head loss iterations not achieved in limit of 40 iterations. Problem calculation continues with next blade row or inputed flow rate.

"Radial equilibrium and streamline radial adjustments not achieved in 10 iterations"

Iterations for blade element leaving streamline positions in subroutine RADEQC did not converge in limit of 10 iterations. Problem calculation continues.

"Radial equilibrium at continuity not achieved in 20 iterations"

Convergence not attained in continuity loop in limit of 20 iterations in subroutine RADEQC. Problem calculation continues.

Computer Program Description

The complete calculation procedure for off-design performance estimation is under the control of program MAIN. Several subprograms or subroutines (as shown in Flow Chart 1) are called upon by MAIN to accomplish certain specific tasks or calculations in the overall program execution. Flow Charts 2-5 give a detailed outline of MAIN. Additional description of MAIN is given below, along with the Fortran symbol definitions. The same procedure is repeated, involving Flow Charts 6-21, in the sections following for the subroutines.

In the Flow Charts, program segments have been identified by horizontal dashed lines for convenient reference. These segments are identified in the program listing (Appendix D) by inserted comments in the appropriate locations. In those instances where program calls of fitting routines FIT1D and FIT2D are made, the purpose of the call is indicated in the Flow Charts by the parameter returned from the subroutine, with those parameter(s) it is a function of in parentheses. Purposes of other subroutine calls are evident in the description and Flow Charts for the particular subroutine.

Program MAIN. — The subprogram BLOCK DATA has been included here as a part of the description and symbol definitions, and as a part of Flow Chart 2 for program MAIN. This subprogram initializes blade element standard reference tables for head loss, deviation angle and incidence reference angle analyses.

A direct responsibility of MAIN is the initialization of the radial equilibrium solution at all axial computing stations for head loss and streamline radii (at equal radial increments) according to the assigned number of streamlines for the solution through the pump. Also MAIN initializes the base streamline axial velocities at all axial computing stations according to the inputed base streamline value at the inlet. (It should be noted here that input card identifications (ID) are checked by the program, in MAIN or in subroutine INPUT during read operations. This checking has not been shown, however, in the Flow Charts. Also, checking of IWARN, and print out of warning messages in MAIN and the

Flow Chart 1.

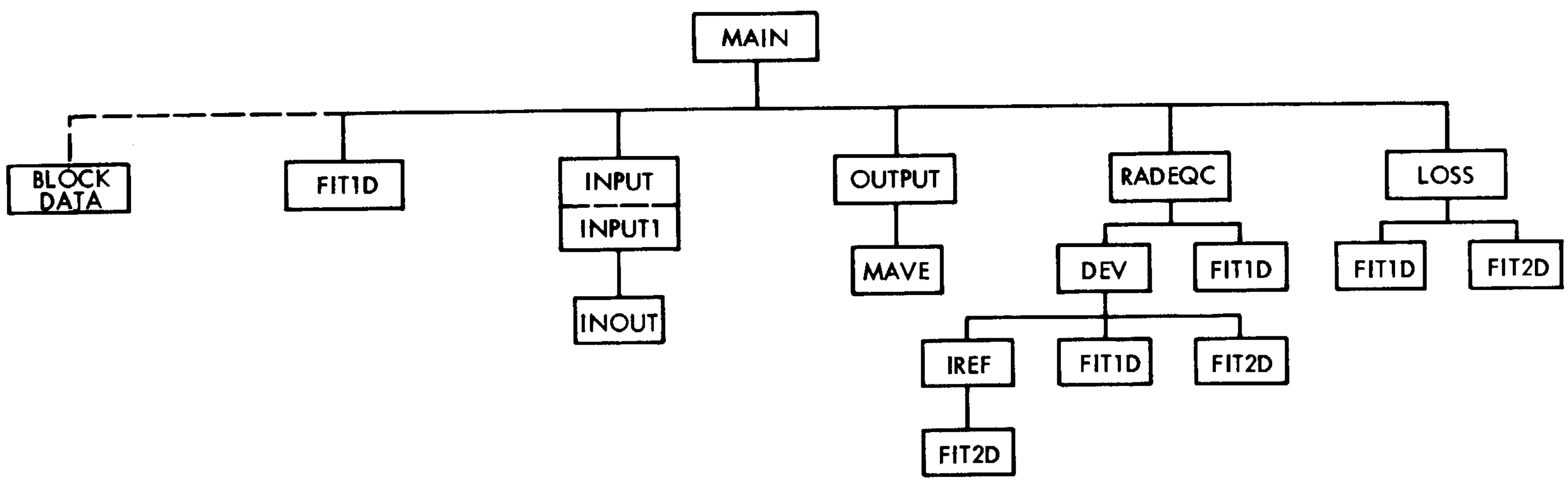

MAIN
BLOCK DATA
FIT1D
INPUT
INPUT1
INOUT
OUTPUT
MAVE
RADEQC
DEV
FIT1D
IREF
FIT2D
FIT1D
FIT2D
LOSS
FIT1D
FIT2D

subroutines noting extrapolation in fitting procedures (IWARN = 2) have not been included in the Flow Charts.)

Also program MAIN is responsible for identifying the Run No. for the pump operating point. Pump inlet flow conditions are set up for the solution according to the given pump operating point conditions and number of streamlines; flow rate, average flow coefficient, and stream-function values are computed by simple quadrature of the inlet station axial velocity profile. Effective flow coefficients per axial computing station for loss and deviation analyses are computed from given effective area factors and blade speeds.

Successive axial calculation stations through the pump are controlled by MAIN; loss and deviation angle reference tables are set up according to the input options per station. Flow conditions entering a blade row are set up prior to the head-loss and radial equilibrium solution for the flow leaving the blade row. Iterations (with a maximum of 40) for head losses are monitored by MAIN with actual loss calculations performed in subroutine LOSS. Convergence of head losses according to a given tolerance value, and revised head loss distribution per head loss iteration are determined by MAIN. Radial equilibrium, continuity and streamline radial adjustment calculations are performed in subroutine RADEQC interior to the head loss iteration loop.

In case of loss of radial equilibrium solution during any one head loss iteration, iterations are re-initialized and then repeated, but only up through the head loss iteration immediate to the unsuccessful one. The calculated results for the final repeated iterations (maximum of three, for four iterations and beyond) are outputed, even though a valid converged solution has not been obtained.

Program parts of MAIN in the accompanying Flow Charts 2-5 are identified as follows:

Flow Chart 2 Program segments "Input problem geometry and reference tables," "Initialize streamline radii, head loss and base streamline velocity" and "Input pump inlet conditions, axial station blockage factors and compute stream function distribution" of program MAIN.

Flow Chart 3 Program segments "Compute station annulus area and effective flow coefficient," and "Transfer loss and deviation angle reference tables per loss and deviation angle options" of program MAIN (continued).

Flow Chart 4 Program segments "Compute blade row inlet conditions," "Save blade row initial head loss," "Interpolate profile maximum thickness and incidence angle correction factor, compute radial equilibrium and continuity solution and determine head loss" of program MAIN (continued).

Flow Chart 5 Program segments "Check head-loss convergence and output computed results," "Revise head loss," "Output message head losses not converged, and output computed results," "Initialize head loss to zero," Reassign head loss and repeat iterations to loss of solution and "Output intermediate iteration results prior to loss of solution" of program MAIN (concluded).

Program MAIN variables:

FZ fraction of annulus passage height from hub to initial streamline radius

I axial station; blade row number, determined by inlet station to blade row

ID input card identification number

II card read reference number

IL ILIM-1

ILIM maximum value of I, the number of blade rows plus one

IO printer reference number

IRUN problem run identification number

IWARN fitting extrapolation warning indicator (- 1, no extrapolation; = 2, extrapolation of reference data table)

IZ index

J streamline number (= 1 at hub)

JBASE base streamline number from which radial equilibrium calculations proceed outward to casing, or inward to hub

JL JLIM-1

JLIM number of streamlines, casing streamline

K index

KHLOSS loss of radial equilibrium solution indicator (= 0, solution not lost; = 1, solution lost)

KK index delimiter

KLK head loss iteration loop index

K1LIM number of elements in array X1

L index

LINDEX head loss calculation option indicator (IEXLOS + 5)

LL index delimiter

LOK KLK

LOK1 LOK-3, or LOK-1, with loss of radial equilibrium solution occurring on head loss iteration number LOK

LOKLIM LOK-1, with loss of radial equilibrium solution occurring on head loss iteration number LOK

PHIB — average flow coefficient at inlet station

PHIRUN — flow rate calculation identification number

QRUN — computed flow rate

THL — tolerance value for convergence of head loss iteration

XJOE — damping factor in reassignment of head loss

XR — IRUN

Z — J

ZL — JL

Program MAIN arrays:

ALF1 — leading edge blade-element camberline tangent angle

ALPHZ — diagnostic alphameric word

ANGSTB — reference table of blade setting angle (YANGS)

AREA — axial calculation station annulus area

ARFAC — axial station effective flow area/ annulus area

BTAP1 — blade-element relative entering fluid flow angle

CS — product of blade-element wheel speed and fluid whirl velocity

DEL2B — reference table of deviation angle (DEL2), function of PHIBB, XPB

DEQBB — reference table of blade-element equivalent diffusion factor (DEQ)

EMB — reference table of deviation angle rule slope factor (EM), function of YANGSB

EXPBB — reference table of camber exponent (EXPB) in deviation angle rule, function of FIDIFB, PPHB

FIDIFB — reference table of blade-element incidence angle minus reference incidence angle (FIDIF)

FI10GB — reference table of blade-element zero-camber incidence angle (FI010G), function of YANGSB, SGMGBB

FNC1 — blade-element incidence angle

H — blade-element total head

HB — total head at inlet station, function of X1

H1 — blade-element total head at inlet station

HL0B — computed blade-element head loss

HLOSS — computed blade-element head loss in preceding head loss iteration

HLOSS1 — initial value of blade-element head loss

IEXDEV — option designation for deviation angle calculation

IEXLOS — option designation for head loss calculation

KLZ number of elements in reference table PHIBB, XDBB, or DEQBB

K2LM number of elements in reference table PHIBB

LLZ number of elements in reference table XPB or RPBB

L2LM number of elements in reference table XPB

OMEGBB reference table of head loss coefficient (OMEGB), function of PHIBB, XPB

PHIBB reference table of PHIEFC

PHIEFC blade row inlet average flow coefficient

PPFT1 streamline location at inlet to blade row as percent of passage height from outer casing

PPHB reference table of percent passage height from outer casing at blade row exit (PPFT2)

QB blade-element quadrature value of flow rate (from hub)

R streamline radius

RN blade row rotational speed

RPBB reference table of percent passage height from outer casing at blade row exit (PPFT2)

RPBB1 reference table of percent passage height from outer casing at blade row exit (PPFT2)

RPBB2 reference table of percent passage height from outer casing at blade row exit (PPFT2)

SGMGBB reference table of blade element solidity (SGMA)

SLP1GB reference table of linear camber coefficient (SLOP1G), function of YANGSB and SGMGBB

SLP2GB reference table of quadratic camber coefficient (SLOP2G), function of YANGSB and SGMGBB

THACBB reference table of wake momentum thickness/chord (THAC), function of DBB or DEQBB, and RPBB

THCBB1 reference table of wake momentum thickness/chord (THAC), function of YXDBB and RPBB1

THCBB2 reference table of wake momentum thickness/chord (THAC), function of YDEQBB and RPBB2

TMAXC blade-element maximum profile thickness/chord

USTAR blade tip speed or reference speed

U1 blade-element velocity at inlet to a blade row

VUB reference table of VU1, function of X1

VU1 blade-element fluid whirl velocity at inlet station

VZ blade-element fluid axial velocity

VZB	reference table of VZ1, function of X1
VZ1	blade-element fluid axial velocity at inlet station
X	reference table of R at inlet to blade row
XDBB	reference table of blade-element diffusion factor (XD)
XP	reference table of R at outlet of blade row
XPB	reference table of R at outlet of blade row
X1	reference table of R at inlet station
YANGSB	reference table of blade-element stagger angle (ANGST)
YDEL2B	reference table of DEL2B
YDEQB	DEQBB
YDEQBB	reference table of blade-element equivalent diffuser factor (DEQ)
YFKIB	reference table of blade-element incidence angle connection factor (FKI), function of YTMACB
YOMGBB	OMEGBB
YPHIBB	PHIBB
YRPB	RPBB
YTHACB	THACBB
YTMACB	reference table of blade-element maximum thickness/chord (TMAXC)
YTMAXC	TMAXC
YXDB	XDBB
YXDBB	reference table of blade-element diffusion factor (XD)
YXPB	XPB

Flow Chart 2.

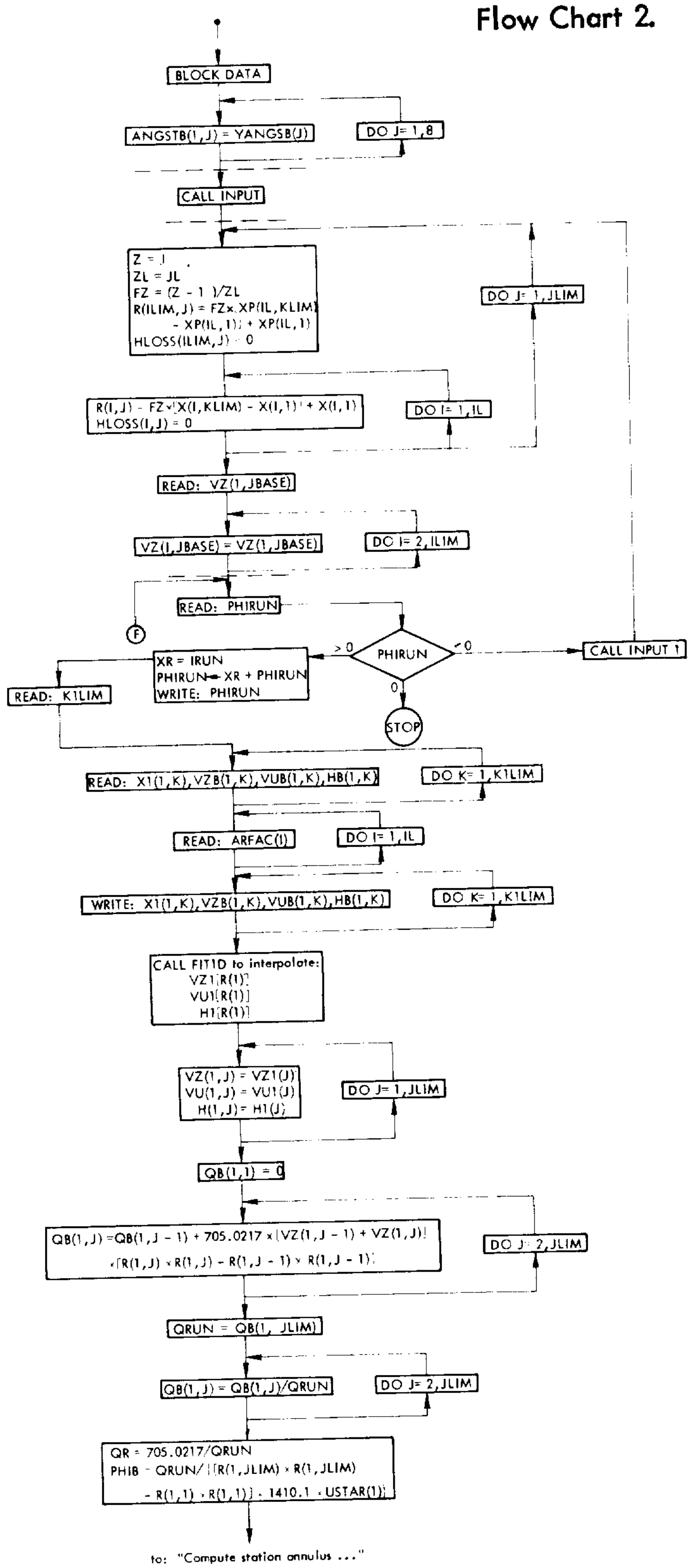
BLOCK DATA
ANGSTB(1,J) = YANGSB(J)
DO J= 1,8
CALL INPUT
Z = J
ZL = JL
FZ = (Z - 1)/ZL
R(ILIM,J) = FZ×XP(IL,KLIM)
- XP(IL,1) + XP(IL,1)
HLOSS(ILIM,J) = 0
DO J= 1,JLIM
R(I,J) = FZ×X(I,KLIM) - X(I,1) + X(I,1)
HLOSS(I,J) = 0
DO I= 1,IL
READ: VZ(1,JBASE)
VZ(I,JBASE) = VZ(1,JBASE)
DO I= 2,ILIM
READ: PHIRUN
F
PHIRUN
> 0
< 0
0
CALL INPUT 1
STOP
XR = IRUN
PHIRUN ← XR + PHIRUN
WRITE: PHIRUN
READ: K1LIM
READ: X1(1,K),VZB(1,K),VUB(1,K),HB(1,K)
DO K= 1,K1LIM
READ: ARFAC(I)
DO I= 1,IL
WRITE: X1(1,K),VZB(1,K),VUB(1,K),HB(1,K)
DO K= 1,K1LIM
CALL FIT1D to interpolate:
VZ1[R(1)]
VU1[R(1)]
H1[R(1)]
VZ(1,J) = VZ1(J)
VU(1,J) = VU1(J)
H(1,J)= H1(J)
DO J= 1,JLIM
QB(1,1) = 0
QB(1,J) =QB(1,J - 1) + 705.0217 × [VZ(1,J - 1) + VZ(1,J)]
×[R(1,J) × R(1,J) - R(1,J - 1) × R(1,J - 1)]
DO J= 2,JLIM
QRUN = QB(1, JLIM)
QB(1,J) = QB(1,J)/QRUN
DO J= 2,JLIM
QR = 705.0217/QRUN
PHIB = QRUN/ [R(1,JLIM) × R(1,JLIM)
- R(1,1) × R(1,1)] ∙ 1410.1 ∙ USTAR(1)
to: "Compute station annulus . . ."

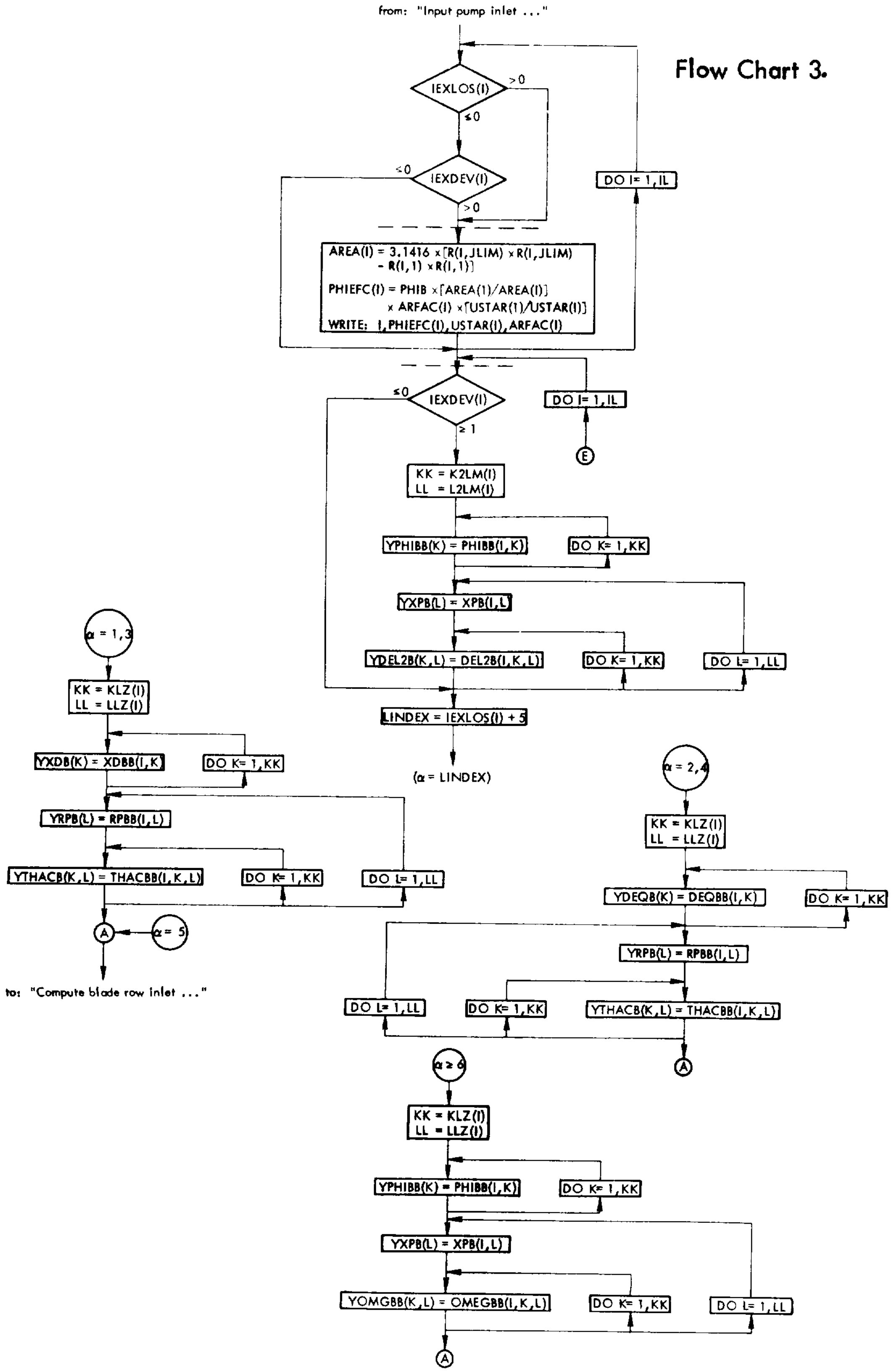
from: "Input pump inlet . . ."
Flow Chart 3.
IEXLOS(I)
> 0
≤ 0
IEXDEV(I)
≤ 0
> 0
DO I = 1, IL
AREA(I) = 3.1416 × [R(I, JLIM) × R(I, JLIM) − R(I, 1) × R(I, 1)]
PHIEFC(I) = PHIB × [AREA(1)/AREA(I)] × ARFAC(I) × [USTAR(1)/USTAR(I)]
WRITE: I, PHIEFC(I), USTAR(I), ARFAC(I)
IEXDEV(I)
≤ 0
≥ 1
DO I = 1, IL
E
KK = K2LM(I)
LL = L2LM(I)
YPHIBB(K) = PHIBB(I, K)
DO K = 1, KK
YXPB(L) = XPB(I, L)
YDEL2B(K, L) = DEL2B(I, K, L)
DO K = 1, KK
DO L = 1, LL
LINDEX = IEXLOS(I) + 5
(α = LINDEX)
α = 1, 3
KK = KLZ(I)
LL = LLZ(I)
YXDB(K) = XDBB(I, K)
DO K = 1, KK
YRPB(L) = RPBB(I, L)
YTHACB(K, L) = THACBB(I, K, L)
DO K = 1, KK
DO L = 1, LL
A
α = 5
to: "Compute blade row inlet . . ."
α = 2, 4
KK = KLZ(I)
LL = LLZ(I)
YDEQB(K) = DEQBB(I, K)
DO K = 1, KK
YRPB(L) = RPBB(I, L)
DO L = 1, LL
DO K = 1, KK
YTHACB(K, L) = THACBB(I, K, L)
A
α ≥ 6
KK = KLZ(I)
LL = LLZ(I)
YPHIBB(K) = PHIBB(I, K)
DO K = 1, KK
YXPB(L) = XPB(I, L)
YOMGBB(K, L) = OMEGBB(I, K, L)
DO K = 1, KK
DO L = 1, LL
A

Flow Chart 4.

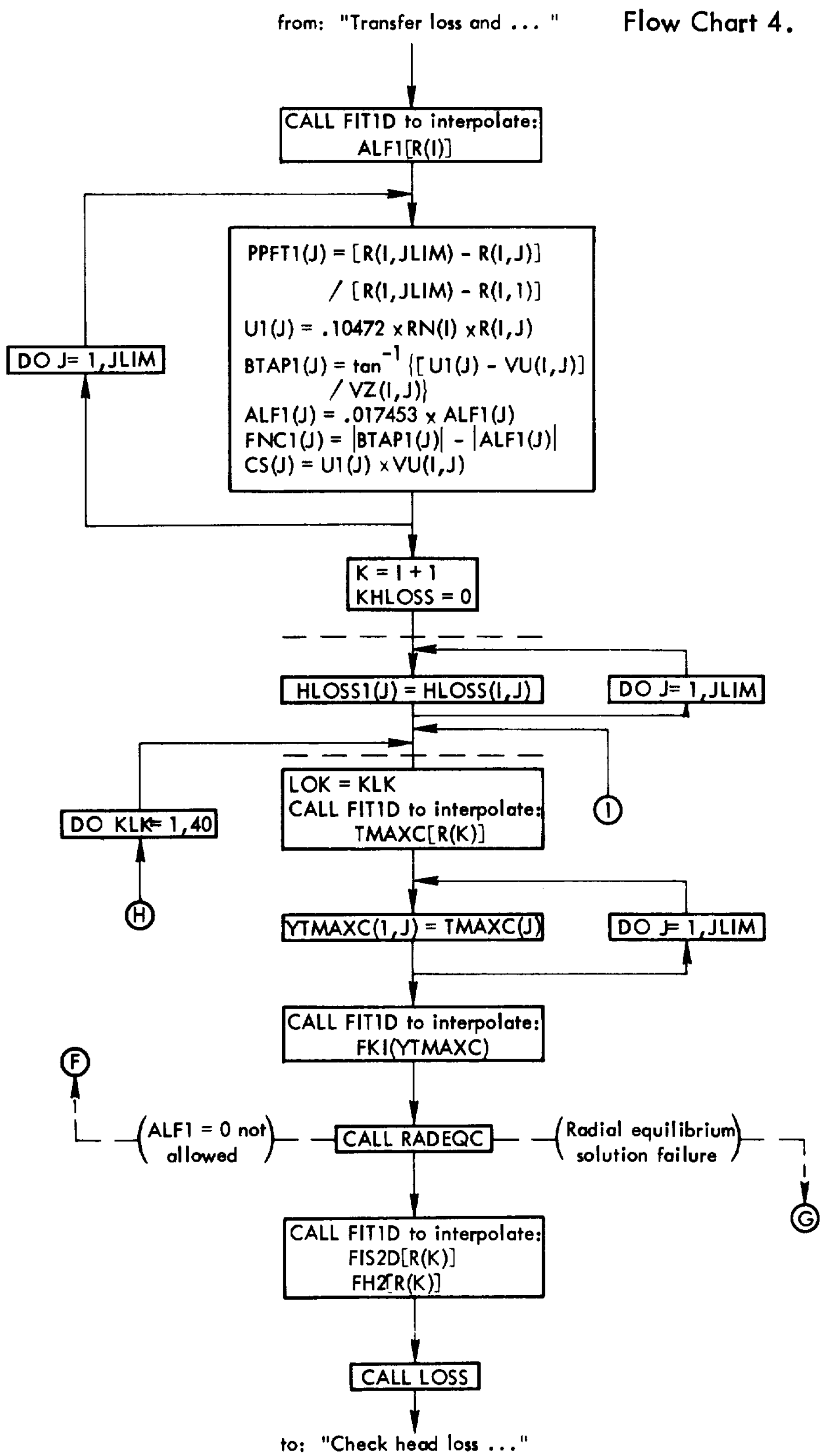
from: "Transfer loss and ... "
CALL FIT1D to interpolate: ALF1[R(I)]
PPFT1(J) = [R(I,JLIM) - R(I,J)] / [R(I,JLIM) - R(I,1)]
U1(J) = .10472 x RN(I) x R(I,J)
BTAP1(J) = tan⁻¹ {[U1(J) - VU(I,J)] / VZ(I,J)}
ALF1(J) = .017453 x ALF1(J)
FNC1(J) = |BTAP1(J)| - |ALF1(J)|
CS(J) = U1(J) x VU(I,J)
DO J= 1,JLIM
K = I + 1
KHLOSS = 0
HLOSS1(J) = HLOSS(I,J)
DO J= 1,JLIM
LOK = KLK
CALL FIT1D to interpolate: TMAXC[R(K)]
DO KLK= 1,40
I
H
YTMAXC(1,J) = TMAXC(J)
DO J= 1,JLIM
CALL FIT1D to interpolate: FKI(YTMAXC)
F
ALF1 = 0 not allowed
CALL RADEQC
Radial equilibrium solution failure
G
CALL FIT1D to interpolate: FIS2D[R(K)] FH2[R(K)]
CALL LOSS
to: "Check head loss ..."

Flow Chart 5.

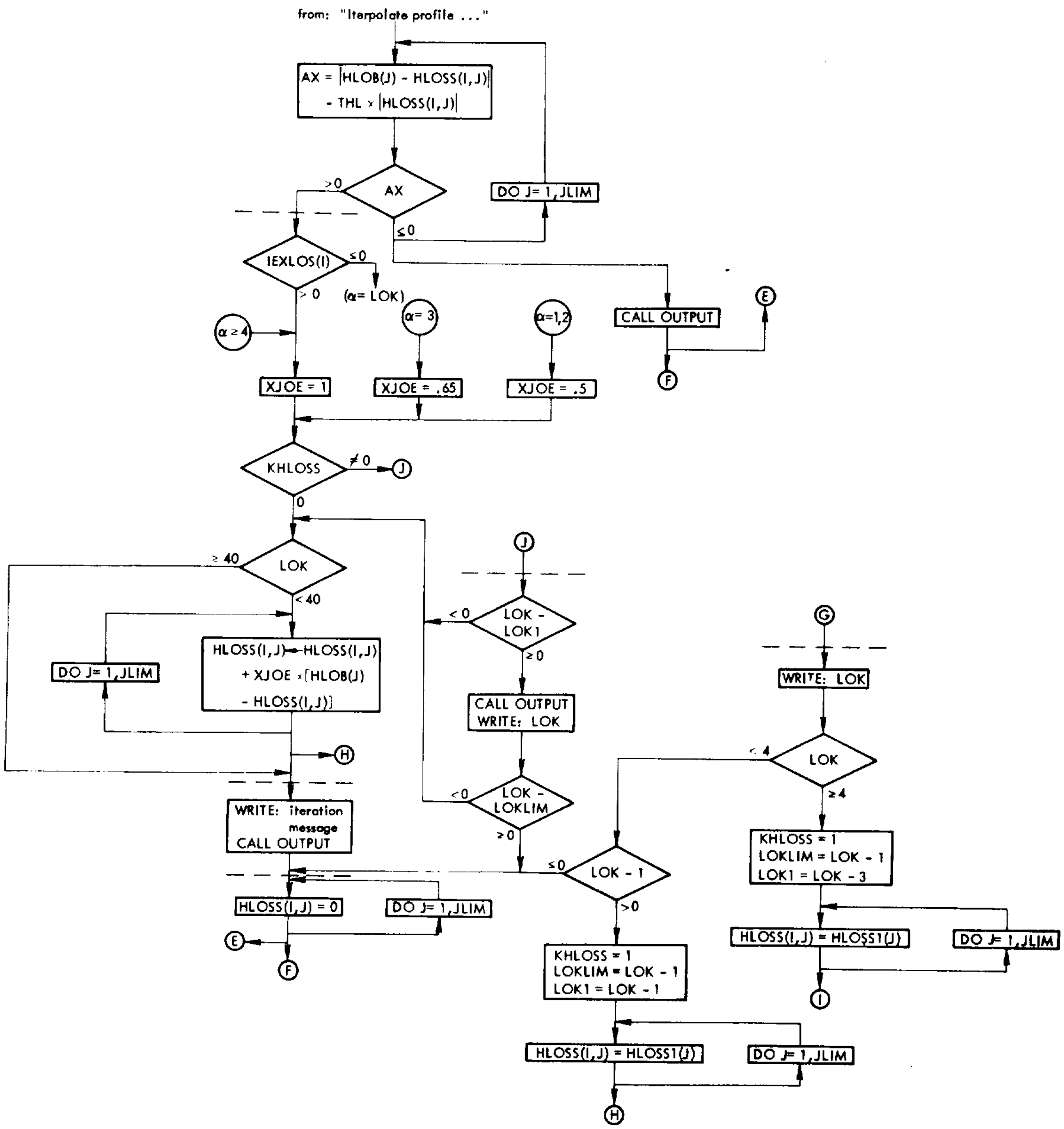

from: "Iterpolate profile ..."
AX = |HLOB(J) - HLOSS(I,J)| - THL × |HLOSS(I,J)|
AX
>0
≤0
DO J= 1,JLIM
IEXLOS(I)
≤0
> 0
(α= LOK)
α ≥ 4
α= 3
α=1,2
CALL OUTPUT
E
F
XJOE = 1
XJOE = .65
XJOE = .5
KHLOSS
≠ 0
J
0
LOK
≥ 40
< 40
HLOSS(I,J)←HLOSS(I,J) + XJOE × [HLOB(J) - HLOSS(I,J)]
DO J= 1,JLIM
H
WRITE: iteration message
CALL OUTPUT
HLOSS(I,J) = 0
DO J= 1,JLIM
E
F
J
LOK - LOK1
< 0
≥ 0
CALL OUTPUT
WRITE: LOK
LOK - LOKLIM
<0
≥ 0
LOK - 1
≤0
>0
KHLOSS = 1
LOKLIM = LOK - 1
LOK1 = LOK - 1
HLOSS(I,J) = HLOSS1(J)
DO J= 1,JLIM
H
G
WRITE: LOK
LOK
< 4
≥ 4
KHLOSS = 1
LOKLIM = LOK - 1
LOK1 = LOK - 3
HLOSS(I,J) = HLOSS1(J)
DO J= 1,JLIM
I

Subroutine DEV. — The purpose of DEV is to compute blade-element flow deviation angles according to the given option value IEXDEV per axial calculation station. In these options, deviation angle is computed based on an inputed correlation of deviation angle, flow coefficient, and radius, or on Carter's deviation angle rule, or on the camber exponent deviation angle rule, using blade-element reference incidence angle and percent passage height location. Details of these methods have been given in the section BLADE-ELEMENT LOSS AND DEVIATION ANGLE PREDICTION.

DEV variables:

IO	printer reference number
IWARN	fitting extrapolation warning indicator
J	streamline number (= 1 at hub)
JLIM	number of streamlines, casing streamline

DEV arrays:

ALF1	leading edge blade-element camberline tangent angle
ALF2	trailing edge blade-element camberline tangent angle
ALPHZ	diagnostic alphameric word
DEL2	blade-element flow deviation angle
EM	blade-element deviation angle rule slope factor
EXPB	blade-element camber exponent in deviation angle rule
FIDIF	FNC1 — STARI
FNC1	blade-element incidence angle
IEXDEV	option designation for deviation angle calculation
PPHT2	streamline location at outlet of a blade row as percent of passage height from outer casing
R	streamline radius
SGMA	blade-element solidity
STARI	blade-element reference incidence angle
THTA	blade-element camber angle

Flow Chart 6.

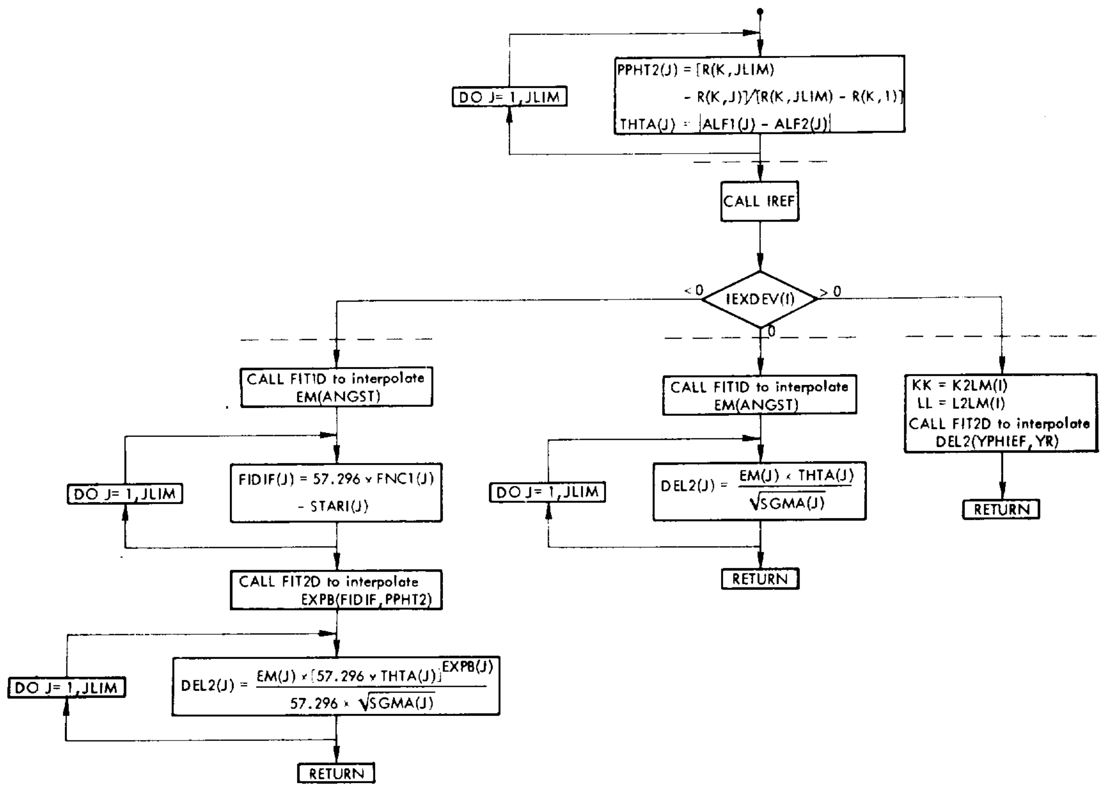
PPHT2(J) = [R(K, JLIM) - R(K,J)]/[R(K,JLIM) - R(K,1)]
THTA(J) = |ALF1(J) - ALF2(J)|
DO J= 1,JLIM
CALL IREF
IEXDEV(I)
< 0
> 0
0
CALL FIT1D to interpolate EM(ANGST)
FIDIF(J) = 57.296 × FNC1(J) - STARI(J)
DO J= 1,JLIM
CALL FIT2D to interpolate EXPB(FIDIF, PPHT2)
DEL2(J) = EM(J) × [57.296 × THTA(J)]^EXPB(J) / 57.296 × √SGMA(J)
DO J= 1,JLIM
RETURN
CALL FIT1D to interpolate EM(ANGST)
DEL2(J) = EM(J) × THTA(J) / √SGMA(J)
DO J= 1,JLIM
RETURN
KK = K2LM(I)
LL = L2LM(I)
CALL FIT2D to interpolate DEL2(YPHIEF, YR)
RETURN

Subroutine FIT1D. — Interpolations for Y(X) are made based on 3-point Lagrange polynomials. Reference data tables are YB, XB, where elements of XB are in monotone nondecreasing order, and KP is the number of point pairs (XB, YB). A total of JP interpolations Y(X) is made. The interpolate X is bracketed (if possible) in each interpolation by three neighboring elements of XB. IWARN = 2 indicates extrapolation of XB array.

FIT1D variables:

I	index
IWARN	extrapolation indicator
J	index
JP	number of fittings made
K	index
KP	number of point pairs (XB, YB)
L	M
M	index
XO	XB value bracketing X
X1	XB value bracketing X
X2	XB value bracketing X

FIT1D arrays:

X	interpolate
XB	reference table of independent variable
Y	interpolated value
YB	reference table of dependent variable

Flow Chart 7.

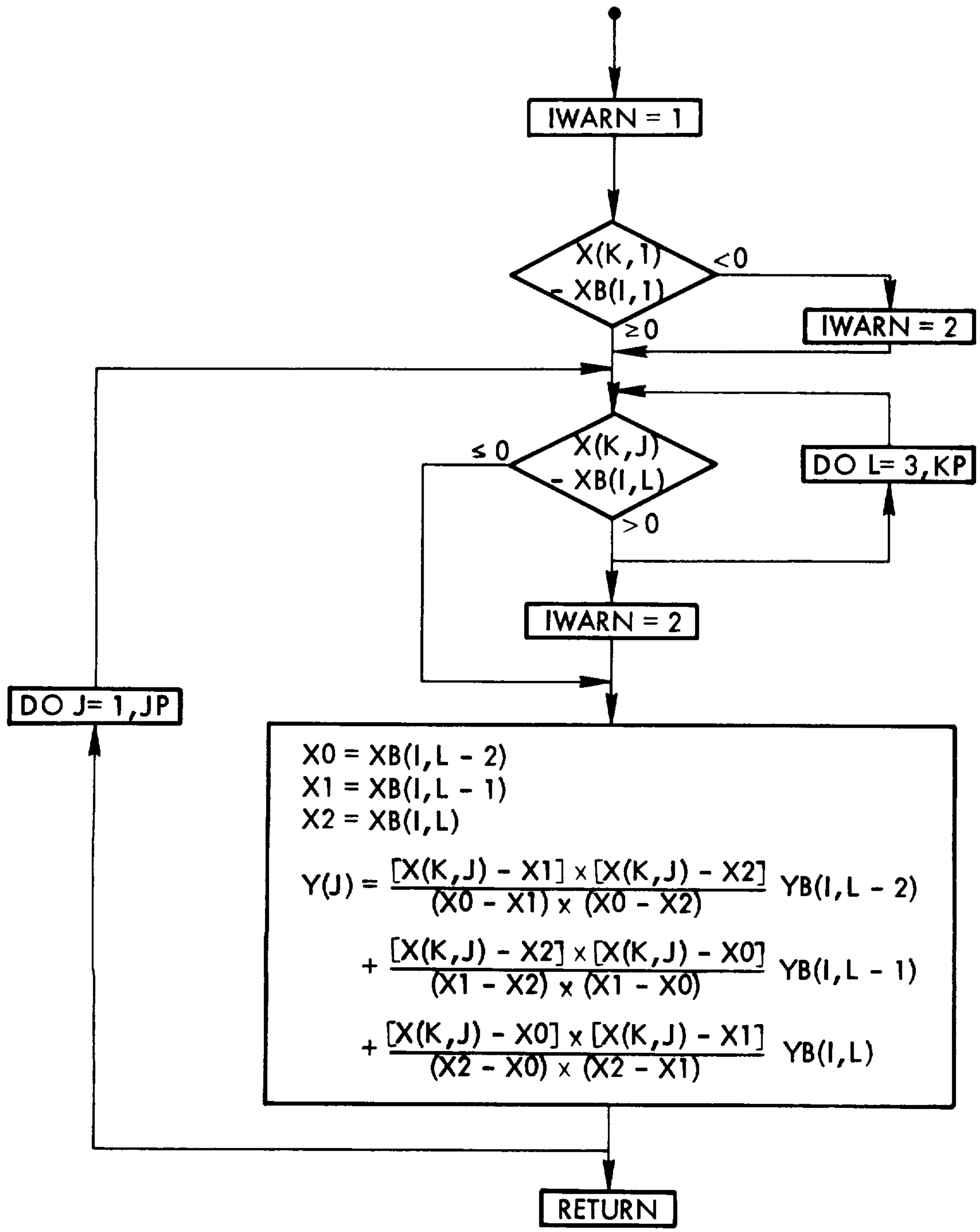

IWARN = 1
X(K,1) - XB(I,1)
<0
≥0
IWARN = 2
≤ 0
X(K,J) - XB(I,L)
> 0
DO L= 3,KP
IWARN = 2
DO J= 1,JP
X0 = XB(I,L - 2)
X1 = XB(I,L - 1)
X2 = XB(I,L)
Y(J) = [X(K,J) - X1] x [X(K,J) - X2] / (X0 - X1) x (X0 - X2) YB(I,L - 2)
+ [X(K,J) - X2] x [X(K,J) - X0] / (X1 - X2) x (X1 - X0) YB(I,L - 1)
+ [X(K,J) - X0] x [X(K,J) - X1] / (X2 - X0) x (X2 - X1) YB(I,L)
RETURN

Subroutine FIT2D. — Interpolations for Y(X, Z) are made based on three-point Lagrange polynomials. Reference data tables are XB, YB, ZB, where elements of XB, ZB are in monotone nondecreasing order. IP is the number of elements in XB, JP the number in ZB. A total of JL interpolations Y(X, Z) is made. The interpolates X, Z are bracketed (if possible) in each interpolation by three neighboring elements of XB and ZB, respectively. IWARN = 2 indicates extrapolation of XB or ZB arrays.

FIT2D variables:

I	M
IQ	dimension size of YB
IWARN	fitting extrapolation warning indicator
J	M
JQ	dimension size of YB
K	index
L	I + K
M	index
N	index
XO	XB or ZB value bracketing X or Z
X1	XB or ZB value bracketing X or Z
X2	XB or ZB value bracketing X or Z
YO	YB element at bracket point (XB, ZB)
Y1	YB element at bracket point (XB, ZB)
Y2	YB element at bracket point (XB, ZB)

FIT2D arrays:

X	interpolate
XB	reference table independent variable
Y	interpolated value
YB	reference table of dependent variable
YST	intermediate interpolated Y value
Z	interpolated value
ZB	reference table of independent

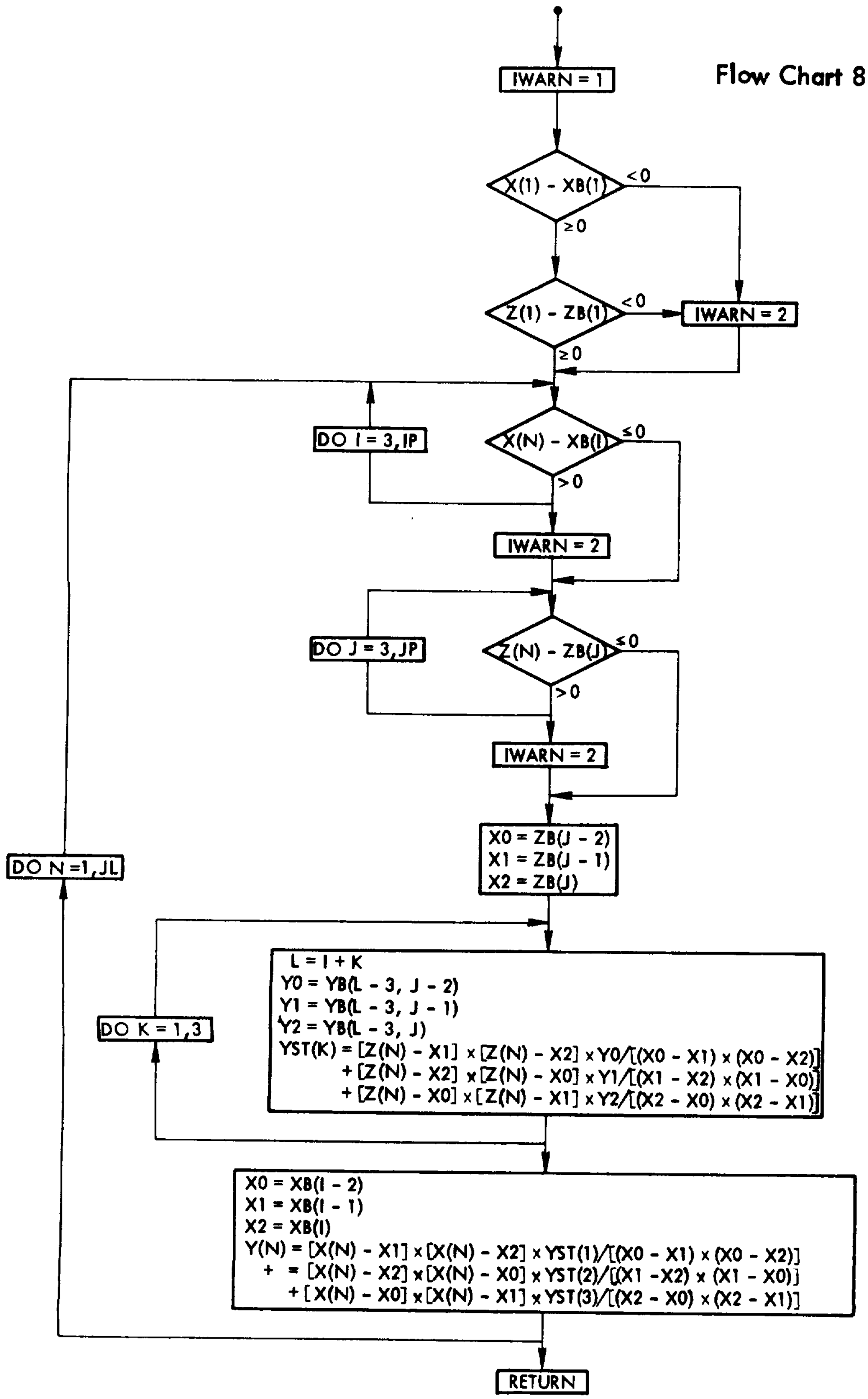
IWARN = 1
X(1) - XB(1)
< 0
≥ 0
Z(1) - ZB(1)
< 0
IWARN = 2
≥ 0
DO I = 3,IP
X(N) - XB(I)
≤ 0
> 0
IWARN = 2
DO J = 3,JP
Z(N) - ZB(J)
≤ 0
> 0
IWARN = 2
DO N =1,JL
X0 = ZB(J - 2)
X1 = ZB(J - 1)
X2 = ZB(J)
L = I + K
Y0 = YB(L - 3, J - 2)
Y1 = YB(L - 3, J - 1)
Y2 = YB(L - 3, J)
YST(K) = [Z(N) - X1] x [Z(N) - X2] x Y0/[(X0 - X1) x (X0 - X2)]
+ [Z(N) - X2] x [Z(N) - X0] x Y1/[(X1 - X2) x (X1 - X0)]
+ [Z(N) - X0] x [Z(N) - X1] x Y2/[(X2 - X0) x (X2 - X1)]
DO K = 1,3
X0 = XB(I - 2)
X1 = XB(I - 1)
X2 = XB(I)
Y(N) = [X(N) - X1] x [X(N) - X2] x YST(1)/[(X0 - X1) x (X0 - X2)]
+ = [X(N) - X2] x [X(N) - X0] x YST(2)/[(X1 -X2) x (X1 - X0)]
+ [X(N) - X0] x [X(N) - X1] x YST(3)/[(X2 - X0) x (X2 - X1)]
RETURN
Flow Chart 8.

Subroutine INOUT. — In this subroutine, the input data to the program for the particular problem are printed out for reference. Problem run number is identified, followed by output of reference incidence angle tables supplied by the BLOCK DATA program (see description of program MAIN). On a blade row by blade row basis, rotational speed and reference geometry tables, and reference deviation angle and loss tables (per designated options) are printed out.

Program parts of INOUT in the accompanying Flow Charts 9 and 10 are identified as follows:

Flow Chart 9	Program segments "Output reference incidence angle tables," "Output blade row RPM, reference radius and loss and deviation angle options," "Output reference blade row geometry tables," "Output reference deviation angle tables" of subroutine INOUT.
Flow Chart 10	Program segment "Output reference blade wake momentum thickness/chord or loss coefficient tables of subroutine INOUT (concluded).

INOUT variables:

I	axial station; blade row number, determined by inlet station to blade row
IL	ILIM-1
ILIM	maximum value of I, the number of blade rows plus one
IOUT	printer reference number
IRUN	problem run identification number
J	streamline number (= 1 at hub)
JBASE	base streamline number
JLIM	number of streamlines, casing streamlines
K	index
KK	index delimiter
KLIM	number of elements in blade row geometry reference tables
K1	index initial value
L	index
LINDEX	IEXLOS + 5
LL	index delimiter
LL1	index delimiter
L1	index

INOUT arrays:

ALFB reference table of leading edge blade-element camber-line tangent angle (ALF1), function of X

ALFPB reference table of trailing edge blade-element camber-line tangent angle (ALF2), function of XP

DEL2B reference table of blade-element flow deviation angle (DEL2), function of PHIBB, XPB

DEQB reference table of blade-element equivalent diffusion factor (DEQ)

DEQBB reference table of blade-element equivalent diffusion factor (DEQ)

EMB reference table of deviation angle rule slope factor (EM), function of YANGSB

EXPBB reference table of camber exponent (EXPB) in deviation angle rule, function of FIDIFB, PPHB

FHB reference table of blade-element wake form factor (FH2), function of XP

FIDIFB reference table of blade-element incidence angle minus reference incidence angle (FIDIF)

FI1OGB reference table of blade-element zero-camber incidence angle (FI010G), function of YANGSB, SGMGBB

FI2DB reference table of blade-element reference incidence minus cascade rule incidence angle (FIS2D), function of XP

FKSHAB reference table of shape correction factor (FKSHA), function of XP

IEXDEV option designation for deviation angle calculation

IEXLOS option designation for head loss calculation

K2LM number of elements in reference table PHIBB

KLZ number of elements in reference table XDBB, YXDBB, DEQBB, YDEQBB, or PHIBB

LLZ number of elements in reference table RPBB or XPB

OMEGBB reference table of head loss coefficient (OMEGB), function of PHIBB, XPB

PHIBB reference table of blade row inlet average flow coefficient (PHIEFC)

PPHB reference table of percent passage height from outer casing at blade row exit (PPFT2)

RN blade row rotational speed

RPBB reference table of percent passage height from outer casing at blade row exit (PPFT2)

RSTAR	blade row reference radius
SGMAB	reference table of blade-element solidity (SGMA), function of XP
SGMGBB	reference table of blade-element solidity (SGMA)
SLP1GB	reference table of linear camber coefficient (SLOP1G) function of YANGSB, SGMGBB
SLP2GB	reference table of quadratic camber coefficient (SLOP2G), function of YANGSB, SGMGBB
THACB	reference table of blade-element wake momentum thickness/chord (THAC), function of DEQB
THACBB	reference table of blade-element wake momentum thickness/chord (THAC), function of RPBB, and DEQBB or XDBB
TMXCB	reference table of blade-element maximum profile thickness/chord (TMAXC), function of XP
X	reference table of streamline radius (R) at inlet to blade row
XDBB	reference table of diffusion factor (XD)
XP	reference table of streamline radius (R) at outlet of blade row
XPB	reference table of streamline radius (R) at outlet of blade row
YANGSB	reference table of blade-element stagger angle (ANGST)
YFKIB	reference table of incidence angle correction factor (FKI), function of YTMACB
YTMACB	reference table of blade-element maximum thickness/chord (TMAXC)

Flow Chart 9.

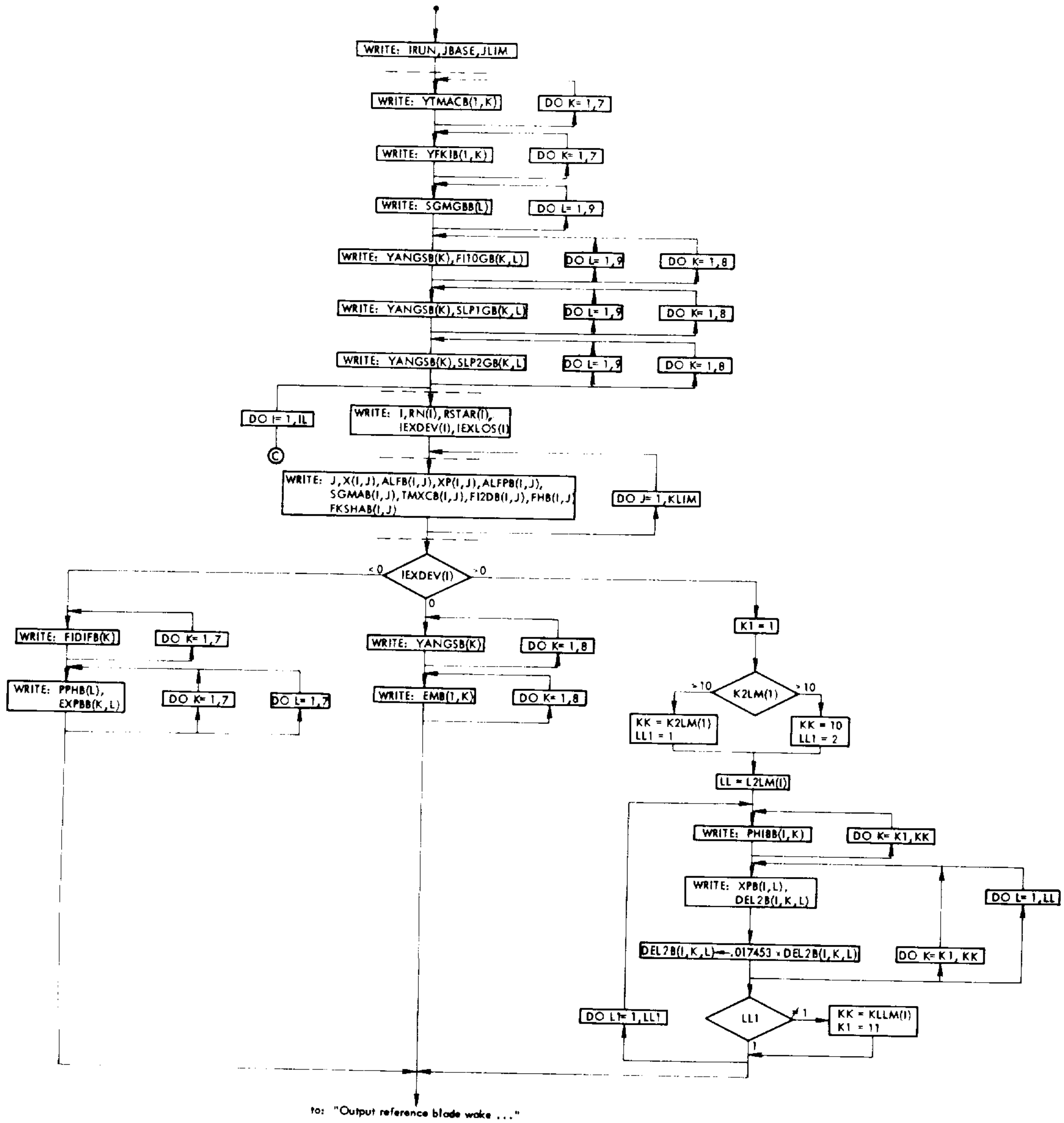

WRITE: IRUN, JBASE, JLIM
WRITE: YTMACB(1,K)
DO K= 1,7
WRITE: YFKIB(1,K)
DO K= 1,7
WRITE: SGMGBB(L)
DO L= 1,9
WRITE: YANGSB(K), FI10GB(K,L)
DO L= 1,9
DO K= 1,8
WRITE: YANGSB(K), SLP1GB(K,L)
DO L= 1,9
DO K= 1,8
WRITE: YANGSB(K), SLP2GB(K,L)
DO L= 1,9
DO K= 1,8
DO I= 1,IL
WRITE: I,RN(I),RSTAR(I), IEXDEV(I),IEXLOS(I)
WRITE: J,X(I,J),ALFB(I,J),XP(I,J),ALFPB(I,J), SGMAB(I,J),TMXCB(I,J),FI2DB(I,J),FHB(I,J) FKSHAB(I,J)
DO J= 1,KLIM
IEXDEV(I)
<0
>0
0
WRITE: FIDIFB(K)
DO K= 1,7
WRITE: PPHB(L), EXPBB(K,L)
DO K= 1,7
DO L= 1,7
WRITE: YANGSB(K)
DO K= 1,8
WRITE: EMB(1,K)
DO K= 1,8
K1 = 1
K2LM(1)
≤10
>10
KK = K2LM(1)
LL1 = 1
KK = 10
LL1 = 2
LL = L2LM(I)
WRITE: PHIBB(I,K)
DO K= K1,KK
WRITE: XPB(I,L), DEL2B(I,K,L)
DO L= 1,LL
DEL2B(I,K,L)←.017453 × DEL2B(I,K,L)
DO K= K1, KK
DO L1= 1,LL1
LL1
≠1
1
KK = KLLM(I)
K1 = 11
to: "Output reference blade wake ..."

Flow Chart 10.

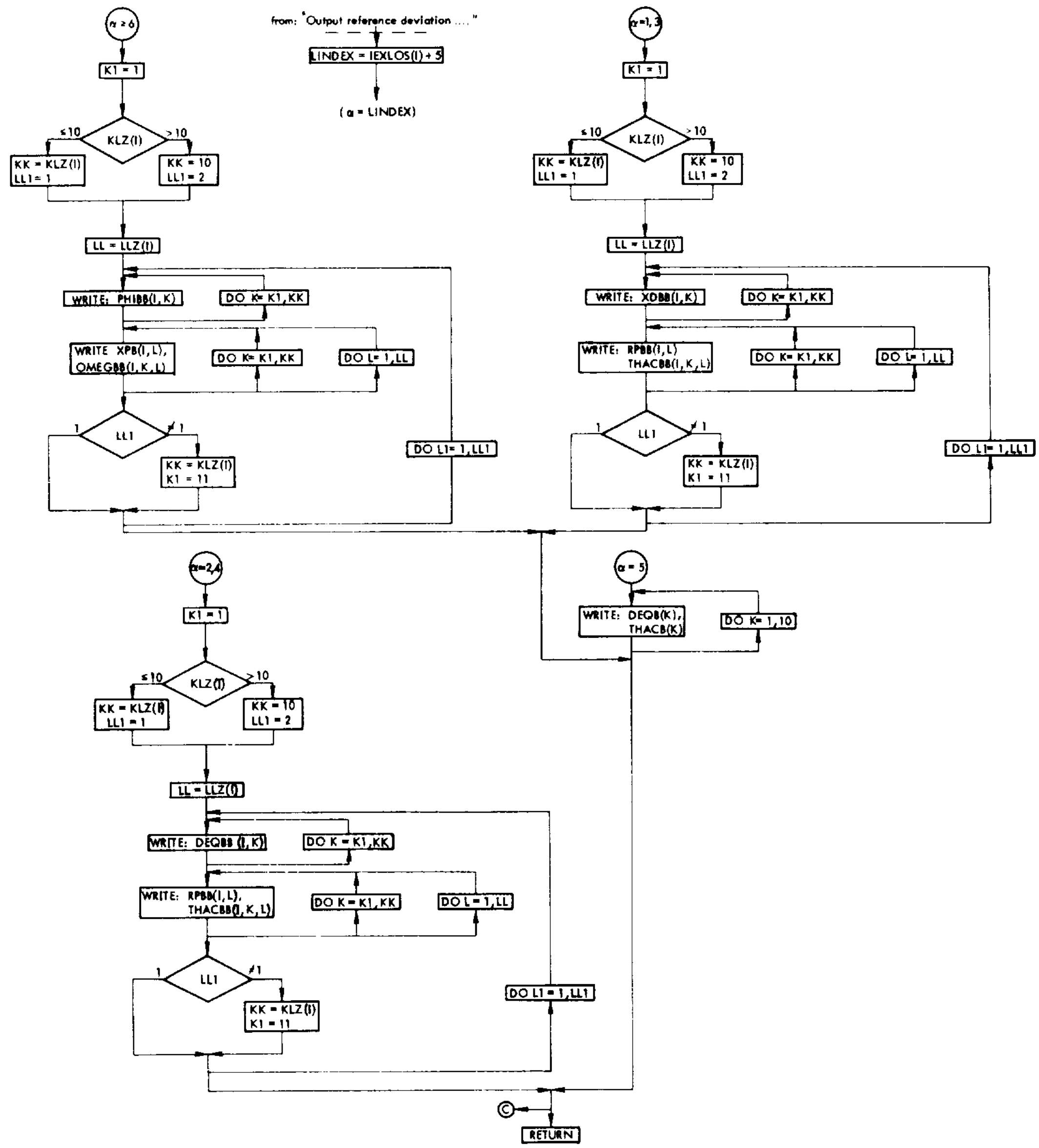

Subroutine INPUT. — Input data are read in on a blade row by blade row basis from cards, or are transferred as necessary from arrays initialized in the BLOCK DATA subprogram. Input data comprise limit parameters and computing run identification, loss and deviation reference tables, blade row geometry reference tables and balde row rotational speed (flow rate, inlet conditions, and area blockage factors are read in by MAIN per flow rate calculation). Multiple rotational speed calculations are handled by ENTRY INPUT1, in which only rotational speeds (per blade row) are read in. Also, reference blade speeds are computed in INPUT, based on blade row rotational speed and reference radius. Subroutine INOUT is called to output the data load for each assigned rotation speed.

Program parts of INPUT in the accompanying Flow Charts 11 and 12 are identified as follows:

Flow Chart 11	Program segments "Input limit values and run identification," "Input loss and deviation option values," "Input reference loss and deviation tables" of subroutine INPUT.
Flow Chart 12	Program segments "Input reference wake momentum/chord (THACBB) tables," "Input reference blade row geometry tables," "Input blade row RPM and compute reference blade speed," "Output problem data load" of subroutine INPUT (concluded).

INPUT variables:

I	axial station; blade row number, determined by inlet station to blade row
ID	input card identification number
IIN	card reader reference number
IL	ILIM-1
ILIM	maximum value of I, the number of blade rows plus one
IOUT	printer reference number
IRUN	problem run identification number
IZ	index
J	I, K, L
JBASE	base streamline number from which radial equilibrium calculations proceed outward to casing, or inward to hub
JL	JLIM-1
JLIM	number of streamlines, casing streamline
K	index
KK	index delimiter
KLIM	index delimiter, number of elements in input blade element geometry arrays
K2LIM	KLZ

L index

LINDEX head loss calculations option indicator (IEXLOS + 5)

LL index delimiter

L2LIM LLZ

RRN RN

THL tolerance value for convergence of head loss iteration

INPUT arrays:

ALFB reference table of leading edge blade-element camberline tangent angle (ALF1), function of X

ALFPB reference table of trailing edge blade-element camberline tangent angle (ALF2), function of XP

ALFPZ diagnostic alphameric word

DEL2B reference table or blade-element flow deviation angle (DEL2), function of PHIBB, XPB

DEQBB reference table of blade-element equivalent diffusion factor (DEQ)

FHB reference table of blade-element wake form factor (FH2), function of XP

FI2DB reference table of blade-element reference incidence minus cascade rule incidence angle (FIS2D), function of XP

FKSHAB reference table of shape correction factor (FKSHA), function of XP

IEXDEV option designation for deviation angle calculation

IEXLOS option designation for head loss calculation

KLZ number of elements in reference table XDBB, DEQBB, or PHIBB

K2LM KLZ

LLZ number of elements in reference table RPBB or XPB

L2LM LLZ

OMEGBB reference table of head loss coefficient (OMEGB), function of PHIBB, XPB

PHIBB reference table of blade row inlet average flow coefficient (PHIEFC)

RN blade row rotational speed

RPBB reference table of percent passage height from outer casing at blade row exit (PPFT2)

RPBB1 reference table of percent passage height from outer casing (PPFT2)

RPBB2 reference table of percent passage height from outer casing (PPFT2)

RSTAR blade row reference radius

SGMAB reference table of blade-element solidity (SGMA), function of XP

THACBB reference table of blade-element wake momentum thickness/chord (THAC), function of RPBB, and DEQBB or XDBB

THCBB1 reference table of wake momentum thickness/chord (THAC), function of YXDBB and RPBB1

THCBB2 reference table of wake momentum thickness/chord (THAC), function of YDEQBB and RPBB2

TMXCB reference table of blade-element maximum profile thickness/chord (TMAXC), function of XP

USTAR blade tip speed or reference speed

X reference table of streamline radius (R) at inlet to blade row

XDBB reference table of diffusion factor (XD)

XP reference table of streamline radius (R) at outlet of blade row

XPB reference table of streamline radius (R) at outlet of blade row

YDEQBB reference table of blade-element equivalent diffusion factor (DEQ)

YXDBB reference table of blade-element diffusion factor (XD)

Flow Chart 11.

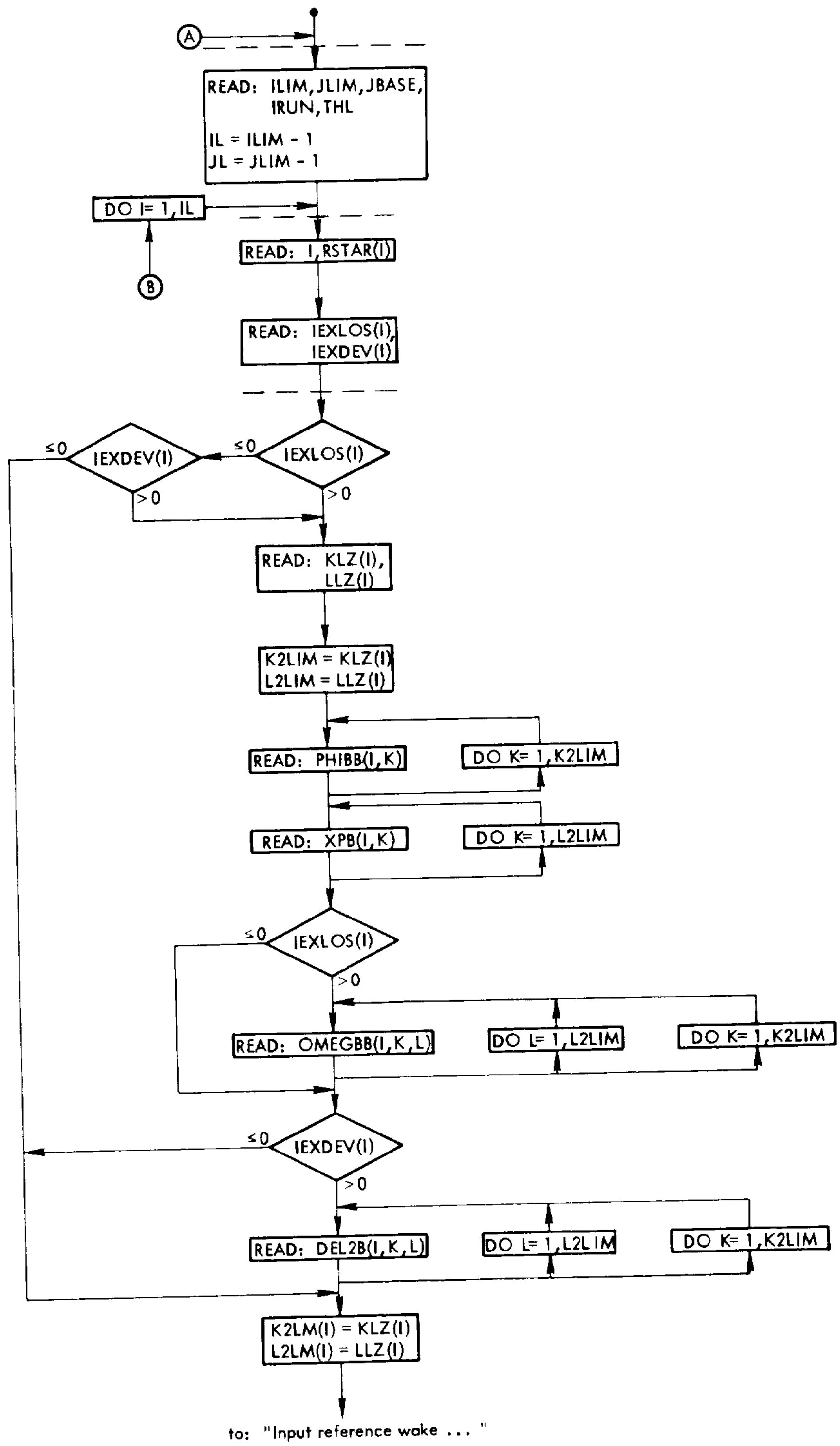

Flow Chart 12.

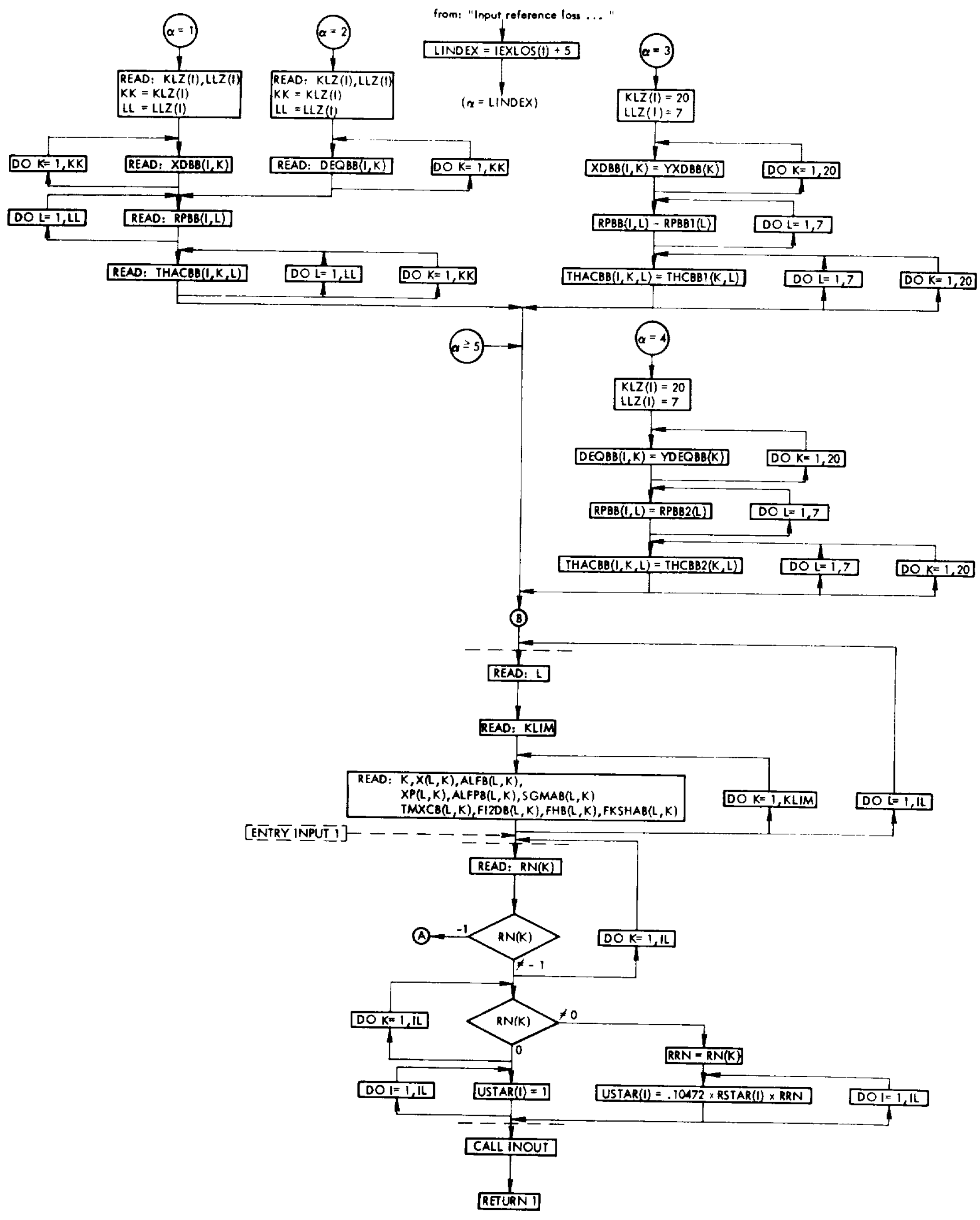

Subroutine IREF. - Blade-element reference incidence angles are computed from camber angle, stagger angle, maximum thickness/chord, solidity, and thickness distribution correction factor. Interpolations for factors FI010G, SLOP1G and SLOP2G from reference tables as functions of YANGS and SGMA are required. Extrapolations of the data for relative inlet angle (BTP1) above 75° are noted by the subroutine.

IREF variables:

BTP1	blade-element relative entering fluid flow angle
IZ	index
IO	printer reference number
J	streamline number (= 1 at hub)
JLIM	number of streamlines, casing streamline

IREF arrays:

ALF1	leading edge blade-element camberline tangent angle
ALPHZ	diagnostic alphameric word
ANGST	blade-element stagger angle
FI010G	blade-element zero-camber incidence angle
FKI	blade-element incidence angle correction factor for maximum thickness/chord and thickness distribution
FKSHA	blade-element shape correction factor
SLOP1G	linear camber coefficient
SLOP2G	quadratic camber coefficient
STARI	blade-element reference incidence angle
THTA	blade-element camber angle
YANGS	ANGST
YANGS1	YANGS

Flow Chart 13.

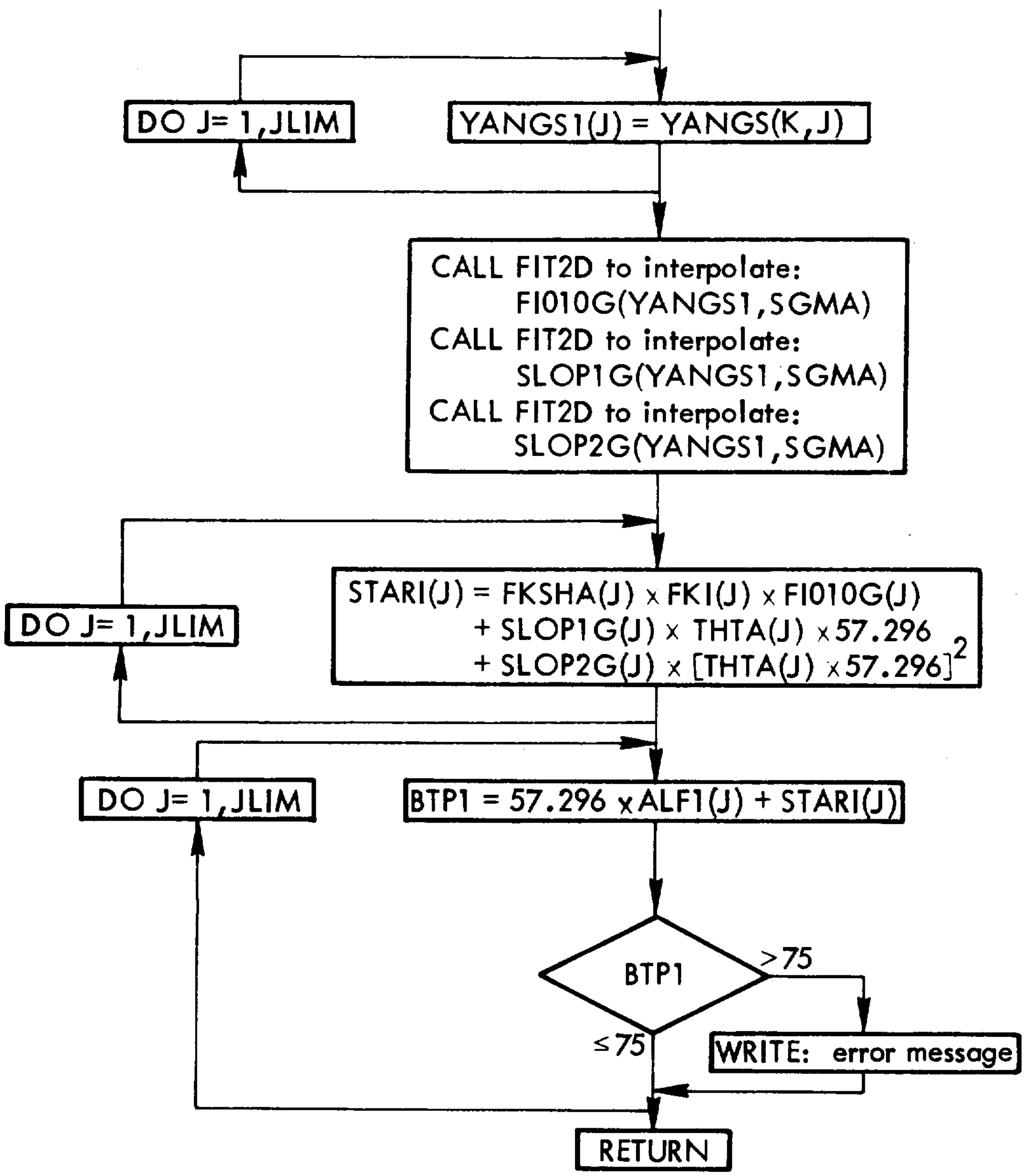

Subroutine LOSS. — Blade-element head losses are computed for all streamlines, hub to casing, in rotors or stationary blade rows. Head losses are computed from reference tables according to specified loss calculation option. These tables consist of (1) blade-element wake momentum thickness/chord and correlated diffusion factor (or both diffusion factor and blade-element radial position), or (2) loss coefficient and correlated effective flow coefficient and radial position.

LOSS variables:

C0117	coefficient in equivalent diffusion factor calculation
C1	ratio of blade-element entering and leaving streamline radii
C2	reciprocal of blade-element relative entering fluid velocity
C3	parameter in blade-element head loss calculation
C4	parameter in blade-element head loss calculation
C61	coefficient in blade-element equivalent diffusion factor calculation, rotor or stationary blade row
FIIPS	absolute value of difference between blade-element incidence angle and reference incidence angle
I	axial station; blade row number, determined by inlet station to blade row
IO	printer reference number
IWARN	fitting extrapolation warning indicator
IZ	index
J	streamline number (= 1 at hub)
JLIM	number of streamlines, casing streamline
KK	KLZ
KSI	coefficient in blade-element diffusion factor calculation, rotor or stationary blade row
LL	LLZ
LINDEX	IEXLOS + 5

LOSS arrays:

ALPHZ	diagnostic alphameric word
BTAP1	blade-element relative entering bluid flow angle
BTAP2	blade-element relative leaving fluid flow angle
DEQ	blade-element equivalent diffusion factor
DEQB	reference table of DEQ
DEQDD	DEQB
FH2	blade-element wake form factor
FNC1	blade-element incidence angle

HLOB	computed blade-element head loss
IEXLOS	option designation for head loss calculation
KLZ	number of elements in reference table of blade element diffusion factor (YXDB or YDEQB), or blade row inlet flow coefficient (YPHIBB)
LLZ	number of elements in reference table of percent passage height from outer casing at blade row exit (YRPB), or streamline radius at outlet of blade row (YXPB)
OMEGB	blade-element head loss coefficient
PPFT2	percent passage height from outer casing at blade row exit
R	streamline radius
RN	blade row rotational speed
SGMA	blade-element solidity
STARI	blade-element reference incidence angle
THAC	blade-element wake momentum thickness/chord
THACB	reference table of THAC, function of DEQB
THACDD	THACB
U1	blade-element velocity at inlet to blade row
VU	blade-element exit fluid whirl velocity
VZ	blade-element fluid axial velocity
XD	blade-element diffusion factor
XDD	DEQ
XVP1	blade-element relative entering fluid velocity
XVP2	blade-element relative leaving fluid velocity

Flow Chart 14.

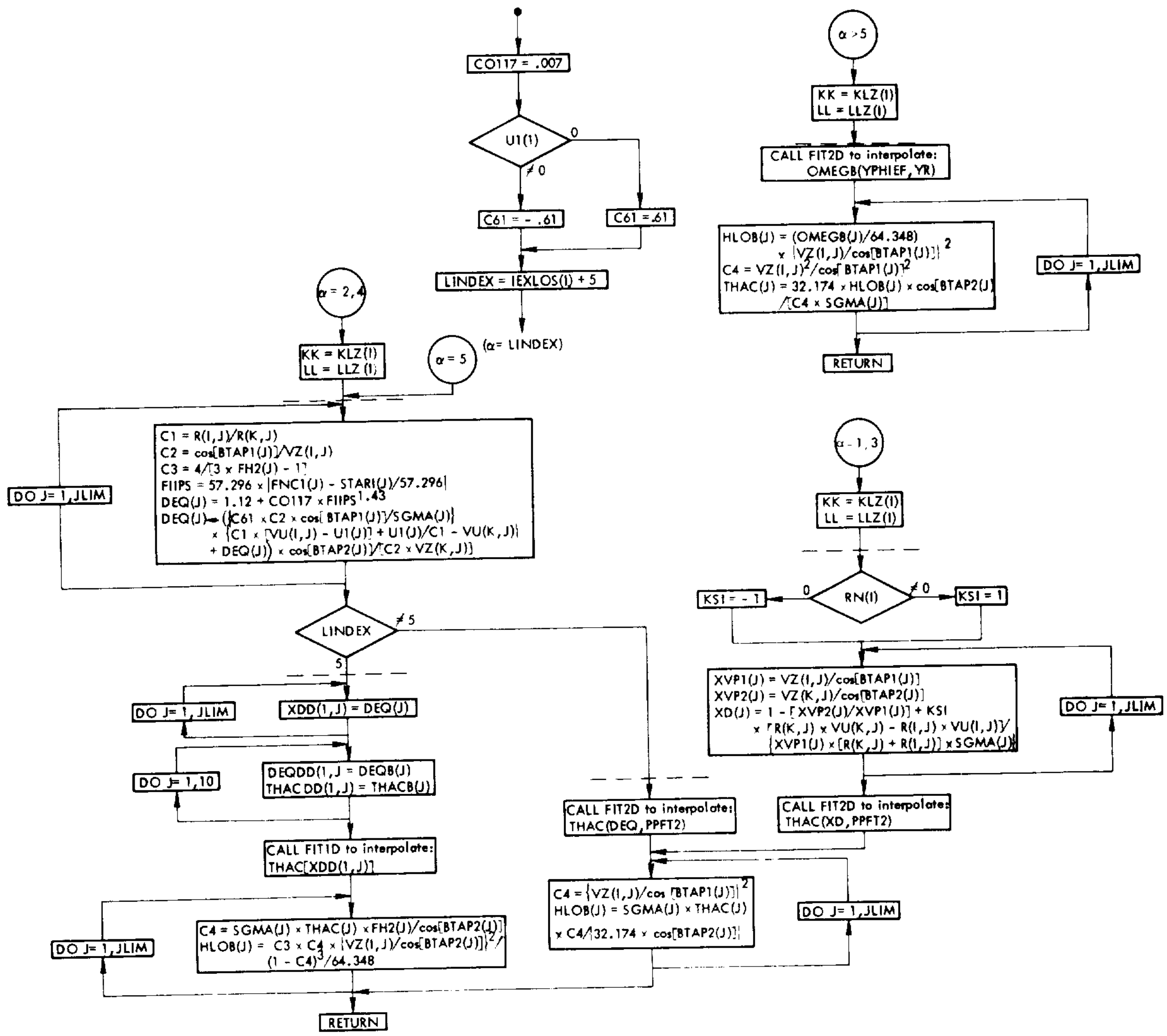

Subroutine MAVE. — Mass-averaged performance results are computed and outputed for a rotating blade row, or for a stage consisting of a rotating and a stationary blade row. Mass-averaged results are based on quadratures of blade-element inlet conditions and determined radial equilibrium outlet conditions.

MAVE variables:

AFLCO	average flow coefficient at blade row inlet
AFLCO1	average flow coefficient at blade row exit
DENOM	quadrature function of R times VZ across annulus
I	axial station; blade row number, determined by inlet station to blade row
IL	maximum value of I (ILIM) minus one
IO	printer reference number
J	streamline number (= 1 at hub)
JL	JLIM-1
JLIM	number of streamlines, casing streamline
QRUN	computed flow rate
REFFI	rotor hydraulic efficiency quadrature function
RHRCO	rotor total head rise coefficient
RHRI	rotor total head rise quadrature function
RMAE	rotor mass-averaged hydraulic efficiency
RMAHR	rotor mass-averaged total head rise
SEFFI	stage hydraulic efficiency quadrature function
SHRCO	stage total head rise coefficient
SHRI	stage total head rise quadrature function
SMAE	stage mass-averaged hydraulic efficiency
SMAHR	stage mass-averaged total head rise

MAVE arrays:

DELH	blade-element total head rise
DELHI	blade-element ideal total head rise
H	blade-element total head
R	streamline radius
REFFP	rotor blade-element hydraulic efficiency product
RHRP	rotor blade-element total head rise product
RN	blade row rotational speed.

RVEL	product of blade-element leaving radius and axial velocity
SDELH	stage total head rise along a streamline
SEFFP	stage hydraulic efficiency for a streamline
SHRP	stage total head rise product for a streamline
TISPD	rotor inlet blade tip velocity
U1	blade-element velocity at inlet to a blade row
U2	blade-element velocity at blade row exit
VZ	blade-element fluid axial velocity
W	DELHI

Flow Chart 15.

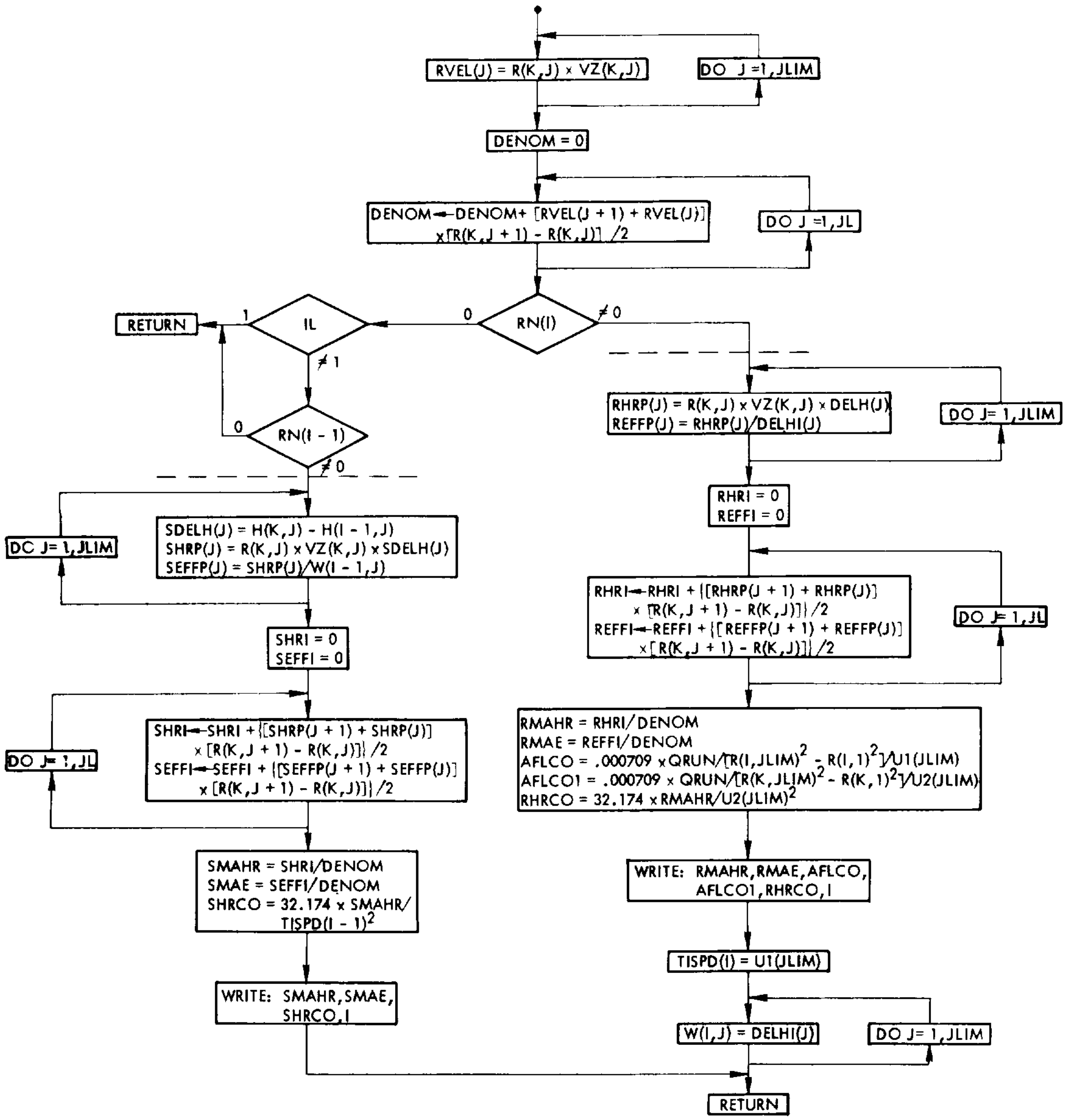

Subroutine OUTPUT. — Additional blade-element results are computed and outputed, based on the blade row entering flow conditions and determined radial equilibrium leaving conditions. Dimensional unit conversions are made for several blade-element results prior to outputing. Subroutine MAVE is called to compute and output mass-averaged blade row results.

Program parts of OUTPUT in the accompanying Flow Charts 16, 17 and 18 are identified as follows:

Flow Chart 16 Program segment "Compute equivalent D-factor and head loss difference" of subroutine OUTPUT.

Flow Chart 17 Program segment "Prepare blade-element results for output" of subroutine OUTPUT (continued).

Flow Chart 18 Program segments "Output blade-element results," and "Output mass-averaged results" of subroutine OUTPUT (concluded).

OUTPUT variables:

C1	ratio of blade-element entering and leaving streamline radii
C2	reciprocal of blade-element relative entering fluid velocity
C61	coefficient in blade-element equivalent diffusion factor calculation, rotor or stationary blade row
FIIPS	absolute value of difference between blade-element incidence angle and reference incidence angle
I	axial station; blade row number, determined by inlet station to blade row
IL	ILIM-1
ILIM	maximum value of I, the number of blade rows plus one
IO	printer reference number
J	streamline number (= 1 at hub)
JLIM	number of streamlines, casing streamline
K	I + 1
KJ	index, streamline number
QRUN	computed flow rate

OUTPUT arrays:

ANGST	blade-element stagger angle
BTAP1	blade-element relative entering fluid flow angle

BTAP2	blade-element relative leaving fluid flow angle
DELH	blade-element total head rise
DELHI	blade-element ideal total head rise
DEL2	blade-element flow deviation angle
DEQ	blade-element equivalent diffusion factor
FNC1	blade-element incidence angle
H	blade-element total head
HLDP	relative difference in computed and estimated blade-element head loss
HLOB	computed blade-element head loss
PPFT1	percent passage height from outer casing at blade row inlet
PPFT2	percent passage height from outer casing at blade row exit
HLOSS	computed blade-element head loss in preceding head loss iteration
R	streamline radius
RN	blade row rotational speed
RRT	streamline radius ratio at inlet to blade element
RRT2	streamline radius ratio at blade-element exit
SGMA	blade-element solidity
STARI	blade-element reference incidence angle
THAC	blade-element wake momentum thickness/chord
THTA	blade-element camber angle
TMAXC	blade-element maximum profile thickness/chord
U1	blade-element velocity at inlet to a blade row
U2	blade-element velocity at blade row exit
VU	blade-element fluid whirl velocity
VZ	blade-element fluid axial velocity
XBETA	blade-element entering fluid flow angle
XBETA2	blade-element leaving fluid flow angle
XBTAP1	BTAP1, deg.
XBTAP2	BTAP2, deg.
XD	blade-element diffusion factor
XDEL2	DEL2, deg.
XEFF	blade-element hydraulic efficiency
XFNC1	FNC1, deg.
XHSTT1	blade-element static head entering blade row
XHSTT2	blade-element static head leaving blade row
XOMEG	blade-element total head loss coefficient

XPFT1	PPFT1, percent
XPFT2	PPFT2, percent
XPHI1	blade-element flow coefficient at blade row inlet
XPHI2	blade-element flow coefficient at blade row exit
XPSI	blade-element head rise coefficient
XPSII	blade-element ideal head rise coefficient
XTHTA	THTA, deg.
XV1	blade-element fluid flow velocity at blade row inlet
XV2	blade-element fluid flow velocity at blade row exit
XVP1	blade-element relative fluid flow velocity at blade row inlet
XVP2	blade-element relative fluid flow velocity at blade row exit

Flow Chart 16.

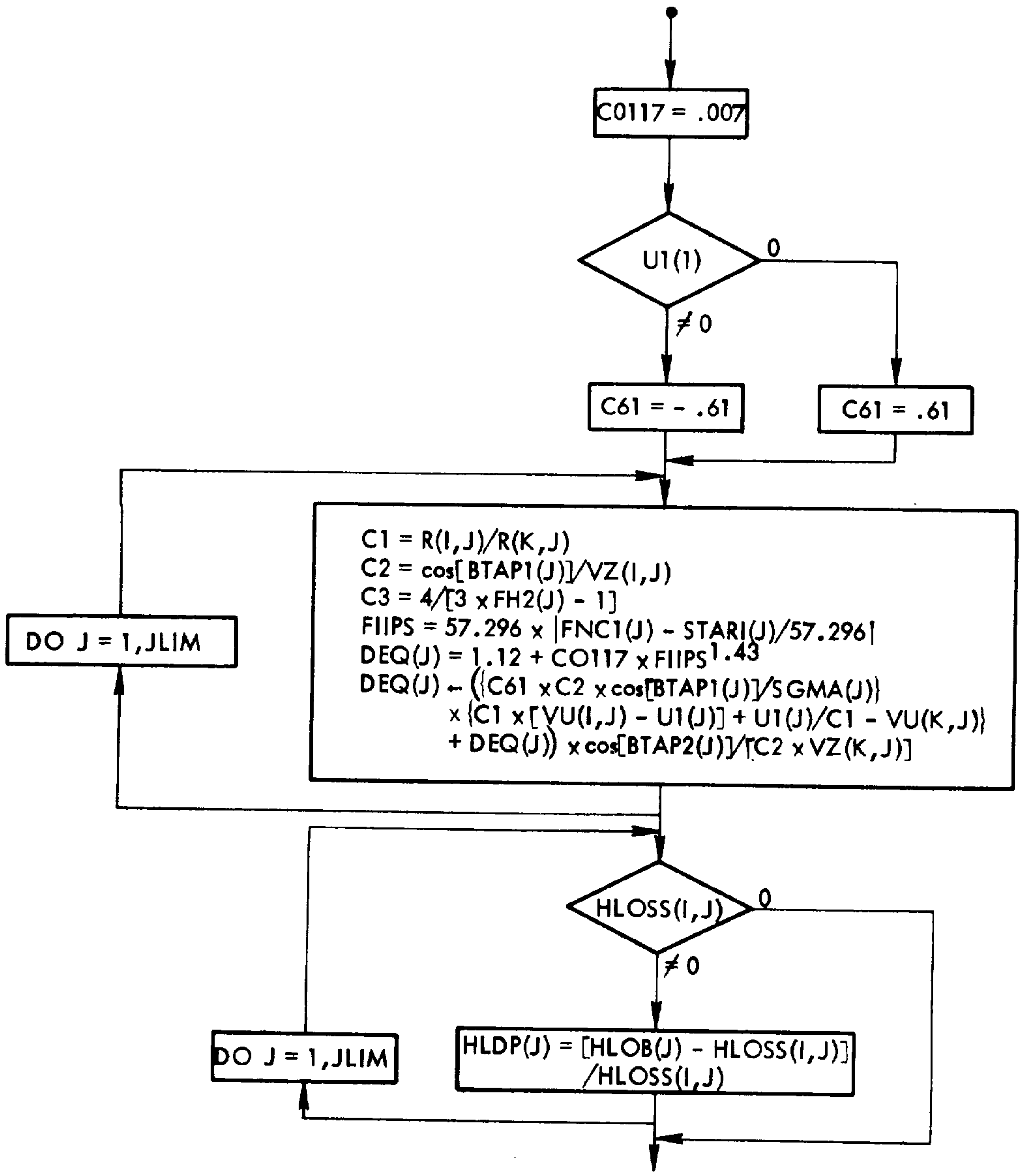

to: "Prepare blade-element ... "

Flow Chart 17.

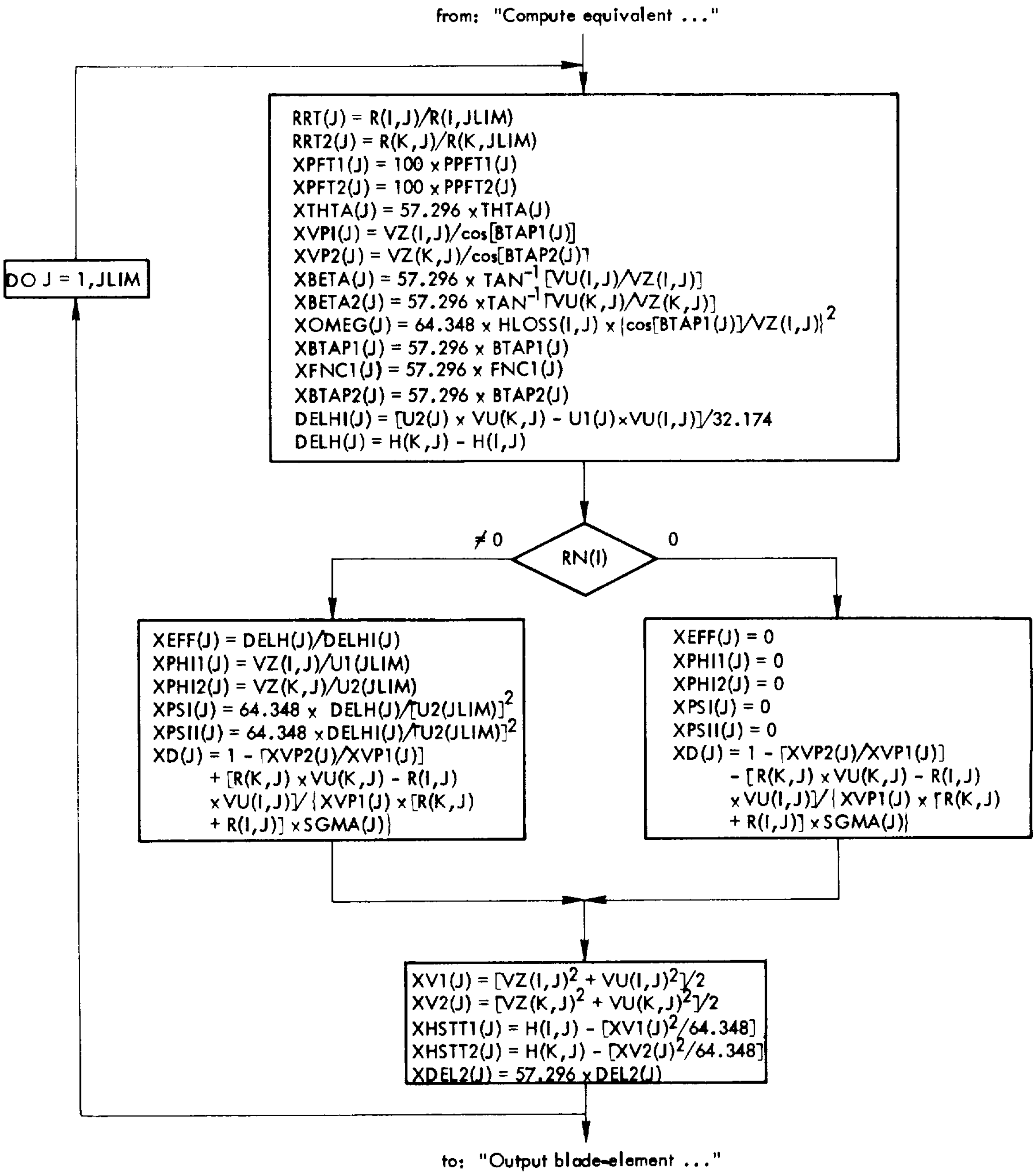

from: "Prepare blade-element ..." **Flow Chart 18.**

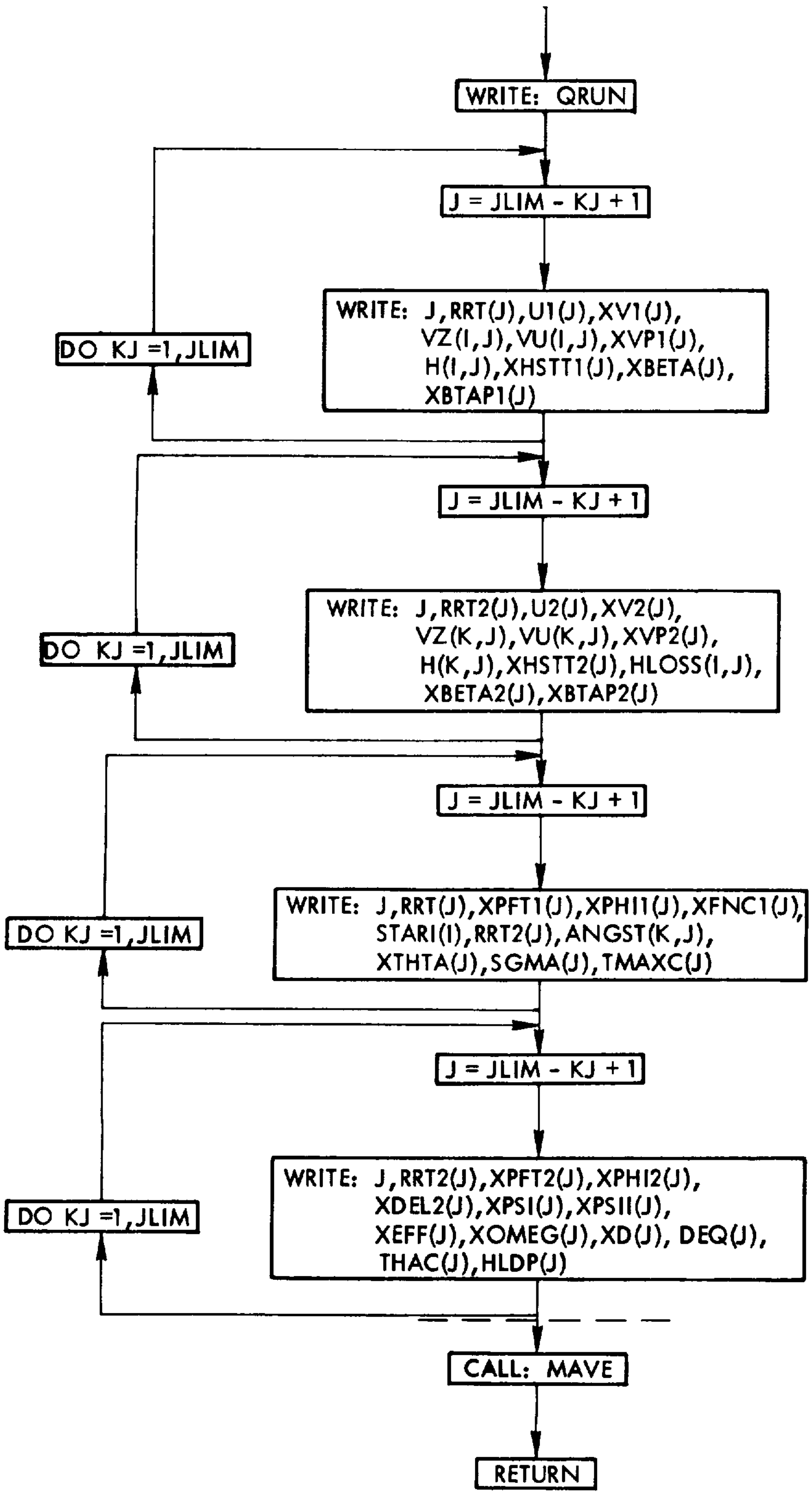

Subroutine RADEQC. — Blade-element radial equilibrium and continuity flow solutions are determined for the flow leaving a given blade row. Iterative adjustment of streamline radii based on radial equilibrium solution and flow continuity requirements are made. Maximum number of adjustments is 10, and a convergence tolerance of ± 1.0% change in streamline radius is used. Maximum number of radial equilibrium and continuity solutions and base streamline axial velocity adjustments is 20, with convergence tolerance set at ± 0.5% of the assigned flow rate.

Abnormal return to the calling program (MAIN) is executed in case of failure of the radial equilibrium solution for leaving axial velocity (VZ) at any blade-element. Also an abnormal return is executed in case a leading edge blade-element camberline tangent angle (ALFI) equal to zero is encountered.

Program parts of RADEQC in the accompanying Flow Charts 19, 20, and 21 are identified as follows:

Flow Chart 19	Program segment "Determine blade-element geometry parameters, wheel speed and relative leaving flow angles" of subroutine RADEQC.
Flow Chart 20	Program segment "Determine leaving whirl velocity, total head and axial velocity satisfying radial equilibrium" of subroutine RADEQC (continued).
Flow Chart 21	Program segments "Compute stream function distribution for leaving flow and revise base streamline velocity" and "Revise leaving flow streamline radii based on stream function distribution of subroutine RADEQC (concluded).

RADEQC variables:

A	factor in radial equilibrium equation
B	factor in radial equilibrium equation
C	factor in radial equilibrium equation
D	streamline radius factor
E	streamline radius factor
I	axial station; blade row number, determined by inlet station to blade row
IO	printer reference number
IWARN	fitting extrapolation warning indicator (= 1, no extrapolation; = 2, extrapolation of reference data table)
IZ	index
J	streamline number (= 1 at hub)
JBASE	base streamline number from which radial equilibrium calculations proceed outward to casing, or inward to hub

JL	JLIM-1
JLIM	number of streamlines, casing streamline
K	I + 1
KJ	J + 1, or J - 1
KKK	index
KNT	integration direction indicator from JBASE streamline (= 1, outward; ≠ 1 inward)
KNTT	radial equilibrium solution failure indicator (= 0, no failure; = 1, failure)
KR	index
RAD	factor in radial equilibrium equation
S	streamline radius factor

RADEQC arrays:

ALF1	leading edge blade-element camberline tangent angle
AFL2	trailing edge blade-element camberline tangent angle
ANGST	blade-element stagger angle
ALPHZ	diagnostic alphameric word
BTAP2	blade-element relative leaving fluid flow angle
CS	product of blade-element wheel speed and fluid whirl velocity
DEL2	blade-element flow deviation angle
FKSHA	blade-element shape correction factor
H	blade-element total head
HLOSS	blade-element total head loss
IEXDEV	option designation for deviation angle calculation
IEXLOS	option designation for head loss calculation
PHIEFC	blade row inlet average flow coefficient
Q	blade-element quadrature value of flow rate (from hub) based on normalized radial equilibrium solution
QB	blade-element quadrature value of normalized flow rate (from hub)
QR	conversion factor in normalized flow rate (Q) calculation
R	streamline radius
RB2	interpolated blade-element leaving streamline radius
RN	blade row rotational speed
SGMA	blade-element solidity
U2	blade-element velocity at blade row exit
VU	blade-element fluid whirl velocity
VZ	blade-element fluid axial velocity

YANGS	|ANGST|	YR	R
YPHIEF	PHIEFC		

Flow Chart 19.

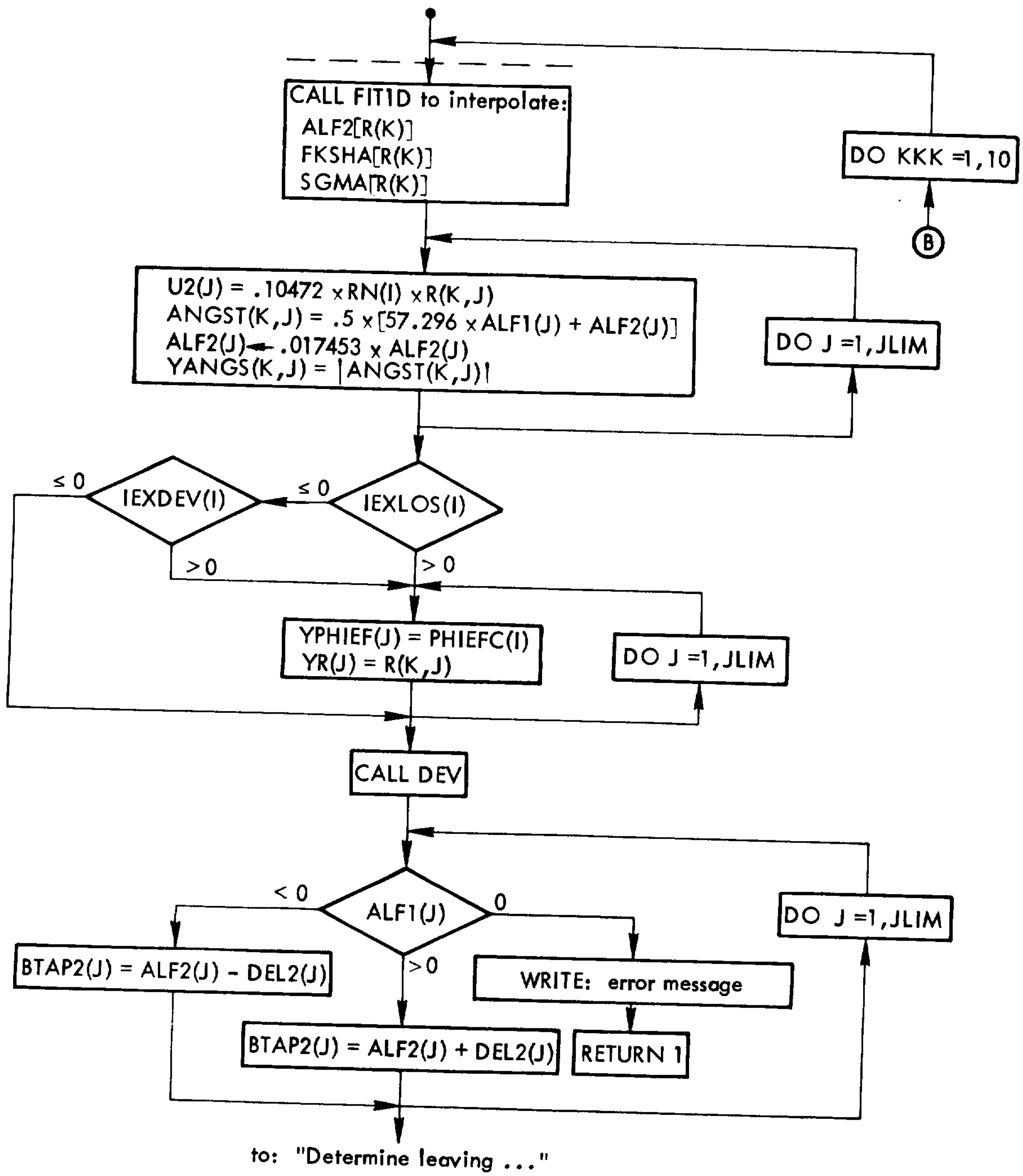

Flow Chart 20.

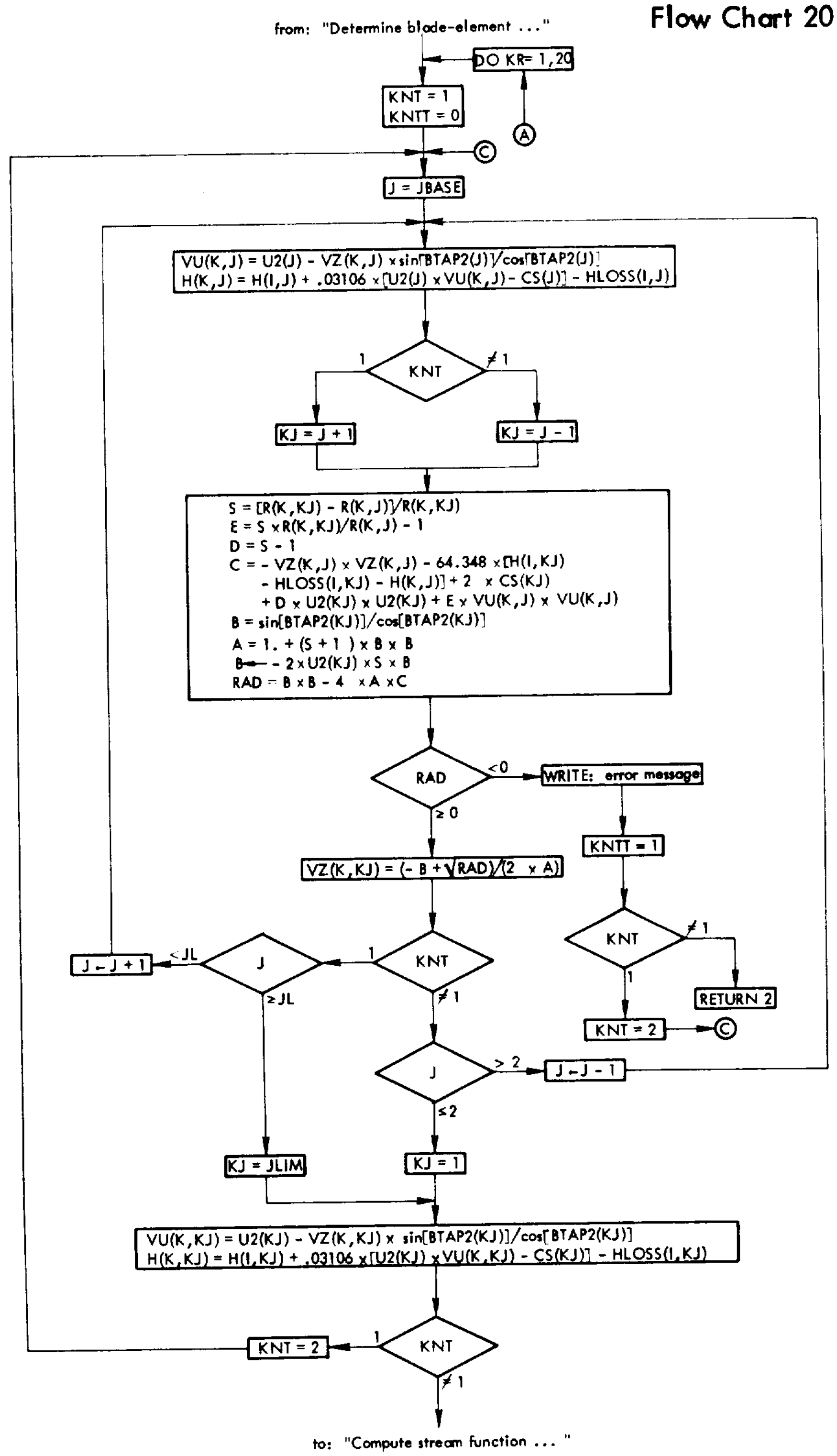

Flow Chart 21.

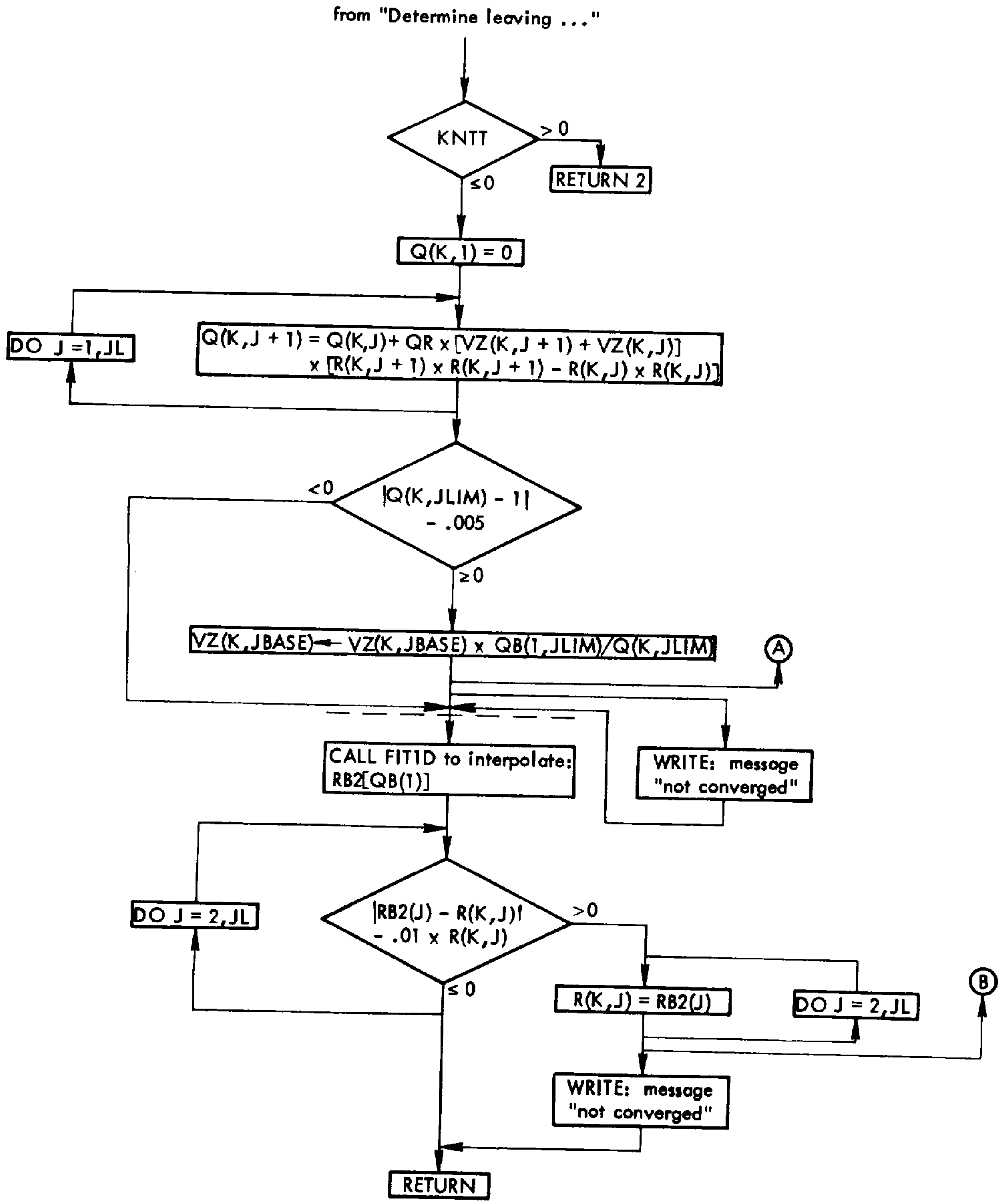

The following examples were selected from a large number of cases considered to represent typical results and to illustrate the significant strengths as well as weaknesses of the proposed pump performance prediction method. Insofar as the primary results shown are computer calculated ones, the calculated mass-averaged flow coefficient without blockage, i.e. $\overline{\phi}_{prog}$, is used throughout the section as the flow level parameter. The experimental flow coefficient values used for comparison were thus appropriately adjusted to reflect the difference between calculated, $\overline{\phi}_{prog}$, and measured, $\overline{\phi}$, flow coefficients.

As mentioned in a previous section, specific correlations of experimentally determined values of blade-element loss and deviation angle were obtained on a three-parameter basis for each rotor geometry and were made available for use in the present program as options associated with IEXLOS > 0 and IEXDEV > 0. For loss, the three correlating parameters are average blade-element loss coefficient, $\overline{\omega}$, exit flow streamline spanwise location (radius from machine axis), and average inlet flow coefficient. For deviation angle the three parameters are deviation angle, δ, exit flow streamline spanwise location (radius from machine axis), and average inlet flow coefficient. These correlations were precise enough to yield estimated average blade-element loss coefficients and deviation angles that are very close to measured values thus providing a means for assessing whether or not the present computer program would produce meaningful results if losses and deviation angles could be estimated accurately. Typical computed results are compared with measured results for a particular rotor, configuration 13A (Table I), in figures 33 and 34. The close agreement between calculated and measured values of mass-averaged hydraulic efficiency, $\overline{\eta}$, head rise coefficient, $\overline{\psi}$, axisymmetric blade-element outlet flow angle, β_2, and axial velocity, $V_{z,2}$, suggests that aside from the procedures used for estimating losses and deviation angles, the basic programming and the axisymmetric, steady-flow, radial equilibrium flow model are as reliable as the available measurements.

Work on the development of semi-empirical and relatively general rotor blade-element loss and deviation estimation procedures based on a large collection of NASA isolated pump rotor data was outlined earlier in the BLADE-ELEMENT LOSS AND DEVIATION ANGLE PREDICTION section of this report.

The recommended procedures for calculating rotor blade-element loss and deviation angles evolving from this work are based on NASA axial-flow pump rotor data (rotor configurations 02, 07, 5, 13A, 14A) correlations. These involve version A of the wake momentum thickness to chord ratio parameter, $(\theta/c)_A$, modified equivalent diffusion ratio, DEQ, and spanwise location (percent of passage height from the outer wall) as loss data correlating parameters (see figure 14) and camber exponent, b, incidence angle difference, $i - i_{ref}$, and spanwise location (percent of passage height from the outer wall) as deviation angle data correlating parameters (see figure 28). These recommended loss and deviation angle estimation procedures are available as the options associated with IEXLOS = - 1 and IEXDEV = - 1 and were used in computing the performance of a NASA axial-flow pump rotor, configuration 15, for which measured data are available but were not used in the above-mentioned correlations. Since the major objective of the blade-element loss and deviation angle estimating procedures development was to realize significant improvement over two-dimensional flow methods (Carter's rule and two-dimensional cascade loss correlation), results obtained using the recommended procedures as well as the two-dimensional flow methods were compared with measured data. Overall-performance results are indicated in figure 35 while blade-element comparisons are shown in figure 36. In general, the overall as well as blade element results related to the recommended procedures for loss and deviation angle prediction were significantly better than those obtained using the two-dimensional flow methods. Note, however, that when using the recommended procedures for calculating blade-element losses and deviation angles, the radial equilibrium condition could not be satisfied for flows corresponding to flow coefficients equal to or less than 0.372. When using the two-dimensional procedures for calculating blade-element losses and deviation angles, the radial equilibrium condition could be satisfied at $\overline{\Phi}_{prog}$ = 0.372 but not at $\overline{\Phi}_{prog}$ = 0.338. As demonstrated in figures 37 and 38, using the more specific $\overline{\omega}$ and δ vs $\overline{\Phi}$ and radius correlations (IEXLOS and IEXDEV > 0) results in the radial equilibrium condition being satisfied at even the lowest flow coefficient, $\overline{\Phi}_{prog}$ = 0.338. These results point out that a failure to satisfy the radial equilibrium condition at lower flow rates in the case of configuration 15, when using either the recommended or the two-dimensional loss and deviation angle estimation procedures, should be interpreted mainly as an indication of the imprecision of these calculating procedures. The more precise loss and deviation estimation procedure did not result in radial equilibrium failure at the lower flow rates. Any statement relating radial equilibrium failure and a reversed flow condition near the hub or tip wall should only be made if the precision of the loss and deviation calculating procedures has been ascertained.

As shown in Appendix F, the radial equilibrium solution loss related to loss and deviation angle estimation procedure imprecision is probably mainly due to a failure to predict loss gradients accurately. Thus, while the $(\theta/c)_A$, DEQ, passage location loss calculation method led to more realistic magnitudes of losses for rotor configuration 15 than the two-dimensional cascade data method did, the predicted gradients were too large at lower flow rates, thus leading to premature radial equilibrium failure. It is interesting to note the computer results of iterations just before a loss of solution occurs. In figure 39, the computed results of each of three iterations before a radial equilibrium solution failure occurred are shown for configuration 15 operating at a flow coefficient, $\phi_{prog} = 0.338$, with the recommended procedures for estimating losses and deviation angles. The predicted deviation angle spanwise variation remained essentially unchanged during iterations 2, 3 and 4, due mainly to the weak dependence between predicted deviation angle and the calculated outlet flow field.

The NASA axial-flow pump experimental research program (see reference 57) involved only one single-stage configuration (ref. 68 to 70). Although measured data from the rotor of this stage were not used in the $(\theta/c)_A$, DEQ and passage location, camber exponent, incidence angle difference and passage location correlations, data from a 16-bladed (the stage rotor had 19 blades) version of the stage rotor (configuration 02) were used. As mentioned previously, no attempt was made to develop an improvement over two-dimensional loss and deviation angle calculation procedures for a stator blade row. The computed results associated with using the recommended loss and deviation angle estimation procedures for the rotor and the two-dimensional procedures for the stator are compared with measured data in figures 40, 41 and 42. The early failure to satisfy the radial equilibrium condition in the stage occurs specifically in the stator row and it most likely is an indication of the inadequacy of the two-dimensional stator loss calculations used. As indicated in figures 43 and 44, the radial equilibrium condition could be satisfied at all flows in the rotor alone.

CONCLUDING REMARKS

The results presented in the current report represent typical examples of computation of axial-flow pump configuration performance using the program described and given in the text. Numerous preliminary versions of the program and its components were modified, combined, and discarded in the process of reaching the format now in use. In retrospect, it is evident that the development of such a computation system is a major undertaking in terms of time and funds that must involve continuity of effort. It is also an undertaking that, considered in a broad sense, is not likely to be completed in the foreseeable future.

At present, it may be concluded that the program logic and the flow model are consistent and adequate in terms of current experimental procedures and design requirements. There does not appear to be a reasonable way to avoid the requirement for introduction of experimental correlations to support the system. This requirement represents a limitation that should be considered in the planning and coordination of future research on axial-flow pump and compressor components.

APPENDIX A

DERIVATION OF RELATIONSHIPS FOR AXIAL-FLOW PUMP ROTOR AND STATOR EQUIVALENT DIFFUSION RATIO

Rotor

For a plane cascade blade element, the equivalent diffusion ratio is an expression intended to serve as a measure of the velocity ratio, $V_{max,s}/V_{2,freestream}$. For a rotor, it is assumed that the appropriate equivalent diffusion ratio to use is one that approximates the velocity ratio, $V'_{max,s}/V'_2$, which can be expressed as follows:

$$\frac{V'_{max,s}}{V'_2} = \frac{V'_{max,s}}{V'_1}\ \frac{V'_1}{V'_2} = \frac{V'_{max,s}}{V'_1}\ \frac{V_{z,1}}{V_{z,2}}\ \frac{\cos \beta'_2}{\cos \beta'_1} \ . \qquad \text{(A-1)}$$

Further, it is assumed that for a rotor, the velocity ratio, $V'_{max,s}/V'_1$, can be expressed in a form similar to that proposed for plane cascade flow by Lieblein (33), namely,

$$\frac{V'_{max,s}}{V'_1} = \left[C_1 + C_2\ (i - i^*)^{C_3} + C_4 (C.P.)'_r\right] \ . \qquad \text{(A-2)}$$

The relative circulation parameter, $C.P.'_r$, deserves further explanation. For axial-flow pump rotor flow, the blade element circulation referenced to a rotating coordinate system is

$$\Gamma'_r = \oint V'_s ds = \left[\left(r_1 V'_{\theta,1} - r_2 V'_{\theta,2}\right)\frac{2\pi}{n}\right]. \qquad \text{(A-3)}$$

With respect to the rotating coordinate system, the circulation parameter, $C.P.'_r$, is

$$C.P.'_r = \frac{\Gamma' \cos \beta'_1}{c V'_1} = \frac{\left[(r_1/r_2) V'_{\theta,1} - V'_{\theta,2}\right] \cos \beta'_1}{\dfrac{nc\ V'_1}{2\pi\ r_2}}$$

$$\text{C.P.}'_r = \frac{\left[\left(r_1/r_2\right)V'_{\theta,1} - V'_{\theta,2}\right] \cos \beta'_1}{\sigma_2 \; V'_1} \quad . \tag{A-4}$$

Since

$$V'_1 = \frac{V_{z,1}}{\cos \beta'_1} \quad ,$$

then it is true that

$$\text{C.P.}'_r = \frac{\cos^2 \beta'_1}{\sigma_2 \; V_{z,1}} \left[\left(r_1/r_2\right)V'_{\theta,1} - V'_{\theta,2}\right] \quad . \tag{A-5}$$

The velocity ratio, $V'_{max,s}/V'_2$, can thus be expressed as

$$\frac{V'_{max,s}}{V'_2} = \frac{V_{z,1} \cos \beta'_2}{V_{z,2} \cos \beta'_1} \left\{ C_1 + C_2 \left(i - i^*\right)^{C_3} + \frac{C_4 \cos^2 \beta'_1}{\sigma_2 \; V_{z,1}} \left[\frac{r_1}{r_2} V'_{\theta,1} - V'_{\theta,2}\right] \right\} \quad . \tag{A-6}$$

Finally, it can be seen that

$$\text{DEQ}_r = \frac{V_{z,1} \cos \beta'_2}{V_{z,2} \cos \beta'_1} \left\{ C_1 + C_2 \left(i - i_{ref}\right)^{C_3} + \frac{C_4 \cos^2 \beta'_1}{\sigma_2 \; V_{z,1}} \left[\frac{r_1}{r_2} V'_{\theta,1} - V'_{\theta,2}\right] \right\} . \tag{A-7}$$

Stator

For a stator, it is assumed that the appropriate equivalent diffusion ratio to use is the one that approximates the ratio, $V_{max,s}/V_2$, which can be expressed as follows:

$$\frac{V_{max,s}}{V_2} = \frac{V_{max,s}}{V_1} \frac{V_1}{V_2} = \frac{V_{max,s}}{V_1} \frac{V_{z,1}}{V_{z,2}} \frac{\cos \beta_2}{\cos \beta_1} . \tag{A-8}$$

It is further assumed that the velocity ratio, $V_{max,s}/V_1$, can be expressed as

$$\frac{V_{max,s}}{V_1} = \left[C_1 + C_2(i - i^*)^{C_3} + C_4\left(C.P._s\right)\right] . \tag{A-9}$$

The circulation for a stator row blade element can be expressed as

$$\Gamma_s = \oint V_s ds = \left(r_2 V_{\theta,2} - r_1 V_{\theta,1}\right) \frac{2\pi}{n} . \tag{A-10}$$

So the stator circulation parameter, $C.P._s$, is

$$C.P._s = \frac{\cos^2 \beta_1}{\sigma_2 V_{z,1}} \left[V_{\theta,2} - \frac{r_1}{r_2} V_{\theta,1}\right] . \tag{A-11}$$

The resulting stator equivalent diffusion ratio is

$$DEQ_s = \frac{V_{z,1}}{V_{z,2}} \frac{\cos \beta_2}{\cos \beta_1} \left\{ C_1 + C_2\left(i - i_{ref}\right)^{C_3} \right.$$

$$\left. + \frac{C_4 \cos^2 \beta_1}{\sigma_2 V_{z,1}} \left[V_{\theta,2} - \frac{r_1}{r_2} V_{\theta,1}\right]\right\} . \tag{A-12}$$

APPENDIX B

DERIVATION OF VERSION B AND C OF THE MOMENTUM THICKNESS-TO-CHORD RATIO RELATIONSHIP

Version B

For plane cascade flow (32):

$$\left(\frac{\theta}{c}\right) = \frac{\bar{\omega}}{2\sigma} \cos \beta_2 \left(\frac{\cos \beta_2}{\cos \beta_1}\right)^2 \frac{\left[1 - \frac{\theta}{c}\, \sigma \frac{H_2}{\cos \beta_2}\right]^3}{\frac{2H_2}{3H_2 - 1}} \tag{B-1}$$

and

$$1 - \left(\frac{\theta}{c}\right)\left(\frac{H_2 \sigma}{\cos \beta_2}\right) = \frac{V_{z,1}}{V_{z,2}} \quad . \tag{B-2}$$

Combining these relationships and using relative flow angles results in

$$\frac{\theta}{c} = \frac{\bar{\omega} \cos^3 \beta_2'}{2\sigma \cos^2 \beta_1'} \left(\frac{V_{z,1}}{V_{z,2}}\right)^3 \left(\frac{3H_2 - 1}{2H_2}\right) \equiv \left(\frac{\theta}{c}\right)_B \quad . \tag{B-3}$$

Version C

If it is assumed that

$$\frac{\left[1 - \frac{\theta}{c}\, \sigma \frac{H_2}{\cos \beta_2}\right]^3}{\frac{2H_2}{3H_2 - 1}} \approx 1.0$$

and

$$V_{z,1} = V_{z,2}$$

or

$$\frac{\cos\ \beta_2}{\cos\ \beta_1} = \frac{V_1}{V_2}\ ,$$

then equation (B-1) becomes

$$\frac{\theta}{c} = \frac{\overline{\omega}}{2\sigma} \cos\ \beta_2 \left(\frac{V_1}{V_2}\right)^2 \quad . \tag{B-4}$$

With relative velocities and exit flow angle for a rotor blade element, the parameter becomes

$$\frac{\theta}{c} = \frac{\overline{\omega}}{2\sigma} \left(\frac{V_1'}{V_2'}\right)^2 \cos\ \beta_2' \equiv \left(\frac{\theta}{c}\right)_C \quad . \tag{B-5}$$

APPENDIX C

DERIVATION OF AXIAL-FLOW PUMP ROTOR AND STATOR BLADE ELEMENT DIFFUSION FACTORS

Rotor

For a plane cascade blade element, the diffusion factor is expressed as

$$D = 1 - \frac{V_2}{V_1} + \frac{\Gamma}{acV_1} \tag{C-1}$$

where a is empirically determined to be equal to 2.0. For a rotor blade element, an appropriate diffusion factor might be

$$D_r = 1 - \frac{V_2'}{V_1'} + \frac{\Gamma_r'}{acV_1'} \quad . \tag{C-2}$$

The relative circulation, Γ_r', could be expressed as

$$\Gamma_r' = \oint V_s' ds = \left(r_1 V_{\theta,1}' - r_2 V_{\theta,2}\right) \frac{2\pi}{n} \quad . \tag{C-3}$$

Thus

$$D_r = 1 - \frac{V_2'}{V_1'} + \left(\frac{r_1 V_{\theta,1}' - r_2 V_{\theta,2}'}{acV_1'}\right)\left(\frac{2\pi}{n}\right) \quad . \tag{C-4}$$

and

$$D_r = 1 - \frac{V_2'}{V_1'} + \frac{r_1 V_{\theta,1}' - r_2 V_{\theta,2}'}{\sigma_{av}\left(r_1 + r_2\right) V_1'} \tag{C-5}$$

if a = 2.0.

Stator

For a stator blade element,

$$\Gamma_s = \oint V_s ds = \left(r_2 V_{\theta,2} - r_1 V_{\theta,1}\right) \frac{2\pi}{n} \quad . \tag{C-6}$$

Thus,

$$D_s = 1 - \frac{V_2}{V_1} + \frac{r_2 V_{\theta,2} - r_1 V_{\theta,1}}{a\sigma_{av}\left(r_1 + r_2\right) V_1} \tag{C-7}$$

if a = 2.0.

```
      BLOCK DATA
      COMMON/BLOCKA/ALFB(5,20),BTA2(20),BTP1B(10),DEQ(20),DEQB(10),FHB
     1(5,20),FH2(20),FIS2D(20),FI10GB(8,9),FI2DB(5,20),FKI(20),FKSHAB
     2(5,20),HLCB(20),SLP1GB(8,9),SLP2GB(8,9),THAC(20),THACB(10),X(5,20)
      COMMON/BLOCKB/ALF1(20),ALF2(20),ALFPB(5,20),ANGST(5,20),ANGSTB
     1(5,8),CS(20),EM(20),EMB(5,8),FKSHA(20),PPFT1(20),PPFT2(20),Q(5,20)
     2,QB(5,20),RB2(20),RN(5),SGMA(20),SGMAB(5,20),SGMGBB(9),THTA(20),
     3TMAXC(20),TMXCB(5,20),XP(5,20),YANGSB(8),YANGS(5,20)
      COMMON/BLOCKI/EXPBB(7,7),FICIFB(7),PPHB(7),STARI(20)
      COMMON/BLOCKM/KLZ(5),LLZ(5),YXDBB(20),RPBB1(7),THCBB1(20,7),
     1RPBB2(7),THCBB2(20,7),YDEGBB(20)
      COMMON/BLOCKP/YFKIB(5,7),YTMACB(5,7)
      DIMENSION FI10I1(40),FI10I2(32),SLP1A(40),SLP1B(32),SLP2A(40),
     1SLP2B(32)
      DIMENSION THCA(40),THCB(40),THCC(40),THCD(20),THCE(40),THCF(40),
     1THCG(40),THCH(20)
      EQUIVALENCE (FI10GB(1),FI10I1(1)),(FI10GB(41),FI10I2(1)),(SLP1GB
     1(1),SLP1A(1)),(SLP1GB(41),SLP1B(1)),(SLP2GB(1),SLP2A(1)),(SLP2GB
     2(41),SLP2B(1))
      EQUIVALENCE (THCBB1(1),THCA(1)),(THCBB1(41),THCB(1)),(THCBB1(81),
     1THCC(1)),(THCBB1(121),THCD(1)),(THCBB2(1),THCE(1)),(THCBB2(41),
     2THCF(1)),(THCBB2(81),THCG(1)),(THCBB2(121),THCH(1))
C
C
C        BLADE-ELEMENT REFERENCE DATATABLES:
C
C
C              REFERENCE TABLES INCIDENCE ANGLE CORRECTION FACTOR FOR
C              MAXIMUM THICKNESS
C
      DATA YTMACB(1,1),YTMACB(1,2),YTMACB(1,3),YTMACB(1,4),YTMACB(1,5),
     1YTMACB(1,6),YTMACB(1,7)/0.0,0.02,0.04,0.06,0.08,0.10,0.12/
      DATA YFKIB(1,1),YFKIB(1,2),YFKIB(1,3),YFKIB(1,4),YFKIB(1,5),YFKIB
     1(1,6),YFKIB(1,7)/0.0,0.334,0.589,0.772,0.903,1.0,1.08/
C
C
C              REFERENCE TABLES CONSTANT STAGGER ANGLE ZERO-CAMBER IN-
C              CIDENCE ANGLE AND CAMBER QUADRATIC COEFFICIENT AS FUNC-
C              TIONS OF STAGGER ANGLE AND SOLIDITY
C
      DATA YANGSB/0.0,10.,20.,30.,40.,50.,60.,70./
      DATA SGMGBB/0.4,0.6,0.8,1.0,1.2,1.4,1.6,2.0,2.6/
      DATA FI10I1/
     1   0.042,  0.413,  0.738,  1.043,  1.360,  1.662,  1.864,  2.042,
     2   0.012,  0.554,  1.085,  1.571,  2.050,  2.485,  2.834,  3.099,
     3   0.003,  0.721,  1.405,  2.105,  2.759,  3.386,  3.835,  4.145,
     4   -.041,  0.853,  1.735,  2.636,  3.488,  4.283,  4.919,  5.276,
     5   -.074,  1.072,  2.146,  3.136,  4.219,  5.215,  5.955,  6.377/
      DATA FI10I2/
     1   -.097,  1.203,  2.476,  3.751,  5.029,  6.214,  7.016,  7.390,
     2   -.124,  1.387,  2.844,  4.346,  5.827,  7.255,  8.100,  8.517,
     3   -.132,  1.764,  3.663,  5.606,  7.591,  9.398, 10.200, 10.850,
```

```
     4   -.186,  2.303,  4.944,  7.694, 10.460, 12.540, 13.550, 14.500/
      DATA SLP1A/
     1-.042758,-.087534,-.138043,-.190901,-.250442,-.321693,-.392870,
     1-.484041,
     2-.022447,-.058126,-.100154,-.148312,-.206059,-.272889,-.352378,
     2-.457603,
     3-.003620,-.032000,-.067203,-.113722,-.166661,-.234563,-.317756,
     3-.448353,
     40.015655,-.008163,-.037928,-.079030,-.130964,-.200632,-.291484,
     4-.433447,
     50.041494,0.019001,-.013239,-.043754,-.096356,-.173708,-.267640,
     5-.408423/
      DATA SLP1B/
     10.059901,0.046889,0.025376,-.009586,-.066273,-.150270,-.249121,
     1-.376220,
     20.082185,0.073090,0.055278,0.018505,-.040472,-.133857,-.236335,
     2-.356545,
     30.116359,0.123619,0.113367,0.079266,0.003457,-.107843,-.194811,
     3-.296872,
     40.162877,0.189407,0.193420,0.147714,0.046888,-.071540,-.156740,
     4-.247098/
      DATA SLP2A/
     1-.001435,-.001385,-.001268,-.001161,-.001019,-.000744,-.000538,
     1-.000113,
     2-.001321,-.001342,-.001331,-.001289,-.001178,-.001022,-.000814,
     2-.000337,
     3-.001225,-.001325,-.001395,-.001370,-.001347,-.001256,-.001107,
     3-.000463,
     4-.001164,-.001293,-.001424,-.001497,-.001533,-.001489,-.001376,
     4-.000607,
     5-.001171,-.001341,-.001418,-.001653,-.001749,-.001639,-.001551,
     5-.000846/
      DATA SLP2B/
     1-.001058,-.001330,-.001604,-.001843,-.001940,-.001797,-.001617,
     1-.001048,
     2-.001045,-.001386,-.001744,-.002001,-.002120,-.001904,-.001656,
     2-.001200,
     3-.000875,-.001462,-.001987,-.002403,-.002377,-.001919,-.001769,
     3-.001514,
     4-.000710,-.001564,-.002445,-.002851,-.002623,-.002108,-.002036,
     4-.002749/
C
C
C           REFERENCE TABLES DEVIATION ANGLE RULE CAMBER EXPONENT AS
C           FUNCTION OF INCIDENT ANGLE MINUS REFERENCE INCIDENT
C           ANGLE AND FRACTION OF PASSAGE HEIGHT FROM OUTER CASING
C           (IEXDEV<0)
C
      DATA FICIFB/-12.,-8.,-4.,0.,4.,8.,10./
      DATA PPHB/0.,.1,.3,.5,.7,.9,1./
      DATA EXPBB/
     1    1.17 ,  1.13 ,  1.10 ,  1.14 ,  1.20 ,  1.28 ,  1.32 ,
```

```
     2      1.15 ,   1.10 ,   1.08 ,   1.11 ,   1.17 ,   1.26 ,   1.31 ,
     3      1.11 ,   1.C7 ,   1.05 ,   1.07 ,   1.13 ,   1.22 ,   1.28 ,
     4      1.C7 ,   1.C6 ,   1.05 ,   1.06 ,   1.C8 ,   1.11 ,   1.13 ,
     5      1.C7 ,   1.C6 ,   1.C5 ,   1.04 ,   1.03 ,   1.02 ,   1.015,
     6      1.06 ,   1.038,   1.016,   0.994,   0.972,   0.95 ,   0.939,
     7      1.C4 ,   1.C1 ,   C.98 ,   0.95 ,   0.92 ,   0.90 ,   0.88 /
C
C
C            REFERENCE TABLE SLOPE FACTOR CARTER DEVIATION ANGLE RULE
C            AS FUNCTICN CF STAGGER (YANGSB) (IEXDEV=0)
C
      DATA EMB(1,1),EMB(1,2),EMB(1,3),EMB(1,4),EMB(1,5),EMB(1,6),
     1EMB(1,7),EMB(1,8)/.217,.227,.245,.268,.295,.328,.368,.425/
C
C
C            REFERENCE TABLES WAKE MCMENTUM THICKNESS/CHORD AS FUNC-
C            TICN CF EQUIVALENT D-FACTOR (IEXLOS=0)
C
      DATA DEQB/ 1.3,1.4,1.5,1.6,1.7,1.8,1.9,2.0,2.1,2.2/
      DATA THACB/.CC5,.C06,.CC7,.CC8,.0094,.011,.013,.0153,.019,.023/
C
C
C            REFERENCE TABLES WAKE MCMENTUM THICKNESS/CHORD AS FUNC-
C            TICN CF D-FACTOR AND FRACTION OF PASSAGE HEIGHT FROM
C            CUTER CASING (IEXLCS=-2)
C
      DATA YXDBB/.05,.1,.15,.2,.25,.3,.35,.4,.45,.5,.55,.6,.65,.7,.75,
     1.8,.85,.9,.95,1.C/
      DATA RPBB1/.0,.1C,.30,.5C,.70,.90,1.0/
      DATA THCA/
     1    .C16 ,.016 ,.C16 ,.016 ,.016 ,.016 ,.017 ,.022 ,.027 ,.032 ,
     1    .C37 ,.C42 ,.C47 ,.052 ,.057 ,.C62 ,.068 ,.073 ,.C78 ,.083 ,
     2    .C16 ,.C16 ,.C16 ,.016 ,.016 ,.016 ,.017 ,.022 ,.027 ,.032 ,
     2    .037 ,.C42 ,.C47 ,.052 ,.057 ,.C62 ,.068 ,.073 ,.078 ,.083 /
      DATA THCB/
     1    .C1  ,.01  ,.C1  ,.01  ,.01  ,.01  ,.01  ,.01  ,.01  ,.014 ,
     1    .023 ,.C32 ,.C41 ,.05  ,.C59 ,.068 ,.C77 ,.086 ,.095 ,.104 ,
     2    .CC59,.C062,.CC65,.0C68,.0071,.0074,.0077,.0C8 ,.0085,.009 ,
     2    .CC95,.C1  ,.C105,.011 ,.0115,.012 ,.0125,.013 ,.0135,.014 /
      DATA THCC/
     1    .CC6 ,.CC65,.CC7 ,.0077,.0084,.0091,.0098,.0105,.0112,.0119,
     1    .0126,.0133,.C14 ,.0147,.0154,.C161,.0168,.0175,.0182,.0189,
     2    .C1  ,.01  ,.C1  ,.01  ,.01  ,.011 ,.012 ,.014 ,.016 ,.018 ,
     2    .C2  ,.C22 ,.C24 ,.C26 ,.028 ,.03  ,.032 ,.034 ,.036 ,.038 /
      DATA THCD/
     1    .C1  ,.C1  ,.C1  ,.01  ,.01  ,.011 ,.012 ,.014 ,.016 ,.018 ,
     1    .02  ,.C22 ,.C24 ,.C26 ,.028 ,.03  ,.032 ,.034 ,.036 ,.038 /
C
C
C            REFERENCE TABLES WAKE MCMENTUM THICKNESS/CHORD AS FUNC-
C            TICN OF EQUIVALENT D-FACTOR AND FRACTION OF PASSAGE HEIGHT
C            FRCM CUTER CASING (IEXLCS=-1)
```

```
C
      CATA YCEQBB/1.2,1.3,1.4,1.5,1.6,1.7,1.8,1.9,2.0,2.1,2.2,2.3,2.4,
     12.5,2.6,2.7,2.8,2.9,3.C,3.4/
      DATA RPBB2/.0,.1C,.30,.5C,.7C,.9C,1.00/
      DATA THCE/
     1   .C14 ,.014 ,.C16 ,.C18 ,.022 ,.026 ,.030 ,.034 ,.038 ,.043 ,
     1   .048 ,.C53 ,.C58 ,.063 ,.068 ,.075 ,.083 ,.C93 ,.108 ,.165 ,
     2   .C14 ,.C14 ,.C16 ,.C18 ,.022 ,.026 ,.030 ,.034 ,.038 ,.043 ,
     2   .C48 ,.C53 ,.C58 ,.C63 ,.068 ,.075 ,.083 ,.093 ,.108 ,.165 /
      DATA THCF/
     1   .01  ,.C1  ,.C1  ,.0105,.0145,.0195,.024 ,.0285,.033 ,.0375,
     1   .042 ,.0465,.C51 ,.0555,.06  ,.0645,.C69 ,.C735,.078 ,.C96 ,
     2   .CC6 ,.CC6 ,.CC6 ,.0C6 ,.0061,.0061,.0061,.0C62,.0066,.0070,
     2   .0074,.0078,.CC82,.CC86,.009C,.0C94,.CC98,.0102,.0106,.0122/
      CATA THCG/
     1   .CC6 ,.CC6 ,.CC65,.0C7 ,.0075,.008 ,.0085,.0C9 ,.01  ,.011 ,
     1   .C12 ,.C13 ,.C14 ,.C15 ,.016 ,.017 ,.018 ,.019 ,.020 ,.024 ,
     2   .CC6 ,.CC6 ,.CC65,.0C75,.0085,.0095,.0105,.0115,.0125,.014 ,
     2   .C155,.C17 ,.C185,.C2  ,.0215,.023 ,.0245,.026 ,.0275,.0335/
      DATA THCH/
     1   .CC6 ,.CC6 ,.CC65,.0C75,.0085,.0095,.0105,.0115,.0125,.014 ,
     1   .0155,.C17 ,.C185,.02  ,.0215,.023 ,.0245,.026 ,.0275,.0335/
      END
```

MAIN PROGRAM
****

```
      COMMON/BLOCKA/ALFB(5,20),BTA2(20),BTP1B(10),DEQ(20),DFQB(10),FHB
     1(5,20),FH2(20),FIS2C(20),FI1OGB(8,9),FI2DB(5,20),FKI(20),FKSHAB
     2(5,20),HLOB(20),SLP1GB(8,9),SLP2GB(8,9),THAC(20),THACB(10),X(5,20)
      COMMON/BLOCKB/ALF1(20),ALF2(20),ALFPB(5,20),ANGST(5,20),ANGSTB
     1(5,8),CS(20),EM(20),EMB(5,8),FKSHA(20),PPFT1(20),PPFT2(20),Q(5,20)
     2,QB(5,20),RB2(20),RN(5),SGMA(20),SGMAB(5,20),SGMGBB(9),THTA(20),
     3TMAXC(20),TMXCB(5,20),XP(5,20),YANGSB(8),YANGS(5,20)
      COMMON/BLOCKC/BTAP1(20),BTAP2(20),DELH(20),DELHI(20),DEL2(20),
     1FNC1(20),H(5,20),HLOSS(5,20),R(5,20),U1(20),U2(20),VU(5,20),VZ(5,
     220)
      COMMON/BLOCKD/I,JBASE,JL,JLIM,K,KLIM,KPRI,QR,QRLN,THL
      COMMON/BLOCKE/X1(5,20),VZB(5,20),VZ1(20),VUB(5,20),VU1(20),
     1HB(5,20),H1(20)
      COMMON/BLOCKF/ILIM,IRUN,IEXLOS(5),IEXDEV(5),K2LM(5),L2LM(5)
     1,LSTAR(5),PHIBB(5,20),XFB(5,20),OMEGBB(5,20,20),DEL2B(5,20,20)
     2,PHIEX(20),RSTAR(5),AREA(5),ARFAC(5)
      COMMON/BLOCKG/K2LIM,L2LIM,YPHIBB(20),YXPB(20),YOMGBB(20,20),YDEL2
     1B(20,20),YPHIEF(20),YR(20),PHIEFC(5)
      COMMON/BLOCKH/IC,IL,IPRI,JPRI,K1LIM
      COMMON/BLOCKI/ EXPBB(7,7),FIDIFB(7),PPHB(7),STARI(20)
      COMMON/BLOCKJ/EMBB(8),FI1OI1(40),FI1OI2(32),FKIB(7),SLP1I1(16),
     1SLP1I2(16),SLP1I3(16),SLP1I4(16),SLP1I5(8),SLP2I1(16),SLP2I2(16),
     2 SLP2I3(16),SLP2I4(16),SLP2I5(8),TMAXCB(7)
      COMMON/BLOCKK/YDEQB(20),YRPB(7),YTHACB(20,7),YXDB(20),DEQBB(5,20)
     X,RPBB(5,7),THACBB(5,20,7),XDBB(5,20),HLOP(20)
      COMMON/BLOCKL/II,IO
      COMMON/BLOCKM/KLZ(5),LLZ(5),YXDBB(20),RPBB1(7),THCBB1(20,7),
     1RPBB2(7),THCBB2(20,7),YDEQBB(20)
      COMMON/BLOCKP/YFKIB(5,7),YTMACB(5,7)
      DIMENSION                        YTMAXC(5,20),HLOSS1(20)
      DIMENSION ALPHZ(20)
      DATA ALPHZ/' VZB','(X1)',' VUB','(X1)','  HB','(X1)',' ALF',
     1           'B(X)','   T','MXCB','(XP)','   Y','FKIB','(YTM',
     2           'ACB)','   F','I2DB','(XP)',' FHB','(XP)'/
      II=5
      IO=6
      DO 340 J=1,8
  340 ANGSTB(1,J)=YANGSB(J)
C
C     INPUT PROBLEM GEOMETRY AND REFERENCE TABLES.
C
      CALL INPUT(&5)
C
C     INITIALIZE STREAMLINE RADII, HEAD LOSS AND BASE STREAMLINE VELOCITY.
C
    5 DO 9 J=1,JLIM
      Z=J
      ZL=JL
```

```
      FZ=(Z-1.)/ZL
      R(ILIM,J)=FZ*(XP(IL,KLIM)-XP(IL,1))+XP(IL,1)
      HLOSS(ILIM,J)=C.
      DO 9 I=1,IL
      R(I,J)=FZ*(X(I,KLIM)-X(I,1))+X(I,1)
    9 HLOSS(I,J)=C.
      READ (II,6CC)IC,VZ(1,JBASE)
      IF(IC-70)14,11,14
   11 DO 12 I=2,ILIM
   12 VZ(I,JBASE)=VZ(1,JBASE)
C
C     INPUT PUMP INLET CONDITIONS, AXIAL STATION BLOCKAGE FACTOR AND
C     COMPUTE STREAMFUNCTION DISTRIBUTION.
C
   13 READ(II,6CC)ID,PHIRUN
      IF(PHIRUN)131,45,133
  131 WRITE(IC,616)
      CALL INPUT1(85)
  133 XR=IRUN
      PHIRUN=XR+PHIRUN
      IF(IC-80)14,113,14
  113 WRITE (IC,519)
      WRITE(IC,601)PHIRUN
      READ(II,615)ID,K1LIM
      IF(IC-81) 14,7C1,14
  701 READ (II,6CC)IC,(X1(1,K),VZB(1,K),VUB(1,K),HB(1,K),K=1,K1LIM)
      IF(IC-82)14,70C,14
  700 READ (II,6CC)IC,(ARFAC(I),I=1,IL)
      IF(IC-83)14,15,14
   15 WRITE (IC,520)
      WRITE (IC,521)(X1(1,K),VZB(1,K),VUB(1,K),HB(1,K),K=1,K1LIM)
   16 CALL FIT1C(R,VZ1,X1,VZB,JLIM,K1LIM,1,1,IWARN)
      GO TC (1CC2,1CC1),IWARN
 1001 WRITE(IO   ,9CC)(ALPHZ(IZ),IZ=1,2)
 1002 CALL FIT1C(R,VU1,X1,VUB,JLIM,K1LIM,1,1,IWARN)
      GO TC (1CC4,1CC3),IWARN
 1003 WRITE(IO   ,900)(ALPHZ(IZ),IZ=3,4)
 1C04 CALL FIT1C(R,H1,X1,HB,JLIM,K1LIM,1,1,IWARN)
      GO TC (10C6,1CC5),IWARN
 1005 WRITE(IO   ,9OC)(ALPHZ(IZ),IZ=5,6)
 1CC6 DO 16C J=1,JLIM
      VZ(1,J)=VZ1(J)
      VU(1,J)=VU1(J)
  160 H(1,J)=H1(J)
      QB(1,1)=C.
      DO 161 J=2,JLIM
  161 QB(1,J)=QB(1,J-1)+705.0217*(VZ(1,J-1)+VZ(1,J))*(R(1,J)*R(1,J)
     1-R(1,J-1)*R(1,J-1))
      QRUN=QB(1,JLIM)
      DO 162 J=2,JLIM
  162 QB(1,J)=QB(1,J)/QRUN
      QR=7C5.C217/QRUN
```

```
      PHIB=GRUN/((R(1,JLIM)*R(1,JLIM)-R(1,1)*R(1,1))*1410.1*USTAR(1))
      DO 67 I=1,IL
      IF(IEXLOS(I))62,62,63
   62 IF(IEXDEV(I))67,67,63
C
C     COMPUTE STATION ANNULUS AREA AND EFFECTIVE FLOW COEFFICIENT.
C
   63 AREA(I)=3.1416*(R(I,JLIM)*R(I,JLIM)-R(I,1)*R(I,1))
   66 PHIEFC(I)=PHIB*(AREA(1)/AREA(I))*ARFAC(I)*(USTAR(1)/USTAR(I))
      IF(I-1)610,611,610
  611 WRITE(IO,612)
  610 WRITE(IO,614)I,PHIEFC(I),USTAR(I),ARFAC(I)
   67 CONTINUE
C
C     TRANSFER LOSS AND DEVIATION ANGLE REFERENCE TABLES PER LOSS AND
C     DEVIATION ANGLE OPTIONS.
C
      DO 42 I=1,IL
   18 IF(IEXDEV(I))232,232,233
  233 KK=K2LM(I)
      LL=L2LM(I)
      DO 230 K=1,KK
  230 YPHIBB(K)=PHIBB(I,K)
      DO 235 L=1,LL
      YXPB(L)=XPB(I,L)
      DO 235 K=1,KK
  235 YDEL2B(K,L)=DEL2B(I,K,L)
  232 LINDEX=IEXLOS(I)+5
      GO TO(401,403,401,403,408,409),LINDEX
  409 KK=KLZ(I)
      LL=LLZ(I)
      DO 2301 K=1,KK
 2301 YPHIBB(K)=PHIBB(I,K)
      DO 2302 L=1,LL
      YXPB(L)=XPB(I,L)
      DO 2302 K=1,KK
 2302 YOMGBB(K,L)=OMEGBB(I,K,L)
      GO TO 408
  401 KK=KLZ(I)
      LL=LLZ(I)
      DO 402 K=1,KK
  402 YXCB(K)=XCBB(I,K)
      DO 406 L=1,LL
      YRPB(L)=RPBB(I,L)
      DO 406 K=1,KK
  406 YTHACB(K,L)=THACBB(I,K,L)
      GO TO 408
  403 KK=KLZ(I)
      LL=LLZ(I)
      DO 404 K=1,KK
  404 YDEQB(K)=DEQBB(I,K)
      DO 407 L=1,LL
```

```
      YRPB(L)=RPEB(I,L)
      DO 407 K=1,KK
  407 YTHACB(K,L)=THACEB(I,K,L)
C
C     COMPUTE BLADE ROW INLET CONDITIONS.
C
  408 CALL FIT1D(R,ALF1,X,ALFB,JLIM,KLIM,I,I,IWARN)
      GO TO (1008,1007),IWARN
 1007 WRITE(IO   ,900)(ALPHZ(IZ),IZ=7,8)
 1008 DO 19 J=1,JLIM
      PPFT1(J)=(R(I,JLIM)-R(I,J))/(R(I,JLIM)-R(I,1))
      U1(J)=.10472*RN(I)*R(I,J)
      BTAP1(J)=ATAN((U1(J)-VU(I,J))/VZ(I,J))
      ALF1(J)=.017453*ALF1(J)
      FNC1(J)=ABS(BTAP1(J))-ABS(ALF1(J))
   19 CS(J)=U1(J)*VU(I,J)
      K=I+1
      KHLOSS=0
C
C     SAVE BLADE ROW INITIAL HEAD LOSS.
C
      DO 850 J=1,JLIM
  850 HLOSS1(J)=HLOSS(I,J)
C
C     INTERPOLATE PROFILE MAXIMUM THICKNESS AND INCIDENCE ANGLE CORRECTI
C     FACTOR, COMPUTE RADIAL EQUILIBRIUM AND CONTINUITY SOLUTION AND
C     DETERMINE HEAD LOSS.
C
  851 DO 41 KLK=1,40
      LOK=KLK
      CALL FIT1D(R,TMAXC,XP,TMXCB,JLIM,KLIM,I,K,IWARN)
      GO TO (1010,1009),IWARN
 1009 WRITE(IO   ,900)(ALPHZ(IZ),IZ=9,11)
 1010 DO 250 J=1,JLIM
  250 YTMAXC(1,J)=TMAXC(J)
      CALL FIT1D (YTMAXC,FKI,YTMACB,YFKIB,JLIM,7,1,1,IWARN)
      GO TO (1012,1011),IWARN
 1011 WRITE(IO   ,900)(ALPHZ(IZ),IZ=12,15)
 1012 CALL RADEQC(&13,&852)
   34 CALL FIT1D(R,FIS2D,XP,FI2DB,JLIM,KLIM,I,K,IWARN)
      GO TO (1014,1013),IWARN
 1013 WRITE(IO   ,900)(ALPHZ(IZ),IZ=16,18)
 1014 CALL FIT1D(R,FH2,XP,FHB,JLIM,KLIM,I,K,IWARN)
      GO TO (1016,1015),IWARN
 1015 WRITE(IO   ,900)(ALPHZ(IZ),IZ=19,20)
 1016 CALL LOSS(R,VZ,VL,BTAP1,BTAP2,FNC1,U1,U2,FH2,
     1FIS2D,DEQB,THACE,I,K,JLIM,HLOB,DEQ,THAC)
C
C     CHECK HEAD LOSS CONVERGENCE AND OUTPUT COMPUTED RESULTS.
C
  801 DO 37 J=1,JLIM
   36 IF(ABS(HLOB(J)-HLOSS(I,J))-THL*ABS(HLOSS(I,J)))37,37,400
```

```
   37 CONTINUE
      CALL OUTPUT
      GO TO 42
C
C     REVISE HEAD LOSS.
C
  400 IF(IEXLOS(I).GT.0) GO TO 413
      GO TO (411,411,412,413),LOK
  413 XJDE=1.0
      GO TO 414
  411 XJDE= .5
      GO TO 414
  412 XJDE= .65
  414 IF(KHLOSS.EQ.0) GO TO 860
C
C     REASSIGN HEAD LOSS AND REPEAT ITERATIONS TO LOSS OF SOLUTION.
C
      IF(LOK.LT.LOK1) GO TO 860
      CALL OUTPUT
      WRITE(IO,880) LOK
      IF(LOK.GE.LOKLIM) GO TO 870
  860 IF(LOK-40)40,841,841
   40 DO 41 J=1,JLIM
   41 HLOSS(I,J)=HLOSS(I,J)+XJDE*(HLOB(J)-HLOSS(I,J))
C
C     OUTPUT MESSAGE HEAD LOSS NOT CONVERGED AND OUTPUT COMPUTED RESULTS.
C
  841 WRITE (IO,513)
      CALL OUTPUT
      GO TO 870
C
C     OUTPUT INTERMEDIATE ITERATION RESULTS PRIOR TO LOSS OF SOLUTION.
C
  852 WRITE(IO,854) LOK
      IF(LOK-4)872,871,871
  872 IF(LOK.GT.1) GO TO 874
      GO TO 870
  871 WRITE(IO,856)
      KHLOSS=1
      LOKLIM=LOK-1
      LOK1=LOK-3
      DO 853 J=1,JLIM
  853 HLOSS(I,J)=HLOSS1(J)
      GO TO 851
  874 WRITE(IO,855)
      KHLOSS=1
      LOKLIM=LOK-1
      LOK1=LOK-1
      DO 873 J=1,JLIM
  873 HLOSS(I,J)=HLOSS1(J)
      GO TO 851
C
```

```
C       INITIALIZE HEAD LOSS TO ZERO.
C
  870 DO 43 J=1,JLIM
   43 HLOSS(I,J)=0
   42 CONTINUE
      GO TO 13
   14 WRITE(IC,510)IC,J,K,L
   45 STOP
  510 FORMAT(//' ERROR IN INPUT DATA CARD ORDER, MAIN PROGRAM.',2X,
     1'IC=',I3,'    J=',I3,'    K=',I3,'    L=',I3)
  513 FORMAT(1H1////44HOLOSS SOLUTION NOT ACHIEVED IN 40 ITERATIONS)
  519 FORMAT(17H1INLET CONDITIONS)
  520 FORMAT(36HO      R          VZ             VU        H)
  521 FORMAT(4F10.4)
  600 FORMAT(I2,(T3,12F6.4))
  601 FORMAT(10X,' PHIRUN NO.',F10.2)
  612 FORMAT(//'        I        PHIEFC        LSTAR            ARFAC'//)
  614 FORMAT(5X,I2,3F12.4)
  615 FORMAT(2I2)
  616 FORMAT(//' FLOW RATES COMPLETED-NEXT READ NEW RPM OR NEW GEOMETRY
     1DATA')
  854 FORMAT(1HO,'SOLUTION FAILURE DUE TO NEGATIVE RADICAND DURING LOSS
     1ITERATION',I3)
  855 FORMAT(1HO,'SOLUTION FOR THE LOSS ITERATION PRECEDING FAILURE IS P
     1RINTED NEXT')
  856 FORMAT(1HO,'SOLUTIONS FOR SEVERAL LOSS ITERATIONS PRECEDING FAILUR
     1E ARE PRINTED NEXT')
  880 FORMAT('  LOSS ITERATION NO.',I4)
  900 FORMAT(//'***** WARNING - FIT1D CALLED IN MAIN - EXTRAPOLATION OF
     1TABLE ',4A4)
      END
```

```
      SUBRCLTINE FITIC
C     ****************
C
C
     1(X,Y,XB,YB,JP,KP,I,K,IWARN)
      COMMCN/BLOCKL/II,IO
      DIMENSICN X(5,1),Y(1),XB(5,1),YB(5,1)
C
C     3-PCINT LAGRANGIAN INTERPCLATION FOR Y(X) FRCM DATA TABLES YB(XB).
C     XB-ARRAY ELEMENTS ARE ARBITRARILY SPACED, MONOTCNE INCREASING.
C     IWARN=2 INCICATES EXTRAPCLATICN CUTSICE RANGE CF XB ARRAY.
C
      IWARN=1
      IF(X(K,1)-XB(I,1)) 15,16,16
   15 IWARN=2
   16 DO 3 J=1,JP
      DO 1 M=3,KP
      L=M
C
C     BRACKET INTERPCLATE X WITH THREE NEIGHBORING POINTS IN XB ARRAY.
C
      IF(X(K,J)-XB(I,L))2,2,1
    1 CONTINUE
      IWARN=2
    2 X0=XB(I,L-2)
      X1=XB(I,L-1)
      X2=XB(I,L)
C
C     CCMPLTE INTERPCLATED Y(X).
C
    3 Y(J)=(X(K,J)-X1)*(X(K,J)-X2)*YB(I,L-2)/((X0-X1)*(X0-X2))
     1+(X(K,J)-X2)*(X(K,J)-X0)*YB(I,L-1)/((X1-X2)*(X1-X0))
     2+(X(K,J)-XC)*(X(K,J)-X1)*YB(I,L)/((X2-X0)*(X2-X1))
      RETURN
      END
```

```
      SUBROUTINE FIT2D
C     ****************
C
C
     1(X,Y,Z,XB,YB,ZB,IP,JP,JL,IQ,JQ,IWARN)
      COMMON/BLOCKL/II,IC
      DIMENSION X(1),Y(1),Z(1),XB(1),ZB(1),YST(3)
      DIMENSION YB(IQ,JQ)
C
C     3-POINT LAGRANGIAN INTERPOLATION FOR Y(X,Z) FROM DATA TABLES
C     YB(XB,ZB). XB,ZB ARRAY ELEMENTS ARE ARBITRARILY SPACED, MONOTONE
C     INCREASING. IWARN=2 INDICATES EXTRAPOLATION OUTSIDE RANGE OF
C     XB, ZB ARRAY.
C
      IWARN=1
      IF(X(1)-XB(1)) 16,17,17
   16 IWARN=2
   17 IF(Z(1)-ZB(1)) 18,19,19
   18 IWARN=2
   19 DO 6 N=1,JL
      DO 1 M=3,IP
      I=M
C
C     BRACKET INTERPOLATE X WITH THREE NEIGHBORING POINTS IN XB ARRAY.
C
      IF(X(N)-XB(I))2,2,1
    1 CONTINUE
      IWARN=2
    2 DO 3 M=3,JP
      J=M
C
C     BRACKET INTERPOLATE Z WITH THREE NEIGHBORING POINTS IN ZB ARRAY.
C
      IF(Z(N)-ZB(J))4,4,3
    3 CONTINUE
      IWARN=2
    4 X0=ZB(J-2)
      X1=ZB(J-1)
      X2=ZB(J)
      DO 5 K=1,3
      L=I+K
      Y0=YB(L-3,J-2)
      Y1=YB(L-3,J-1)
      Y2=YB(L-3,J)
C
C     COMPUTE INTERPOLATED YST(XB,Z) AT THREE NEIGHBORING POINTS IN
C     XB ARRAY.
C
    5 YST(K)=(Z(N)-X1)*(Z(N)-X2)*Y0/((X0-X1)*(X0-X2))
     1+(Z(N)-X2)*(Z(N)-X0)*Y1/((X1-X2)*(X1-X0))
     2+(Z(N)-X0)*(Z(N)-X1)*Y2/((X2-X0)*(X2-X1))
      X0=XB(I-2)
```

```
      X1=XB(I-1)
      X2=XB(I)
C
C     COMPUTE INTERPOLATED Y(X,Z).
C
    6 Y(N)=(X(N)-X1)*(X(N)-X2)*YST(1)/((X0-X1)*(X0-X2))
     1+(X(N)-X2)*(X(N)-X0)*YST(2)/((X1-X2)*(X1-X0))
     2+(X(N)-X0)*(X(N)-X1)*YST(3)/((X2-X0)*(X2-X1))
      RETURN
      END
```

```
      SUBROUTINE DEV
C     *************
C
C
      COMMON/BLOCKA/ALFB(5,20),BTA2(20),BTP1B(10),DEQ(20),DEQB(10),FHB
     1(5,20),FH2(20),FIS2D(20),FI10GB(8,9),FI2DB(5,20),FKI(20),FKSHAB
     2(5,20),HLCB(20),SLP1GB(8,9),SLP2GB(8,9),THAC(20),THACB(10),X(5,20)
      COMMON/BLOCKB/ALF1(20),ALF2(20),ALFPB(5,20),ANGST(5,20),ANGSTB
     1(5,8),CS(20),EM(20),EMB(5,8),FKSHA(20),PPFT1(20),PPFT2(20),Q(5,20)
     2,QB(5,20),RB2(20),RN(5),SGMA(20),SGMAB(5,20),SGMGBB(9),THTA(20),
     3TMAXC(20),TMXCB(5,20),XP(5,20),YANGSB(8),YANGS(5,20)
      COMMON/BLOCKC/BTAP1(20),BTAP2(20),DELH(20),DELHI(20),DEL2(20),
     1FNC1(20),H(5,20),HLOSS(5,20),R(5,20),U1(20),U2(20),VU(5,20),VZ(5,
     220)
      COMMON/BLOCKD/I,JBASE,JL,JLIM,K,KLIM,KPRI,QR,QRUN,THL
      COMMON/BLOCKF/ILIM,IRUN,IEXLOS(5),IEXDEV(5),K2LM(5),L2LM(5)
     1,LSTAR(5),PHIBB(5,20),XPB(5,20),CMEGBB(5,20,20),DEL2B(5,20,20)
     2,PHIEX(20),RSTAR(5),AREA(5),ARFAC(5)
      COMMON/BLOCKG/K2LIM,L2LIM,YPHIBB(20),YXPB(20),YCMGBB(20,20),YDEL2
     1B(20,20),YPHIEF(20),YR(20),PHIEFC(5)
      COMMON/BLOCKI/ EXPBB(7,7),FIDIFB(7),PPHB(7),STARI(20)
      COMMON/BLOCKJ/EMBB(8),FI1CI1(40),FI10I2(32),FKIB(7),SLP1I1(16),
     1SLP1I2(16),SLP1I3(16),SLP1I4(16),SLP1I5(8),SLP2I1(16),SLP2I2(16),
     2 SLP2I3(16),SLP2I4(16),SLP2I5(8),TMAXCB(7)
      COMMON/BLOCKL/II,IC
      DIMENSION EXPB(20),FIDIF(20)
      DIMENSION ALPHZ(10)
      DATA ALPHZ/' YDE','L2B(','YPHI','BB,Y','XPB)','  EX','PBB(',
     1          'FIDI','FB,P','PHB)'/
C
C     CALCULATE REFERENCE INCIDENCE ANGLES.
C
      DO 45 J=1,JLIM
      PPFT2(J)=(R(K,JLIM)-R(K,J))/(R(K,JLIM)-R(K,1))
   45 THTA(J)=ABS(ALF1(J)-ALF2(J))
      CALL IREF
      IF(IEXDEV(I))43,40,42
C
C     CALCULATE DEVIATION ANGLES USING CARTER'S RULE.
C
   40 CALL FIT1D(YANGS,EM,ANGSTB,EMB,JLIM,8,1,K,IWARN)
      GO TO (51,50),IWARN
   50 WRITE(IO,100)
   51 DO 41 J=1,JLIM
   41 DEL2(J)=EM(J)*THTA(J)/SQRT(SGMA(J))
      RETURN
C
C     CALCULATE DEVIATION ANGLES FROM INPUTED REFERENCE TABLE.
C
   42 KK=K2LM(I)
      LL=L2LM(I)
```

```
      CALL FIT2C(YPHIEF,DEL2,YR,YPHIBB,YDEL2B,YXPB,KK    ,LL    ,JLIM,20,
     1 2C,IWARN)
      GO TO (55,54),IWARN
   54 WRITE(IO,101)(ALFHZ(IZ),IZ=1,5)
   55 RETLRN
C
C     CALCLLATE DEVIATICN ANGLES USING CAMBER EXPONENT RULE.
C
   43 CALL FIT1C(YANGS,EM,ANGSTB,EMB,JLIM,8,1,K,IWARN)
      GO TC (53,52),IWARN
   52 WRITE(IO,1CO)
   53 DO 47 J=1,JLIM
   47 FICIF(J)=FNC1(J)*57.29578-STARI(J)
      CALL FIT2D(FIDIF,EXPB,PPFT2,FIDIFB,EXPBB,PPHB,7,7,JLIM,7,7,IWARN)
      GO TC (57,56),IWARN
   56 WRITE(IO,101)(ALPHZ(IZ),IZ=6,10)
   57 DO 46 J=1,JLIM
   46 DEL2(J)=EM(J)*((THTA(J)*57.29578)**EXPB(J))/(57.29578*
     1 SQRT(SGMA(J)))
      RETLRN
  100 FORMAT(//'***** WARNING - EXTRAPOLATICN OF TABLE EMB(ANGSTB) IN FI
     1T1C-CALLEC IN CEV')
  101 FORMAT(//'***** WARNING - FIT2D CALLED IN DEV - EXTRAPOLATICN OF T
     1ABLE ',5A4)
      END
```

```
      SUBROUTINE INOUT
C     ****************
C
C
      COMMON/BLOCKA/ALFB(5,20),BTA2(20),BTP1B(10),DEQ(20),DEQB(10),FHB
     1(5,20),FH2(20),FIS2C(20),FI10GB(8,9),FI2DB(5,20),FKI(20),FKSHAB
     2(5,20),HLCE(20),SLP1GB(8,9),SLP2GB(8,9),THAC(20),THACB(10),X(5,20
      COMMON/BLOCKB/ALF1(20),ALF2(20),ALFPB(5,20),ANGST(5,20),ANGSTB
     1(5,8),CS(20),EM(20),EMB(5,8),FKSHA(20),PPFT1(20),PPFT2(20),Q(5,20
     2,QE(5,20),RB2(20),RN(5),SGMA(20),SGMAB(5,20),SGMGBB(9),THTA(20),
     3TMAXC(20),TMXCE(5,20),XP(5,20),YANGSB(8),YANGS(5,20)
      COMMON/BLOCKD/I,JBASE,JL,JLIM,K,KLIM,KPRI,QR,QRUN,THL
      COMMON/BLOCKF/ILIM,IRUN,IEXLOS(5),IEXDEV(5),K2LM(5),L2LM(5)
     1,USTAR(5),PHIBE(5,20),XFB(5,20),OMEGBB(5,20,20),DEL2B(5,20,20)
     2,PHIEX(20),RSTAR(5),AREA(5),ARFAC(5)
      COMMON/BLOCKH/ID,IL,IPRI,JPRI,K1LIM
      COMMON/BLOCKI/ EXPBB(7,7),FIDIFB(7),PPHB(7),STARI(20)
      COMMON/BLOCKK/YDEQB(20),YRPE(7),YTHACB(20,7),YXDB(20),DEQBB(5,20)
     X,RPBE(5,7),THACBE(5,20,7),XDBB(5,20),HLDP(20)
      COMMON/BLOCKL/IIN,IOUT
      COMMON/BLOCKM/KLZ(5),LLZ(5),YXDBB(20),RPBB1(7),THCBB1(20,7),
     1RPBB2(7),THCBB2(20,7),YDEQBB(20)
      COMMON/BLOCKP/YFKIB(5,7),YTMACB(5,7)
      WRITE(IOUT,9125)
      WRITE(IOUT,5074)
    8 WRITE(IOUT,503)IRUN,JBASE,JLIM
      WRITE(IOUT,5076)
C
C     OUTPUT REFERENCE INCIDENCE ANGLE TABLES.
C
      WRITE(IOUT,5031)(YTMACB(1,K),K=1,7)
      WRITE(IOUT,5078)(YFKIB(1,K),K=1,7)
      WRITE(IOUT,5077)
      WRITE(IOUT,5034)
      WRITE(IOUT,5032)(SGMGBB(L),L=1,9)
      DO 61 K=1,8
      WRITE(IOUT,5033) YANGSB(K),(FI10GB(K,L),L=1,9)
   61 CONTINUE
      WRITE(IOUT,9124)
      DO 62 K=1,8
      WRITE(IOUT,5033) YANGSB(K),(SLP1GB(K,L),L=1,9)
   62 CONTINUE
      WRITE(IOUT,9124)
      DO 63 K=1,8
      WRITE(IOUT,5033) YANGSB(K),(SLP2GB(K,L),L=1,9)
   63 CONTINUE
C
C     OUTPUT BLADE ROW RPM, REFERENCE RADIUS AND LOSS AND DEVIATION
C     ANGLE OPTIONS.
C
      DO 93 I=1,IL
      WRITE(IOUT,5038)
```

```
      WRITE(IOUT,505) I,RN(I),RSTAR(I),IEXDEV(I),IEXLOS(I)
      WRITE(IOUT,506)
      WRITE(IOUT,507)
C
C     OUTPUT REFERENCE BLADE ROW GEOMETRY TABLES.
C
   81 WRITE(IOUT,508)(J,X(I,J),ALFB(I,J),XP(I,J),ALFPB(I,J),SGMAB(I,J),
     1TMXCB(I,J),FI2CB(I,J),FHB(I,J),FKSHAB(I,J),J=1,KLIM)
C
C     OUTPUT REFERENCE DEVIATION ANGLE TABLES.
C
      IF(IEXDEV(I)) 9113,911,9112
 9113 WRITE(IOUT,5081)
      WRITE(IOUT,5091)
      WRITE(IOUT,600)(FIDIFB(K),K=1,7)
      WRITE(IOUT,9124)
      DO 360 L=1,7
  360 WRITE(IOUT,630) FPHB(L),(EXPBB(K,L),K=1,7)
      GO TO 900
  911 WRITE(IOUT,5082)
      WRITE(IOUT,6001)(YANGSB(K),K=1,8)
      WRITE(IOUT,6002)(EMB(1,K),K=1,8)
      GO TO 900
 9112 K1=1
      IF(K2LM(I)-10)912,912,921
  921 KK=10
      LL1=2
      GO TO 9211
  912 KK=K2LM(I)
      LL1=1
 9211 LL=L2LM(I)
      WRITE(IOUT,5083)
      WRITE(IOUT,9122)
      DO 981 L1=1,LL1
      WRITE(IOUT,9123)(PHIBB(I,K),K=K1,KK)
      WRITE(IOUT,9124)
      DO 98 L=1,LL
      WRITE(IOUT,542) XPB(I,L),(DEL2B(I,K,L),K=K1,KK)
      DO 98 K=K1,KK
   98 DEL2B(I,K,L)=0.017453*DEL2B(I,K,L)
      IF(LL1-1)982,981,982
  982 KK=K2LM(I)
      K1=11
      WRITE(IOUT,9124)
  981 CONTINUE
C
C     OUTPUT REFERENCE BLADE WAKE MOMENTUM THICKNESS/CHORD OR LOSS
C     COEFFICIENT TABLES.
C
  900 LINDEX=IEXLOS(I)+5
      GO TO (899,898,899,898,897,896),LINDEX
  896 K1=1
```

```
      IF( KLZ(I)-1C) 8563,8963,8961
 8961 KK=10
      LL1=2
      GO TC 8962
 8963 KK= KLZ(I)
      LL1=1
 8962 LL= LLZ(I)
      WRITE(IOUT,553)
      WRITE(IOUT,543)
      DO S2 L1=1,LL1
      WRITE(IOUT,9123)(PHIBB(I,K),K=K1,KK)
      WRITE(IOUT,S124)
      DO S5 L=1,LL
      WRITE(IOUT,5422) XPB(I,L),(CMEGBB(I,K,L),K=K1,KK)
   95 CONTINUE
      IF(LL1-1) S7,S2,S7
   97 KK= KLZ(I)
      K1=11
      WRITE(IOUT,9124)
   92 CONTINUE
      GO TC S3
  899 K1=1
      IF(KLZ(I)-10)8S92,8992,89S1
 8991 KK=10
      LL1=2
      GO TO 902
 8992 KK=KLZ(I)
      LL1=1
  902 LL=LLZ(I)
      WRITE(IOUT,554)
      WRITE(IOUT,566)
      DO S021 L1=1,LL1
      WRITE(IOUT,563)(XCBB(I,K),K=K1,KK)
      WRITE(ICUT,9124)
      DO S04 L=1,LL
      WRITE(IOUT,564) RPBB(I,L),(THACBB(I,K,L),K=K1,KK)
  904 CONTINUE
      IF(LL1-1) 9041,SC21,9041
 9041 KK=KLZ(I)
      K1=11
      WRITE(IOUT,9124)
 9021 CONTINUE
      GO TC S3
  898 K1=1
      IF(KLZ(I)-10) 89E2,8982,8S81
 8981 KK=1C
      LL1=2
      GO TO 901
 8982 KK=KLZ(I)
      LL1=1
  901 LL=LLZ(I)
      WRITE(IOUT,57C)
```

```
      WRITE(IOUT,562)
      DO 9011 L1=1,LL1
      WRITE(IOUT,563)(CEQBB(I,K),K=K1,KK)
      WRITE(IOUT,9124)
      DO 903 L=1,LL
      WRITE(IOUT,564) RPBB(I,L),(THACBB(I,K,L),K=K1,KK)
  903 CONTINUE
      IF(LL1-1) 9031,9011,9031
 9031 KK=KLZ(I)
      K1=11
      WRITE(IOUT,9124)
 9011 CONTINUE
      GO TO 93
  897 WRITE(ICUT,550)
      WRITE(IOUT,551) (DEQB(K),K=1,10)
      WRITE(IOUT,552) (THACB(K),K=1,10)
   93 CONTINUE
      RETURN
  503 FORMAT(4X,'IRUN=',I4,10X,'JBASE=',I3,10X,'JLIM=',I3)
  505 FORMAT(7X,'I=',I2,10X,'RN=',F7.1,' RPM',10X,'RSTAR=',F8.5,' FT',10
     1X,'IEXDEV=',I2,10X,'IEXLCS=',I2,//)
  506 FORMAT(7X,'REFERENCE TABLES FOR BLADE ROW GEOMETRY AND GEOMETRY-DE
     1PENDENT LCSS CATA'//)
  507 FORMAT(10X,'J',5X,'X',9X,'ALFB',7X,'XP',7X,'ALFPB',5X,'SGMAB',5X,
     1'TMXCB',5X,'FI2CE',5X,'FHB',6X,'FKSHAB'/)
  508 FORMAT(9X,I2,9F10.4)
  542 FCRMAT(9X,F8.4,2X,10F8.4)
  543 FORMAT(12X,'XPB',43X,'PHIBB'/)
  550 FORMAT(//,7X,'REFERENCE TABLE LOSS(THACB)'//)
  551 FORMAT(/10X,'CEQB= ',10F8.2)
  552 FORMAT( 10X,'THACB=',10F8.2)
  553 FORMAT(//,7X,'REFERENCE TABLE LCSS(OMEGBB)'//)
  554 FORMAT(//,7X,'REFERENCE TABLE LOSS(THACBB)'//)
  562 FORMAT(11X,'RPBB',45X,'CECBB'/)
  563 FORMAT(17X,10F10.4)
  564 FORMAT(6X,F10.4,1X,10F10.4)
  566 FORMAT(11X,'RPBB',45X,'XDBB'/)
  570 FORMAT(//7X,'REFERENCE TABLE LCSS(THACBB)'//)
  600 FORMAT(17X,7F10.1)
  630 FORMAT( 5X,F10.3,2X,7F10.3)
 5031 FORMAT(7X,'YTMACB=',7F8.2)
 5032 FORMAT(13X,9F10.1/)
 5033 FORMAT(5X,F7.2,2X,9F10.3)
 5034 FORMAT(7X,'YANGSB',43X,'SGMGBB'/)
 5038 FORMAT(//4X,'BLACE ROW CATA'//)
 5074 FORMAT(//2X,'AXIAL-FLOW PUMP PERFORMANCE PREDICTION - - INPUT'//)
 5076 FORMAT(//4X,'REFERENCE TABLE INCIDENCE ANGLE BLADE THICKNESS CORRE
     1CTICN'/)
 5077 FORMAT(//4X,'REFERENCE TABLE ZERO-CAMBER INCIDENCE ANGLE AND CAMBE
     1R CCEFFICIENTS (FI10GB,SLP1GB,SLP2GB)'//)
 5078 FORMAT(7X,'YFKIB= ',7F8.2)
```

```
5081 FORMAT(//7X,'REFERENCE TABLE DEVIATION ANGLE-CAMBER EXPONENT(EXPBB
    1)'//)
5082 FORMAT(//7X,'REFERENCE TABLE DEVIATION ANGLE-SLOPE FACTOR(EMB)'//)
5083 FORMAT(//7X,'REFERENCE TABLE DEVIATION ANGLE(DEL2B)'//)
5091 FORMAT(11X,'PPHB',45X,'FICIFB'/)
5422 FORMAT(8X,F8.4,2X,10F8.4)
6001 FORMAT(/10X,'YANGSB=',8F8.2)
6002 FORMAT( 10X,'EMB=   ',8F8.2)
9122 FORMAT(14X,'XPB',45X,'PHIBB'/)
9123 FORMAT(18X,10F8.4)
9124 FORMAT(1H )
9125 FORMAT(1H1)
     END
```

```
      SUBROUTINE INPUT
      ****************
C
C
C
C
     1(*)
      COMMON/BLOCKA/ALFB(5,20),BTA2(20),BTP1B(10),DEQ(20),DEQB(10),FHB
     1(5,20),FH2(20),FIS2D(20),FI10GB(8,9),FI2DB(5,20),FKI(20),FKSHAB
     2(5,20),HLOB(20),SLP1GB(8,9),SLP2GB(8,9),THAC(20),THACB(10),X(5,20)
      COMMON/BLOCKB/ALF1(20),ALF2(20),ALFPB(5,20),ANGST(5,20),ANGSTB
     1(5,8),CS(20),EM(20),EMB(5,8),FKSHA(20),PPFT1(20),PPFT2(20),Q(5,20)
     2,QB(5,20),RB2(20),RN(5),SGMA(20),SGMAB(5,20),SGMGBB(9),THTA(20),
     3TMAXC(20),TMXCB(5,20),XP(5,20),YANGSB(8),YANGS(5,20)
      COMMON/BLOCKD/I,JBASE,JL,JLIM,K,KLIM,KPRI,QR,QRUN,THL
      COMMON/BLOCKF/ILIM,IRUN,IEXLOS(5),IEXDEV(5),K2LM(5),L2LM(5)
     1,LSTAR(5),PHIBB(5,20),XPB(5,20),OMEGBB(5,20,20),DEL2B(5,20,20)
     2,PHIEX(20),RSTAR(5),AREA(5),ARFAC(5)
      COMMON/BLOCKG/K2LIM,L2LIM,YPHIBB(20),YXPB(20),YOMGBB(20,20),YDEL2
     1B(20,20),YPHIEF(20),YR(20),PHIEFC(5)
      COMMON/BLOCKH/IC,IL,IPRI,JPRI,K1LIM
      COMMON/BLOCKI/ EXPBB(7,7),FIDIFB(7),PPHB(7),STARI(20)
      COMMON/BLOCKJ/EMBB(8),FI10I1(40),FI10I2(32),FKIB(7),SLP1I1(16),
     1SLP1I2(16),SLP1I3(16),SLP1I4(16),SLP1I5(8),SLP2I1(16),SLP2I2(16),
     2 SLP2I3(16),SLP2I4(16),SLP2I5(8),TMAXCB(7)
      COMMON/BLOCKK/YDEQB(20),YRPB(7),YTHACB(20,7),YXDB(20),DEQBB(5,20)
     X,RPBB(5,7),THACBB(5,20,7),XDBB(5,20),HLDP(20)
      COMMON/BLOCKL/IIN,IOUT
      COMMON/BLOCKM/KLZ(5),LLZ(5),YXDBB(20),RPBB1(7),THCBB1(20,7),
     1RPBB2(7),THCBB2(20,7),YDECBB(20)
      DIMENSION ALPHZ(6)
      DATA ALPHZ/'  KL','Z(I)','  LL','Z(I)','    ','KLIM'/
C
C     INPUT LIMIT VALUES AND RUN IDENTIFICATION.
C
   73 READ (IIN,501)IC,ILIM,JLIM,JBASE,IRUN,THL
      IF(IC-10)14,3,14
    3 IL=ILIM-1
      JL=JLIM-1
      DO 99 I=1,IL
C
C     INPUT LOSS AND DEVIATION OPTION VALUES.
C
      READ (IIN,5021)IC,J,RSTAR(I)
      IF(IC-18)14,100,14
  100 IF(I-J)14,101,14
  101 READ (IIN,501 )IC,IEXLOS(I),IEXDEV(I)
      IF(IC-19)14,74,14
C
C     INPUT REFERENCE LOSS AND DEVIATION TABLES.
C
   74 IF(IEXLOS(I))75,75,76
   75 IF(IEXDEV(I))800,800,76
   76 READ (IIN,501 )IC, KLZ(I), LLZ(I)
```

```
      IF(IC-20) 14,86,14
   86 IF(KLZ(I)-3) 600,601,601
  600 WRITE(IOUT,1000)(ALPHZ(IZ),IZ=1,2),I,ID
      STOP
  601 IF(LLZ(I)-3) 602,603,603
  602 WRITE(IOUT,1000)(ALPHZ(IZ),IZ=3,4),I,ID
      STOP
  603 K2LIM=KLZ(I)
      L2LIM= LLZ(I)
      READ (IIN,533)ID,(PHIBB(I,K),K=1,K2LIM)
      IF(ID-21)14,78,14
   78 READ (IIN,533)ID,(XPB(I,K),K=1,L2LIM)
      IF(ID-22)14,102,14
  102 IF(IEXLOS(I))89,89,79
   79 DO 80 K=1,K2LIM
      READ (IIN,532)ID,(OMEGBB(I,K,L),L=1,L2LIM)
      IF(ID-23)14,80,14
   80 CONTINUE
   89 IF(IEXDEV(I))99,99,103
  103 DO 85 L=1,K2LIM
      READ (IIN,532)ID,(DEL2B(I,L,K),K=1,L2LIM)
      IF(ID-24)14,85,14
   85 CONTINUE
      K2LM(I)=KLZ(I)
      L2LM(I)=LLZ(I)
C
C     INPUT REFERENCE WAKE MOMENTUM/CHORD (THACBB) TABLES.
C
  800 LINDEX=IEXLOS(I)+5
      GO TO (812,813,814,815,811),LINDEX
  811 GO TO 99
  812 READ (IIN,501 )ID,KLZ(I),LLZ(I)
      IF(ID-25)14,816,14
  816 IF(KLZ(I)-3) 604,605,605
  604 WRITE(IOUT,1000)(ALPHZ(IZ),IZ=1,2),I,ID
      STOP
  605 IF(LLZ(I)-3) 606,607,607
  606 WRITE(IOUT,1000)(ALPHZ(IZ),IZ=3,4),I,ID
      STOP
  607 KK=KLZ(I)
      LL=LLZ(I)
  802 READ(IIN,500) ID,(XCBB(I,K),K=1,KK)
      IF(ID-26)14,803,14
  813 READ (IIN,501 )ID,KLZ(I),LLZ(I)
      IF(ID-25)14,817,14
  817 IF(KLZ(I)-3) 608,609,609
  608 WRITE(IOUT,1000)(ALPHZ(IZ),IZ=1,2),I,ID
      STOP
  609 IF(LLZ(I)-3) 610,611,611
  610 WRITE(IOUT,1000)(ALPHZ(IZ),IZ=3,4),I,ID
      STOP
  611 KK=KLZ(I)
```

```
      LL=LLZ(I)
  801 READ(IIN,500) IC,(DEQBB(I,K),K=1,KK)
      IF(IC-26)14,803,14
  803 READ(IIN,500) IC,(RPBB(I,L),L=1,LL)
      IF(IC-27) 14,804,14
  804 DO 805 K=1,KK
  805 READ(IIN,500) IC,(THACBB(I,K,L),L=1,LL)
      IF(IC-28) 14,99,14
  814 KLZ(I)=20
      LLZ(I)=7
      DO 8141 K=1,20
 8141 XDBB(I,K)=YXDBB(K)
      DO 8142 L=1,7
 8142 RPBB(I,L)=RPBB1(L)
      DO 8143 K=1,20
      DO 8143 L=1,7
 8143 THACBB(I,K,L)=THCBB1(K,L)
      GO TO 99
  815 KLZ(I)=20
      LLZ(I)=7
      DO 8151 K=1,20
 8151 DEQBB(I,K)=YDEQBB(K)
      DO 8152 L=1,7
 8152 RPBB(I,L)=RPBB2(L)
      DO 8153 K=1,20
      DO 8153 L=1,7
 8153 THACBB(I,K,L)=THCBB2(K,L)
   99 CONTINUE
C
C     INPUT REFERENCE BLADE ROW GEOMETRY TABLES.
C
      DO 6 L=1,IL
      READ (IIN,501)IC,J
      IF(IC-30)14,4,14
    4 IF(L-J)14,44,14
   44 READ (IIN,501 )IC,KLIM
      IF(IC-31)14,444,14
  444 IF(KLIM-3) 612,613,613
  612 WRITE(IOUT,1000)(ALPHZ(IZ),IZ=5,6),L,ID
      STOP
  613 DO 6 K=1,KLIM
      READ (IIN,5021)IC,J,X(L,K),ALFB(L,K),XP(L,K),ALFPB(L,K),
     1SGMAB(L,K),TMXCB(L,K),F12CB(L,K),FHB(L,K),FKSHAB(L,K)
      IF(IC-32)14,5,14
    5 IF(J-K)14,6,14
    6 CONTINUE
      ENTRY INPUT1(*)
      CONTINUE
C
C     INPUT BLADE ROW RPM AND COMPUTE REFERENCE BLADE SPEED.
C
```

```
   72 DC 7 K=1,IL
      REAC (IIN,500)IC,RN(K)
      IF(IC-50)14,71,14
   71 IF(RN(K)+1.)7,73,7
    7 CONTINLE
      DO 250 K=1,IL
      IF(RN(K))251,250,251
  251 RRN=RN(K)
      GO TC 253
  250 CONTINUE
      DO 255 I=1,IL
  255 USTAR(I)=1
      GO TC 256
  253 DO 252 I=1,IL
  252 USTAR(I)=0.10472*RSTAR(I)*RRN
C
C     OUTPLT PRCBLEM DATA LOAC.
C
  256 CALL INCLT
      RETURN 1
   14 WRITE (IOLT,557)   ID,I,K,L,J
      STCP
  500 FORMAT(I2,(T3,12F6.4))
  501 FORMAT(4I2,I6,F6.4)
  532 FORMAT(I2,(T5,14F5.4))
  533 FORMAT(I2,(T3,14F5.4))
  557 FORMAT(//' ERROR IN INPLT DATA CARD ORDER, SUBRCUTINE INPUT.',2X,
     1'IC=',I3,'I=',I3,'K=',I3,'L=',I3,'J=',I3)
 1000 FORMAT(//'***** ERRCR IN INPUT - ',2A4,' MUST BE GREATER THAN 2 FO
     1R INTERPCLATICN, I= ',I2,' ID= ',I2)
 5021 FORMAT(I2,2X,I2,9F7.4)
      END
```

```
      SUBROUTINE IREF
C     ***************
C
C
C     COMPUTE REFERENCE INCIDENCE ANGLE FOR CONSTANT STAGGER CASCADES
C     BASED ON CAMBER ANGLE, STAGGER ANGLE, MAXIMUM THICKNESS TO CHORD
C     RATIO, SOLIDITY, AND CORRECTION FACTOR FOR THICKNESS DISTRIBUTION.
C
C
      COMMON/BLOCKA/ALFB(5,20),ETA2(20),BTP1B(10),DEQ(20),DEQB(10),FHB
     1(5,20),FH2(20),FIS2D(20),FI10GB(8,9),FI2DB(5,20),FKI(20),FKSHAB
     2(5,20),HLCB(20),SLP1GB(8,9),SLP2GB(8,9),THAC(20),THACB(10),X(5,20)
      COMMON/BLOCKB/ALF1(20),ALF2(20),ALFPB(5,20),ANGST(5,20),ANGSTB
     1(5,8),CS(20),EM(20),EMB(5,8),FKSHA(20),PPFT1(20),PPFT2(20),Q(5,20)
     2,QE(5,20),RB2(20),RN(5),SGMA(20),SGMAB(5,20),SGMGBB(9),THTA(20),
     3TMAXC(20),TMXCB(5,20),XP(5,20),YANGSB(8),YANGS(5,20)
      COMMON/BLOCKD/I,JBASE,JL,JLIM,K,KLIM,KPRI,QR,QRUN,THL
      COMMON/BLOCKI/ EXPBB(7,7),FIDIFB(7),PPHB(7),STARI(20)
      COMMON/BLOCKJ/EMBB(8),FI10I1(40),FI10I2(32),FKIB(7),SLP1I1(16),
     1SLP1I2(16),SLP1I3(16),SLP1I4(16),SLP1I5(8),SLP2I1(16),SLP2I2(16),
     2 SLP2I3(16),SLP2I4(16),SLP2I5(8),TMAXCB(7)
      COMMON/BLOCKL/II,IO
      DIMENSION FI010G(20),SLOP1G(20),SLOP2G(20),YANGS1(20)
      DIMENSION ALPHZ(18)
      DATA ALPHZ/'   F','I10G','B(YA','NGSB',',SGM','GBB)','   S',
     1           'LP1G','B(YA','NGSB',',SGM','GBB)','   S','LP2G',
     2           'B(YA','NGSB',',SGM','GBB)'/
C
C
      DO 10 J=1,JLIM
   10 YANGS1(J)=YANGS(K,J)
      CALL FIT2D(YANGS1,FI010G,SGMA,YANGSB,FI10GB,SGMGBB,8,9,
     XJLIM,8,9,IWARN)
      GO TO (201,200),IWARN
  200 WRITE(IO,501)(ALPHZ(IZ),IZ=1,6)
  201 CALL FIT2D(YANGS1,SLOP1G,SGMA,YANGSB,SLP1GB,SGMGBB,8,9,
     XJLIM,8,9,IWARN)
      GO TO (203,202),IWARN
  202 WRITE(IO,501)(ALPHZ(IZ),IZ=7,12)
  203 CALL FIT2D(YANGS1,SLOP2G,SGMA,YANGSB,SLP2GB,SGMGBB,8,9,
     XJLIM,8,9,IWARN)
      GO TO (205,204),IWARN
  204 WRITE(IO,501)(ALPHZ(IZ),IZ=13,18)
  205 DO 100 J=1,JLIM
  100 STARI(J)=FKSHA(J)*FKI(J)*FI010G(J)+SLOP1G(J)*THTA(J)*57.29578
     X +SLOP2G(J)*THTA(J)*THTA(J)*57.29578*57.29578
      DO 60 J=1,JLIM
      BTP1=57.29578*ALF1(J)+STARI(J)
      IF(BTP1.LE.75.)  GO TO 60
      WRITE (IO,500) J,BTP1
   60 CONTINUE
```

```
      RETURN
  500 FORMAT(/'  IREF AT STREAMLINE',I4,' REQUIRED EXTRAPOLATION OF TABL
     1ES BECAUSE BTP1=',F7.2,' DEG'/)
  501 FORMAT(//'***** WARNING - FIT2D CALLED IN IREF - EXTRAPOLATION OF
     1TABLE ',6A4)
      END
```

```
      SUBROUTINE LOSS
C     ***************
C
C
     1(R,VZ,VU,BTAP1,BTAP2,FNC1,U1,U2,FH2,FIS2D,DEQB,THACB,I,K,JLIM,
     2HLOB,DEQ,THAC)
      DIMENSION BTAP1(20),BTAP2(20),DEQ(20),DEQB(10),
     1FH2(20),FIS2D(20),FNC1(20),HLOB(20),R(5,20),
     2THAC(20),THACB(10),U1(20),U2(20),VU(5,20),VZ(5,20),OMEGB(20)
      DIMENSION XVP1(20),XVP2(20),XD(20),XDD(5,20),DEQDD(5,20),THACDD(5,
     120)
      COMMON/BLOCKB/ALF1(20),ALF2(20),ALFPB(5,20),ANGST(5,20),ANGSTB
     1(5,8),CS(20),EM(20),EMB(5,8),FKSHA(20),PPFT1(20),PPFT2(20),Q(5,20)
     2,QB(5,20),RB2(20),RN(5),SGMA(20),SGMAB(5,20),SGMGBB(9),THTA(20),
     3TMAXC(20),TMXCB(5,20),XP(5,20),YANGSB(8),YANGS(5,20)
      COMMON/BLOCKF/ILIM,IRUN,IEXLOS(5),IEXDEV(5),K2LM(5),L2LM(5)
     1,USTAR(5),PHIBB(5,20),XPB(5,20),OMEGBB(5,20,20),DEL2B(5,20,20)
     2,PHIEX(20),RSTAR(5),AREA(5),ARFAC(5)
      COMMON/BLOCKG/K2LIM,L2LIM,YPHIBB(20),YXPB(20),YOMGBB(20,20),YDEL2
     1B(20,20),YPHIEF(20),YR(20),PHIEFC(5)
      COMMON/BLOCKI/ EXPBB(7,7),FIDIFB(7),PPHB(7),STARI(20)
      COMMON/BLOCKJ/EMEB(8),FI1CI1(40),FI1OI2(32),FKIB(7),SLP1I1(16),
     1SLP1I2(16),SLP1I3(16),SLP1I4(16),SLP1I5(8),SLP2I1(16),SLP2I2(16),
     2 SLP2I3(16),SLP2I4(16),SLP2I5(8),TMAXCB(7)
      COMMON/BLOCKK/YDEQB(20),YRPB(7),YTHACB(20,7),YXDB(20),DEQBB(5,20)
     1,RPBB(5,7),THACBB(5,20,7),XDBB(5,20),HLOP(20)
      COMMON/BLOCKL/II,IC
      COMMON/BLOCKM/KLZ(5),LLZ(5),YXDBB(20),RPBB1(7),THCBB1(20,7),
     1RPBB2(7),THCBB2(20,7),YDEQBB(20)
      DIMENSION ALPHZ(15)
      DATA ALPHZ/'    Y','THAC','B(YX','DB,Y','RPB)','    YT','HACB',
     1            '(YDE','QB,Y','RPB)',' YOM','GBB(','YPHI','BB,Y',
     2            'YPB)'/
      C0117=.007
      IF(U1(1))10,11,10
   10 C61=-.61
      GO TO 12
   11 C61=.61
   12 LINDEX=IEXLOS(I)+5
      GO TO (30,20,30,20,50,40),LINDEX
   30 KK=KLZ(I)
      LL=LLZ(I)
C
C     COMPUTE THETA OVER CHORD RATIO(THAC) FROM D-FACTOR AND BLADE-
C     ELEMENT LOCATION.
C
      IF(RN(I)) 32,33,32
   32 KSI=1
      GO TO 34
   33 KSI=-1
   34 DO 31 J=1,JLIM
      XVP1(J)=VZ(I,J)/(COS(BTAP1(J)))
```

```
      XVP2(J)=VZ(K,J)/(COS(BTAP2(J)))
   31 XD(J)=1.-(XVP2(J)/XVP1(J))+KSI*(R(K,J)*VU(K,J)-R(I,J)*VU(I,J))/
     1(XVP1(J)*(R(K,J)+R(I,J))*SGMA(J))
      CALL FIT2C(XC,THAC,PPFT2,YXCB,YTHACB,YRPB,KK,LL,JLIM,20,7,IWARN)
      GO TC (61,60),IWARN
   60 WRITE(IC,1C1)(ALPHZ(IZ),IZ=1,5)
   61 GO TC 25
   20 KK=KLZ(I)
      LL=LLZ(I)
C
C     COMPUTE DEQ.
C
   50 DO 21 J=1,JLIM
      C1=R(I,J)/R(K,J)
      C2=CCS(BTAP1(J))/VZ(I,J)
      C3=4./(3.*FH2(J)-1.)
      FIIPS=57.29578*ABS(FNC1(J)-STARI(J)/57.29578)
      DEQ(J)=1.12+C0117*FIIPS**1.43
      DEQ(J)=((C61*C2*COS(BTAP1(J))/SGMA(J))*(C1*(VU(I,J)-U1(J))
     1+U1(J)/C1-VU(K,J))+DEQ(J))*COS(BTAP2(J))/(C2*VZ(K,J))
   21 CONTINUE
      IF(LINDEX-5) 22,23,22
C
C     COMPUTE THAC AND HEAD LOSS FROM DEQ AND BLADE-ELEMENT LOCATION.
C
   22 CALL FIT2C(DEQ,THAC,PPFT2,YDEQB,YTHACB,YRPB,KK,LL,JLIM,20,7,IWARN)
      GO TC (25,62),IWARN
   62 WRITE(IO,101)(ALPHZ(IZ),IZ=6,10)
   25 DO 24 J=1,JLIM
      C4=(VZ(I,J)*VZ(I,J)/(CCS(BTAP1(J))*COS(BTAP1(J))))
   24 HLCB(J)=SGMA(J)*THAC(J)*C4/(32.174*COS(BTAP2(J)))
      RETURN
C
C     COMPUTE THAC AND HEAD LOSS FROM DEQ.
C
   23 DO 26 J=1,JLIM
   26 XDC(1,J)=DEQ(J)
      DO 28 J=1,10
      DEQDD(1,J)=DEQB(J)
   28 THACDD(1,J)=THACB(J)
      CALL FIT1C(XDC,THAC,DEQDD,THACDD,JLIM,10,1,1,IWARN)
      GO TC (67,66),IWARN
   66 WRITE(IO,100)
   67 DO 27 J=1,JLIM
      C4=SGMA(J)*THAC(J)*FH2(J)/CCS(BTAP2(J))
   27 HLCB(J)=(C3*C4*((VZ(I,J)/CCS(BTAP2(J)))*(VZ(I,J)/COS(BTAP2(J))))/
     1((1.0-C4)**3))/64.348
      RETURN
   40 KK=KLZ(I)
      LL=LLZ(I)
C
C     COMPUTE LOSS COEFFICIENT AND HEAD LOSS FROM EFFECTIVE FLOW
```

```
C      COEFFICIENT ANC RACIAL PCSITION.
C
      CALL FIT2C(YPHIEF,OMEGB,YR,YPHIBB,YOMGBB,YXPB,KK,LL,JLIM,20,20,
     1IWARN)
      GC TC (65,64),IWARN
   64 WRITE(IO,101)(ALFHZ(IZ),IZ=11,15)
   65 DO 41 J=1,JLIM
      HLCB(J)=CMEGB(J)*((VZ(I,J)/CCS(BTAP1(J)))**2)/64.348
      C4=VZ(I,J)*VZ(I,J)/(COS(BTAP1(J))*COS(BTAP1(J)))
   41 THAC(J)=(HLCB(J)*32.174*CCS(BTAP2(J)))/(C4*SGMA(J))
      RETURN
  100 FORMAT(//'***** WARNING - EXTRAPOLATICN OF TABLE THACDD(DEQDD) IN
     1FIT1C-CALLED IN LCSS')
  101 FORMAT(//'***** WARNING - FIT2D CALLED IN LOSS - EXTRAPOLATICN OF
     1TABLE ',5A4)
      END
```

```
      SUBROUTINE MAVE
C     ***************
C
C
     1(I,J,K,R,VZ,VU,H,U1,U2,QRUN,JLIM,JL,DELH,DELHI,RN,IL)
      COMMON/BLOCKL/II,IO
      DIMENSION DELH(20),DELHI(20),H(5,20),R(5,20),REFFP(20),
     1RHRP(20),RVEL(20),SEFFP(20),SHRP(20),SDELH(20),TISPD(5),U1(20),
     2U2(20),VU(5,20),VZ(5,20),W(5,20),RN(5)
      DO 1 J=1,JLIM
    1 RVEL(J)=R(K,J)*VZ(K,J)
      DENOM=0
      DO 2 J=1,JL
    2 DENOM=DENOM+((RVEL(J+1)+RVEL(J))*(R(K,J+1)-R(K,J)))/2.0
      IF(RN(I)) 3,12,3
   12 IF(IL-1) 13,10,13
   13 IF(RN(I-1)) 7,10,7
    3 DO 4 J=1,JLIM
      RHRP(J)=R(K,J)*VZ(K,J)*DELH(J)
    4 REFFP(J)=RHRP(J)/DELHI(J)
      RHRI=0
      REFFI=0
      DO 5 J=1,JL
      RHRI=RHRI+((RHRP(J+1)+RHRP(J))*(R(K,J+1)-R(K,J)))/2.0
    5 REFFI=REFFI+((REFFP(J+1)+REFFP(J))*(R(K,J+1)-R(K,J)))/2.0
      RMAHR=RHRI/DENOM
      RMAE=REFFI/DENOM
      AFLCO=.000709*QRUN/((R(I,JLIM)*R(I,JLIM)-R(I,1)*R(I,1))*U1(JLIM))
      AFLCO1=.000709*QRUN/((R(K,JLIM)*R(K,JLIM)-R(K,1)*R(K,1))*U2(JLIM))
      RHRCO=32.174*RMAHR/(U2(JLIM)*U2(JLIM))
      WRITE (IO,100)RMAHR,RMAE,AFLCO,AFLCO1,RHRCO,I
      TISPD(I)=U1(JLIM)
      DO 6 J=1,JLIM
    6 W(I,J)=DELHI(J)
      GO TO 10
    7 DO 8 J=1,JLIM
      SDELH(J)=H(K,J)-H(I-1,J)
      SHRP(J)=R(K,J)*VZ(K,J)*SDELH(J)
    8 SEFFP(J)=SHRP(J)/W(I-1,J)
      SHRI=0
      SEFFI=0
      DO 9 J=1,JL
      SHRI=SHRI+((SHRP(J+1)+SHRP(J))*(R(K,J+1)-R(K,J)))/2.0
    9 SEFFI=SEFFI+((SEFFP(J+1)+SEFFP(J))*(R(K,J+1)-R(K,J)))/2.0
      SMAHR=SHRI/DENOM
      SMAE=SEFFI/DENOM
      SHRCO=32.174*SMAHR/(TISPD(I-1)*TISPD(I-1))
      WRITE (IO,101)SMAHR,SMAE,SHRCO,I
   10 CONTINUE
      RETURN
```

```
100 FORMAT(1HO,46H ROTOR MASS AVERAGED HEAD RISE FROM I TO I+1 =,F10.4
   1,3H FT/52H  ROTOR MASS AVERAGED EFFICIENCY BETWEEN I AND I+1 =,F6.
   24,/33H  AVERAGE FLOW COEFFICIENT AT I =,F6.4/35H  AVERAGE FLOW COE
   3FFICIENT AT I+1 =,F6.4/38H  ROTOR HEAD RISE COEFFICIENT AT I+1 =,
   4F6.4/4H   I=,I2)
101 FORMAT(1HO,48H STAGE MASS AVERAGED HEAD RISE FROM I-1 TO I+1 =,F10
   1.4,3H FT/54H  STAGE MASS AVERAGED EFFICIENCY BETWEEN I-1 AND I+1 =
   2,F6.4/50H  STAGE HEAD RISE COEFFICIENT (ROTOR IN TIP SPD) =,F6.4/
   3 4H   I=,I2)
    END
```

```
      SUBROUTINE OUTPUT
C     ****************
C
C
      COMMON/BLOCKA/ALFE(5,20),BTA2(20),BTP1B(10),DEQ(20),DEQB(10),FHB
     1(5,20),FH2(20),FIS2D(20),FI10GB(8,9),FI2DB(5,20),FKI(20),FKSHAB
     2(5,20),HLCB(20),SLP1GB(8,9),SLP2GB(8,9),THAC(20),THACB(10),X(5,20
      COMMON/BLOCKB/ALF1(20),ALF2(20),ALFPB(5,20),ANGST(5,20),ANGSTB
     1(5,8),CS(20),EM(20),EMB(5,8),FKSHA(20),PPFT1(20),PPFT2(20),Q(5,20
     2,QB(5,20),RB2(20),RN(5),SGMA(20),SGMAB(5,20),SGMGBB(9),THTA(20),
     3TMAXC(20),TMXCB(5,20),XP(5,20),YANGSB(8),YANGS(5,20)
      COMMON/BLOCKC/BTAP1(20),BTAP2(20),DELH(20),DELHI(20),DEL2(20),
     1FNC1(20),H(5,20),HLOSS(5,20),R(5,20),U1(20),U2(20),VU(5,20),VZ(5,
     220)
      COMMON/BLOCKD/I,JBASE,JL,JLIM,K,KLIM,KPRI,QR,QRUN,THL
      COMMON/BLOCKF/ILIM,IRUN,IEXLOS(5),IEXDEV(5),K2LM(5),L2LM(5)
     1,USTAR(5),PHIBB(5,20),XPB(5,20),OMEGBB(5,20,20),DEL2B(5,20,20)
     2,PHIEX(20),RSTAR(5),AREA(5),ARFAC(5)
      COMMON/BLOCKI/ EXPBB(7,7),FIDIFB(7),PPHB(7),STARI(20)
      COMMON/BLOCKK/YDEQB(20),YRPB(7),YTHACB(20,7),YXDB(20),DEQBB(5,20)
     X,RPBB(5,7),THACBB(5,20,7),XDBB(5,20),HLDP(20)
      COMMON/BLOCKL/II,IO
      DIMENSION RRT(20),XBETA(20),XBETA2(20),XOMEG(20),RRT2(20),XEFF(20
     1,XVP1(20),XVP2(20),XV1(20),XV2(20),XHSTT1(20),XHSTT2(20),XPHI1(20
     2,XPHI2(20),XPSI(20),XPSII(20),XD(20),XBTAP1(20),XFNC1(20)
     3,XBTAP2(20),XDEL2(20),XPFT1(20),XPFT2(20),XTHTA(20)
C
C     COMPUTE EQUIVALENT D-FACTOR AND HEAD LOSS DIFFERENCE.
C
      C0117=.007
      IF(U1(1))10,11,10
   10 C61=-.61
      GO TO 12
   11 C61=.61
   12 DO 20 J=1,JLIM
      C1=R(I,J)/R(K,J)
      C2=COS(BTAP1(J))/VZ(I,J)
      C3=4./(3.*FH2(J)-1.)
      FIIPS=57.29578*ABS(FNC1(J)-STARI(J)/57.29578)
      DEQ(J)=1.12+C0117*FIIPS**1.43
      DEQ(J)=((C61*C2*COS(BTAP1(J))/SGMA(J))*(C1*(VU(I,J)-U1(J))
     1+U1(J)/C1-VU(K,J))+DEQ(J))*COS(BTAP2(J))/(C2*VZ(K,J))
   20 CONTINUE
      DO 30 J=1,JLIM
      IF(HLOSS(I,J)) 30,31,30
   30 HLDP(J)=(HLCB(J)-HLOSS(I,J))/HLOSS(I,J)
   31 CONTINUE
C
C     PREPARE BLADE-ELEMENT RESULTS FOR OUTPUT.
C
   42 DO 43 J=1,JLIM
      RRT(J)=R(I,J)/R(I,JLIM)
```

```
      RRT2(J)=R(K,J)/R(K,JLIM)
      XPFT1(J)=100.*PPFT1(J)
      XPFT2(J)=100.*PPFT2(J)
      XTHTA(J)=57.29578*THTA(J)
      XVP1(J)=VZ(I,J)/(COS(BTAP1(J)))
      XVP2(J)=VZ(K,J)/(COS(BTAP2(J)))
      XBETA(J)=57.29578*ATAN(VU(I,J)/VZ(I,J))
      XBETA2(J)=57.29578*ATAN(VU(K,J)/VZ(K,J))
      XOMEG(J)=64.348*HLOSS(I,J)*COS(BTAP1(J))*COS(BTAP1(J))/(VZ(I,J)*
     1VZ(I,J))
      XBTAP1(J)=57.29578*BTAP1(J)
      XFNC1(J)=57.29578*FNC1(J)
      XBTAP2(J)=57.29578*BTAP2(J)
      DELHI(J)=(U2(J)*VU(K,J)-U1(J)*VU(I,J))/32.174
      DELH(J)=H(K,J)-H(I,J)
      XV1(J)=(VZ(I,J)*VZ(I,J)+VU(I,J) *VU(I,J))**0.5
      XV2(J)=(VZ(K,J)*VZ(K,J)+VU(K,J) *VU(K,J))**0.5
      XHSTT1(J)=H(I,J)-((XV1(J)*XV1(J))/64.348)
      XHSTT2(J)=H(K,J)-((XV2(J)*XV2(J))/64.348)
      XDEL2(J)=57.29578*DEL2(J)
      IF(RN(I))44,45,44
   44 XEFF(J)=DELH(J)/DELHI(J)
      XPHI1(J)=VZ(I,J)/U1(JLIM)
      XPHI2(J)=VZ(K,J)/U2(JLIM)
      XPSI(J) =64.348*DELH(J) /(U2(JLIM)*U2(JLIM))
      XPSII(J)=64.348*DELHI(J)/(U2(JLIM)*U2(JLIM))
      XD(J)=1.-(XVP2(J)/XVP1(J))+(R(K,J)*VU(K,J)-R(I,J)*VU(I,J))/(XVP1(J
     1)*(R(K,J)+R(I,J))*SGMA(J))
      GO TO 43
   45 XEFF(J)=0
      XPHI1(J)=0
      XPHI2(J)=0
      XPSI(J)=0
      XPSII(J)=0
      XD(J)=1.-(XVP2(J)/XVP1(J))-(R(K,J)*VU(K,J)-R(I,J)*VU(I,J))/(XVP1(J
     1)*(R(K,J)+R(I,J))*SGMA(J))
   43 CONTINUE
C
C     OUTPUT BLADE-ELEMENT RESULTS.
C
      WRITE (IO,514)GRUN
      WRITE (IO,525)
      WRITE (IO,515)
      WRITE (IO,519)
      DO 50 KJ=1,JLIM
      J=JLIM-KJ+1
   50 WRITE(IO,516)J,RRT(J) ,U1(J),XV1(J),VZ(I,J),VU(I,J),XVP1(J),H(I,J)
     1,XHSTT1(J),XBETA(J),XBTAP1(J)
      WRITE (IO,519)
      WRITE (IO,530)
      WRITE (IO,515)
      WRITE (IO,519)
```

```
      DO 60 KJ=1,JLIM
      J=JLIM-KJ+1
   60 WRITE(IC,518)J,RRT2(J),U2(J),XV2(J),VZ(K,J),VU(K,J),XVP2(J),H(K,J)
     1,XHSTT2(J),HLOSS(I,J),XBETA2(J),XBTAP2(J)
      WRITE (IC,535)
      WRITE (IC,540)
      WRITE (IO,521)
      DO 70 KJ=1,JLIM
      J=JLIM-KJ+1
   70 WRITE(IO,520) J,RRT(J),XPFT1(J),XPHI1(J),XFNC1(J),STARI(J),
     1 RRT2(J),ANGST(K,J),XTHTA(J),SGMA(J),TMAXC(J)
      WRITE (IO,519)
      WRITE (IC,530)
      WRITE(IO,522)
      DO 80 KJ=1,JLIM
      J=JLIM-KJ+1
   80 WRITE(IO,523) J,RRT2(J),XPFT2(J),XPHI2(J),XDEL2(J),XPSI(J),
     1XPSII(J),XEFF(J),XOMEG(J),XC(J),DEQ(J),THAC(J),HLOP(J)
C
C     OUTPUT MASS AVERAGED RESULTS.
C
      IL=ILIM-1
      CALL MAVE(I,J,K,R,VZ,VU,H,U1,U2,QRUN,JLIM,JL,DELH,DELHI,RN,IL)
      RETURN
  514 FORMAT(11H1FLOW RATE=,F8.1,4H GPM///)
  515 FORMAT(   '  J      R/R(TIP)          U,FPS          V,FPS       VZ,FPS
     1 VU,FPS    V(REL),FPS   TOT HD,FT    STAT HD,FT   HD LOSS,FT    BETA,DEG
     2   BETAP,DEG')
  516 FORMAT(I3,F12.3,7F12.2,12X,2F11.2)
  518 FORMAT(I3,F12.3,8F12.2,2F11.2)
  519 FORMAT(1H0)
  520 FORMAT(I3,F11.3,F11.1,F11.3,2F11.2,F15.3,2F10.2,F10.3,F10.4)
  521 FORMAT('    J      R/RT(I)      %PH F T        PHI1     INCID,DEG     REF IN
     1C         R2/RT(I)   STAG,DEG   CMBR,DEG   SOLIDITY     TMAX/C'//)
  522 FORMAT(   '  J      R/RT(I)      %PH F T         PHI2     DEV,DEG          P
     1SI          PSI I        EFFIC    OMEGABAR   D-FACTOR   EQ D-FAC (THTA/C)A
     1LOSS DIFF'//)
  523 FORMAT(I3,F11.3,F11.1,F11.3,F11.2,4F11.3,2F10.3,2F10.4)
  525 FORMAT('  ENTRANCE QUANTITIES'/)
  530 FORMAT ('  EXIT QUANTITIES'/)
  535 FORMAT (1H1/)
  540 FORMAT (21H  ENTRANCE QUANTITIES 44X 21H GEOMETRIC PARAMETERS/)
      END
```

```
      SUBRCUTINE RADEGC
      *****************

 1(*,*)
      RACIAL EQUILIBRIUM AND CONTINUITY ITERATIONS.

      COMMCN/BLCCKA/ALFB(5,20),BTA2(20),BTP1B(10),DEQ(20),DEQB(10),FHB
     1(5,2C),FH2(20),FIS2C(20),FI10GB(8,9),FI2DB(5,20),FKI(20),FKSHAB
     2(5,20),HLCB(20),SLP1GB(8,9),SLP2GB(8,9),THAC(20),THACB(10),X(5,20)
      COMMCN/BLCCKB/ALF1(20),ALF2(20),ALFPB(5,20),ANGST(5,20),ANGSTB
     1(5,8),CS(2C),EM(20),EMB(5,8),FKSHA(20),PPFT1(20),PPFT2(20),Q(5,20)
     2,QE(5,2C),RB2(20),RN(5),SCMA(20),SGMAB(5,20),SGMGBB(9),THTA(2C),
     3TMAXC(2C),TMXCB(5,20),XP(5,20),YANGSB(8),YANGS(5,20)
      CCMMCN/BLCCKC/BTAP1(20),BTAP2(20),DELH(20),DELHI(20),DEL2(20),
     1FNC1(2C),H(5,20),HLOSS(5,20),R(5,20),U1(20),U2(20),VU(5,20),VZ(5,
     220)
      COMMCN/BLCCKD/I,JBASE,JL,JLIM,K,KLIM,KPRI,QR,QRUN,THL
      COMMCN/BLOCKF/ILIM,IRUN,IEXLOS(5),IEXDEV(5),K2LM(5),L2LM(5)
     1,USTAR(5),PHIBB(5,20),XFB(5,20),OMEGBB(5,20,20),DEL2B(5,20,20)
     2,PHIEX(2C),RSTAR(5),AREA(5),ARFAC(5)
      COMMCN/BLOCKG/K2LIM,L2LIM,YPHIBB(20),YXPB(20),YCMGBB(20,20),YDEL2
     1B(20,20),YPHIEF(20),YR(20),PHIEFC(5)
      COMMCN/BLCCKJ/EMEB(8),FI1CI1(40),FI10I2(32),FKIB(7),SLP1I1(16),
     1SLP1I2(16),SLP1I3(16),SLP1I4(16),SLP1I5(8),SLP2I1(16),SLP2I2(16),
     2 SLP2I3(16),SLP2I4(16),SLP2I5(8),TMAXCB(7)
      COMMCN/BLCCKL/II,IO
      DIMENSICN ALPHZ(10)
      DATA ALPHZ/'    A','LFPB','(XP)','   FK','SHAB','(XP)','    S',
     1           'GMAB','(XP)','R(Q)'/

      DETERMINE BLADE-ELEMENT GECMETRY PARAMETERS, WHEEL SPEED AND RELATIVE
      LEAVING FLOW ANGLES.

      DO 33 KKK=1,1C
      CALL FIT1C(R,ALF2,XP,ALFPB,JLIM,KLIM,I,K,IWARN)
      GO TC (4C1,400),IWARN
  400 WRITE(IO,7CC)(ALFHZ(IZ),IZ=1,3)
  401 CALL FIT1C (R,FKSHA,XP,FKSHAB,JLIM,KLIM,I,K,IWARN)
      GO TC (403,402),IWARN
  402 WRITE(IO,7CC)(ALPHZ(IZ),IZ=4,6)
  403 CALL FIT1C(R,SCMA,XP,SGMAB,JLIM,KLIM,I,K,IWARN)
      GO TC (405,404),IWARN
  404 WRITE(IO,7CO)(ALPHZ(IZ),IZ=7,9)
  405 DO 43 J=1,JLIM
      U2(J)=.1C472*RN(I)*R(K,J)
      ANGST(K,J)=C.5*57.29578*ALF1(J)+.5*ALF2(J)
      YANGS(K,J)=ABS(ANGST(K,J))
   43 ALF2(J)=.017453*ALF2(J)
      IF(IEXLCS(I))45,45,47
   45 IF(IEXDEV(I))44,44,47
   47 DO 46 J=1,JLIM
```

```
      YPHIEF(J)=PHIEFC(I)
   46 YR(J)=R(K,J)
C
C     COMPLTE CEVIATICN ANGLES
C
   44 CALL DEV
C
C
      DO 20 J=1,JLIM
      IF(ALF1(J))201,2C2,200
  200 BTAP2(J)=ALF2(J)+DEL2(J)
      GO TC 20
  201 BTAP2(J)=ALF2(J)-DEL2(J)
      GO TC 20
  202 WRITE (IO,511)
      RETURN 1
   20 CONTINUE
C
C     DETERMINE LEAVING WHIRL VELOCITY, TOTAL HEAD ANC AXIAL VELOCITY
C     SATISFYING RACIAL EQUILIBRIUM.
C
      DO 29 KR=1,20
      KNT=1
      KNTT=0
  3C0 J=JBASE
  301 VU(K,J)=U2(J)-VZ(K,J)*SIN(BTAP2(J))/COS(BTAP2(J))
      H(K,J)=H(I,J)+.03106*(U2(J)*VU(K,J)-CS(J))-HLOSS(I,J)
      IF(KNT-1) 1C1,1CC,101
  101 KJ=J-1
      GO TO 102
  100 KJ=J+1
  102 S=(R(K,KJ)-R(K,J))/R(K,KJ)
      E=S*R(K,KJ)/R(K,J)-1.
      D=S-1.
      C=-(VZ(K,J)*VZ(K,J))-64.348*(H(I,KJ)-HLOSS(I,KJ)-H(K,J))
     1+2.*CS(KJ)+D*U2(KJ)*U2(KJ)+E*VU(K,J)*VU(K,J)
      B=SIN(BTAP2(KJ))/COS(BTAP2(KJ))
      A=1.+(S+1.)*B*B
      B=-2.*U2(KJ)*S*B
      RAC=B*B-4.*A*C
      IF(RAC)25,21,21
   25 WRITE (IO,512)
      KNTT=1
      IF(KNT-1) 103,104,103
  103 RETURN 2
  104 KNT=2
      GO TC 300
   21 VZ(K,KJ)=(-B+SQRT(RAC))/(2.*A)
      IF(KNT-1) 106,105,106
  106 IF(J-2) 112,112,111
  111 J=J-1
```

```
      GO TO 301
  112 KJ=1
      GO TO 108
  105 IF(J-JL) 600,107,107
  600 J=J+1
      GO TO 301
  107 KJ=JLIM
  108 VU(K,KJ)=U2(KJ)-VZ(K,KJ)*SIN(BTAP2(KJ))/COS(BTAP2(KJ))
      H(K,KJ)=H(I,KJ)+.03106*(U2(KJ)*VU(K,KJ)-CS(KJ))-HLOSS(I,KJ)
      IF(KNT-1) 110,109,110
  109 KNT=2
      GO TO 300
  110 IF(KNTT.GT.0) GO TO 103
C
C     COMPUTE STREAM FUNCTION DISTRIBUTION FOR LEAVING FLOW AND REVISE
C     BASE STREAMLINE VELOCITY.
C
      Q(K,1)=0.
      DO 28 J=1,JL
   28 Q(K,J+1)=Q(K,J)+CR*(VZ(K,J+1)+VZ(K,J))*(R(K,J+1)*R(K,J+1)
     1-R(K,J)*R(K,J))
      IF(ABS(Q(K,JLIM)-1.)-.005)30,29,29
   29 VZ(K,JBASE)=VZ(K,JBASE)*QB(1,JLIM)/Q(K,JLIM)
      WRITE(IO,515)
C
C     REVISE LEAVING FLOW STREAMLINE RADII BASED ON STREAM FUNCTION
C     DISTRIBUTION.
C
   30 CALL FIT1D(QB,RB2,Q,R,JL   ,JLIM,K,1,IWARN)
      GO TO (407,406),IWARN
  406 WRITE(IO,700) ALPHZ(10)
  407 DO 31 J=2,JL
      IF(ABS(RB2(J)-R(K,J))-.01*R(K,J))31,31,32
   31 CONTINUE
      RETURN
   32 DO 33 J=2,JL
      R(K,J)=RB2(J)
   33 CONTINUE
      WRITE(IO,514)
      RETURN
  511 FORMAT(21H1ALF1 = 0 NOT ALLOWED)
  512 FORMAT(1H1////35HORADIAL EQUILIBRIUM SOLUTION FAILED)
  514 FORMAT(1H0,'RADIAL EQUILIBRIUM SOLUTION AND STREAMLINE RADIAL ADJU
     1STMENTS NOT ACHIEVED IN 10 ITERATIONS')
  515 FORMAT(1H0,'RADIAL EQUILIBRIUM AT CONTINUITY NOT ACHIEVED IN 20 IT
     1ERATIONS')
  700 FORMAT(//'***** WARNING - FIT1D CALLED IN RADEQC - EXTRAPOLATION O
     1F TABLE ',3A4)
      END
```

Sample Input Load 1.

```
10 32010    820    .01
18   1    .375
19-1-1
18   2    .375
19
30 1
31 7
32 1 1 .1500  49.50  .1500 -10.7   2.52   .100   0.     1.08   .7
32 1 2 .1725  55.60  .1725  11.10  2.19   .097   0.     1.08   .7
32 1 3 .2175  62.50  .2175  38.60  1.74   .091   0.     1.08   .7
32 1 4 .2625  66.40  .2625  52.40  1.44   .085   0.     1.08   .7
32 1 5 .3075  69.40  .3075  60.30  1.23   .079   0.     1.08   .7
32 1 6 .3525  71.80  .3525  65.40  1.07   .073   0.     1.08   .7
32 1 7 .3750  72.80  .3750  67.50  1.00   .070   0.     1.08   .7
30 2
31 7
32 2 1 .1500 -51.44  .1500  10.76  2.34   .08    0.     1.08   .7
32 2 2 .1725 -49.00  .1725  10.60  2.09   .08    0.     1.08   .7
32 2 3 .2175 -44.30  .2175  10.90  1.65   .08    0.     1.08   .7
32 2 4 .2625 -40.20  .2625  11.20  1.36   .08    0.     1.08   .7
32 2 5 .3075 -36.40  .3075  11.60  1.16   .08    0.     1.08   .7
32 2 6 .3525 -33.10  .3525  12.20  1.01   .08    0.     1.08   .7
32 2 7 .3750 -31.69  .3750  12.47  0.96   .08    0.     1.08   .7
50 3910.
50    0.
70 51.78
80   .01
81 9
82 .1500   53.3      115.2  .1625  53.3      115.2 .1710  54.2      115
82 .2165   53.7      115.2  .2625  53.1      115.2 .3085  51.8      115
82 .3540   50.2      115.2  .3625  48.0      115.2 .3750  48.0      115
83 0.967 0.967
80   .02
81 9
82 .1500   44.6      115.2  .1625  44.6      115.2 .1710  45.4      115
82 .2165   45.4      115.2  .2625  46.2      115.2 .3085  45.0      115
82 .3540   43.1      115.2  .3625  40.8      115.2 .3750  40.8      115
83  0.97 0.97
80
```

Sample Output 1

AXIAL-FLOW PUMP PERFORMANCE PREDICTION - - INPUT

IRUN= 820　　JBASE= 10　　JLIM= 20

REFERENCE TABLE INCIDENCE ANGLE BLADE THICKNESS CORRECTION

YTMACB=	0.0	0.02	0.04	0.06	0.08	0.10	0.12
YFKIB=	0.0	0.33	0.59	0.77	0.90	1.00	1.08

REFERENCE TABLE ZERO-CAMBER INCIDENCE ANGLE AND CAMBER COEFFICIENTS (FI10GB,SLP1GB,SLP2GB)

YANGSB	SGMGBB								
	0.4	0.6	0.8	1.0	1.2	1.4	1.6	2.0	2.6
0.0	0.042	0.012	0.003	-0.041	-0.074	-0.097	-0.124	-0.132	-0.186
10.00	0.413	0.554	0.721	0.853	1.072	1.203	1.387	1.764	2.303
20.00	0.738	1.085	1.405	1.735	2.146	2.476	2.844	3.663	4.944
30.00	1.043	1.571	2.105	2.636	3.136	3.751	4.346	5.606	7.694
40.00	1.360	2.050	2.759	3.488	4.219	5.029	5.827	7.591	10.460
50.CC	1.662	2.485	3.386	4.283	5.215	6.214	7.255	9.398	12.540
60.00	1.864	2.834	3.835	4.919	5.955	7.016	8.100	10.200	13.550
70.00	2.042	3.099	4.145	5.276	6.377	7.390	8.517	10.850	14.500
0.0	-0.043	-0.022	-0.004	0.016	0.041	0.060	0.082	0.116	0.163
10.00	-0.088	-0.058	-0.032	-0.008	0.019	0.047	0.073	0.124	0.189
20.00	-0.138	-0.100	-0.067	-0.038	-0.013	0.025	0.055	0.113	0.193
30.00	-0.191	-0.148	-0.114	-0.079	-0.044	-0.010	0.019	0.079	0.148
40.00	-0.250	-0.206	-0.167	-0.131	-0.096	-0.066	-0.040	0.003	0.047
50.00	-0.322	-0.273	-0.235	-0.201	-0.174	-0.150	-0.134	-0.108	-0.072
60.00	-0.393	-0.352	-0.318	-0.291	-0.268	-0.249	-0.236	-0.195	-0.157
70.00	-0.484	-0.458	-0.448	-0.433	-0.408	-0.376	-0.357	-0.297	-0.247
0.0	-0.001	-0.001	-0.001	-0.001	-0.001	-0.001	-0.001	-0.001	-0.001
10.00	-0.001	-0.001	-0.001	-0.001	-0.001	-0.001	-0.001	-0.001	-0.002
20.00	-0.001	-0.001	-0.001	-0.001	-0.001	-0.002	-0.002	-0.002	-0.002
30.00	-0.001	-0.001	-0.001	-0.001	-0.002	-0.002	-0.002	-0.002	-0.003
40.00	-0.001	-0.001	-0.001	-0.002	-0.002	-0.002	-0.002	-0.002	-0.003
50.CC	-0.001	-0.001	-0.001	-0.001	-0.002	-0.002	-0.002	-0.002	-0.003
60.00	-0.001	-0.001	-0.001	-0.001	-0.002	-0.002	-0.002	-0.002	-0.002
70.00	-0.000	-0.000	-0.000	-0.001	-0.001	-0.001	-0.001	-0.002	-0.003

BLADE ROW DATA

I= 1　　RN= 3910.0 RPM　　RSTAR= 0.37500 FT　　IEXDEV=-1　　IEXLOS=-1

REFERENCE TABLES FOR BLADE ROW GEOMETRY AND GEOMETRY-DEPENDENT LOSS DATA

J	X	ALFB	XP	ALFPB	SGMAB	TMXCB	FI20B	FHB	FKSHAB

1	0.1500	49.5000	0.1500	-10.7000	2.5200	0.1000	0.0	1.0800	0.7000
2	0.1725	55.6000	0.1725	11.1000	2.1900	0.0970	0.0	1.0800	0.7000
3	0.2175	62.5000	0.2175	38.6000	1.7400	0.0910	0.0	1.0800	0.7000
4	0.2625	66.4000	0.2625	52.4000	1.4400	0.0850	0.0	1.0800	0.7000
5	0.3075	69.4000	0.3075	60.3000	1.2300	0.0790	0.0	1.0800	0.7000
6	0.3525	71.8000	0.3525	65.4000	1.0700	0.0730	0.0	1.0800	0.7000
7	0.3750	72.8000	0.3750	67.5000	1.0000	0.0700	0.0	1.0800	0.7000

REFERENCE TABLE DEVIATION ANGLE-CAMBER EXPONENT(EXPBB)

PPHB				FIDIFB			
	-12.0	-8.0	-4.0	0.0	4.0	8.0	10.0
0.0	1.170	1.130	1.100	1.140	1.200	1.280	1.320
0.100	1.150	1.100	1.080	1.110	1.170	1.260	1.310
C.300	1.110	1.070	1.050	1.070	1.130	1.220	1.280
0.500	1.070	1.060	1.050	1.060	1.080	1.110	1.130
0.700	1.070	1.060	1.050	1.040	1.030	1.020	1.015
C.900	1.060	1.038	1.016	0.994	0.972	0.950	0.939
1.000	1.040	1.010	0.980	0.950	0.920	0.900	0.880

REFERENCE TABLE LOSS(THACBB)

RPBB					DEQBB					
	1.2000	1.3000	1.4000	1.5000	1.6000	1.7000	1.8000	1.9000	2.0000	2.1000
0.0	0.0140	0.0140	0.0160	0.0180	0.0220	0.0260	0.0300	0.0340	0.0380	0.0430
0.1000	0.0140	0.0140	0.0160	0.0180	0.0220	0.0260	0.0300	0.0340	0.0380	0.0430
0.3000	0.0100	0.0100	0.0100	0.0105	0.0145	0.0195	0.0240	0.0285	0.0330	0.0375
0.5000	0.0060	0.0060	0.0060	0.0060	0.0061	0.0061	0.0061	0.0062	0.0066	0.0070
0.7000	0.0060	0.0060	0.0065	0.0070	0.0075	0.0080	0.0085	0.0090	0.0100	0.0110
0.9000	0.0060	0.0060	0.0065	0.0075	0.0085	0.0095	0.0105	0.0115	0.0125	0.0140
1.0000	0.0060	0.0060	0.0065	0.0075	0.0085	0.0095	0.0105	0.0115	0.0125	0.0140
	2.2000	2.3000	2.4000	2.5000	2.6000	2.7000	2.8000	2.9000	3.0000	3.4000
0.0	0.0480	0.0530	0.0580	0.0630	0.0680	0.0750	0.0830	0.0930	0.1080	0.1650
0.1000	0.0480	0.0530	0.0580	0.0630	0.0680	0.0750	0.0830	0.0930	0.1080	0.1650
C.3000	0.0420	0.0465	0.0510	0.0555	0.0600	0.0645	0.0690	0.0735	0.0780	0.0960
0.5C00	0.0074	0.0078	0.0082	0.0086	0.0090	0.0094	0.0098	0.0102	0.0106	0.0122
0.7000	0.0120	0.0130	0.0140	0.0150	0.0160	0.0170	0.0180	0.0190	0.0200	0.0240
0.9000	0.0155	0.0170	0.0185	0.0200	0.0215	0.0230	0.0245	0.0260	0.0275	0.0335
1.0000	0.0155	0.0170	0.0185	0.0200	0.0215	0.0230	0.0245	0.0260	0.0275	0.0335

BLADE ROW DATA

I= 2 RN= 0.0 RPM RSTAR= 0.37500 FT IEXDEV= 0 IEXLOS= 0

REFERENCE TABLES FOR BLADE ROW GEOMETRY AND GEOMETRY-DEPENDENT LOSS DATA

J	X	ALFB	XP	ALFPB	SGMAB	TMXCB	FI2DB	FHB	FKSHAB
1	0.1500	-51.4400	0.1500	10.7600	2.3400	0.0800	0.0	1.0800	0.7000
2	0.1725	-49.0000	0.1725	10.6000	2.0900	0.0800	0.0	1.0800	0.7000
3	0.2175	-44.3000	0.2175	10.9000	1.6500	0.0800	0.0	1.0800	0.7000
4	0.2625	-40.2000	0.2625	11.2000	1.3600	0.0800	0.0	1.0800	0.7000
5	0.3075	-36.4000	0.3075	11.6000	1.1600	0.0800	0.0	1.0800	0.7000
6	0.3525	-33.1000	0.3525	12.2000	1.0100	0.0800	0.0	1.0800	0.7000
7	0.3750	-31.6900	0.3750	12.4700	0.9600	0.0800	0.0	1.0800	0.7000

REFERENCE TABLE DEVIATICN ANGLE-SLOPE FACTOR(EMB)

YANGSB=	0.0	10.00	20.00	30.00	40.00	50.00	60.00	70.00
EMB=	0.22	0.23	0.24	0.27	0.29	0.33	0.37	0.42

REFERENCE TABLE LOSS(THACB)

DEQB=	1.30	1.40	1.50	1.60	1.70	1.80	1.90	2.00	2.10	2.20
THACB=	0.00	0.01	0.01	0.01	0.01	0.01	0.01	0.02	0.02	0.02

```
INLET CONDITIONS
         PHIRUN NO.     820.01

     R         VZ          VU          H
  0.1500    53.3000     0.0       115.2000
  0.1625    53.3000     0.0       115.2000
  0.1710    54.2000     0.0       115.2000
  0.2165    53.7000     0.0       115.2000
  0.2625    53.1000     0.0       115.2000
  0.3085    51.8000     0.0       115.2000
  0.3540    50.2000     0.0       115.2000
  0.3625    48.0000     0.0       115.2000
  0.3750    48.0000     0.0       115.2000

**** WARNING - FIT2D CALLED IN IREF - EXTRAPOLATION OF TABLE    FI1OGB(YANGSB,SGMGBB)

**** WARNING - FIT2D CALLED IN IREF - EXTRAPOLATION OF TABLE    SLP1GB(YANGSB,SGMGBB)

**** WARNING - FIT2D CALLED IN IREF - EXTRAPOLATION OF TABLE    SLP2GB(YANGSB,SGMGBB)

**** WARNING - EXTRAPOLATION CF TABLE EMB(ANGSTB) IN FIT1D-CALLED IN DEV

**** WARNING - FIT2D CALLED IN IREF - EXTRAPOLATION OF TABLE    FI1OGB(YANGSB,SGMGBB)

**** WARNING - FIT2D CALLED IN IREF - EXTRAPOLATION OF TABLE    SLP1GB(YANGSB,SGMGBB)

**** WARNING - FIT2D CALLED IN IREF - EXTRAPOLATION OF TABLE    SLP2GB(YANGSB,SGMGBB)

**** WARNING - EXTRAPOLATION OF TABLE EMB(ANGSTB) IN FIT1D-CALLED IN DEV

**** WARNING - FIT2D CALLED IN IREF - EXTRAPOLATION OF TABLE    FI1OGB(YANGSB,SGMGBB)

**** WARNING - FIT2D CALLED IN IREF - EXTRAPOLATION OF TABLE    SLP1GB(YANGSB,SGMGBB)

**** WARNING - FIT2D CALLED IN IREF - EXTRAPOLATION OF TABLE    SLP2GB(YANGSB,SGMGBB)

**** WARNING - EXTRAPOLATION CF TABLE EMB(ANGSTB) IN FIT1D-CALLED IN DEV

**** WARNING - FIT2D CALLED IN IREF - EXTRAPOLATION OF TABLE    FI1OGB(YANGSB,SGMGBB)

**** WARNING - FIT2C CALLED IN IREF - EXTRAPOLATION OF TABLE    SLP1GB(YANGSB,SGMGBB)

**** WARNING - FIT2C CALLED IN IREF - EXTRAPOLATION OF TABLE    SLP2GB(YANGSB,SGMGBB)

**** WARNING - EXTRAPOLATION CF TABLE EMB(ANGSTB) IN FIT1D-CALLED IN DEV
```

```
**** WARNING - FIT2D CALLED IN IREF - EXTRAPOLATION OF TABLE    FI1OGB(YANGSB,SGMGBB)

**** WARNING - FIT2D CALLED IN IREF - EXTRAPOLATION OF TABLE    SLP1GB(YANGSB,SGMGBB)

**** WARNING - FIT2D CALLED IN IREF - EXTRAPOLATION OF TABLE    SLP2GB(YANGSB,SGMGBB)

**** WARNING - EXTRAPOLATION OF TABLE EMB(ANGSTB) IN FIT1D-CALLED IN DEV

**** WARNING - FIT2D CALLED IN IREF - EXTRAPOLATION OF TABLE    FI1OGB(YANGSB,SGMGBB)

**** WARNING - FIT2D CALLED IN IREF - EXTRAPOLATION OF TABLE    SLP1GB(YANGSB,SGMGBB)

**** WARNING - FIT2D CALLED IN IREF - EXTRAPOLATION OF TABLE    SLP2GB(YANGSB,SGMGBB)

**** WARNING - EXTRAPOLATION OF TABLE EMB(ANGSTB) IN FIT1D-CALLED IN DEV

**** WARNING - FIT2D CALLED IN IREF - EXTRAPOLATION OF TABLE    FI1OGB(YANGSB,SGMGBB)

**** WARNING - FIT2D CALLED IN IREF - EXTRAPOLATION OF TABLE    SLP1GB(YANGSB,SGMGBB)

**** WARNING - FIT2D CALLED IN IREF - EXTRAPOLATION OF TABLE    SLP2GB(YANGSB,SGMGBB)

**** WARNING - EXTRAPOLATION OF TABLE EMB(ANGSTB) IN FIT1D-CALLED IN DEV
```

FLOW RATE= 8681.2 GPM

ENTRANCE QUANTITIES

J	R/R(TIP)	U,FPS	V,FPS	VZ,FPS	VU,FPS	V(REL),FPS	TOT HD,FT	STAT HD,FT	HD LOSS,FT	BETA,DEG	BETAP,DEG
20	1.000	153.55	48.00	48.00	0.0	160.87	115.20	79.39		0.0	72.64
19	0.968	148.70	47.90	47.90	0.0	156.22	115.20	79.54		0.0	72.14
18	0.937	143.85	50.30	50.30	0.0	152.39	115.20	75.88		0.0	70.73
17	0.905	139.00	50.74	50.74	0.0	147.97	115.20	75.18		0.0	69.94
16	0.874	134.15	51.17	51.17	0.0	143.58	115.20	74.52		0.0	69.12
15	0.842	129.30	51.56	51.56	0.0	139.20	115.20	73.88		0.0	68.26
14	0.811	124.45	51.96	51.96	0.0	134.86	115.20	73.24		0.0	67.34
13	0.779	119.60	52.34	52.34	0.0	130.56	115.20	72.62		0.0	66.36
12	0.747	114.76	52.68	52.68	0.0	126.27	115.20	72.07		0.0	65.34
11	0.716	109.91	52.97	52.97	0.0	122.01	115.20	71.59		0.0	64.27
10	0.684	105.06	53.18	53.18	0.0	117.75	115.20	71.25		0.0	63.15
9	0.653	100.21	53.34	53.34	0.0	113.52	115.20	70.98		0.0	61.97
8	0.621	95.36	53.50	53.50	0.0	109.34	115.20	70.72		0.0	60.71
7	0.589	90.51	53.64	53.64	0.0	105.21	115.20	70.48		0.0	59.35
6	0.558	85.66	54.38	54.38	0.0	101.47	115.20	69.24		0.0	57.59
5	0.526	80.81	55.00	55.00	0.0	97.75	115.20	68.19		0.0	55.76
4	0.495	75.96	55.01	55.01	0.0	93.79	115.20	68.17		0.0	54.09
3	0.463	71.12	54.42	54.42	0.0	89.55	115.20	69.18		0.C	52.58
2	0.432	66.27	53.26	53.26	0.0	85.02	115.20	71.12		0.0	51.21
1	0.400	61.42	53.30	53.30	0.0	81.32	115.20	71.05		0.0	49.05

EXIT QUANTITIES

J	R/R(TIP)	U,FPS	V,FPS	VZ,FPS	VU,FPS	V(REL),FPS	TOT HD,FT	STAT HD,FT	HD LOSS,FT	BETA,DEG	BETAP,DEG
20	1.000	153.55	52.06	47.10	22.18	139.55	186.81	144.69	34.18	25.22	70.28
19	0.970	149.01	52.58	47.48	22.61	135.03	187.27	144.30	32.57	25.46	69.41
18	0.939	144.20	53.25	47.89	23.27	130.08	187.89	143.83	31.53	25.51	68.40
17	0.907	139.29	53.62	48.22	23.47	125.46	188.00	143.31	28.72	25.95	67.40
16	0.875	134.35	54.14	48.79	23.47	121.14	188.31	142.76	24.83	25.69	66.25
15	0.843	129.41	54.80	49.60	23.30	117.13	188.87	142.19	19.99	25.16	64.95
14	0.811	124.46	55.46	50.41	23.13	113.18	189.40	141.60	15.20	24.64	63.55
13	C.778	119.48	56.01	50.89	23.39	108.74	189.72	140.97	12.29	24.69	62.09
12	0.746	114.49	56.88	51.59	23.96	104.20	190.57	140.29	9.84	24.91	60.32
11	C.713	109.51	58.01	52.43	24.84	99.58	191.82	139.52	7.87	25.35	58.23
10	0.681	104.51	58.68	52.73	25.75	94.78	192.17	138.65	6.63	26.C3	56.20
9	0.648	99.50	59.67	53.18	27.06	89.87	192.85	137.52	5.97	26.97	53.72
8	0.616	94.52	61.44	54.10	29.11	84.88	194.86	136.20	5.81	28.28	50.40
7	0.584	89.60	63.76	55.16	31.98	79.76	197.75	134.58	6.43	30.10	46.25
6	0.552	84.70	65.82	55.92	34.70	75.02	199.89	132.57	6.61	31.82	41.80
5	0.520	79.83	68.79	57.12	38.34	70.59	203.58	130.04	6.69	33.87	35.99
4	0.489	75.02	72.63	58.54	42.99	66.72	208.73	126.75	6.66	36.30	28.68
3	0.458	70.34	77.15	59.92	48.60	63.75	214.95	122.45	6.43	39.04	19.95
2	0.429	65.82	82.51	61.23	55.31	62.13	222.55	116.75	5.72	42.09	9.74
1	C.400	61.42	88.34	61.82	63.10	61.85	230.33	109.05	5.25	45.59	-1.56

ENTRANCE QUANTITIES

GEOMETRIC PARAMETERS

J	R/RT(I)	%PH F T	PHI1	INCID,DEG	REF INC	R2/RT(I)	STAG,DEG	CMBR,DEG	SOLIDITY	TMAX/C
20	1.000	0.0	0.313	-0.16	0.79	1.000	70.15	5.30	1.000	0.0700
19	0.968	5.3	0.312	-0.15	0.80	0.970	69.40	5.79	1.034	0.0715
18	0.937	10.5	0.328	-1.02	0.81	0.939	68.56	6.37	1.071	0.0730
17	0.905	15.8	0.330	-1.22	0.86	0.907	67.72	6.88	1.109	0.0746
16	0.874	21.1	0.333	-1.42	0.90	0.875	66.77	7.56	1.150	0.0762
15	0.842	26.3	0.336	-1.63	0.91	0.843	65.69	8.40	1.196	0.0779
14	0.811	31.6	0.338	-1.86	0.94	0.811	64.54	9.30	1.243	0.0795
13	0.779	36.8	0.341	-2.11	0.99	0.778	63.34	10.26	1.293	0.0811
12	0.747	42.1	0.343	-2.35	1.00	0.746	61.90	11.59	1.349	0.0827
11	0.716	47.4	0.345	-2.58	0.99	0.713	60.20	13.29	1.413	0.0843
10	0.684	52.6	0.346	-2.91	1.02	0.681	58.58	14.96	1.478	0.0860
9	0.653	57.9	0.347	-3.24	1.04	0.648	56.66	17.11	1.552	0.0876
8	0.621	63.2	0.348	-3.46	1.05	0.616	54.15	20.05	1.635	0.0892
7	0.589	68.4	0.349	-3.57	1.14	0.584	51.06	23.72	1.729	0.0908
6	0.558	73.7	0.354	-4.17	1.31	0.552	47.90	27.72	1.821	0.0924
5	0.526	78.9	0.358	-4.53	1.68	0.520	43.90	32.78	1.930	0.0940
4	0.495	84.2	0.358	-4.24	2.33	0.489	38.96	38.72	2.057	0.0956
3	0.463	89.5	0.354	-3.30	3.26	0.458	33.18	45.37	2.199	0.0971
2	0.432	94.7	0.347	-1.72	4.43	0.429	26.66	52.55	2.354	0.0986
1	0.400	100.0	0.347	-0.45	5.86	0.400	19.40	60.20	2.520	0.1000

EXIT QUANTITIES

J	R/RT(I)	%PH F T	PHI2	DEV,DEG	PSI	PSI I	EFFIC	OMEGABAR	D-FACTOR	EQ D-FAC	(THTA/C)A	LOSS DIFF
20	1.000	0.0	0.307	2.78	0.195	0.289	0.676	0.085	0.201	1.328	0.0144	0.0007
19	0.970	4.9	0.309	2.91	0.197	0.286	0.688	0.086	0.206	1.333	0.0146	0.0008
18	0.939	10.1	0.312	3.02	0.198	0.285	0.697	0.087	0.218	1.364	0.0150	0.0016
17	0.907	15.5	0.314	3.12	0.199	0.277	0.717	0.084	0.224	1.379	0.0147	0.0015
16	0.875	20.8	0.318	3.27	0.200	0.268	0.746	0.078	0.227	1.391	0.0136	0.0009
15	0.843	26.2	0.323	3.46	0.201	0.256	0.786	0.066	0.229	1.400	0.0118	0.0002
14	0.811	31.6	0.328	3.66	0.203	0.244	0.829	0.054	0.230	1.410	0.0096	0.0000
13	0.778	37.0	0.331	3.88	0.203	0.237	0.858	0.046	0.236	1.428	0.0084	0.0000
12	0.746	42.4	0.336	4.22	0.206	0.233	0.884	0.040	0.245	1.449	0.0073	0.0000
11	0.713	47.8	0.341	4.68	0.209	0.231	0.906	0.034	0.256	1.473	0.0063	0.0
10	0.681	53.2	0.343	5.10	0.210	0.228	0.920	0.031	0.269	1.506	0.0058	0.0
9	0.648	58.7	0.346	5.61	0.212	0.228	0.928	0.030	0.285	1.544	0.0057	-0.0000
8	0.616	64.1	0.352	6.28	0.217	0.233	0.931	0.031	0.305	1.587	0.0061	-0.0000
7	0.584	69.4	0.359	7.05	0.225	0.243	0.927	0.037	0.329	1.638	0.0075	-0.0000
6	0.552	74.7	0.364	7.76	0.231	0.249	0.927	0.041	0.354	1.710	0.0085	-0.0000
5	0.520	80.0	0.372	8.48	0.241	0.260	0.929	0.045	0.379	1.784	0.0094	-0.0001
4	0.489	85.2	0.381	9.08	0.255	0.274	0.933	0.049	0.399	1.836	0.0104	-0.0001
3	0.458	90.3	0.390	9.45	0.272	0.290	0.939	0.052	0.411	1.851	0.0110	-0.0002
2	0.429	95.2	0.399	9.36	0.293	0.309	0.949	0.051	0.407	1.808	0.0107	-0.0003
1	0.400	100.0	0.403	9.14	0.314	0.329	0.956	0.051	0.393	1.763	0.0101	-0.0003

ROTOR MASS AVERAGED HEAD RISE FROM I TO I+1 =   79.5418 FT
ROTOR MASS AVERAGED EFFICIENCY BETWEEN I AND I+1 =0.8435
AVERAGE FLOW COEFFICIENT AT I =0.3394
AVERAGE FLOW COEFFICIENT AT I+1 =0.3394
ROTOR HEAD RISE COEFFICIENT AT I+1 =0.1085
I= 1

FLOW RATE= 8681.2 GPM

ENTRANCE QUANTITIES

J	R/R(TIP)	U,FPS	V,FPS	VZ,FPS	VU,FPS	V(REL),FPS	TOT HD,FT	STAT HD,FT	HD LOSS,FT	BETA,DEG	BETAP,DEG
20	1.000	0.0	52.06	47.10	22.18	52.06	186.81	144.69		25.22	-25.22
19	0.970	0.0	52.58	47.48	22.61	52.58	187.27	144.30		25.46	-25.46
18	0.939	0.0	53.25	47.89	23.27	53.25	187.89	143.83		25.91	-25.91
17	0.907	0.0	53.62	48.22	23.47	53.62	188.00	143.31		25.95	-25.95
16	0.875	0.0	54.14	48.79	23.47	54.14	188.31	142.76		25.69	-25.69
15	0.843	0.0	54.80	49.60	23.30	54.80	188.87	142.19		25.16	-25.16
14	0.811	0.0	55.46	50.41	23.13	55.46	189.40	141.60		24.64	-24.64
13	0.778	0.0	56.01	50.89	23.39	56.01	189.72	140.97		24.69	-24.69
12	0.746	0.0	56.88	51.59	23.96	56.88	190.57	140.29		24.91	-24.91
11	0.713	0.0	58.01	52.43	24.84	58.01	191.82	139.52		25.35	-25.35
10	0.681	0.0	58.68	52.73	25.75	58.68	192.17	138.65		26.03	-26.03
9	0.648	0.0	59.67	53.18	27.06	59.67	192.85	137.52		26.97	-26.97
8	0.616	0.0	61.44	54.10	29.11	61.44	194.86	136.20		28.28	-28.28
7	0.584	0.0	63.76	55.16	31.98	63.76	197.75	134.58		30.10	-30.10
6	0.552	0.0	65.82	55.92	34.70	65.82	199.89	132.57		31.82	-31.82
5	0.520	0.0	68.79	57.12	38.34	68.79	203.58	130.04		33.87	-33.87
4	0.489	0.0	72.63	58.54	42.99	72.63	208.73	126.75		36.30	-36.30
3	0.458	0.0	77.15	59.92	48.60	77.15	214.95	122.45		39.04	-39.04
2	0.429	0.0	82.51	61.23	55.31	82.51	222.55	116.75		42.09	-42.09
1	0.400	0.0	88.34	61.82	63.10	88.34	230.33	109.05		45.59	-45.59

EXIT QUANTITIES

J	R/R(TIP)	U,FPS	V,FPS	VZ,FPS	VU,FPS	V(REL),FPS	TOT HD,FT	STAT HD,FT	HD LOSS,FT	BETA,DEG	BETAP,DEG
20	1.000	0.0	48.63	48.59	-1.92	48.63	186.33	149.57	0.48	-2.26	2.26
19	0.968	0.0	48.92	48.88	-1.80	48.92	186.76	149.57	0.51	-2.10	2.10
18	0.936	0.0	49.31	49.28	-1.67	49.31	187.35	149.57	0.54	-1.94	1.94
17	0.903	0.0	49.35	49.33	-1.51	49.35	187.42	149.56	0.58	-1.76	1.76
16	0.869	0.0	49.52	49.50	-1.38	49.52	187.67	149.56	0.64	-1.59	1.59
15	0.836	0.0	49.82	49.80	-1.26	49.82	188.13	149.56	0.74	-1.44	1.44
14	0.803	0.0	50.09	50.08	-1.14	50.09	188.55	149.56	0.85	-1.30	1.30
13	0.769	0.0	50.22	50.21	-1.03	50.22	188.75	149.56	0.97	-1.17	1.17
12	0.735	0.0	50.67	50.67	-0.94	50.67	189.46	149.55	1.11	-1.06	1.06
11	0.702	0.0	51.36	51.35	-0.87	51.36	190.54	149.55	1.28	-0.98	0.98
10	0.668	0.0	51.47	51.46	-0.81	51.47	190.72	149.55	1.45	-0.90	0.90
9	0.635	0.0	51.77	51.76	-0.76	51.77	191.20	149.55	1.65	-0.84	0.84
8	0.602	0.0	52.87	52.87	-0.74	52.87	192.99	149.55	1.87	-0.80	0.80
7	0.570	0.0	54.48	54.47	-0.71	54.48	195.67	149.55	2.08	-0.75	0.75
6	0.539	0.0	55.56	55.56	-0.65	55.56	197.52	149.55	2.37	-0.67	0.67
5	0.508	0.0	57.49	57.48	-0.64	57.49	200.90	149.55	2.67	-0.64	0.64
4	0.478	0.0	60.16	60.16	-0.66	60.16	205.79	149.55	2.94	-0.63	0.63
3	0.450	0.0	63.31	63.30	-0.73	63.31	211.83	149.55	3.12	-0.66	0.66
2	0.424	0.0	67.01	67.01	-0.82	67.01	219.33	149.54	3.22	-0.70	0.70
1	0.400	0.0	70.67	70.66	-0.95	70.67	227.15	149.54	3.18	-0.77	0.77

ENTRANCE QUANTITIES

GEOMETRIC PARAMETERS

J	R/RT(I)	%PH F T	PHI1	INCID,DEG	REF INC	R2/RT(I)	STAG,DEG	CMBR,DEG	SOLIDITY	TMAX/C
20	1.000	0.0	0.0	-6.47	-2.54	1.000	-9.61	44.16	0.960	0.0800
19	0.970	4.9	0.0	-6.90	-2.50	0.968	-10.02	44.69	0.985	0.0800
18	0.939	10.1	0.0	-7.21	-2.44	0.936	-10.47	45.30	1.014	0.0800
17	0.907	15.5	0.0	-8.00	-2.33	0.903	-10.98	45.95	1.051	0.0800
16	0.875	20.8	0.0	-9.13	-2.20	0.869	-11.50	46.65	1.092	0.0800
15	0.843	26.2	0.0	-10.57	-2.04	0.836	-12.03	47.40	1.137	0.0800
14	0.811	31.6	0.0	-12.04	-1.88	0.803	-12.58	48.22	1.184	0.0800
13	0.778	37.0	0.0	-13.00	-1.68	0.769	-13.14	49.11	1.234	0.0800
12	0.746	42.4	0.0	-13.80	-1.40	0.735	-13.71	50.02	1.292	0.0800
11	0.713	47.8	0.0	-14.42	-1.05	0.702	-14.28	50.97	1.356	0.0800
10	0.681	53.2	0.0	-14.79	-0.68	0.668	-14.85	51.94	1.422	0.0800
9	0.648	58.7	0.0	-14.93	-0.30	0.635	-15.43	52.94	1.499	0.0800
8	0.616	64.1	0.0	-14.74	0.10	0.602	-16.03	53.98	1.585	0.0800
7	0.584	69.4	0.0	-14.07	0.61	0.570	-16.66	55.01	1.683	0.0800
6	0.552	74.7	0.0	-13.57	1.22	0.539	-17.34	56.09	1.793	0.0800
5	0.520	80.0	0.0	-12.75	1.85	0.508	-18.00	57.24	1.905	0.0800
4	0.489	85.2	0.0	-11.56	2.49	0.478	-18.63	58.45	2.018	0.0800
3	0.458	90.3	0.0	-10.03	3.06	0.450	-19.23	59.69	2.129	0.0800
2	0.429	95.2	0.0	-8.17	3.56	0.424	-19.80	60.94	2.236	0.0800
1	0.400	100.0	0.0	-5.85	4.00	0.400	-20.34	62.20	2.340	0.0800

EXIT QUANTITIES

J	R/RT(I)	%PH F T	PHI2	DEV,DEG	PSI	PSI I	EFFIC	OMEGABAR	D-FACTOR	EQ D-FAC	(THTA/C)A	LOSS DIFF
20	1.000	0.0	0.0	10.21	0.0	0.0	0.0	0.011	0.307	1.537	0.0074	-0.0025
19	0.968	5.3	0.0	10.23	0.0	0.0	0.0	0.012	0.306	1.546	0.0075	-0.0024
18	0.936	10.7	0.0	10.24	0.0	0.0	0.0	0.012	0.305	1.555	0.0075	-0.0023
17	0.903	16.2	0.0	10.24	0.0	0.0	0.0	0.013	0.302	1.573	0.0077	-0.0022
16	0.869	21.8	0.0	10.23	0.0	0.0	0.0	0.014	0.296	1.601	0.0080	-0.0024
15	0.836	27.3	0.0	10.22	0.0	0.0	0.0	0.016	0.289	1.638	0.0085	-0.0023
14	0.803	32.9	0.0	10.23	0.0	0.0	0.0	0.018	0.283	1.683	0.0091	-0.0021
13	0.769	38.5	0.0	10.25	0.0	0.0	0.0	0.020	0.281	1.721	0.0097	-0.0017
12	0.735	44.1	0.0	10.24	0.0	0.0	0.0	0.022	0.280	1.758	0.0103	-0.0012
11	0.702	49.7	0.0	10.23	0.0	0.0	0.0	0.024	0.279	1.794	0.0109	-0.0006
10	0.668	55.3	0.0	10.22	0.0	0.0	0.0	0.027	0.283	1.831	0.0116	0.0
9	0.635	60.9	0.0	10.20	0.0	0.0	0.0	0.030	0.289	1.864	0.0122	0.0008
8	0.602	66.3	0.0	10.16	0.0	0.0	0.0	0.032	0.294	1.882	0.0126	0.0017
7	0.570	71.7	0.0	10.10	0.0	0.0	0.0	0.033	0.299	1.885	0.0127	0.0025
6	0.539	76.9	0.0	10.03	0.0	0.0	0.0	0.035	0.307	1.905	0.0131	0.0036
5	0.508	82.0	0.0	9.99	0.0	0.0	0.0	0.036	0.315	1.912	0.0133	0.0045
4	0.478	87.0	0.0	9.96	0.0	0.0	0.0	0.036	0.322	1.903	0.0131	0.0050
3	0.450	91.6	0.0	9.95	0.0	0.0	0.0	0.034	0.331	1.879	0.0125	0.0051
2	0.424	95.9	0.0	9.97	0.0	0.0	0.0	0.030	0.341	1.842	0.0118	0.0045
1	0.400	100.0	0.0	9.99	0.0	0.0	0.0	0.026	0.355	1.796	0.0109	0.0035

STAGE MASS AVERAGED HEAD RISE FROM I-1 TO I+1 = 77.8024 FT
STAGE MASS AVERAGED EFFICIENCY BETWEEN I-1 AND I+1 =0.8243
STAGE HEAD RISE COEFFICIENT (ROTOR IN TIP SPD) =0.1062
I= 2

INLET CCNDITICNS
PHIRUN NO. 820.02

R	VZ	VU	H
0.1500	44.6000	0.0	115.2000
0.1625	44.6000	0.0	115.2000
0.1710	45.4000	0.0	115.2000
0.2165	45.4000	0.0	115.2000
0.2625	46.2000	0.0	115.2000
0.3085	45.0000	0.0	115.2000
0.3540	43.1000	0.0	115.2000
0.3625	40.8000	0.0	115.2000
0.3750	40.8000	0.0	115.2000

```
**** WARNING - FIT2D CALLED IN IREF - EXTRAPOLATION OF TABLE    FI10GB(YANGSB,SGMGBB)

**** WARNING - FIT2D CALLED IN IREF - EXTRAPOLATION OF TABLE    SLP1GB(YANGSB,SGMGBB)

**** WARNING - FIT2D CALLED IN IREF - EXTRAPOLATION OF TABLE    SLP2GB(YANGSB,SGMGBB)

**** WARNING - EXTRAPOLATION OF TABLE EMB(ANGSTB) IN FIT1D-CALLED IN DEV

**** WARNING - FIT2D CALLED IN IREF - EXTRAPOLATION OF TABLE    FI10GB(YANGSB,SGMGBB)

**** WARNING - FIT2D CALLED IN IREF - EXTRAPOLATION OF TABLE    SLP1GB(YANGSB,SGMGBB)

**** WARNING - FIT2D CALLED IN IREF - EXTRAPOLATION OF TABLE    SLP2GB(YANGSB,SGMGBB)

**** WARNING - EXTRAPOLATION OF TABLE EMB(ANGSTB) IN FIT1D-CALLED IN DEV

**** WARNING - FIT2D CALLED IN IREF - EXTRAPOLATION OF TABLE    FI10GB(YANGSB,SGMGBB)

**** WARNING - FIT2D CALLED IN IREF - EXTRAPOLATION OF TABLE    SLP1GB(YANGSB,SGMGBB)

**** WARNING - FIT2D CALLED IN IREF - EXTRAPOLATION OF TABLE    SLP2GB(YANGSB,SGMGBB)

**** WARNING - EXTRAPOLATION OF TABLE EMB(ANGSTB) IN FIT1D-CALLED IN DEV

**** WARNING - FIT2D CALLED IN IREF - EXTRAPOLATION OF TABLE    FI10GB(YANGSB,SGMGBB)

**** WARNING - FIT2D CALLED IN IREF - EXTRAPOLATION OF TABLE    SLP1GB(YANGSB,SGMGBB)

**** WARNING - FIT2D CALLED IN IREF - EXTRAPOLATION OF TABLE    SLP2GB(YANGSB,SGMGBB)

**** WARNING - EXTRAPOLATION OF TABLE EMB(ANGSTB) IN FIT1D-CALLED IN DEV
```

```
**** WARNING - FIT2D CALLED IN IREF - EXTRAPOLATION OF TABLE    FI1OGB(YANGSB,SGMGBB)

**** WARNING - FIT2D CALLED IN IREF - EXTRAPOLATION OF TABLE    SLP1GB(YANGSB,SGMGBB)

**** WARNING - FIT2D CALLED IN IREF - EXTRAPOLATION OF TABLE    SLP2GB(YANGSB,SGMGBB)

**** WARNING - EXTRAPOLATION CF TABLE EMB(ANGSTB) IN FIT1D-CALLED IN DEV

**** WARNING - FIT2D CALLED IN IREF - EXTRAPOLATION OF TABLE    FI1OGB(YANGSB,SGMGBB)

**** WARNING - FIT2D CALLED IN IREF - EXTRAPOLATION OF TABLE    SLP1GB(YANGSB,SGMGBB)

**** WARNING - FIT2D CALLED IN IREF - EXTRAPOLATION OF TABLE    SLP2GB(YANGSB,SGMGBB)

**** WARNING - EXTRAPOLATION CF TABLE EMB(ANGSTB) IN FIT1D-CALLED IN DEV
```

FLOW RATE= 7445.6 GPM

ENTRANCE QUANTITIES

J	R/R(TIP)	U,FPS	V,FPS	VZ,FPS	VU,FPS	V(REL),FPS	TOT HD,FT	STAT HD,FT	HD LOSS,FT	BETA,DEG	BETAP,DEG
20	1.000	153.55	40.80	4C.80	0.0	158.87	115.20	89.33		0.C	75.12
19	0.968	148.70	40.70	40.70	0.0	154.17	115.20	89.46		0.0	74.69
18	C.937	143.85	43.23	43.23	0.0	150.20	115.20	86.16		0.0	73.27
17	0.905	139.00	43.78	43.78	0.0	145.73	115.20	85.41		0.0	72.52
16	C.874	134.15	44.29	44.29	0.0	141.27	115.20	84.72		0.0	71.73
15	C.842	129.30	44.74	44.74	0.0	136.82	115.20	84.09		0.C	70.91
14	0.811	124.45	45.21	45.21	0.0	132.41	115.20	83.44		0.0	70.C4
13	C.779	119.60	45.66	45.66	0.0	128.02	115.20	82.80		0.C	69.11
12	0.747	114.76	45.97	45.97	0.0	123.62	115.20	82.35		0.0	68.17
11	0.716	109.91	46.16	46.16	0.0	119.21	115.20	82.09		0.0	67.22
10	C.684	105.06	46.05	46.05	0.0	114.71	115.20	82.24		0.0	66.33
9	0.653	100.21	45.80	45.80	0.0	110.18	115.20	82.61		0.0	65.44
8	0.621	95.36	45.59	45.59	0.0	105.70	115.20	82.90		0.0	64.45
7	0.589	90.51	45.44	45.44	0.0	101.28	115.20	83.11		0.C	63.34
6	C.558	85.66	45.89	45.89	0.0	97.18	115.20	82.48		0.0	61.82
5	0.526	80.81	46.28	46.28	0.0	93.13	115.20	81.92		0.0	60.20
4	0.495	75.96	46.18	46.18	0.0	88.90	115.2C	82.05		0.0	58.70
3	C.463	71.12	45.60	45.60	0.0	84.48	115.20	82.89		0.0	57.33
2	C.432	66.27	44.57	44.57	0.0	79.86	115.20	84.34		0.0	56.08
1	C.400	61.42	44.60	44.60	0.0	75.90	115.20	84.29		0.0	54.01

EXIT QUANTITIES

J	R/R(TIP)	U,FPS	V,FPS	VZ,FPS	VU,FPS	V(REL),FPS	TOT HD,FT	STAT HD,FT	HD LOSS,FT	BETA,DEG	BETAP,DEG
20	1.000	153.55	54.12	42.74	33.20	127.71	233.79	188.28	39.73	37.84	70.45
19	C.970	148.97	54.62	42.81	33.92	122.76	233.68	187.33	38.45	38.39	69.59
18	C.940	144.30	55.18	43.12	34.43	118.03	233.60	186.28	35.93	38.61	68.57
17	C.908	139.48	55.40	43.29	34.57	113.49	232.82	185.12	32.15	38.61	67.58
16	0.877	134.62	55.63	43.68	34.44	109.29	232.00	183.91	27.21	38.25	66.44
15	0.845	129.75	55.90	44.27	34.14	105.36	231.22	182.66	21.55	37.64	65.16
14	0.813	124.88	56.20	44.84	33.87	101.45	230.46	181.38	16.13	37.C7	63.77
13	C.781	119.99	56.53	44.85	34.42	96.62	229.69	180.02	13.77	37.50	62.34
12	C.750	115.08	57.11	45.02	35.15	91.74	229.23	178.54	11.60	37.98	60.61
11	C.718	110.18	57.85	45.43	35.81	87.14	228.92	176.92	8.83	38.25	58.58
10	0.686	105.26	58.29	45.55	36.38	82.58	227.96	175.15	6.19	38.62	56.53
9	0.654	100.35	58.89	45.42	37.48	77.56	226.93	173.04	5.09	39.53	54.15
8	0.622	95.45	60.16	45.51	39.34	72.25	226.90	170.66	4.92	40.84	50.95
7	C.590	90.58	61.91	45.45	42.04	66.49	227.44	167.88	6.04	42.77	46.88
6	0.558	85.68	63.35	45.02	44.57	60.97	226.92	164.55	6.89	44.71	42.40
5	0.526	80.72	65.23	44.80	47.41	55.83	226.66	160.54	7.41	46.62	36.63
4	C.493	75.75	67.70	44.77	50.78	51.26	226.89	155.67	7.79	48.60	29.15
3	C.461	70.84	70.63	44.94	54.48	47.83	227.32	149.80	7.76	50.48	20.00
2	C.430	66.07	74.38	45.74	58.66	46.34	228.73	142.74	6.84	52.05	9.20
1	C.400	61.42	78.93	46.56	63.74	46.62	230.94	134.12	5.85	53.85	-2.85

ENTRANCE QUANTITIES

GEOMETRIC PARAMETERS

J	R/RT(I)	%PH F T	PHI1	INCID,DEG	REF INC	R2/RT(I)	STAG,DEG	CMBR,DEG	SOLIDITY	TMAX/C
20	1.000	0.0	0.266	2.32	0.79	1.000	70.15	5.30	1.000	0.0700
19	0.968	5.3	0.265	2.40	0.80	0.970	69.39	5.80	1.034	0.0715
18	0.937	10.5	0.282	1.53	0.81	0.940	68.57	6.35	1.070	0.0730
17	0.905	15.8	0.285	1.35	0.87	0.908	67.75	6.84	1.107	0.0746
16	0.874	21.1	0.288	1.18	0.91	0.877	66.80	7.49	1.148	0.0762
15	0.842	26.3	0.291	1.03	0.93	0.845	65.74	8.29	1.193	0.0777
14	0.811	31.6	0.294	0.84	0.96	0.813	64.60	9.18	1.239	0.0793
13	0.779	36.8	0.297	0.63	1.02	0.781	63.44	10.07	1.288	0.0809
12	0.747	42.1	0.299	0.48	1.04	0.750	62.03	11.32	1.342	0.0825
11	0.716	47.4	0.301	0.37	1.03	0.718	60.38	12.92	1.404	0.0841
10	0.684	52.6	0.300	0.27	1.05	0.686	58.76	14.59	1.468	0.0857
9	0.653	57.9	0.298	0.22	1.09	0.654	56.95	16.54	1.538	0.0873
8	0.621	63.2	0.297	0.28	1.11	0.622	54.56	19.23	1.619	0.0889
7	0.589	68.4	0.296	0.42	1.19	0.590	51.59	22.66	1.710	0.0905
6	0.558	73.7	0.299	0.07	1.33	0.558	48.46	26.59	1.801	0.0921
5	0.526	78.9	0.301	-0.08	1.68	0.526	44.55	31.46	1.909	0.0937
4	0.495	84.2	0.301	0.38	2.30	0.493	39.61	37.43	2.037	0.0953
3	0.463	89.5	0.297	1.46	3.22	0.461	33.70	44.34	2.183	0.0969
2	0.432	94.7	0.290	3.15	4.39	0.430	26.95	51.96	2.345	0.0985
1	0.400	100.0	0.290	4.51	5.86	0.400	19.40	60.20	2.520	0.1000

EXIT QUANTITIES

J	R/RT(I)	%PH F T	PHI2	DEV,DEG	PSI	PSI I	EFFIC	OMEGABAR	D-FACTOR	EQ D-FAC	(THTA/C)A	LOSS DIFF
20	1.000	0.0	0.278	2.95	0.324	0.432	0.749	0.101	0.301	1.450	0.0170	0.0031
19	0.970	5.0	0.279	3.10	0.323	0.429	0.755	0.104	0.310	1.466	0.0176	0.0035
18	0.940	10.0	0.281	3.18	0.323	0.422	0.767	0.102	0.321	1.477	0.0175	0.0029
17	0.908	15.3	0.282	3.25	0.321	0.409	0.785	0.097	0.329	1.490	0.0168	0.0023
16	0.877	20.5	0.284	3.38	0.319	0.393	0.810	0.088	0.333	1.500	0.0153	0.0018
15	0.845	25.8	0.288	3.56	0.317	0.376	0.843	0.074	0.335	1.508	0.0131	0.0029
14	0.813	31.1	0.292	3.76	0.315	0.359	0.877	0.059	0.337	1.517	0.0106	0.0026
13	0.781	36.4	0.292	3.93	0.312	0.350	0.892	0.054	0.350	1.545	0.0098	0.0051
12	0.750	41.7	0.293	4.24	0.311	0.343	0.907	0.049	0.364	1.577	0.0090	0.0062
11	0.718	47.1	0.296	4.66	0.310	0.335	0.927	0.040	0.376	1.606	0.0074	0.0015
10	0.686	52.4	0.297	5.06	0.308	0.325	0.947	0.030	0.388	1.635	0.0057	0.0
9	0.654	57.7	0.296	5.47	0.305	0.319	0.956	0.027	0.407	1.678	0.0051	0.0003
8	0.622	63.1	0.296	6.01	0.305	0.319	0.957	0.028	0.431	1.735	0.0055	0.0002
7	0.590	68.3	0.296	6.63	0.306	0.323	0.948	0.038	0.465	1.814	0.0076	0.0000
6	0.558	73.7	0.293	7.23	0.305	0.324	0.941	0.047	0.500	1.918	0.0096	0.0011
5	0.526	79.0	0.292	7.81	0.304	0.325	0.937	0.055	0.534	2.030	0.0116	0.0029
4	0.493	84.4	0.292	8.26	0.305	0.326	0.934	0.063	0.563	2.129	0.0137	0.0049
3	0.461	89.8	0.293	8.47	0.306	0.327	0.935	0.070	0.581	2.180	0.0152	0.0064
2	0.430	95.0	0.298	8.23	0.310	0.329	0.943	0.069	0.576	2.132	0.0146	0.0053
1	0.400	100.0	0.303	7.85	0.316	0.332	0.951	0.065	0.552	2.035	0.0130	0.0024

ROTOR MASS AVERAGED HEAD RISE FROM I TO I+1 = 114.6787 FT
ROTOR MASS AVERAGED EFFICIENCY BETWEEN I AND I+1 =0.8774
AVERAGE FLOW COEFFICIENT AT I =0.2910
AVERAGE FLOW COEFFICIENT AT I+1 =0.2910
ROTOR HEAD RISE COEFFICIENT AT I+1 =0.1565
I= 1

```
**** WARNING - EXTRAPOLATION OF TABLE THACDD(CEQDD) IN FIT1D-CALLED IN LOSS

**** WARNING - EXTRAPOLATION OF TABLE THACDD(DEQDD) IN FIT1D-CALLED IN LOSS

**** WARNING - EXTRAPOLATION OF TABLE THACDD(DEQDD) IN FIT1D-CALLED IN LOSS

**** WARNING - EXTRAPOLATION OF TABLE THACDD(DEQDD) IN FIT1D-CALLEC IN LOSS

**** WARNING - EXTRAPOLATION OF TABLE THACDD(DEQDD) IN FIT1D-CALLED IN LOSS

**** WARNING - EXTRAPOLATION OF TABLE THACDD(DEQDD) IN FIT1D-CALLED IN LOSS

**** WARNING - EXTRAPOLATION OF TABLE THACDD(DEQDD) IN FIT1D-CALLEC IN LOSS
```

FLOW RATE= 7445.6 GPM

ENTRANCE QUANTITIES

J	R/R(TIP)	U,FPS	V,FPS	VZ,FPS	VU,FPS	V(REL),FPS	TOT HD,FT	STAT HD,FT	HD LOSS,FT	BETA,DEG	BETAP,DEG
20	1.CCO	0.0	54.12	42.74	33.20	54.12	233.79	188.28		37.84	-37.84
19	C.970	0.0	54.62	42.81	33.92	54.62	233.68	187.33		38.39	-38.39
18	C.940	0.0	55.18	43.12	34.43	55.18	233.60	186.28		38.61	-38.61
17	0.908	0.0	55.40	43.29	34.57	55.40	232.82	185.12		38.61	-38.61
16	C.877	0.0	55.63	43.68	34.44	55.63	232.00	183.91		38.25	-38.25
15	0.845	0.0	55.90	44.27	34.14	55.90	231.22	182.66		37.64	-37.64
14	0.813	0.0	56.20	44.84	33.87	56.20	230.46	181.38		37.07	-37.07
13	C.781	0.0	56.53	44.85	34.42	56.54	229.69	180.02		37.50	-37.50
12	C.750	0.0	57.11	45.02	35.15	57.11	229.23	178.54		37.98	-37.98
11	0.718	0.0	57.85	45.43	35.81	57.85	228.92	176.92		38.25	-38.25
10	0.686	0.0	58.29	45.55	36.38	58.29	227.96	175.15		38.62	-38.62
9	0.654	0.0	58.89	45.42	37.48	58.89	226.93	173.04		39.53	-39.53
8	0.622	0.0	60.16	45.51	39.34	60.16	226.90	170.66		40.84	-40.84
7	C.590	0.0	61.91	45.45	42.04	61.91	227.44	167.88		42.77	-42.77
6	C.558	0.0	63.35	45.02	44.57	63.35	226.92	164.55		44.71	-44.71
5	0.526	0.0	65.23	44.80	47.41	65.23	226.66	160.54		46.62	-46.62
4	0.493	0.0	67.70	44.77	50.78	67.70	226.89	155.67		48.60	-48.60
3	0.461	0.0	70.63	44.94	54.48	70.63	227.32	149.80		50.48	-50.48
2	C.430	0.0	74.38	45.74	58.66	74.38	228.73	142.74		52.05	-52.05
1	0.400	0.0	78.93	46.56	63.74	78.93	230.94	134.12		53.65	-53.85

EXIT QUANTITIES

J	R/R(TIP)	U,FPS	V,FPS	VZ,FPS	VU,FPS	V(REL),FPS	TOT HD,FT	STAT HD,FT	HD LOSS,FT	BETA,DEG	BETAP,DEG
20	1.000	0.0	47.99	47.95	-1.90	47.99	233.19	197.40	0.6C	-2.26	2.26
19	0.973	0.0	47.91	47.87	-1.75	47.91	233.06	197.39	0.63	-2.10	2.10
18	C.945	0.0	47.84	47.81	-1.61	47.84	232.96	197.39	0.65	-1.93	1.93
17	C.917	0.0	47.31	47.28	-1.44	47.31	232.16	197.39	0.66	-1.75	1.75
16	C.888	0.0	46.73	46.72	-1.28	46.73	231.33	197.39	0.67	-1.57	1.57
15	C.858	0.0	46.19	46.18	-1.13	46.19	230.54	197.38	0.69	-1.40	1.40
14	0.828	0.0	45.64	45.63	-0.99	45.64	229.75	197.38	0.71	-1.25	1.25
13	0.797	0.0	45.07	45.06	-0.86	45.07	228.95	197.38	0.75	-1.09	1.09
12	0.766	0.0	44.70	44.70	-0.75	44.70	228.44	197.38	0.79	-0.96	0.96
11	C.734	0.0	44.43	44.43	-0.66	44.43	228.06	197.38	0.86	-0.85	0.85
10	0.702	0.0	43.65	43.65	-0.58	43.65	226.99	197.38	0.96	-0.76	0.76
9	C.670	0.0	42.79	42.79	-0.51	42.79	225.84	197.38	1.10	-0.68	0.68
8	0.637	0.0	42.66	42.66	-0.46	42.66	225.67	197.38	1.24	-0.62	0.62
7	0.604	0.0	42.98	42.98	-0.43	42.98	226.08	197.38	1.36	-0.58	0.58
6	0.570	0.0	42.44	42.43	-0.39	42.44	225.36	197.38	1.56	-0.53	0.53
5	0.536	0.0	42.02	42.02	-0.34	42.02	224.82	197.38	1.85	-0.47	0.47
4	0.502	0.0	41.82	41.82	-0.34	41.82	224.55	197.38	2.34	-0.46	0.46
3	C.467	0.0	41.54	41.53	-0.37	41.54	224.19	197.38	3.13	-0.51	0.51
2	C.433	0.0	41.76	41.76	-0.45	41.76	224.48	197.38	4.25	-0.62	0.62
1	0.400	0.0	42.43	42.42	-0.57	42.43	225.35	197.38	5.59	-0.77	0.77

ENTRANCE QUANTITIES / GEOMETRIC PARAMETERS

J	R/RT(I)	%PH F T	PHI1	INCID,DEG	REF INC	R2/RT(I)	STAG,DEG	CMBR,DEG	SOLIDITY	TMAX/C
20	1.000	0.0	0.0	6.15	-2.54	1.000	-9.61	44.16	0.960	0.0800
19	0.970	5.0	0.0	6.02	-2.53	0.973	-10.01	44.72	0.980	0.0800
18	C.940	10.0	0.0	5.50	-2.50	0.945	-10.44	45.33	1.005	0.0800
17	0.908	15.3	0.0	4.69	-2.43	0.917	-10.93	45.99	1.035	0.0800
16	0.877	20.5	0.0	3.48	-2.35	0.888	-11.43	46.69	1.069	0.0800
15	0.845	25.8	0.0	1.97	-2.24	0.858	-11.95	47.44	1.107	0.0800
14	0.813	31.1	0.0	0.47	-2.12	0.828	-12.48	48.24	1.148	0.0800
13	0.781	36.4	0.0	-0.09	-1.99	0.797	-13.03	49.10	1.191	0.0800
12	0.750	41.7	0.0	-0.62	-1.80	0.766	-13.59	50.00	1.239	0.0800
11	0.718	47.1	0.0	-1.38	-1.54	0.734	-14.16	50.93	1.294	0.0800
10	0.686	52.4	0.0	-2.04	-1.20	0.702	-14.73	51.87	1.356	0.0800
9	0.654	57.7	0.0	-2.19	-0.85	0.670	-15.30	52.84	1.419	0.0800
8	0.622	63.1	0.0	-1.97	-0.49	0.637	-15.88	53.85	1.494	0.0800
7	0.590	68.3	0.0	-1.17	-0.08	0.604	-16.49	54.90	1.581	0.0800
6	0.558	73.7	0.0	-0.43	0.44	0.570	-17.15	55.99	1.683	0.0800
5	0.526	79.0	0.0	0.23	1.10	0.536	-17.85	57.09	1.801	0.0800
4	0.493	84.4	0.0	0.93	1.84	0.502	-18.53	58.28	1.929	0.0800
3	0.461	89.8	0.0	1.54	2.61	0.467	-19.17	59.54	2.063	0.0800
2	0.430	95.0	0.0	1.85	3.33	0.433	-19.78	60.85	2.201	0.0800
1	0.400	100.0	0.0	2.41	4.00	0.400	-20.34	62.20	2.340	0.0800

EXIT QUANTITIES

J	R/RT(I)	%PH F T	PHI2	DEV,DEG	PSI	PSI I	EFFIC	OMEGABAR	D-FACTOR	EQ D-FAC	(THTA/C)A	LOSS DIFF
20	1.000	0.0	0.0	10.21	0.0	0.0	0.0	0.013	0.451	1.804	0.0111	0.0003
19	0.973	4.5	0.0	10.25	0.0	0.0	0.0	0.013	0.455	1.811	0.0112	0.0003
18	0.945	9.1	0.0	10.29	0.0	0.0	0.0	0.014	0.457	1.805	0.0111	0.0003
17	0.917	13.8	0.0	10.32	0.0	0.0	0.0	0.014	0.459	1.795	0.0109	0.0003
16	0.888	18.7	0.0	10.35	0.0	0.0	0.0	0.014	0.458	1.775	0.0106	0.0003
15	0.858	23.6	0.0	10.37	0.0	0.0	0.0	0.014	0.457	1.750	0.0102	0.0002
14	0.828	28.6	0.0	10.39	0.0	0.0	0.0	0.014	0.456	1.731	0.0099	0.0002
13	0.797	33.8	0.0	10.42	0.0	0.0	0.0	0.015	0.462	1.739	0.0100	0.0002
12	0.766	39.0	0.0	10.45	0.0	0.0	0.0	0.016	0.468	1.747	0.0101	0.0002
11	0.734	44.3	0.0	10.46	0.0	0.0	0.0	0.017	0.473	1.756	0.0103	0.0001
10	0.702	49.6	0.0	10.45	0.0	0.0	0.0	0.018	0.482	1.794	0.0109	0.0
9	0.670	55.0	0.0	10.45	0.0	0.0	0.0	0.020	0.498	1.843	0.0118	-0.0003
8	0.637	60.5	0.0	10.42	0.0	0.0	0.0	0.022	0.510	1.878	0.0125	-0.0005
7	0.604	66.1	0.0	10.38	0.0	0.0	0.0	0.023	0.520	1.898	0.0130	-0.0006
6	0.570	71.6	0.0	10.32	0.0	0.0	0.0	0.025	0.539	1.948	0.0141	-0.0009
5	0.536	77.3	0.0	10.23	0.0	0.0	0.0	0.028	0.557	2.007	0.0155	-0.0026
4	0.502	83.1	0.0	10.15	0.0	0.0	0.0	0.033	0.576	2.075	0.0179	-0.0054
3	0.467	88.9	0.0	10.08	0.0	0.0	0.0	0.040	0.599	2.163	0.0215	-0.0054
2	0.433	94.6	0.0	10.03	0.0	0.0	0.0	0.049	0.619	2.257	0.0254	-0.0049
1	0.400	100.0	0.0	9.99	0.0	0.0	0.0	0.058	0.637	2.342	0.0292	-0.0010

STAGE MASS AVERAGED HEAD RISE FROM I-1 TO I+1 = 113.4721 FT
STAGE MASS AVERAGED EFFICIENCY BETWEEN I-1 AND I+1 =0.8675
STAGE HEAD RISE COEFFICIENT (ROTOR IN TIP SPD) =0.1549
I= 2

Sample Input Load 2.

```
10 22010  1000   .01
18   1   .375
19 1 1
20 9 9
21 .260 .284 .290 .302 .324 .352 .381 .405 .420
22 2625 2729 2850 2979 3188 3396 3500 3646 3750
23 1 051  042  024  016  057  062  140  380  440
23 2 052  045  036  029  036  044  082  201  262
23 3 052  046  038  032  032  040  068  160  214
23 4 051  046  041  036  029  039  056  089  118
23 5 038  033  028  026  044  060  070  090  105
23 6 053  047  039  030  013  019  042  103  164
23 7 092  067  043  031  036  040  056  090  117
23 8 066  054  040  033  064  047  063  096  116
23 9 040  038  036  034  083  048  064  104  116
24 1 1.65 4.20 6.30 7.25 6.05 4.85 3.50 0.0  0.0
24 2 4.75 6.26 7.58 8.14 7.68 6.53 4.60 1.73 0.50
24 3 5.25 6.60 7.70 8.25 7.95 6.90 5.95 4.10 2.55
24 4 6.30 7.11 7.88 8.23 8.11 7.21 6.72 6.18 5.90
24 5 6.60 7.31 7.43 7.65 7.55 6.46 6.12 5.82 5.70
24 6 9.25 8.02 6.95 6.45 6.53 5.88 5.60 5.36 5.19
24 7 7.95 7.28 6.60 6.17 5.98 5.43 5.36 5.40 5.50
24 8 8.25 7.33 6.33 5.75 5.28 4.90 4.92 5.47 6.08
24 9 8.65 7.45 6.35 5.50 4.80 4.50 4.70 5.38 6.50
30 1
3110
32 1 1 .2625  66.00  .2625  38.40  1.44  .0850  0.     1.08   .7
32 1 2 .2700  66.60  .2700  40.30  1.40  .0840  0.     1.08   .7
32 1 3 .2800  67.50  .2800  42.70  1.35  .0826  0.     1.08   .7
32 1 4 .2900  68.50  .2900  45.10  1.30  .0813  0.     1.08   .7
32 1 5 .3000  69.30  .3000  47.20  1.26  .0800  0.     1.08   .7
32 1 6 .3200  70.50  .3200  51.00  1.18  .0773  0.     1.08   .7
32 1 7 .3400  71.10  .3400  55.20  1.11  .0746  0.     1.08   .7
32 1 8 .3600  70.30  .3600  60.20  1.05  .0720  0.     1.08   .7
32 1 9 .3700  68.40  .3700  63.70  1.02  .0706  0.     1.08   .7
32 110 .3750  67.10  .3750  67.10  1.01  .0700  0.     1.08   .7
50 3620.
70 55.0
80    .01
81 7
82 .2625 59.81      188.36 .2729 59.81      188.36 .2979 58.95      188.36
82 .3188 59.39      188.46 .3396 58.93      188.52 .3646 55.92      185.66
82 .3750 55.92      185.66
83 0.984
80    .02
81 7
```

```
82 .2625 51.81        188.57 .2729 51.81        188.57 .2979 51.15        188.41
82 .3188 51.34        188.84 .3396 51.17        188.89 .3646 48.80        186.90
82 .3750 48.80        186.90
83 0.985
80 -1.0
50 2890.
70 47.7
80   .05
81 7
82 .2625 48.01        188.36 .2729 48.01        188.36 .2979 47.32        188.36
82 .3188 47.68        188.46 .3396 47.31        188.52 .3646 44.89        185.66
82 .3750 44.89        185.66
83 0.984
80
```

Sample Output 2

AXIAL-FLOW PUMP PERFORMANCE PREDICTION - - INPUT

IRUN=1000 JBASE= 10 JLIM= 20

REFERENCE TABLE INCIDENCE ANGLE BLADE THICKNESS CORRECTION

YTMACB=	0.0	0.02	0.04	0.06	0.08	0.10	0.12
YFKIB=	0.0	0.33	0.59	0.77	0.90	1.00	1.08

REFERENCE TABLE ZERO-CAMBER INCIDENCE ANGLE AND CAMBER COEFFICIENTS (FI10GB,SLP1GB,SLP2GB)

YANGSB	SGMGBB								
	0.4	0.6	0.8	1.0	1.2	1.4	1.6	2.0	2.6
0.0	0.042	0.012	0.003	-0.041	-0.074	-0.097	-0.124	-0.132	-0.186
10.00	0.413	0.554	0.721	0.853	1.072	1.203	1.387	1.764	2.303
20.00	0.738	1.085	1.405	1.735	2.146	2.476	2.844	3.663	4.944
30.00	1.043	1.571	2.105	2.636	3.136	3.751	4.346	5.606	7.694
40.00	1.360	2.050	2.759	3.488	4.219	5.029	5.827	7.591	10.460
50.00	1.662	2.485	3.386	4.283	5.215	6.214	7.255	9.398	12.540
60.00	1.864	2.834	3.835	4.919	5.955	7.016	8.100	10.200	13.550
70.00	2.042	3.099	4.145	5.276	6.377	7.390	8.517	10.850	14.500
0.0	-0.043	-0.022	-0.004	0.016	0.041	0.060	0.082	0.116	0.163
10.00	-0.088	-0.058	-0.032	-0.008	0.019	0.047	0.073	0.124	0.189
20.00	-0.138	-0.100	-0.067	-0.038	-0.013	0.025	0.055	0.113	0.193
30.00	-0.191	-0.148	-0.114	-0.079	-0.044	-0.010	0.019	0.079	0.148
40.00	-0.250	-0.206	-0.167	-0.131	-0.096	-0.066	-0.040	0.003	0.047
50.00	-0.322	-0.273	-0.235	-0.201	-0.174	-0.150	-0.134	-0.108	-0.072
60.00	-0.393	-0.352	-0.318	-0.291	-0.268	-0.249	-0.236	-0.195	-0.157
70.00	-0.484	-0.458	-0.448	-0.433	-0.408	-0.376	-0.357	-0.297	-0.247
0.0	-0.001	-0.001	-0.001	-0.001	-0.001	-0.001	-0.001	-0.001	-0.001
10.00	-0.001	-0.001	-0.001	-0.001	-0.001	-0.001	-0.001	-0.001	-0.002
20.00	-0.001	-0.001	-0.001	-0.001	-0.001	-0.002	-0.002	-0.002	-0.002
30.00	-0.001	-0.001	-0.001	-0.001	-0.002	-0.002	-0.002	-0.002	-0.003
40.00	-0.001	-0.001	-0.001	-0.002	-0.002	-0.002	-0.002	-0.002	-0.003
50.00	-0.001	-0.001	-0.001	-0.001	-0.002	-0.002	-0.002	-0.002	-0.002
60.00	-0.001	-0.001	-0.001	-0.001	-0.002	-0.002	-0.002	-0.002	-0.002
70.00	-0.000	-0.000	-0.000	-0.001	-0.001	-0.001	-0.001	-0.002	-0.003

BLADE ROW DATA

I= 1 RN= 3620.0 RPM RSTAR= 0.37500 FT IEXDEV= 1 IEXLOS= 1

REFERENCE TABLES FOR BLADE ROW GEOMETRY AND GEOMETRY-DEPENDENT LOSS DATA

J	X	ALFB	XP	ALFPB	SGMAB	TMXCB	FI2DB	FHB	FKSHAB

1	0.2625	66.0000	0.2625	38.4000	1.4400	0.0850	0.0	1.0800	0.7000
2	0.2700	66.6000	0.2700	40.3000	1.4000	0.0840	0.0	1.0800	0.7000
3	0.2800	67.5000	0.2800	42.7000	1.3500	0.0826	0.0	1.0800	0.7000
4	0.2900	68.5000	0.2900	45.1000	1.3000	0.0813	0.0	1.0800	0.7000
5	0.3000	69.3000	0.3000	47.2000	1.2600	0.0800	0.0	1.0800	0.7000
6	0.3200	70.5000	0.3200	51.0000	1.1800	0.0773	0.0	1.0800	0.7000
7	0.3400	71.1000	0.3400	55.2000	1.1100	0.0746	0.0	1.0800	0.7000
8	0.3600	70.3000	0.3600	60.2000	1.0500	0.0720	0.0	1.0800	0.7000
9	0.3700	68.4000	0.3700	63.7000	1.0200	0.0706	0.0	1.0800	0.7000
10	0.3750	67.1000	0.3750	67.1000	1.0100	0.0700	0.0	1.0800	0.7000

REFERENCE TABLE DEVIATION ANGLE(DEL2B)

XPB	PHIBB								
	0.2600	0.2840	0.2900	0.3020	0.3240	0.3520	0.3810	0.4050	0.4200
0.2625	1.6500	4.7500	5.2500	6.3000	6.6000	9.2500	7.9500	8.2500	8.6500
0.2729	4.2000	6.2600	6.6000	7.1100	7.3100	8.0200	7.2800	7.3300	7.4500
0.2850	6.3000	7.5800	7.7000	7.8800	7.4300	6.9500	6.6000	6.3300	6.3500
0.2979	7.2500	8.1400	8.2500	8.2300	7.6500	6.4500	6.1700	5.7500	5.5000
0.3188	6.0500	7.6800	7.9500	8.1100	7.5500	6.5300	5.9800	5.2800	4.8000
0.3396	4.8500	6.5300	6.9000	7.2100	6.4600	5.8800	5.4300	4.9000	4.5000
0.3500	3.5000	4.6000	5.9500	6.7200	6.1200	5.6000	5.3600	4.9200	4.7000
0.3646	0.0	1.7300	4.1000	6.1800	5.8200	5.3600	5.4000	5.4700	5.3800
0.3750	0.0	0.5000	2.5500	5.9000	5.7000	5.1900	5.5000	6.0800	6.5000

REFERENCE TABLE LOSS(OMEGBB)

XPB	PHIBB								
	0.2600	0.2840	0.2900	0.3020	0.3240	0.3520	0.3810	0.4050	0.4200
0.2625	0.0510	0.0520	0.0520	0.0510	0.0380	0.0530	0.0920	0.0660	0.0400
0.2729	0.0420	0.0450	0.0460	0.0460	0.0330	0.0470	0.0670	0.0540	0.0380
0.2850	0.0240	0.0360	0.0380	0.0410	0.0280	0.0390	0.0430	0.0400	0.0360
0.2979	0.0160	0.0290	0.0320	0.0360	0.0260	0.0300	0.0310	0.0330	0.0340
0.3188	0.0570	0.0360	0.0320	0.0290	0.0440	0.0130	0.0360	0.0640	0.0830
0.3396	0.0620	0.0440	0.0400	0.0390	0.0600	0.0190	0.0400	0.0470	0.0480
0.3500	0.1400	0.0820	0.0680	0.0560	0.0700	0.0420	0.0560	0.0630	0.0640
0.3646	0.3800	0.2010	0.1600	0.0890	0.0900	0.1030	0.0900	0.0960	0.1040
0.3750	0.4400	0.2620	0.2140	0.1180	0.1050	0.1640	0.1170	0.1160	0.1160

INLET CONDITIONS

PHIRUN NO. 1000.01

R	VZ	VU	H
0.2625	59.8100	0.0	188.3600
0.2729	59.8100	0.0	188.3600
0.2979	58.9500	0.0	188.3600
0.3188	59.3900	0.0	188.4600
0.3396	58.9300	0.0	188.5200
0.3646	55.9200	0.0	185.6600
0.3750	55.9200	0.0	185.6600

I	PHIEFC	USTAR	ARFAC
1	0.4052	142.1574	0.9840

FLOW RATE= 5920.6 GPM

ENTRANCE QUANTITIES

J	R/R(TIP)	U,FPS	V,FPS	VZ,FPS	VU,FPS	V(REL),FPS	TOT HD,FT	STAT HD,FT	HD LOSS,FT	BETA,DEG	BETAP,DEG
20	1.000	142.16	55.92	55.92	0.0	152.76	185.66	137.06		0.0	68.53
19	0.984	139.91	55.83	55.83	0.0	150.64	185.57	137.14		0.0	68.25
18	0.968	137.67	56.17	56.17	0.0	148.68	185.91	136.89		0.0	67.81
17	0.953	135.42	57.09	57.09	0.0	146.96	186.83	136.19		0.0	67.14
16	0.937	133.18	57.85	57.85	0.0	145.20	187.58	135.56		0.0	66.52
15	0.921	130.93	58.47	58.47	0.0	143.40	188.14	135.01		0.0	65.94
14	0.905	128.69	58.94	58.94	0.0	141.54	188.52	134.54		0.0	65.39
13	0.889	126.45	59.16	59.16	0.0	139.60	188.51	134.12		0.0	64.93
12	0.874	124.20	59.30	59.30	0.0	137.63	188.49	133.83		0.0	64.48
11	0.858	121.96	59.38	59.38	0.0	135.64	188.47	133.68		0.0	64.04
10	0.842	119.71	59.26	59.26	0.0	133.58	188.44	133.86		0.0	63.66
9	0.826	117.47	59.07	59.07	0.0	131.48	188.41	134.18		0.0	63.30
8	0.811	115.22	58.97	58.97	0.0	129.43	188.38	134.34		0.0	62.90
7	0.795	112.98	58.95	58.95	0.0	127.43	188.36	134.36		0.0	62.45
6	0.779	110.73	59.26	59.26	0.0	125.59	188.36	133.79		0.0	61.85
5	0.763	108.49	59.50	59.50	0.0	123.74	188.36	133.33		0.0	61.26
4	0.747	106.24	59.68	59.68	0.0	121.86	188.36	133.00		0.0	60.67
3	0.732	104.00	59.79	59.79	0.0	119.96	188.36	132.80		0.0	60.10
2	0.716	101.75	59.84	59.84	0.0	118.04	188.36	132.72		0.0	59.54
1	0.700	99.51	59.81	59.81	0.0	116.10	188.36	132.77		0.0	58.99

EXIT QUANTITIES

J	R/R(TIP)	U,FPS	V,FPS	VZ,FPS	VU,FPS	V(REL),FPS	TOT HD,FT	STAT HD,FT	HD LOSS,FT	BETA,DEG	BETAP,DEG
20	1.000	142.16	42.39	36.39	21.74	125.79	239.60	211.67	42.07	30.86	73.18
19	0.979	139.22	51.79	45.95	23.89	124.15	253.08	211.40	35.77	27.46	68.27
18	0.961	136.61	56.53	50.93	24.55	123.09	260.79	211.12	29.28	25.74	65.56
17	0.944	134.18	59.68	54.31	24.74	122.17	266.20	210.85	23.75	24.49	63.61
16	0.927	131.84	62.18	56.95	24.95	121.11	270.67	210.59	19.09	23.66	61.95
15	0.911	129.57	64.18	58.98	25.31	119.79	274.33	210.31	15.67	23.23	60.50
14	0.896	127.34	65.55	59.94	26.54	117.27	276.80	210.02	16.70	23.88	59.26
13	0.880	125.12	66.60	60.45	27.94	114.45	278.61	209.68	18.46	24.80	58.12
12	0.865	122.91	67.50	60.96	28.97	111.99	280.11	209.31	18.97	25.42	57.02
11	0.849	120.71	68.23	61.49	29.57	109.94	281.24	208.91	18.10	25.68	56.00
10	0.834	118.55	68.97	62.45	29.27	108.95	282.41	208.49	13.80	25.11	55.03
9	0.819	116.42	69.61	63.18	29.22	107.68	283.24	207.94	10.83	24.82	54.08
8	0.804	114.32	70.13	63.66	29.42	106.11	283.81	207.38	9.03	24.81	53.14
7	0.789	112.23	70.51	63.86	29.88	104.21	284.07	206.81	8.46	25.08	52.20
6	0.775	110.14	70.82	63.88	30.58	102.04	284.15	206.20	8.82	25.58	51.24
5	0.760	108.05	71.11	63.81	31.37	99.76	284.14	205.56	9.50	26.18	50.23
4	0.745	105.94	71.06	63.39	32.11	97.31	283.34	204.87	10.68	26.87	49.35
3	0.730	103.82	70.90	62.87	32.77	94.86	282.25	204.14	11.79	27.53	48.49
2	0.715	101.67	70.73	62.33	33.42	92.43	281.10	203.35	12.81	28.20	47.59
1	0.700	99.51	70.55	61.78	34.05	90.01	279.86	202.52	13.75	28.86	46.65

ENTRANCE QUANTITIES

J	R/RT(I)	%PH F T	PHI1	INCID,DEG	REF INC	R2/RT(I)	STAG,DEG	CMBR,DEG	SOLIDITY	TMAX/C
						GEOMETRIC PARAMETERS				
20	1.000	0.0	0.393	1.43	3.11	1.000	67.10	0.0	1.010	0.0700
19	0.984	5.3	0.393	-0.37	0.97	0.979	65.64	5.95	1.028	0.0710
18	0.968	10.5	0.395	-2.00	-0.20	0.961	65.06	9.49	1.049	0.0720
17	0.953	15.8	0.402	-3.35	-0.93	0.944	64.55	11.89	1.067	0.0728
16	0.937	21.1	0.407	-4.30	-1.43	0.927	63.93	13.77	1.085	0.0736
15	0.921	26.3	0.411	-5.08	-1.82	0.911	63.32	15.40	1.104	0.0744
14	0.905	31.6	0.415	-5.70	-2.09	0.896	62.70	16.78	1.124	0.0752
13	0.889	36.8	0.416	-6.04	-2.25	0.880	62.02	17.91	1.144	0.0759
12	0.874	42.1	0.417	-6.32	-2.36	0.865	61.33	18.95	1.164	0.0767
11	0.858	47.4	0.418	-6.53	-2.41	0.849	60.65	19.85	1.186	0.0775
10	0.842	52.6	0.417	-6.63	-2.40	0.834	59.98	20.61	1.209	0.0783
9	0.826	57.9	0.416	-6.65	-2.39	0.819	59.28	21.35	1.232	0.0791
8	0.811	63.2	0.415	-6.68	-2.35	0.804	58.55	22.06	1.254	0.0798
7	0.795	68.4	0.415	-6.71	-2.30	0.789	57.78	22.75	1.275	0.0805
6	0.779	73.7	0.417	-6.84	-2.23	0.775	56.95	23.46	1.298	0.0812
5	0.763	78.9	0.419	-6.85	-2.12	0.760	56.01	24.20	1.325	0.0819
4	0.747	84.2	0.420	-6.85	-1.99	0.745	55.05	24.95	1.353	0.0827
3	0.732	89.5	0.421	-6.87	-1.86	0.730	54.11	25.73	1.380	0.0835
2	0.716	94.7	0.421	-6.92	-1.75	0.715	53.16	26.62	1.409	0.0842
1	0.700	100.0	0.421	-7.01	-1.65	0.700	52.20	27.60	1.440	0.0850

EXIT QUANTITIES

J	R/RT(I)	%PH F T	PHI2	DEV,DEG	PSI	PSI I	EFFIC	OMEGABAR	D-FACTOR	EQ D-FAC	(THTA/C)A	LOSS DIFF
20	1.000	0.0	0.256	6.09	0.172	0.306	0.561	0.116	0.247	1.416	0.0166	0.0
19	0.979	6.9	0.323	5.61	0.215	0.329	0.653	0.101	0.253	1.417	0.0183	0.0
18	0.961	13.0	0.358	5.25	0.238	0.332	0.718	0.085	0.251	1.420	0.0168	0.0
17	0.944	18.7	0.382	5.01	0.253	0.329	0.769	0.071	0.247	1.427	0.0147	0.0
16	0.927	24.2	0.401	4.90	0.265	0.326	0.813	0.058	0.245	1.432	0.0126	0.0
15	0.911	29.5	0.415	4.89	0.274	0.325	0.846	0.049	0.244	1.439	0.0109	0.0
14	0.896	34.8	0.422	4.95	0.281	0.334	0.840	0.054	0.254	1.461	0.0122	0.0
13	0.880	40.0	0.425	5.06	0.287	0.346	0.829	0.061	0.267	1.484	0.0141	0.0
12	0.865	45.1	0.429	5.17	0.292	0.352	0.828	0.064	0.276	1.502	0.0151	0.0
11	0.849	50.3	0.433	5.28	0.295	0.353	0.836	0.063	0.281	1.513	0.0149	0.0
10	0.834	55.4	0.439	5.35	0.299	0.343	0.871	0.050	0.275	1.505	0.0118	0.0
9	0.819	60.4	0.444	5.47	0.302	0.337	0.897	0.040	0.271	1.500	0.0096	0.0
8	0.804	65.3	0.448	5.62	0.304	0.333	0.913	0.035	0.270	1.501	0.0083	0.0
7	0.789	70.2	0.449	5.80	0.305	0.332	0.918	0.034	0.274	1.508	0.0081	0.0
6	0.775	75.1	0.449	6.02	0.305	0.333	0.915	0.036	0.281	1.524	0.0087	0.0
5	0.760	80.0	0.449	6.33	0.305	0.335	0.909	0.040	0.289	1.541	0.0096	0.0
4	0.745	84.9	0.446	6.78	0.302	0.337	0.898	0.046	0.299	1.561	0.0111	0.0
3	0.730	89.9	0.442	7.25	0.299	0.337	0.888	0.053	0.308	1.582	0.0127	0.0
2	0.715	94.9	0.438	7.74	0.295	0.336	0.878	0.059	0.317	1.604	0.0142	0.0
1	0.700	100.0	0.435	8.25	0.291	0.335	0.869	0.066	0.327	1.627	0.0156	0.0

ROTOR MASS AVERAGED HEAD RISE FROM I TO I+1 = 87.9479 FT
ROTOR MASS AVERAGED EFFICIENCY BETWEEN I AND I+1 =0.8346
AVERAGE FLOW COEFFICIENT AT I =0.4117
AVERAGE FLOW COEFFICIENT AT I+1 =0.4117
ROTOR HEAD RISE COEFFICIENT AT I+I =0.1400
I= 1

INLET CONDITIONS
PHIRUN NO. 1000.02

R	VZ	VU	H
0.2625	51.8100	0.0	188.5700
0.2729	51.8100	0.0	188.5700
0.2979	51.1500	0.0	188.4100
0.3188	51.3400	0.0	188.8400
0.3396	51.1700	0.0	188.8900
0.3646	48.8000	0.0	186.9000
0.3750	48.8000	0.0	186.9000

I	PHIEFC	USTAR	ARFAC
1	0.3521	142.1574	0.9850

FLOW RATE= 5139.1 GPM

ENTRANCE QUANTITIES

J	R/R(TIP)	U,FPS	V,FPS	VZ,FPS	VU,FPS	V(REL),FPS	TOT HD,FT	STAT HD,FT	HD LOSS,FT	BETA,DEG	BETAP,DEG
20	1.000	142.16	48.80	48.80	0.0	150.30	186.90	149.89		0.0	71.05
19	0.984	139.91	48.73	48.73	0.0	148.16	186.84	149.94		0.0	70.80
18	0.968	137.67	49.00	49.00	0.0	146.13	187.08	149.76		0.0	70.41
17	0.953	135.42	49.74	49.74	0.0	144.27	187.72	149.26		0.0	69.83
16	0.937	133.18	50.35	50.35	0.0	142.38	188.24	148.83		0.0	69.29
15	0.921	130.93	50.83	50.83	0.0	140.45	188.63	148.47		0.0	68.78
14	0.905	128.69	51.17	51.17	0.0	138.49	188.89	148.20		0.0	68.32
13	0.889	126.45	51.26	51.26	0.0	136.44	188.91	148.09		0.0	67.93
12	0.874	124.20	51.31	51.31	0.0	134.38	188.91	147.99		0.0	67.55
11	0.858	121.96	51.34	51.34	0.0	132.32	188.87	147.91		0.0	67.17
10	0.842	119.71	51.27	51.27	0.0	130.23	188.75	147.89		0.0	66.82
9	0.826	117.47	51.18	51.18	0.0	128.13	188.59	147.89		0.0	66.46
8	0.811	115.22	51.14	51.14	0.0	126.06	188.48	147.85		0.0	66.07
7	0.795	112.98	51.15	51.15	0.0	124.02	188.41	147.75		0.0	65.64
6	0.779	110.73	51.39	51.39	0.0	122.07	188.47	147.43		0.0	65.11
5	0.763	108.49	51.58	51.58	0.0	120.12	198.51	147.18		0.0	64.57
4	0.747	106.24	51.71	51.71	0.0	118.16	188.55	146.99		0.0	64.05
3	0.732	104.00	51.80	51.80	0.0	116.18	188.57	146.87		0.0	63.52
2	0.716	101.75	51.83	51.83	0.0	114.19	188.57	146.83		0.0	63.01
1	0.700	99.51	51.81	51.81	0.0	112.19	188.57	146.85		0.0	62.50

EXIT QUANTITIES

J	R/R(TIP)	U,FPS	V,FPS	VZ,FPS	VU,FPS	V(REL),FPS	TOT HD,FT	STAT HD,FT	HD LOSS,FT	BETA,DEG	BETAP,DEG
20	1.000	142.16	50.83	33.07	38.61	108.71	299.77	259.62	57.58	49.41	72.29
19	0.979	139.22	55.45	41.38	36.93	110.33	306.59	258.80	39.95	41.76	67.98
18	0.961	136.61	57.76	45.66	35.37	111.06	309.98	258.14	27.16	37.76	65.72
17	0.944	134.18	59.35	48.52	34.18	111.15	312.31	257.57	17.84	35.16	64.12
16	0.927	131.84	60.82	50.69	33.61	110.54	314.52	257.04	11.33	33.54	62.71
15	0.911	129.57	62.12	52.31	33.50	109.39	316.49	256.53	6.96	32.64	61.43
14	0.896	127.34	63.06	53.23	33.82	107.61	317.81	256.00	4.84	32.43	60.35
13	0.880	125.12	63.87	53.79	34.43	105.44	318.85	255.46	3.87	32.62	59.33
12	0.865	122.91	64.64	54.21	35.20	103.11	319.80	254.88	3.46	32.99	58.28
11	0.849	120.71	65.33	54.45	36.10	100.63	320.59	254.26	3.62	33.54	57.24
10	0.834	118.55	66.18	54.60	37.40	97.81	321.65	253.59	4.81	34.41	56.07
9	0.819	116.42	66.85	54.62	38.54	95.12	322.13	252.68	5.84	35.21	54.96
8	0.804	114.32	67.36	54.52	39.57	92.52	322.24	251.72	6.73	35.97	53.90
7	0.789	112.23	67.72	54.30	40.47	89.99	321.99	250.71	7.49	36.69	52.88
6	0.775	110.14	68.01	54.05	41.27	87.55	321.52	249.64	8.15	37.37	51.87
5	0.760	108.05	68.23	53.74	42.04	85.12	320.85	248.51	8.75	38.04	50.85
4	0.745	105.94	68.17	53.19	42.63	82.69	319.53	247.32	9.29	38.71	49.96
3	0.730	103.82	67.91	52.49	43.08	80.28	317.73	246.07	9.75	39.37	49.16
2	0.715	101.67	67.54	51.71	43.44	77.88	315.64	244.76	10.11	40.03	48.39
1	0.700	99.51	67.06	50.86	43.71	75.50	313.29	243.40	10.39	40.68	47.65

ENTRANCE QUANTITIES / GEOMETRIC PARAMETERS

J	R/RT(I)	%PH F T	PHI1	INCID,DEG	REF INC	R2/RT(I)	STAG,DEG	CMBR,DEG	SOLIDITY	TMAX/C
20	1.000	0.0	0.343	3.95	3.11	1.000	67.10	0.0	1.010	0.0700
19	0.984	5.3	0.343	2.18	0.97	0.979	65.64	5.95	1.028	0.0710
18	0.968	10.5	0.345	0.60	-0.20	0.961	65.06	9.49	1.049	0.0720
17	0.953	15.8	0.350	-0.66	-0.93	0.944	64.55	11.89	1.067	0.0728
16	0.937	21.1	0.354	-1.53	-1.43	0.927	63.93	13.77	1.085	0.0736
15	0.921	26.3	0.358	-2.24	-1.82	0.911	63.32	15.40	1.104	0.0744
14	0.905	31.6	0.360	-2.78	-2.09	0.896	62.70	16.78	1.124	0.0752
13	0.889	36.8	0.361	-3.04	-2.25	0.880	62.02	17.91	1.144	0.0759
12	0.874	42.1	0.361	-3.25	-2.36	0.865	61.33	18.95	1.164	0.0767
11	0.858	47.4	0.361	-3.40	-2.41	0.849	60.65	19.85	1.186	0.0775
10	0.842	52.6	0.361	-3.48	-2.40	0.834	59.98	20.61	1.209	0.0783
9	0.826	57.9	0.360	-3.50	-2.39	0.819	59.28	21.35	1.232	0.0791
8	0.811	63.2	0.360	-3.51	-2.35	0.804	58.55	22.06	1.254	0.0798
7	0.795	68.4	0.360	-3.51	-2.30	0.789	57.78	22.75	1.275	0.0805
6	0.779	73.7	0.361	-3.58	-2.23	0.775	56.95	23.46	1.298	0.0812
5	0.763	78.9	0.363	-3.53	-2.12	0.760	56.01	24.20	1.325	0.0819
4	0.747	84.2	0.364	-3.48	-1.99	0.745	55.05	24.95	1.353	0.0827
3	0.732	89.5	0.364	-3.45	-1.86	0.730	54.11	25.73	1.380	0.0835
2	0.716	94.7	0.365	-3.46	-1.75	0.715	53.16	26.62	1.409	0.0842
1	0.700	100.0	0.364	-3.50	-1.65	0.700	52.20	27.60	1.440	0.0850

EXIT QUANTITIES

J	R/RT(I)	%PH F T	PHI2	DEV,DEG	PSI	PSI I	EFFIC	OMEGABAR	D-FACTOR	EQ D-FAC	(THTA/C)A LOSS	DIFF
20	1.000	0.0	0.233	5.19	0.359	0.543	0.662	0.164	0.404	1.626	0.0247	0.0
19	0.979	6.9	0.291	5.32	0.381	0.509	0.749	0.117	0.376	1.584	0.0213	0.0
18	0.961	13.0	0.321	5.41	0.391	0.478	0.818	0.082	0.355	1.546	0.0160	0.0
17	0.944	18.7	0.341	5.52	0.397	0.454	0.874	0.055	0.340	1.520	0.0113	0.0
16	0.927	24.2	0.357	5.66	0.402	0.438	0.917	0.036	0.332	1.508	0.0076	0.0
15	0.911	29.5	0.368	5.82	0.407	0.430	0.948	0.023	0.329	1.507	0.0049	0.0
14	0.896	34.8	0.374	6.05	0.410	0.426	0.963	0.016	0.331	1.515	0.0036	0.0
13	0.880	40.0	0.378	6.27	0.414	0.426	0.970	0.013	0.337	1.526	0.0030	0.0
12	0.865	45.1	0.381	6.43	0.417	0.428	0.974	0.012	0.345	1.541	0.0028	0.0
11	0.849	50.3	0.383	6.52	0.419	0.431	0.973	0.013	0.354	1.558	0.0030	0.0
10	0.834	55.4	0.384	6.39	0.423	0.439	0.964	0.018	0.367	1.582	0.0042	0.0
9	0.819	60.4	0.384	6.35	0.425	0.444	0.957	0.023	0.379	1.604	0.0053	0.0
8	0.804	65.3	0.383	6.38	0.426	0.448	0.951	0.027	0.391	1.626	0.0064	0.0
7	0.789	70.2	0.382	6.48	0.425	0.449	0.946	0.031	0.402	1.648	0.0074	0.0
6	0.775	75.1	0.380	6.65	0.424	0.450	0.942	0.035	0.413	1.673	0.0084	0.0
5	0.760	80.0	0.378	6.95	0.421	0.450	0.937	0.039	0.423	1.697	0.0093	0.0
4	0.745	84.9	0.374	7.39	0.417	0.447	0.933	0.043	0.433	1.721	0.0102	0.0
3	0.730	89.9	0.369	7.92	0.411	0.443	0.929	0.046	0.443	1.747	0.0110	0.0
2	0.715	94.9	0.364	8.54	0.405	0.437	0.926	0.050	0.453	1.774	0.0118	0.0
1	0.700	100.0	0.358	9.25	0.397	0.430	0.923	0.053	0.462	1.803	0.0124	0.0

ROTOR MASS AVERAGED HEAD RISE FROM I TO I+1 = 128.6317 FT
ROTOR MASS AVERAGED EFFICIENCY BETWEEN I AND I+1 =0.9169
AVERAGE FLOW COEFFICIENT AT I =0.3574
AVERAGE FLOW COEFFICIENT AT I+1 =0.3574
ROTOR HEAD RISE COEFFICIENT AT I+1 =0.2048
I= 1

AXIAL-FLOW PUMP PERFORMANCE PREDICTION - - INPUT

IRUN=1000 JBASE= 10 JLIM= 20

REFERENCE TABLE INCIDENCE ANGLE BLADE THICKNESS CORRECTION

YTMACB=	0.0	0.02	0.04	0.06	0.08	0.10	0.12
YFKIB=	0.0	0.33	0.59	0.77	0.90	1.00	1.08

REFERENCE TABLE ZERO-CAMBER INCIDENCE ANGLE AND CAMBER COEFFICIENTS (FI10GB,SLP1GB,SLP2GB)

YANGSB	SGMGBB								
	0.4	0.6	0.8	1.0	1.2	1.4	1.6	2.0	2.6
0.0	0.042	0.012	0.003	-0.041	-0.074	-0.097	-0.124	-0.132	-0.186
10.00	0.413	0.554	0.721	0.853	1.072	1.203	1.387	1.764	2.303
20.00	0.738	1.085	1.405	1.735	2.146	2.476	2.844	3.663	4.944
30.00	1.043	1.571	2.105	2.636	3.136	3.751	4.346	5.606	7.694
40.00	1.360	2.050	2.759	3.488	4.219	5.029	5.827	7.591	10.460
50.00	1.662	2.485	3.386	4.283	5.215	6.214	7.255	9.398	12.540
60.00	1.864	2.834	3.835	4.919	5.955	7.016	8.100	10.200	13.550
70.00	2.042	3.099	4.145	5.276	6.377	7.390	8.517	10.850	14.500
0.0	-0.043	-0.022	-0.004	0.016	0.041	0.060	0.082	0.116	0.163
10.00	-0.088	-0.058	-0.032	-0.008	0.019	0.047	0.073	0.124	0.189
20.00	-0.138	-0.100	-0.067	-0.038	-0.013	0.025	0.055	0.113	0.193
30.00	-0.191	-0.148	-0.114	-0.079	-0.044	-0.010	0.019	0.079	0.148
40.00	-0.250	-0.206	-0.167	-0.131	-0.096	-0.066	-0.040	0.003	0.047
50.00	-0.322	-0.273	-0.235	-0.201	-0.174	-0.150	-0.134	-0.108	-0.072
60.00	-0.393	-0.352	-0.318	-0.291	-0.268	-0.249	-0.236	-0.195	-0.157
70.00	-0.484	-0.458	-0.448	-0.433	-0.408	-0.376	-0.357	-0.297	-0.247
0.0	-0.001	-0.001	-0.001	-0.001	-0.001	-0.001	-0.001	-0.001	-0.001
10.00	-0.001	-0.001	-0.001	-0.001	-0.001	-0.001	-0.001	-0.001	-0.002
20.00	-0.001	-0.001	-0.001	-0.001	-0.001	-0.002	-0.002	-0.002	-0.002
30.00	-0.001	-0.001	-0.001	-0.001	-0.002	-0.002	-0.002	-0.002	-0.003
40.00	-0.001	-0.001	-0.001	-0.002	-0.002	-0.002	-0.002	-0.002	-0.003
50.00	-0.001	-0.001	-0.001	-0.001	-0.002	-0.002	-0.002	-0.002	-0.002
60.00	-0.001	-0.001	-0.001	-0.001	-0.002	-0.002	-0.002	-0.002	-0.002
70.00	-0.000	-0.000	-0.000	-0.001	-0.001	-0.001	-0.001	-0.002	-0.003

BLADE ROW DATA

I= 1 RN= 2890.0 RPM RSTAR= 0.37500 FT IEXDEV= 1 IEXLOS= 1

REFERENCE TABLES FOR BLADE ROW GEOMETRY AND GEOMETRY-DEPENDENT LOSS DATA

J	X	ALFB	XP	ALFPB	SGMAB	TMXCB	FI2DB	FHB	FKSHAB

FLOW RATES COMPLETED-NEXT READ NEW RPM OR NEW GEOMETRY DATA

1	0.2625	66.0000	0.2625	38.4000	1.4400	0.0850	0.0	1.0800	0.7000
2	0.2700	66.6000	0.2700	40.3000	1.4000	0.0840	0.0	1.0800	0.7000
3	0.2800	67.5000	0.2800	42.7000	1.3500	0.0826	0.0	1.0800	0.7000
4	0.2900	68.5000	0.2900	45.1000	1.3000	0.0813	0.0	1.0800	0.7000
5	0.3000	69.3000	0.3000	47.2000	1.2600	0.0800	0.0	1.0800	0.7000
6	0.3200	70.5000	0.3200	51.0000	1.1800	0.0773	0.0	1.0800	0.7000
7	0.3400	71.1000	0.3400	55.2000	1.1100	0.0746	0.0	1.0800	0.7000
8	0.3600	70.3000	0.3600	60.2000	1.0500	0.0720	0.0	1.0800	0.7000
9	0.3700	68.4000	0.3700	63.7000	1.0200	0.0706	0.0	1.0800	0.7000
10	0.3750	67.1000	0.3750	67.1000	1.0100	0.0700	0.0	1.0800	0.7000

REFERENCE TABLE DEVIATION ANGLE(DEL2B)

XPB	PHIBB								
	0.2600	0.2840	0.2900	0.3020	0.3240	0.3520	0.3810	0.4050	0.4200
0.2625	0.0288	0.0829	0.0916	0.1100	0.1152	0.1614	0.1388	0.1440	0.1510
0.2729	0.0733	0.1093	0.1152	0.1241	0.1276	0.1400	0.1271	0.1279	0.1300
0.2850	0.1100	0.1323	0.1344	0.1375	0.1297	0.1213	0.1152	0.1105	0.1108
0.2979	0.1265	0.1421	0.1440	0.1436	0.1335	0.1126	0.1077	0.1004	0.0960
0.3188	0.1056	0.1340	0.1388	0.1415	0.1318	0.1140	0.1044	0.0922	0.0838
0.3396	0.0846	0.1140	0.1204	0.1258	0.1127	0.1026	0.0948	0.0855	0.0785
0.3500	0.0611	0.0803	0.1038	0.1173	0.1068	0.0977	0.0935	0.0859	0.0820
0.3646	0.0	0.0302	0.0716	0.1079	0.1016	0.0935	0.0942	0.0955	0.0939
0.3750	0.0	0.0087	0.0445	0.1030	0.0995	0.0906	0.0960	0.1061	0.1134

REFERENCE TABLE LOSS(OMEGBB)

XPB	PHIBB								
	0.2600	0.2840	0.2900	0.3020	0.3240	0.3520	0.3810	0.4050	0.4200
0.2625	0.0510	0.0520	0.0520	0.0510	0.0380	0.0530	0.0920	0.0660	0.0400
0.2729	0.0420	0.0450	0.0460	0.0460	0.0330	0.0470	0.0670	0.0540	0.0380
0.2850	0.0240	0.0360	0.0380	0.0410	0.0280	0.0390	0.0430	0.0400	0.0360
0.2979	0.0160	0.0290	0.0320	0.0360	0.0260	0.0300	0.0310	0.0330	0.0340
0.3188	0.0570	0.0360	0.0320	0.0290	0.0440	0.0130	0.0360	0.0640	0.0830
0.3396	0.0620	0.0440	0.0400	0.0390	0.0600	0.0190	0.0400	0.0470	0.0480
0.3500	0.1400	0.0820	0.0680	0.0560	0.0700	0.0420	0.0560	0.0630	0.0640
0.3646	0.3800	0.2010	0.1600	0.0890	0.0900	0.1030	0.0900	0.0960	0.1040
0.3750	0.4400	0.2620	0.2140	0.1180	0.1050	0.1640	0.1170	0.1160	0.1160

INLET CONDITIONS

PHIRUN NO. 1000.05

R	VZ	VU	H
0.2625	48.0100	0.0	188.3600
0.2729	48.0100	0.0	188.3600
0.2979	47.3200	0.0	188.3600
0.3188	47.6800	0.0	188.4600
0.3396	47.3100	0.0	188.5200
0.3646	44.8900	0.0	185.6600
0.3750	44.8900	0.0	185.6600

I	PHIEFC	USTAR	ARFAC
1	0.4075	113.4903	0.9840

FLOW RATE= 4752.8 GPM

ENTRANCE QUANTITIES

J	R/R(TIP)	U,FPS	V,FPS	VZ,FPS	VU,FPS	V(REL),FPS	TOT HD,FT	STAT HD,FT	HD LOSS,FT	BETA,DEG	BETAP,DEG
20	1.000	113.49	44.89	44.89	0.0	122.05	185.66	154.34		0.0	68.42
19	0.984	111.70	44.82	44.82	0.0	120.35	185.57	154.36		0.0	68.14
18	0.968	109.91	45.09	45.09	0.0	118.80	185.91	154.32		0.0	67.69
17	0.953	108.11	45.83	45.83	0.0	117.43	186.83	154.20		0.0	67.03
16	0.937	106.32	46.44	46.44	0.0	116.02	187.58	154.06		0.0	66.40
15	0.921	104.53	46.94	46.94	0.0	114.59	188.14	153.90		0.0	65.82
14	0.905	102.74	47.31	47.31	0.0	113.11	188.52	153.73		0.0	65.27
13	0.889	100.95	47.49	47.49	0.0	111.56	188.51	153.45		0.0	64.80
12	0.874	99.15	47.61	47.61	0.0	109.99	188.49	153.26		0.0	64.35
11	0.858	97.36	47.67	47.67	0.0	108.41	188.47	153.15		0.0	63.91
10	0.842	95.57	47.58	47.58	0.0	106.76	188.44	153.27		0.0	63.54
9	0.826	93.78	47.42	47.42	0.0	105.09	188.41	153.46		0.0	63.18
8	0.811	91.99	47.34	47.34	0.0	103.45	188.38	153.56		0.0	62.77
7	0.795	90.19	47.32	47.32	0.0	101.85	188.36	153.56		0.0	62.32
6	0.779	88.40	47.57	47.57	0.0	100.39	188.36	153.20		0.0	61.72
5	0.763	86.61	47.76	47.76	0.0	98.91	188.36	152.90		0.0	61.12
4	0.747	84.82	47.91	47.91	0.0	97.41	188.36	152.69		0.0	60.54
3	0.732	83.03	48.00	48.00	0.0	95.90	188.36	152.56		0.0	59.97
2	0.716	81.24	48.03	48.03	0.0	94.37	188.36	152.51		0.0	59.41
1	0.700	79.44	48.01	48.01	0.0	92.82	188.36	152.54		0.0	58.85

EXIT QUANTITIES

J	R/R(TIP)	U,FPS	V,FPS	VZ,FPS	VU,FPS	V(REL),FPS	TOT HD,FT	STAT HD,FT	HD LOSS,FT	BETA,DEG	BETAP,DEG
20	1.000	113.49	46.50	34.67	30.98	89.50	268.03	234.43	26.84	41.78	67.21
19	0.984	111.70	51.23	39.54	32.58	88.45	274.79	234.01	23.81	39.49	63.45
18	0.968	109.91	53.45	42.09	32.95	87.72	277.94	233.54	20.43	38.05	61.33
17	0.953	108.11	55.11	44.26	32.83	87.34	280.26	233.07	16.81	36.56	59.55
16	0.937	106.32	56.43	45.93	32.78	86.70	282.06	232.58	13.77	35.52	58.02
15	0.921	104.53	57.63	47.36	32.83	85.93	283.70	232.09	11.05	34.73	56.55
14	0.905	102.74	58.68	48.37	33.23	84.68	285.09	231.57	9.47	34.49	55.17
13	0.889	100.95	59.50	48.32	34.72	81.98	286.02	231.01	11.33	35.70	53.89
12	0.874	99.15	60.17	48.32	35.86	79.63	286.66	230.39	12.26	36.58	52.64
11	0.858	97.36	60.72	48.40	36.66	77.63	287.02	229.72	12.33	37.15	51.43
10	0.842	95.57	61.07	48.81	36.71	76.47	286.98	229.02	10.42	36.94	50.33
9	0.826	93.78	61.41	49.40	36.47	75.66	286.77	228.16	7.88	36.44	49.23
8	0.811	91.99	61.75	49.78	36.53	74.52	286.54	227.29	6.22	36.28	48.09
7	0.795	90.19	62.04	49.92	36.84	73.06	286.21	226.40	5.36	36.43	46.91
6	0.779	88.40	62.29	49.75	37.47	71.20	285.76	225.47	5.50	36.99	45.67
5	0.763	86.61	62.61	49.57	38.26	69.25	285.41	224.48	5.87	37.66	44.29
4	0.747	84.82	62.87	49.22	39.11	67.17	284.87	223.44	6.53	38.47	42.88
3	0.732	83.03	63.01	48.78	39.89	65.11	284.04	222.34	7.19	39.28	41.49
2	0.716	81.24	63.13	48.31	40.64	63.11	283.10	221.17	7.79	40.07	40.04
1	0.700	79.44	63.22	47.83	41.34	61.15	282.04	219.93	8.33	40.84	38.54

ENTRANCE QUANTITIES

GEOMETRIC PARAMETERS

J	R/RT(I)	%PH F T	PHI1	INCID,DEG	REF INC	R2/RT(I)	STAG,DEG	CMBR,DEG	SOLIDITY	TMAX/C
20	1.000	0.0	0.396	1.32	3.11	1.000	67.10	0.0	1.010	0.0700
19	0.984	5.3	0.395	-0.48	1.18	0.984	65.98	5.27	1.023	0.0707
18	0.968	10.5	0.397	-2.11	0.06	0.968	65.52	8.57	1.041	0.0716
17	0.953	15.8	0.404	-3.46	-0.71	0.953	64.98	11.03	1.058	0.0724
16	0.937	21.1	0.409	-4.42	-1.23	0.937	64.37	12.89	1.075	0.0731
15	0.921	26.3	0.414	-5.20	-1.64	0.921	63.75	14.55	1.093	0.0739
14	0.905	31.6	0.417	-5.82	-1.95	0.905	63.09	16.01	1.112	0.0747
13	0.889	36.8	0.418	-6.17	-2.13	0.889	62.39	17.17	1.131	0.0755
12	0.874	42.1	0.420	-6.45	-2.25	0.874	61.68	18.24	1.152	0.0763
11	0.858	47.4	0.420	-6.66	-2.33	0.859	60.96	19.23	1.174	0.0771
10	0.842	52.6	0.419	-6.75	-2.34	0.842	60.27	20.05	1.197	0.0779
9	0.826	57.9	0.418	-6.78	-2.32	0.826	59.55	20.82	1.221	0.0787
8	0.811	63.2	0.417	-6.81	-2.30	0.811	58.79	21.59	1.244	0.0795
7	0.795	68.4	0.417	-6.84	-2.26	0.795	57.98	22.35	1.267	0.0803
6	0.779	73.7	0.419	-6.97	-2.20	0.779	57.13	23.12	1.291	0.0810
5	0.763	78.9	0.421	-6.98	-2.09	0.763	56.14	23.92	1.319	0.0818
4	0.747	84.2	0.422	-6.98	-1.98	0.747	55.14	24.76	1.349	0.0826
3	0.732	89.5	0.423	-7.01	-1.86	0.732	54.17	25.62	1.378	0.0834
2	0.716	94.7	0.423	-7.06	-1.75	0.716	53.19	26.56	1.408	0.0842
1	0.700	100.0	0.423	-7.14	-1.65	0.700	52.20	27.60	1.440	0.0850

EXIT QUANTITIES

J	R/RT(I)	%PH F T	PHI2	DEV,DEG	PSI	PSI I	EFFIC	OMEGABAR	D-FACTOR	EQ D-FAC	(THTA/C)A	LOSS DIFF
20	1.000	0.0	0.306	0.11	0.412	0.546	0.754	0.116	0.392	1.626	0.0222	0.0
19	0.984	5.3	0.348	0.10	0.446	0.565	0.789	0.106	0.397	1.625	0.0231	0.0
18	0.968	10.5	0.371	0.09	0.460	0.562	0.818	0.093	0.395	1.629	0.0215	0.0
17	0.953	15.8	0.390	0.09	0.467	0.551	0.847	0.078	0.388	1.630	0.0188	0.0
16	0.937	21.1	0.405	0.09	0.472	0.541	0.872	0.066	0.384	1.634	0.0162	0.0
15	0.921	26.3	0.417	0.08	0.477	0.533	0.896	0.054	0.381	1.638	0.0137	0.0
14	0.905	31.6	0.426	0.08	0.482	0.530	0.910	0.048	0.383	1.651	0.0122	0.0
13	0.889	36.8	0.426	0.09	0.487	0.544	0.895	0.059	0.403	1.691	0.0153	0.0
12	0.874	42.1	0.426	0.09	0.490	0.552	0.888	0.065	0.417	1.725	0.0172	0.0
11	0.858	47.4	0.426	0.09	0.492	0.554	0.888	0.068	0.428	1.751	0.0179	0.0
10	0.842	52.6	0.430	0.09	0.492	0.545	0.904	0.059	0.427	1.754	0.0157	0.0
9	0.826	57.9	0.435	0.09	0.491	0.531	0.925	0.046	0.422	1.747	0.0123	0.0
8	0.811	63.2	0.439	0.10	0.490	0.522	0.940	0.037	0.422	1.749	0.0100	0.0
7	0.795	68.4	0.440	0.10	0.489	0.516	0.947	0.033	0.425	1.760	0.0090	0.0
6	0.779	73.7	0.438	0.10	0.487	0.514	0.946	0.035	0.435	1.789	0.0095	0.0
5	0.763	78.9	0.437	0.11	0.485	0.514	0.942	0.039	0.447	1.820	0.0105	0.0
4	0.747	84.2	0.434	0.12	0.482	0.515	0.936	0.044	0.459	1.855	0.0120	0.0
3	0.732	89.5	0.430	0.13	0.478	0.514	0.929	0.050	0.472	1.893	0.0137	0.0
2	0.716	94.7	0.426	0.14	0.473	0.513	0.923	0.056	0.484	1.931	0.0153	0.0
1	0.700	100.0	0.421	0.14	0.468	0.510	0.918	0.062	0.496	1.970	0.0169	0.0

ROTOR MASS AVERAGED HEAD RISE FROM I TO I+1 =   95.7524 FT
ROTOR MASS AVERAGED EFFICIENCY BETWEEN I AND I+1 =0.8960
AVERAGE FLOW COEFFICIENT AT I =0.4140
AVERAGE FLOW COEFFICIENT AT I+1 =0.4140
ROTOR HEAD RISE COEFFICIENT AT I+1 =0.2392
I= 1

APPENDIX F

ANALYSIS OF RADIAL EQUILIBRIUM SOLUTION FAILURE

In the formulation of the pump off-design performance prediction problem, the radial equilibrium equation in finite difference form was obtained in equation (13). Coefficient C in that equation is repeated here, with subscripts 1 and 2 denoting blade row entering and leaving stations:

$$C = - V_{z\ 2,j}^2 - 2g\left(H_{1,j+1} - H_{loss,j+1} - H_{2,j}\right) + 2\left(UV_o\right)_{1,j+1}$$

$$- \frac{r_{2,j}}{r_{2,j+1}} U_{2,j+1}^2 + \left(\frac{r_{2,j+1} - r_{2,j}}{r_{2,j}} - 1\right) V_{\theta\ 2,j+1}^2 .$$

The coefficient C can be expressed in terms of a difference in loss, $H_{loss,j+1} - H_{loss,j}$.

Since

$$H_{2,j} - H_{1,j} = \Delta H_{ideal,j} - H_{loss,j}$$

and

$$\Delta H_{ideal,j} = \frac{\left(UV_\theta\right)_{2,j} - \left(UV_\theta\right)_{1,j}}{g} ,$$

then

$$H_{2,j} = H_{1,j} + \frac{\left(UV_\theta\right)_{2,j} - \left(UV_\theta\right)_{1,j}}{g} - H_{loss,j} .$$

Therefore

$$C = -V_{z\ 2,j}^{2} - 2g\left(H_{1,j+1} - H_{loss,j+1} - H_{1,j} - \left[\frac{(UV_{\theta})_{2,j} - (UV_{\theta})_{1,j}}{g}\right] + H_{loss,j}\right) + 2(UV_{\theta})_{1,j+1} - \frac{r_{2,j}}{r_{2,j+1}} U_{2,j+1}^{2} + \left(\frac{r_{2,j+1} - r_{2,j}}{r_{2,j}} - 1\right) V_{\theta\ 2,j}^{2}$$

or

$$C = -V_{z\ 2,j}^{2} - 2g\left(H_{1,j+1} - H_{1,j}\right) + 2g\left(H_{loss,j+1} - H_{loss,j}\right) + 2(UV_{\theta})_{2,j} - 2(UV_{\theta})_{1,j} + 2(UV_{\theta})_{1,j+1} - \frac{r_{2,j}}{r_{2,j+1}} U_{2,j+1}^{2} + \left(\frac{r_{2,j+1} - r_{2,j}}{r_{2,j}} - 1\right) V_{\theta\ 2,j}^{2} \ .$$

Radial equilibrium solution failure is defined as the condition related to the radicand of the quadratic equation root formula, namely, $B^2 - 4AC$, becoming negative.

In figure 39, the computed results of each of three iterations before a radial equilibrium failure occurred are shown for pump configuration 15 operating at a flow coefficient, $\bar{\phi}_{prog} = 0.338$. The recommended procedures associated with figures 14 and 28 were used for predicting losses and deviation angles. The results indicate that the spanwise variation of predicted deviation angle did not vary appreciably during successive iterations. Thus it can be concluded that the spanwise variations with iteration of the blade row exit relative flow angle, β_2, and hence the quadratic equation coefficients A and B, were very small. Stability of successive predicted loss variations was, however, never achieved before a radial equilibrium solution was obtained. The main reason for this circumstance is thought to be the imprecision of the recommended loss prediction method which, in the case of radial equilibrium solution failure, seems to generate spanwise gradients of loss that cause the quadratic equation coefficient C to become large enough in a positive sense to result in a negative radicand $B^2 - 4AC$

before equilibrium is achieved. It is easily seen from the quadratic formula as well as the relationship for the coefficient C that a large spanwise gradient of loss will lead to a small $V_{z,2}$ and a large $V_{\theta,2}$. The large difference in H_{loss}, the small $V_{z,2}$, and the large $V_{\theta,2}$ all tend to make C a large positive number.

APPENDIX G

SYMBOLS

In addition to the following list of symbols, glossaries of Fortran computer program symbols and description of program input load and output variables are included in the section, Computer Program Capability and Utilization.

A	coefficient (see equation 14)
a	empirical constant (see equation 19)
AVR	ratio of blade leaving to entering axial velocity
B	coefficient (see equation 15)
b	empirical constant (see equation 19); camber exponent (see equation 43)
C	coefficient (see equation 16)
c	blade chord
C.P.	circulation parameter (see equation 21)
C_p	pressure coefficient
$C_1, \ldots C_4$	coefficients (see equation 21)
D	diffusion factor (see equation 19)
DEQ	equivalent diffusion factor (see equation 21)
g	acceleration of gravity
H	stagnation head
$\mathcal{H}$	blade wake form factor
h	static head
H_{loss}	head loss
i	blade incidence angle (see figure 6)

$(K_\delta)_{sh}$ deviation angle blade shape correction factor

$(K_\delta)_t$ deviation angle blade thickness correction factor

m slope factor, deviation angle function of blade camber for compressors (see equation 23) for compressors

m_c coefficient in Carter's deviation angle rule for compressors (see equation 22)

n exponent (equation 18); number of blades in blade row

P stagnation pressure

p static pressure

Q measure of volume flow rate (see equation 17)

q volume flow rate

r radius from machine axis

s blade spacing in cascade

U tangential blade speed

$\mathcal{U}$ free stream velocity

V flow velocity

x a distance

z axial coordinate

α blade angle (see figure 6)

β flow angle, measured from axial direction (see figure 6)

Γ blade circulation (see equation 26); Buri shape factor (see equation 18)

γ blade setting angle, angle between chord and axial direction

δ flow deviation angle (see figure 4)

δ_o zero camber reference deviation angle (see equation 23)

$(\delta_o)_{10}$ 10% thickness reference value of δ_o, NACA 65-series blading (see equation 24)

ϵ turning angle, $\beta_1 - \beta_2$

η hydraulic efficiency

θ blade wake momentum thickness

$(\theta/c)_A, \ldots (\theta/c)_E$ blade wake momentum thickness to chord ratio (see equations 29-33)

ν kinematic viscosity

σ solidity, c/s

ϕ flow coefficient, V_z/U_t

ϕ^o blade camber angle (see figure 6)

ψ head rise coefficient, $g(H_2 - H_1)/U_t^2$

$\bar{\omega}$ head loss coefficient, $2g(H'_{2,i} - H'_2)/(V'_1)^2$

Subscripts

A, ... E versions of momentum thickness to chord ratio parameter

AV average

c corrected

eq equivalent

exp experimental

i axial station, between blade rows

j blade element or streamline radial station

j_{base} radial equilibrium calculation starting value of j

j_{lim} outer casing

min minimum value

nom nominal

prog program

r rotor

ref reference

s blade suction surface; stator

st stage

t blade tip

z axial

θ tangential

1 blade row entrance

2 blade row exit

2-D two-dimensional

Superscripts

' relative to blades

* reference value

- mass averaged

REFERENCES

1. Finger, H. B. and Dugan, J. F., Jr. Analysis of Stage Matching and Off-Design Performance of Multistage Axial-Flow Compressors. NACA RM E52D07. 1952.

2. Doyle, M. D. C. and Dixon, S. L. The Stacking of Compressor Stage Characteristics to Give an Overall Compressor Performance Map. Aeronautical Quarterly. 13:349-367. 1962.

3. Hostetler, G. W. Prediction of Off-Design Performance of Multi-Stage Compressors. A. E. Thesis. California Institute of Technology. 1965.

4. Horlock, J. H. Axial-Flow Compressors. London. Butterworths Scientific Publications. 1958. pp. 119-124.

5. Robbins, W. H. and Dugan, J.F., Jr. Prediction of Off-Design Performance of Multistage Compressors. Chapter X of Aerodynamic Design of Axial-Flow Compressors. NASA SP-36. 1965.

6. Serovy, G. K. A Method for the Prediction of the Off-Design Performance of Axial-Flow Compressors. Ph.D. Dissertation. Iowa State University. Ames, Iowa. 1958.

7. Serovy, G. K. and Anderson, E. W. Method for Predicting Off-Design Performance of Axial-Flow Compressor Blade Rows. NASA TN D-110. 1959.

8. Swan, W. C. A Practical Engineering Solution of the Three-Dimensional Flow in Transonic Type Axial Flow Compressors. WADC Technical Report 58-57. February 1958.

9. Swan, W. C. A Practical Method of Predicting Transonic-Compressor Performance. Journal of Engineering for Power, Trans. ASME, Series A, 83:322-330. 1961.

10. Bullock, R. O. and Johnsen, I. A. Compressor Design System. Chapter III of Aerodynamic Design of Axial-Flow Compressors. NASA SP-36. 1965.

11. Giamati, C. C., Jr. and Finger, H. B. Design Velocity Distribution in Meridional Plane. Chapter VIII of Aerodynamic Design of Axial-Flow Compressors. NASA SP-36. 1965.

12. Holmquist, C. O. and Rannie, W. D. An Approximate Method of Calculating Three-Dimensional Compressible Flow in Axial Turbomachines. Journal of the Aeronautical Sciences. 23:543-556, 582. 1956.

13. Jansen, W. and Moffatt, W. C. The Off-Design Analysis of Axial-Flow Compressors. Journal of Engineering for Power, Trans. ASME, Series A. 89:453-462. 1967.

14. Novak, R. A. Streamline Curvature Computing Procedures for Fluid-Flow Problems. Journal of Engineering for Power, Trans. ASME, Series A. 89:478-490. 1967.

15. Davis, W. R. A Computer Program for the Analysis and Design of Turbomachinery--Revision. Report ME/A 71-5. Division of Aerothermodynamics. Carleton University. September, 1971.

16. Davis, W. R. A Computer Program for the Analysis and Design of the Flow in Turbomachinery. Part B - Loss and Deviation Correlations. Report ME/A 70-1. Division of Aerothermodynamics. Carleton University. July, 1970.

17. Creveling, H. F. and Carmody, R. H. Axial Flow Compressor Computer Program for Calculating Off-Design Performance (Program IV). NASA CR-72427. August, 1968.

18. Daneshyar, H. The Off-Design Analysis of Flow in Axial Compressors. CUED/A-Turbo/TR 19. Department of Engineering, University of Cambridge. 1970.

19. Grahl, K. Beitrag zur Berechnung des Teillastverhaltens von Axialverdichterstufen mit Berücksichtigung der unterschiedlichen Strömungsverhältnisse in den Stufenelementen. Dissertation, Technische Hochschule Aachen. 1970.

20. Grahl, K. Teillastberchnung für Axialverdichterstufen. Zeitschrift für Flugwissenschaften. 20:42-51. 1972.

21. Marsh, H. The Uniqueness of Turbomachinery Flow Calculations. Report CUED/A-Turbo/TR-24. Department of Engineering, Cambridge University. February, 1971.

22. Wilkinson, D. H. Stability, Convergence, and Accuracy of Two-Dimensional Streamline Curvature Methods Using Quasi-Orthogonals. Proceedings of the IME. 184: Part 3G (1): 108-119. 1969-1970.

23. Marsh, H. A Digital Computer Program for the Through-Flow Fluid Mechanics in an Arbitrary Turbomachine Using a Matrix Method. Aeronautical Research Council, R + M 3509. 1968.

24. Gregory-Smith, D. G. An Investigation of Annulus Wall Boundary Layers in Axial Flow Turbomachines. Journal of Engineering for Power, Trans. ASME, Series A. 92:369-376. 1970.

25. Flagg, E. E. Analytical Procedure and Computer Program for Determining the Off-Design Performance of Axial Flow Turbines. NASA CR-710. 1967.

26. Renaudin, A. and Somm, E. Quasi-Three-Dimensional Flow in a Multistage Turbine — Calculation and Experimental Verification. In Dzung. L. S., ed. Flow Research on Blading. Amsterdam. Elsevier Publishing Company. 1970.

27. Novak, R. A. and Hearsey, R. M. The Performance Prediction of Multi-stage Axial Compressors of Arbitrary Geometry Operating with Combined Radial and Circumferential Distributions. In Proceedings of the Air Force Airborne-Propulsion Compatibility Symposium, 24-26 June, 1969. AFAPL-TR-69-103, pp. 627-672. 1970.

28. Ribaut, M. Three-Dimensional Calculation of Flow in Turbomachines with the Aid of Singularities. Journal of Engineering for Power, Trans. ASME, Series A. 90:258-264. 1968.

29. Smith, L. H., Jr. and Yeh, H. Sweep and Dihedral Effects in Axial-Flow Turbomachinery. Journal of Basic Engineering, Trans. ASME, Series D. 85:401-416. 1963.

30. Lieblein, Seymour, Schwenk, Francis C., and Broderick, Robert L. Diffusion Factor for Estimating Losses and Limiting Blade Loadings in Axial-Flow-Compressor Blade Elements. NACA RM E53D01. 1953.

31. Lieblein, S. and Roudebush, W. H. Low-Speed Wake Characteristics of Two-Dimensional Cascade and Isolated Airfoil Sections. NACA TN 3771. 1956.

32. Lieblein, S. and Roudebush, W. H. Theoretical Loss Relations for Low-Speed Two-Dimensional-Cascade Flow. NACA TN 3662. 1956.

33. Lieblein, S. Analysis of Experimental Low-Speed Loss and Stall Characteristics of Two-Dimensional Compressor Blade Cascades. NACA RM E57A28. 1957.

34. Lieblein, S. Loss and Stall Analysis of Compressor Cascades. Journal of Basic Engineering, Trans. ASME, Series D. 81:387-400. 1959.

35. Schlichting. H. Boundary Layer Theory. New York, N.Y. McGraw-Hill Book Co., Inc. 1968.

36. Lieblein, S. Experimental Flow in Two-Dimensional Cascades. Chapter VI of Aerodynamic Design of Axial-Flow Compressors. NASA SP-36. 1965.

37. Herrig, L. J., Emery, J. C. and Erwin, J. R. Effect of Section Thickness and Trailing-Edge Radius on the Performance of NACA 65-series Compressor Blades in Cascade at Low Speeds. NACA RM L51J16. 1951.

38. Reeman, J. and Simonis, E. A. The Effect of Trailing Edge Thickness on Blade Loss. Great Britain RAE Tech. Note 116. 1943.

39. Bailey, W. and Jefferson, J. L. Compressibility Effects on Cascades of Low Cambered Compressor Blades. Great Britain RAE Report E3972. 1943.

40. Emery, James C., Herrig, L. Joseph, Erwin, John R., and Felix A. Richard. Systematic Two-Dimensional Cascade Tests of NACA 65-series Compressor Blades at Low Speeds. NACA Report 1368. 1958.

41. Schlichting, H. and Das, A. On the Influence of Turbulence Level on the Aerodynamic Losses of Axial Turbomachines. In Dzung, L.S., ed. Flow Research on Blading. Amsterdam. Elservier Publishing Company. 1969.

42. Carter, A.D.S. The Low Speed Performance of Related Aerofoils in Cascades. Great Britain ARC Current Paper No. 29. 1950.

43. Carter, A.D.S. and Hughes, Hazel, P., A Theroretical Investigation Into the Effect of Profile Shape on the Performance of Aerofoils in Cascade. Great Britain ARC Reports and Memoranda No. 2384. 1946.

44. Howell, A. R. The Present Basis of Axial Flow Compressor Design. Part 1. Cascade Theory and Performance. Great Britain ARC Reports and Memoranda No. 2095. 1942.

45. Constant, H. Performance of Cascades of Aerofoils. Great Britain ARC No. 4155. 1939.

46. Lieblein, Seymour. Incidence and Deviation-Angle Correlations for Compressor Cascades. Journal of Basic Engineering, Trans. ASME, Series D. 82:575-584. 1960.

47. Weinig, Fritz. Die Strömung um die Schaufeln von Turbomaschinen. Leipzig Johann Ambrosius Barth. 1935.

48. Smith, Leroy H., Jr. Discussion. Journal of Basic Engineering, Trans. ASME, Series D. 82:585-596. 1960.

49. Howell, A. R. Flow in Cascades. In Hawthorne, W. R., ed. High Speed Aerodynamics and Jet Propulsion, Vol. 10, Aerodynamics of Turbines and Compressors. Princeton, New Jersey. Princeton Univ. Press. 1964.

50. Katzoff, S., Bogdonoff, Harriet E., and Boyet, Howard. Comparisons of Theoretical and Experimental Lift and Pressure Distributions on Airfoils in Cascade. NACA TN 1376. 1947.

51. Erwin, John R., and Emery, James C. Effect of Tunnel Configuration and Testing Technique on Cascade Performance. NACA Report 1016. 1951.

52. Pollard, D. and Gostelow, J. P. Some Experiments at Low Speed on Compressor Cascades. Journal of Engineering for Power, Trans. ASME, Series A. 89:427-436. 1967.

53. Montgomery, S. R. Spanwise Variations of Lift in Compressor Cascades. Part 1. Experiments. Journal of Mechanical Engineering Science. 1:293-304. 1959.

54. Miller, M. J. Deviation Angle Prediction Methods--A Review. Iowa State University Engineering Research Institute Report 580. 1969.

55. Erwin, J. R., Savage, M., and Emery, J. C. Two-Dimensional Low-Speed Cascade Investigation of NACA Compressor Blade Sections Having a Systematic Variation in Mean-Line Loading. NACA TN 3817. 1956.

56. Moses, J. J. and Serovy, G. K. Some Effects of Blade Trailing-Edge Thickness on Performance of a Single-Stage Axial-Flow Compressor. NACA RM E51F28. 1951.

57. Miller, M. J., Okiishi, T. H., Serovy, G. K., Sandercock, D. M. and Britsch, W. R. Summary of Design and Blade-Element Performance Data for 12 Axial-Flow Pump Rotor Configuration NASA TN D-7074. 1973.

58. Miller, M. J., Okiishi, T. H., Kavanagh, P. and Serovy, G. K. Application of Blade-Element Techniques to Designed Performance Prediction Problems for Axial-Flow Turbomachinery. ISU-ERI-AMES-77900. Engineering Research Institute, Iowa State University. July, 1970.

59. Hawthorne, W. R. Secondary Circulation in Fluid Flow. Proc. of the Royal Society. London. Series A. 206:374. 1951.

60. Lakshminarayana, B. and Horlock, J. H. Effects of Shear Flows on the Outlet Angle in Axial Compressor Cascades – Methods of Prediction and Correlation with Experiments. Journal of Basic Engineering, Trans. ASME Series D. 89:191-200. 1967.

61. Smith, L. H., Jr. Secondary Flow in Axial-Flow Turbomachinery. Trans. ASME. 77:1065-1976. 1955.

62. Lieblein, S. and Ackley, R. H. Secondary Flows in Annular Cascades and Effects on Flow in Inlet Guide Vanes, NACA RM E51G27. 1951.

63. Schulze, Wallace M., Erwin, John R., and Ashby, George C. NACA 65-series Compressor Rotor Performance with Varying Annulus-Area Ratio, Solidity, Blade Angle, and Reynolds Number and Comparisons with Cascade Results. NACA TN 4130. 1957.

64. Scholz, N. Two-Dimensional Correction of the Outlet Angle in Cascade Flow. Journal of the Aeronautical Sciences, Readers Forum. 20: 786-787. 1953.

65. Soltis, Richard F., Urasek, Donald C., and Miller, Max J. Blade-Element Performance of a Tandem-Bladed Inducer Tested in Water. NASA TN D-5562. 1969.

66. Westphal, Willard R., and Godwin, William R. Comparison of NACA 65-series Compressor-Blade Pressure Distributions and Performance in a Rotor and in Cascade. NACA TN 3806. 1957.

67. Miller, M. J. and Skånberg, T. Reference Incidence Angles in Constant Stagger Cascades. ISU-ERI-AMES-99985. Engineering Research Institute, Iowa State University. 1971.

68. Miller, M. J., Crouse, J. E. and Sandercock, D. M. Summary of Experimental Investigation of Three Axial-Flow Pump Rotors Tested in Water. Journal of Engineering For Power, Trans. ASME, Series A. 89:589-599. 1967.

69. Crouse, J. E., Montgomery, J. C. and Soltis, R. F. Investigation of the Performance of an Axial-Flow-Pump Stage Designed by the Blade-Element Theory – Design and Overall Performance. NASA TN D-591. 1961.

70. Crouse, J. E., Soltis, R. F. and Montgomery, J. C. Investigation of the Performance of an Axial-Flow-Pump Stage Designed by the Blade-Element Theory – Blade-Element Data. NASA TN D-1109. 1961.

Table I. NASA axial-flow pump rotor configuration descriptions.[a]

NASA configuration number	Tip diameter, inches	r_h/r_t	Number of blades	Blade section profile[b]	Blade chord length,[c] inches	Radial tip clearance,[d] inches	Design tip section D-factor	Design point flow coefficient	Minimum blade chord Reynolds number
*02	9.0	0.4	16	DCA	1.5	0.013 - 0.020	0.23	0.293	$1.0x10^6$
*07	9.0	0.7	19	DCA	1.5	0.005 - 0.012	0.43	0.294	$1.5x10^6$
09	9.0	0.7	8	DCA	3.04	0.013 - 0.020	0.46	0.294	$3.0x10^6$
*5	9.0	0.8	19	DCA	1.5	0.015 - 0.017	0.66	0.466	$1.5x10^6$
6	9.0	0.8	19	DCA	1.5	0.025 - 0.027	0.66	0.466	$1.5x10^6$
8	5.0	0.8	19	DCA	0.834	0.007 - 0.009	0.66	0.466	$8.0x10^6$
9	5.0	0.8	19	DCA	0.834	0.015 - 0.017	0.66	0.466	$8.0x10^6$
10	5.0	0.8	19	DCA	0.834	0.022 - 0.024	0.66	0.466	$8.0x10^6$
*13A	9.0	0.85	33	DCA	1.172	0.009 - 0.011	0.72	0.5	$1.0x10^6$
*14A	9.0	0.9	19	DCA	1.5	0.009 - 0.011	0.63	0.7	$1.5x10^6$
15	9.0	0.8	19	DCA	1.5	0.009 - 0.010	0.55	0.466	$1.5x10^6$
16	9.0	0.85	33	CUBIC	1.172	0.009 - 0.011	0.72	0.5	$1.0x10^6$

[a]All rotors were tested without inlet guide vanes and downstream stator blades. Data are presented in reference 57.

[b]DCA indicates a DOUBLE CIRCULAR ARC blade section profile.

[c]All blade chord lengths were uniform along the blade span.

[d]The range of circumferential variation of radial tip clearance is indicated.

*Rotors used for obtaining loss and deviation angle correlations.

Table II. Comparison of measured deviation angles with those computed from Carter's rule and equation (45).

Percent passage height from tip	b	Configuration 02		Configuration 07		Configuration 5		Configuration 13		Configuration 14	
		$\delta_{exp}-\delta_{2-D}$	$\delta_{exp}-\delta_c$	$\delta_{exp}-\delta_{2-D}$	$\delta_{exp}-\delta_c$	$\delta_{exp}-\delta_{2-D}$	$\delta_{exp}-\delta_c$	$\delta_{exp}-\delta_{2-D}$	$\delta_{exp}-\delta_c$	$\delta_{exp}-\delta_{2D}$	$\delta_{exp}-\delta_c$
10	1.11	-0.7	-1.5	2.2	1.3	6.3	1.6	6.9	-1.4	7.6	-1.3
30	1.07	0.2	-0.4	0.8	-0.5	3.6	0.3	7.9	2.6	5.8	0.6
50	1.07	0.1	-0.9	0.9	-0.8	3.9	0.0	8.0	2.1	5.1	-0.1
70	1.06	1.5	0.1	1.2	-0.3	2.8	-0.3	6.9	1.8	2.4	-2.2
90	0.98	3.3	4.0	-0.4	0.0	-0.1	0.8	-1.7	-1.0	0.1	1.6

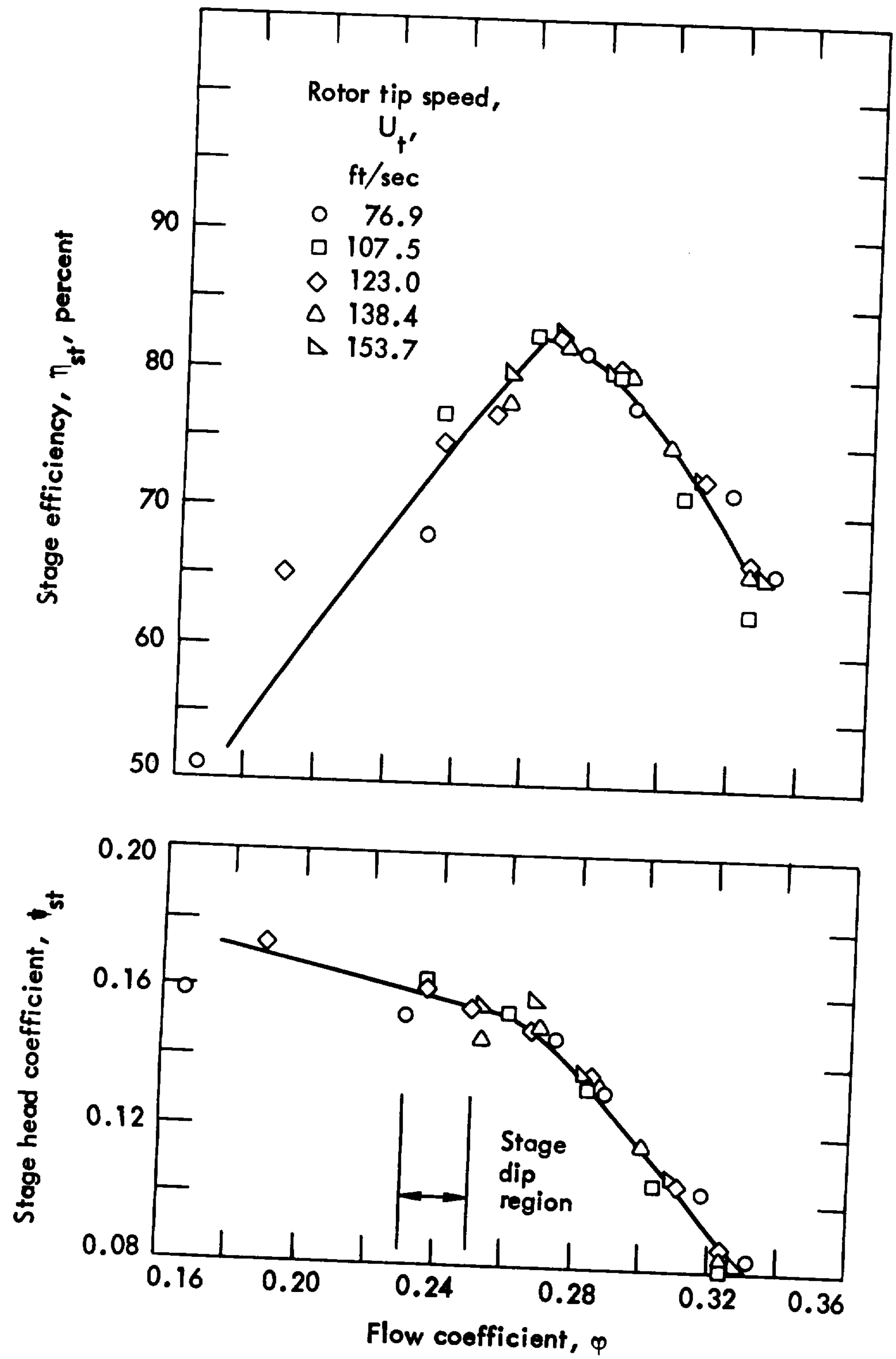

Figure 1. - Noncavitating overall performance of an axial-flow pump stage (ref.69).

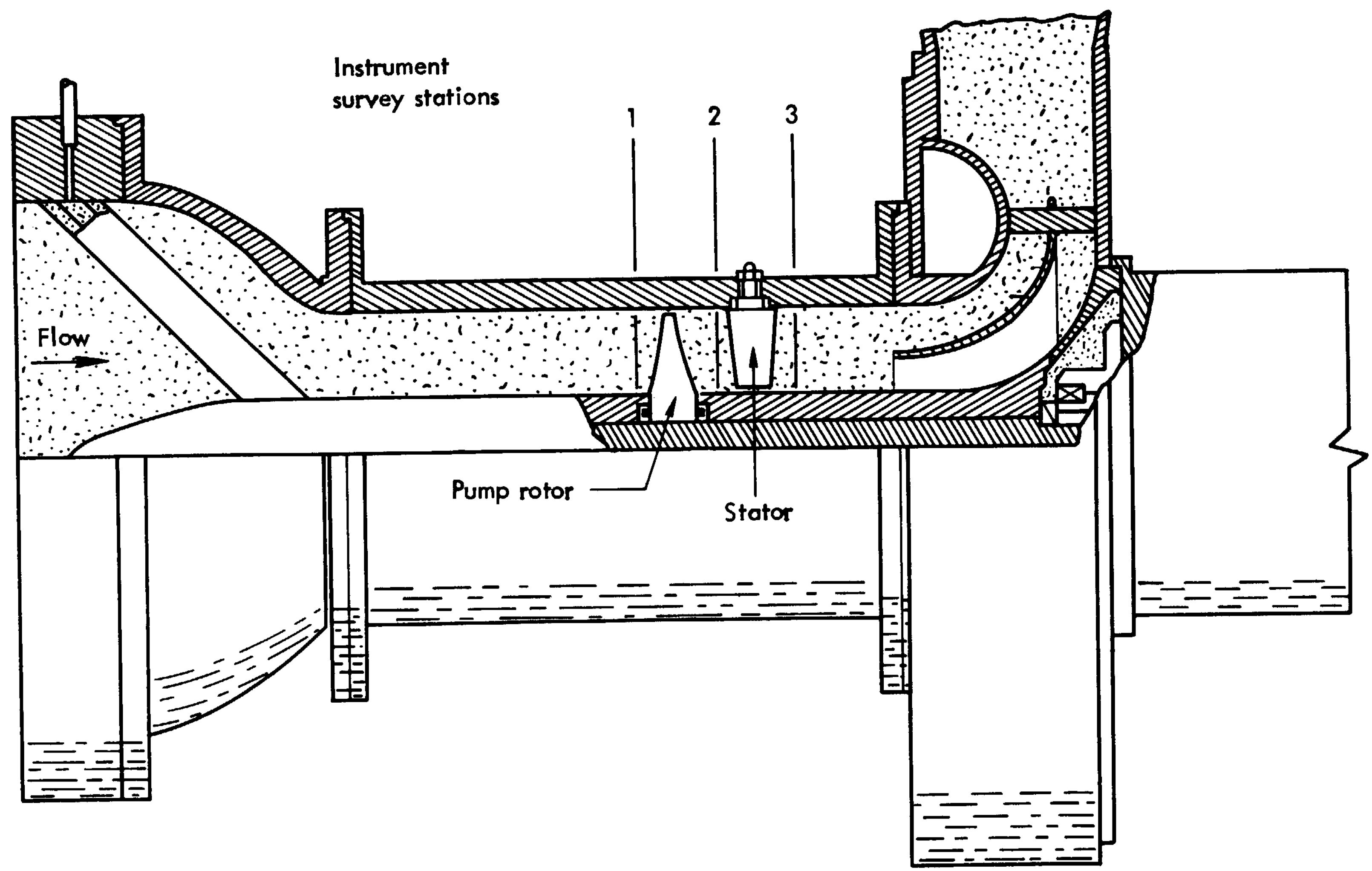

Figure 2. - Typical axial-flow pump stage test installation (ref. 69).

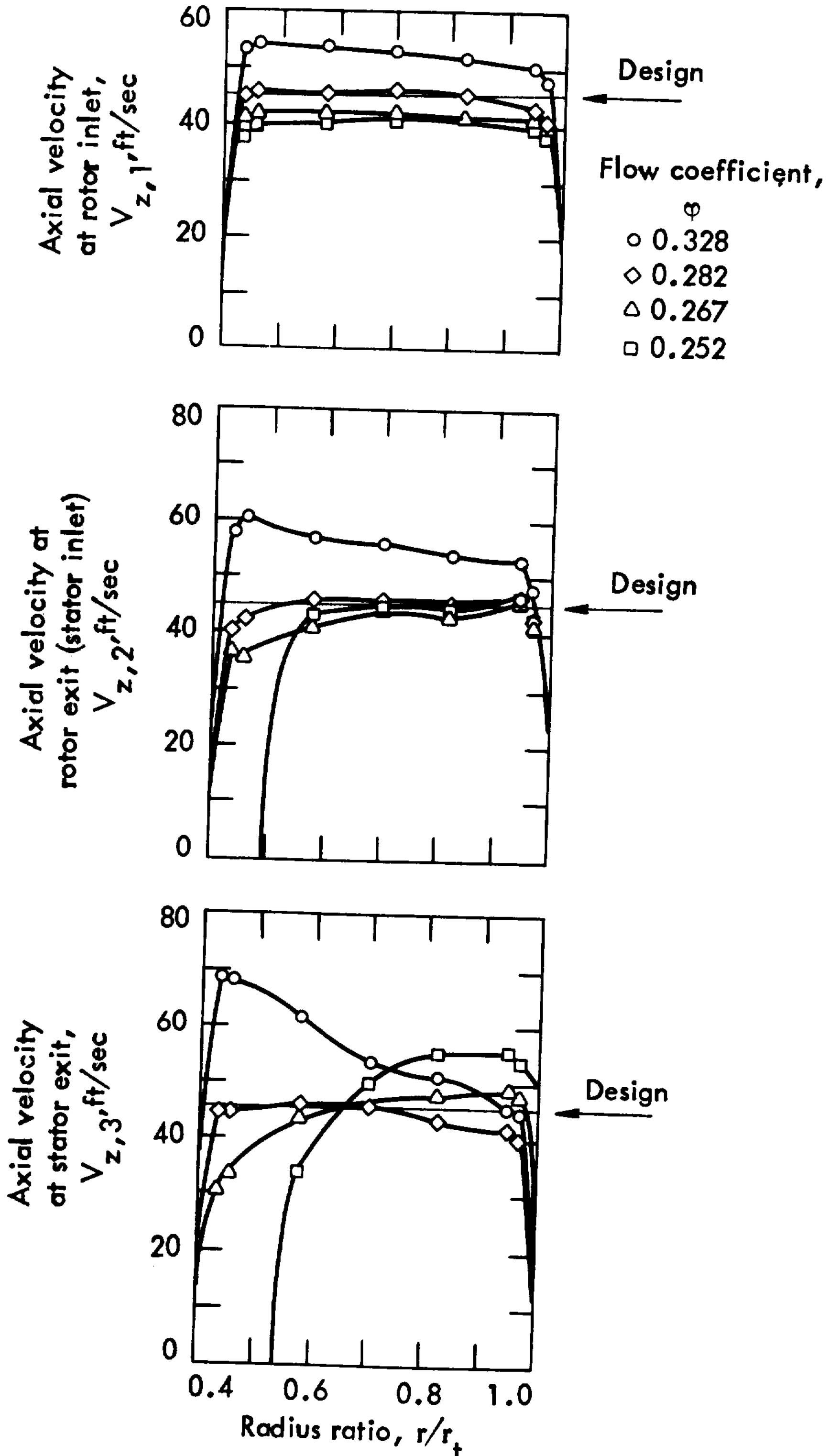

(a) Axial velocity

Figure 3. - Radial distributions of flow parameters at rotor inlet, rotor exit (stator inlet) and stator exit of an axial-flow pump stage; rotor tip speed 153.7 feet per second (ref. 69).

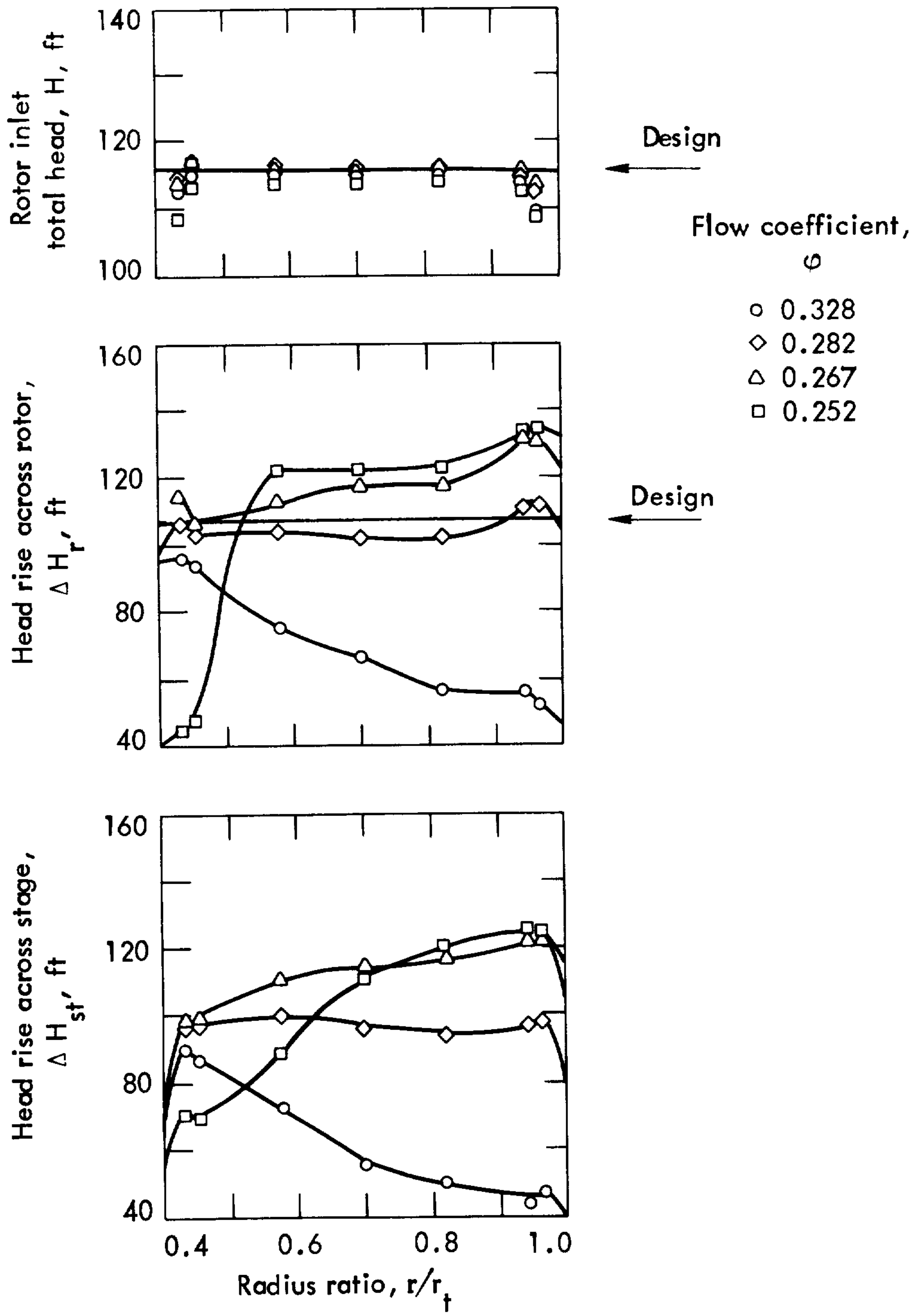

(b) Inlet head and head rise

Figure 3. - Continued.

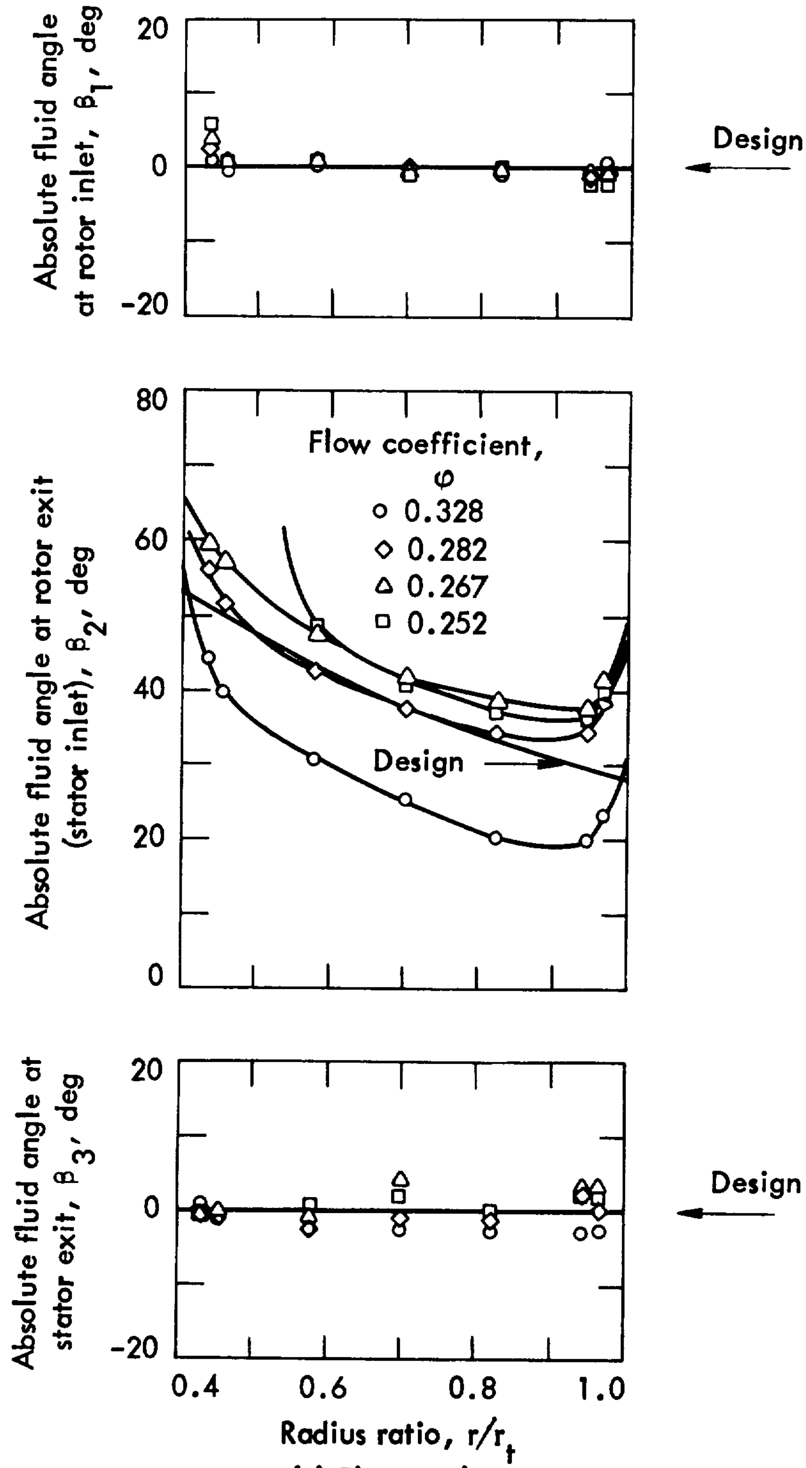

(c) Flow angle

Figure 3. - Concluded.

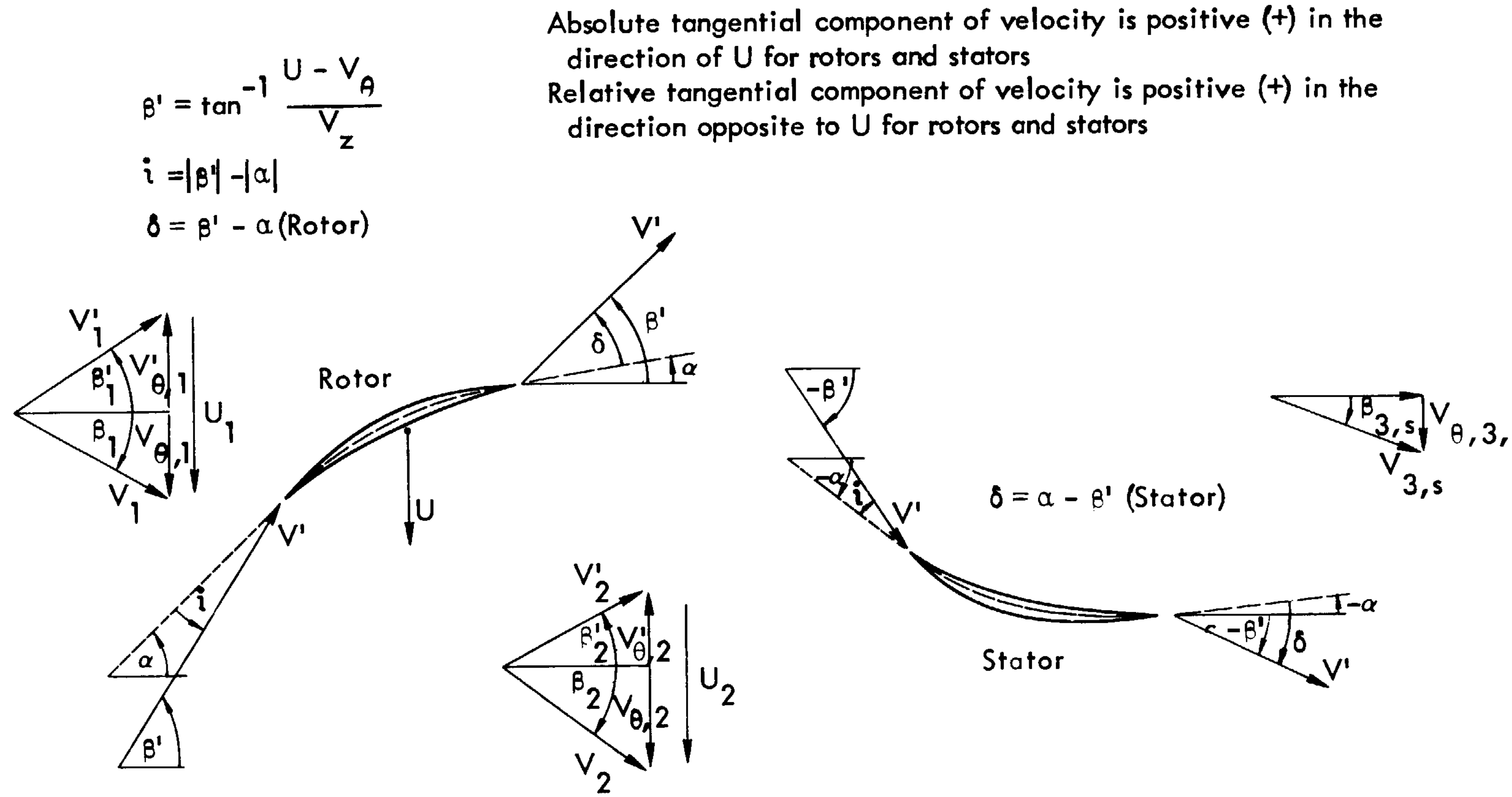

Figure 4. - Sign convention for blade-element parameters.

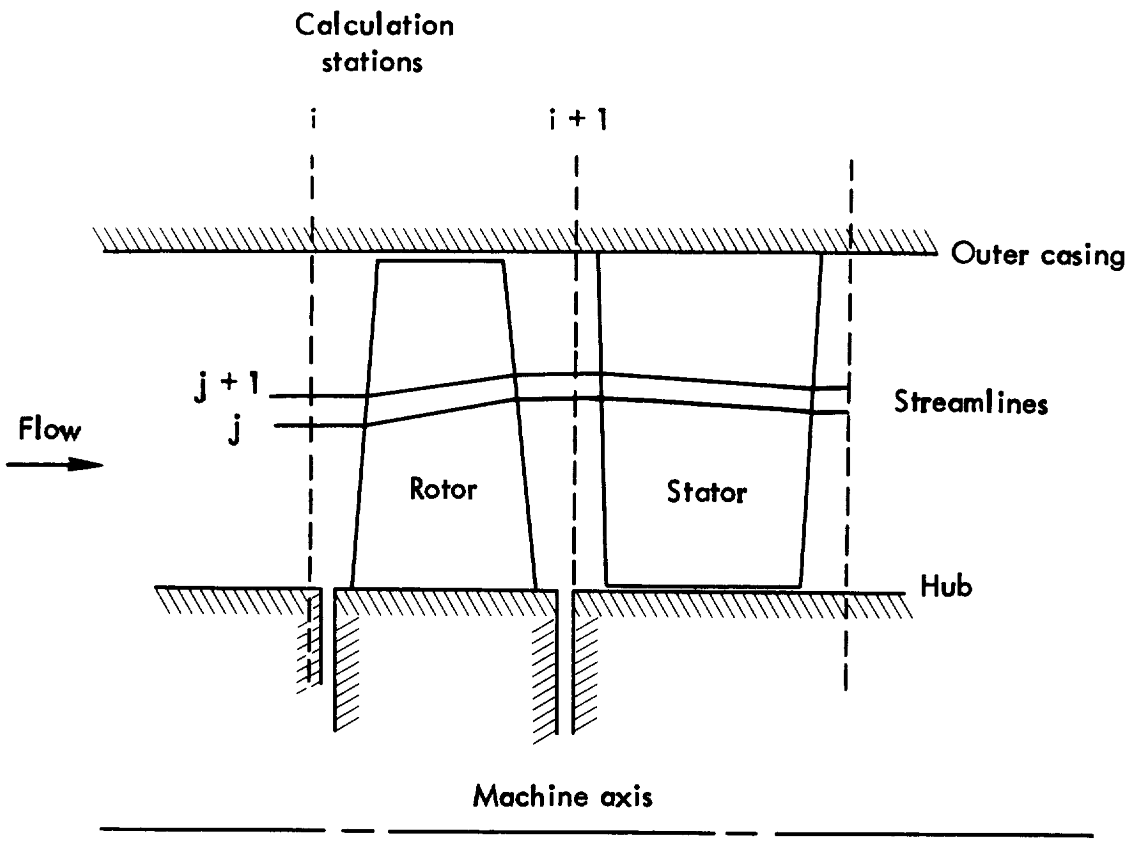

Figure 5. - Meridional plane view of a typical axial-flow pump stage.

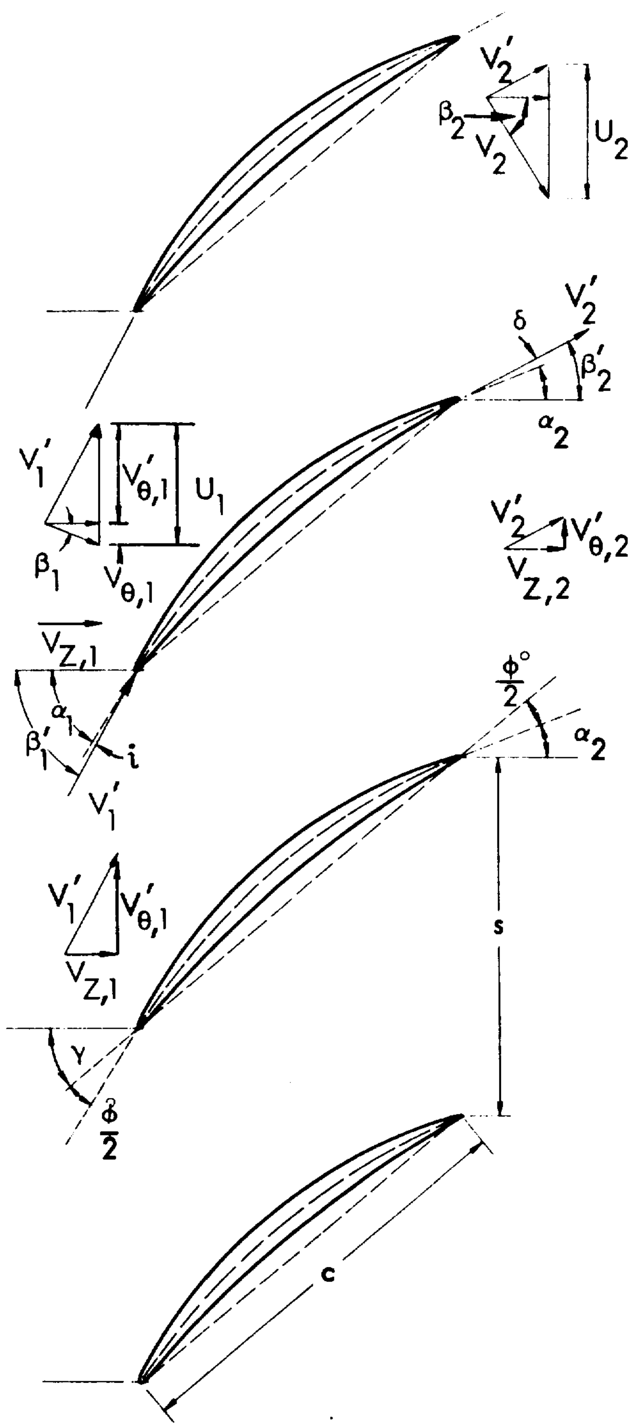

Figure 6. - Typical blade elements and nomenclature.

(a) Effect of blade setting angle

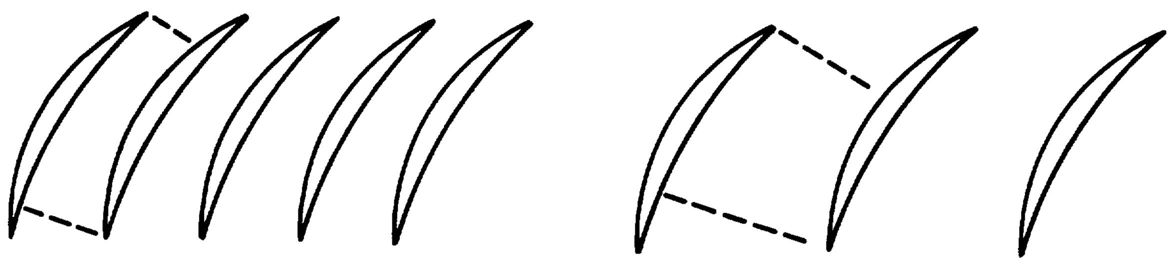

(b) Effect of solidity

(c) Effect of camber

Figure 7. - Effect of geometric parameters on deviation angle.

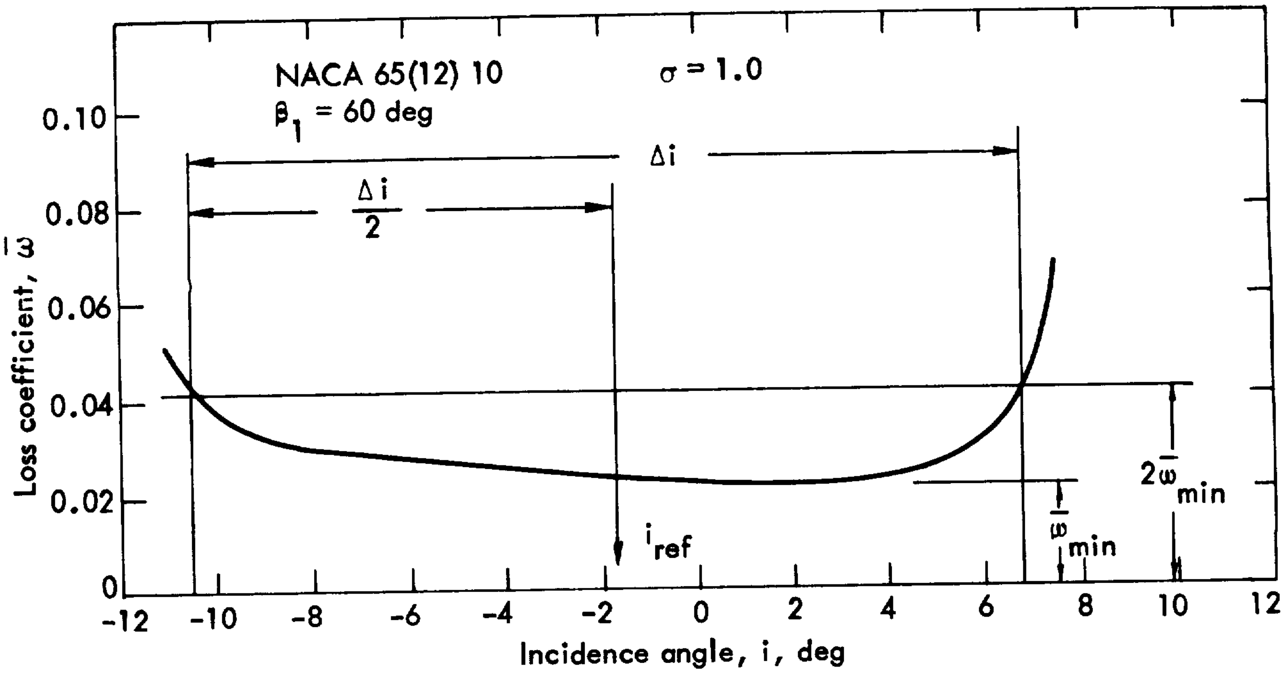

Figure 8. - Schematic definition of reference incidence angle.
Data from reference 40.

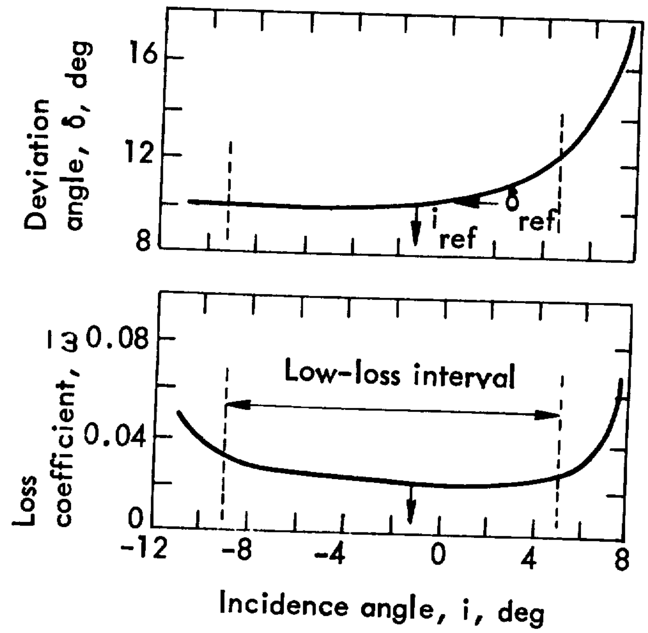

Figure 9. - Typical cascade results.

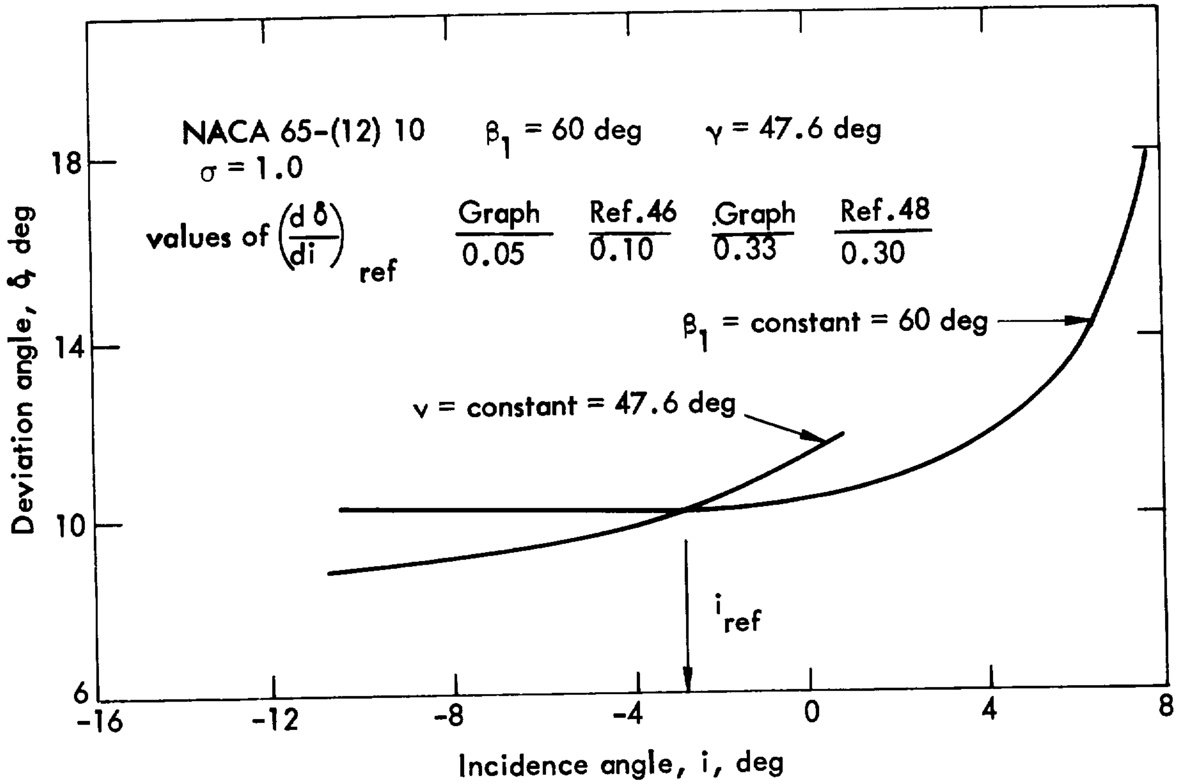

Figure 10. - Comparison of deviation angle as a function of incidence angle for constant inlet angle and constant blade setting angle. Data from reference 40.

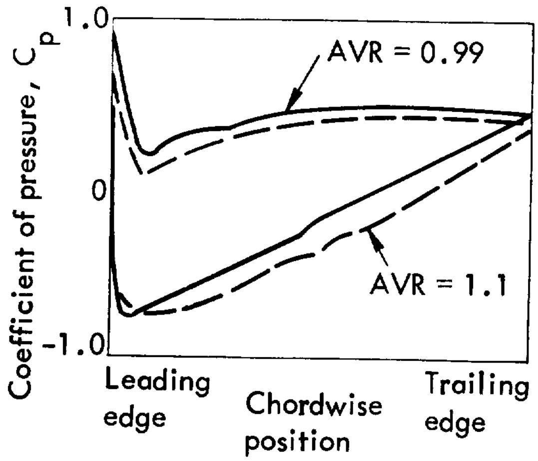

Figure 11. - Effect of axial velocity ratio on cascade blade pressure distribution (ref. 52).

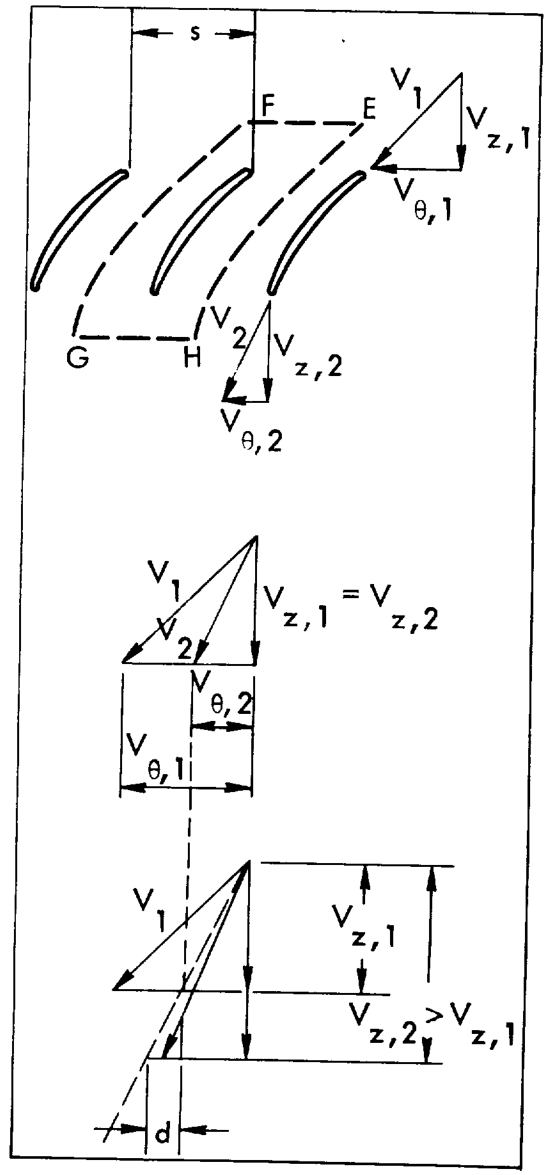

Figure 12. - Effect of axial velocity ratio on plane cascade velocity diagrams.

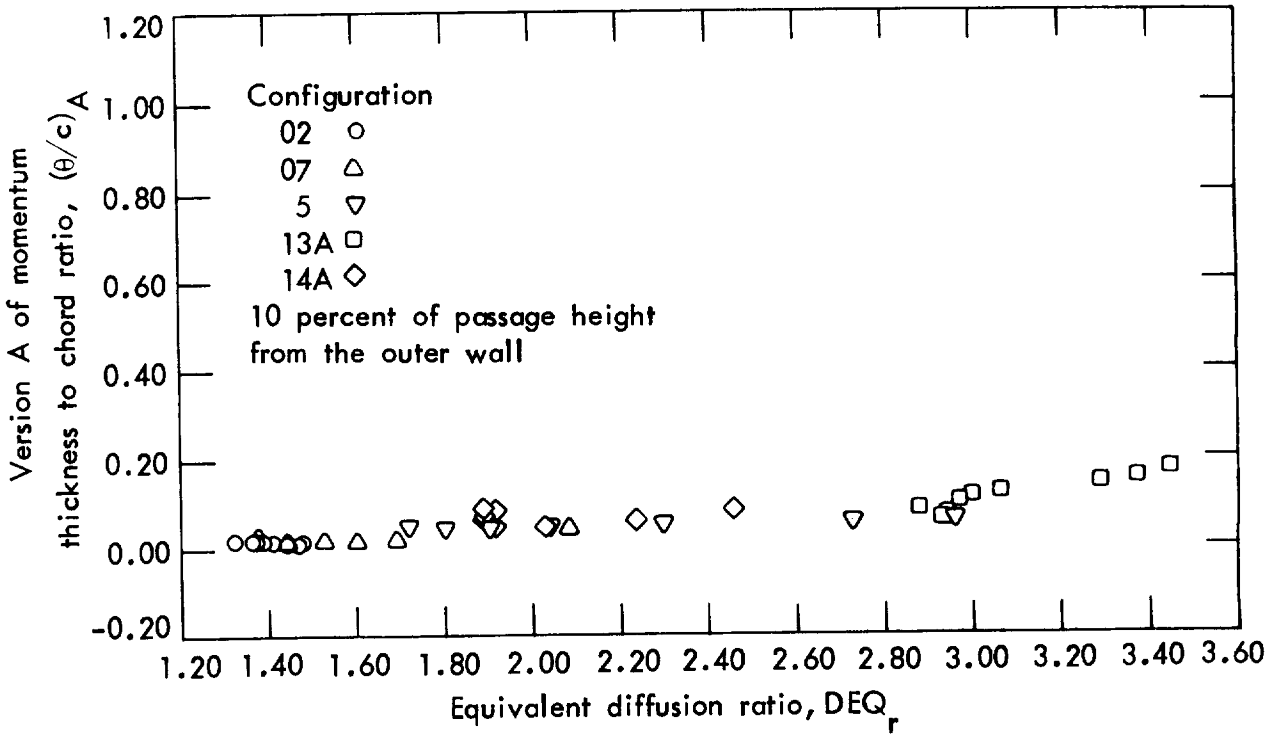

(a) Version A of momentum thickness to chord ratio; 10 percent of passage height from the outer wall.

Figure 13. - Variation of blade-element wake momentum thickness parameter with loading (equivalent diffusion ratio).

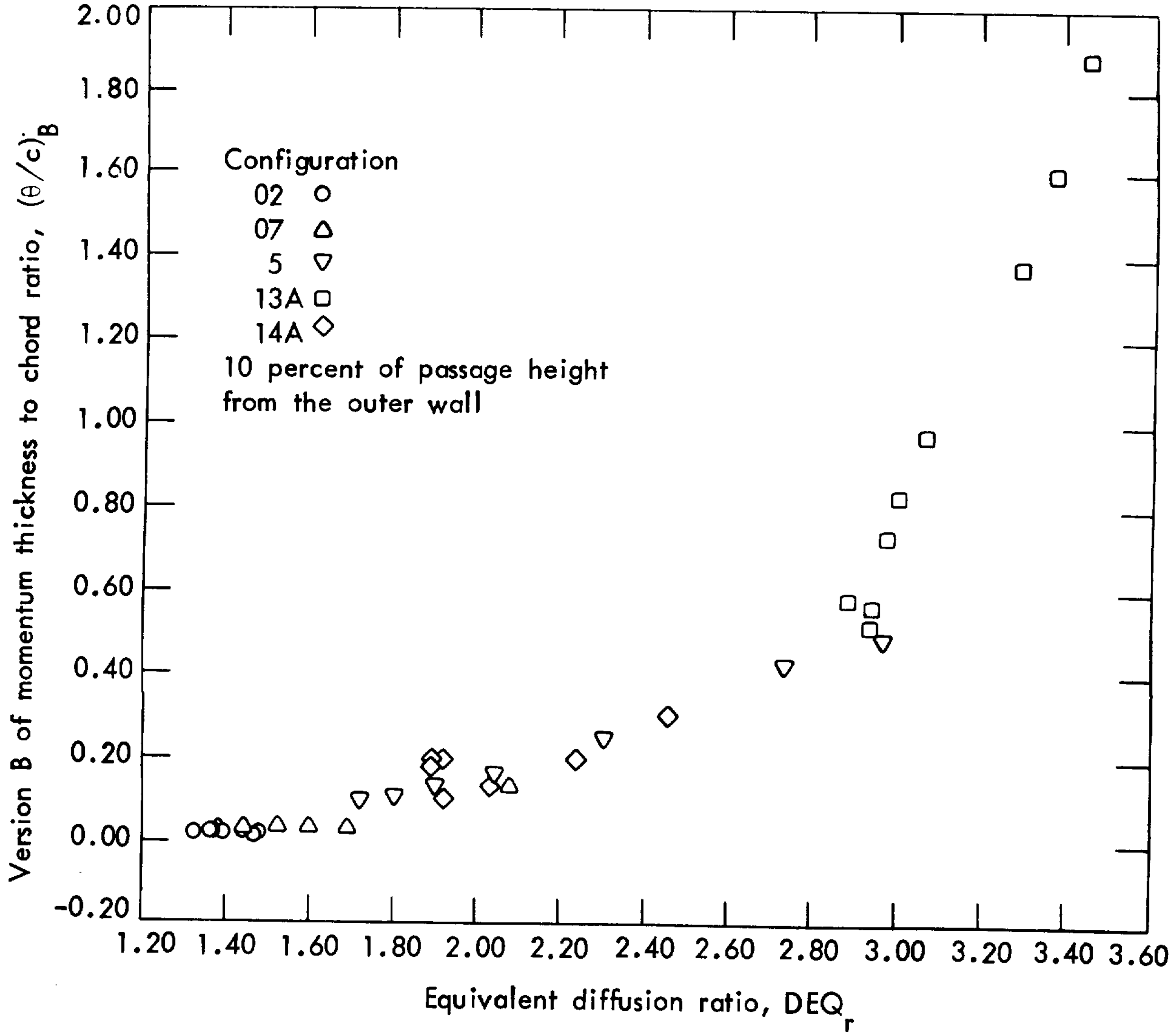

(b) Version B of momentum thickness to chord ratio; 10 percent of passage height from the outer wall.

Figure 13. - Continued.

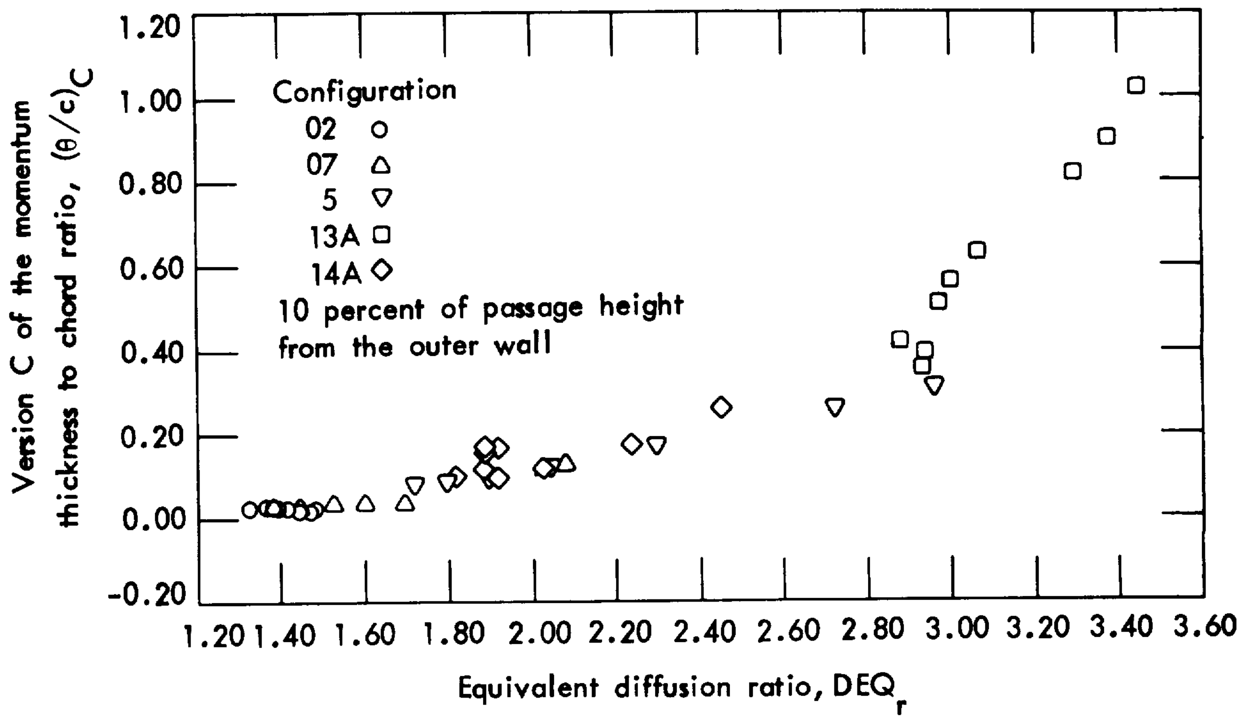

(c) Version C of the momentum thickness to chord ratio; 10 percent of passage height from the outer wall.

Figure 13. - Continued.

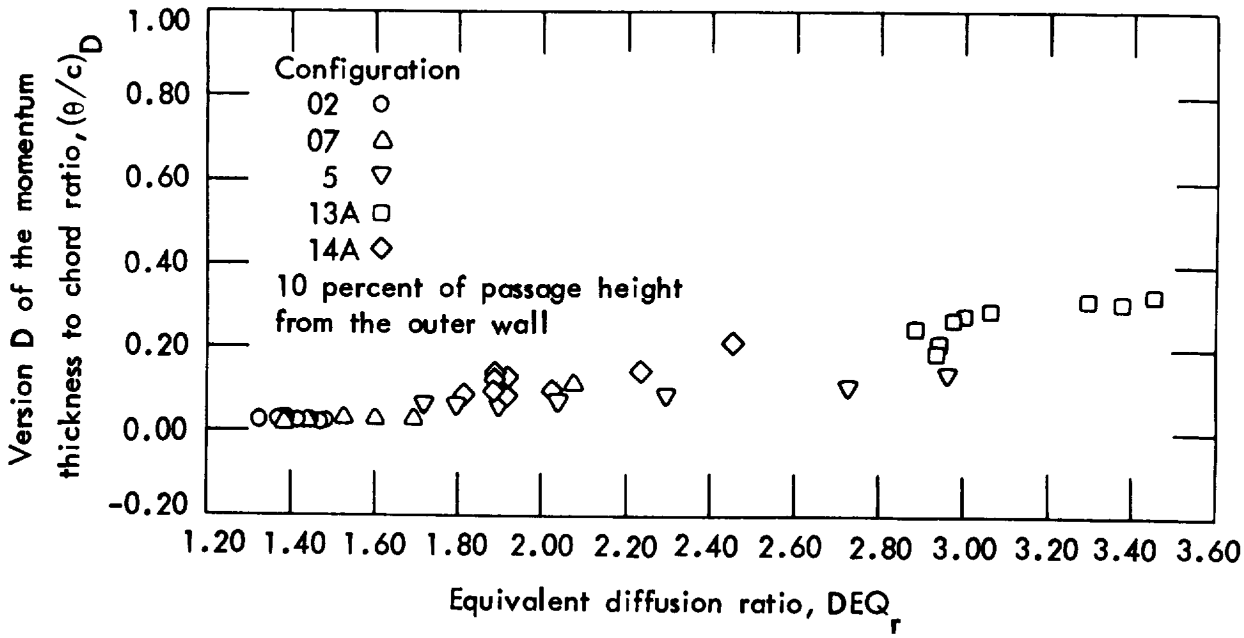

(d) Version D of the momentum thickness to chord ratio; 10 percent of passage height from the outer wall.

Figure 13. - Continued.

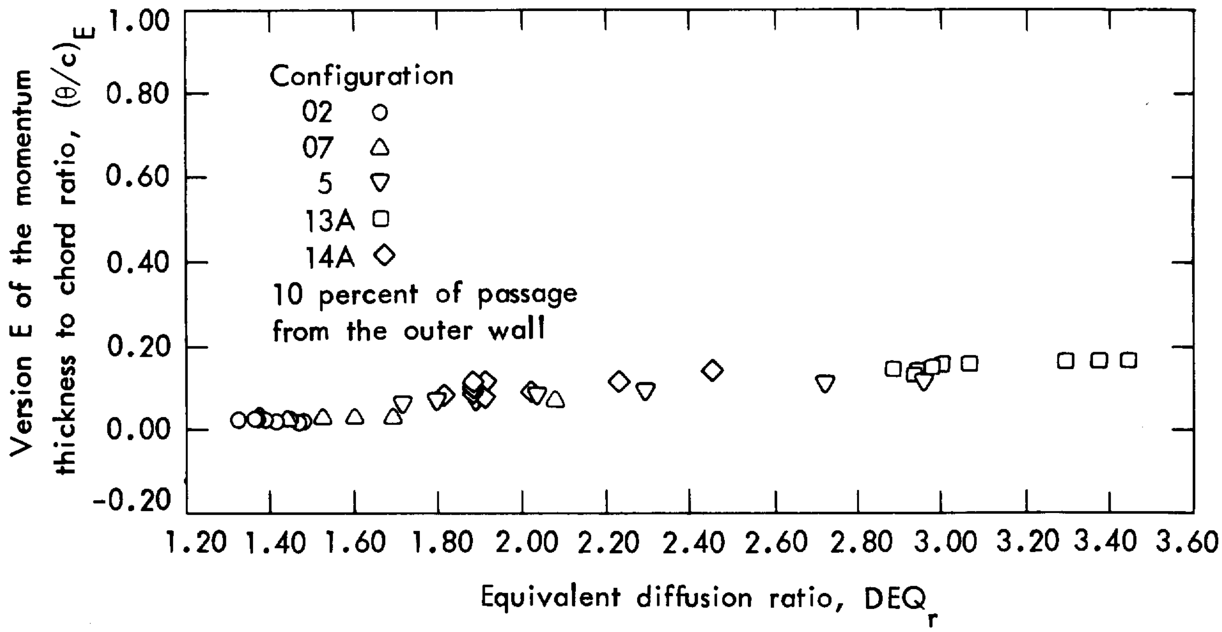

(e) Version E of the momentum thickness to chord ratio; 10 percent of passage height from the outer wall.

Figure 13. - Continued.

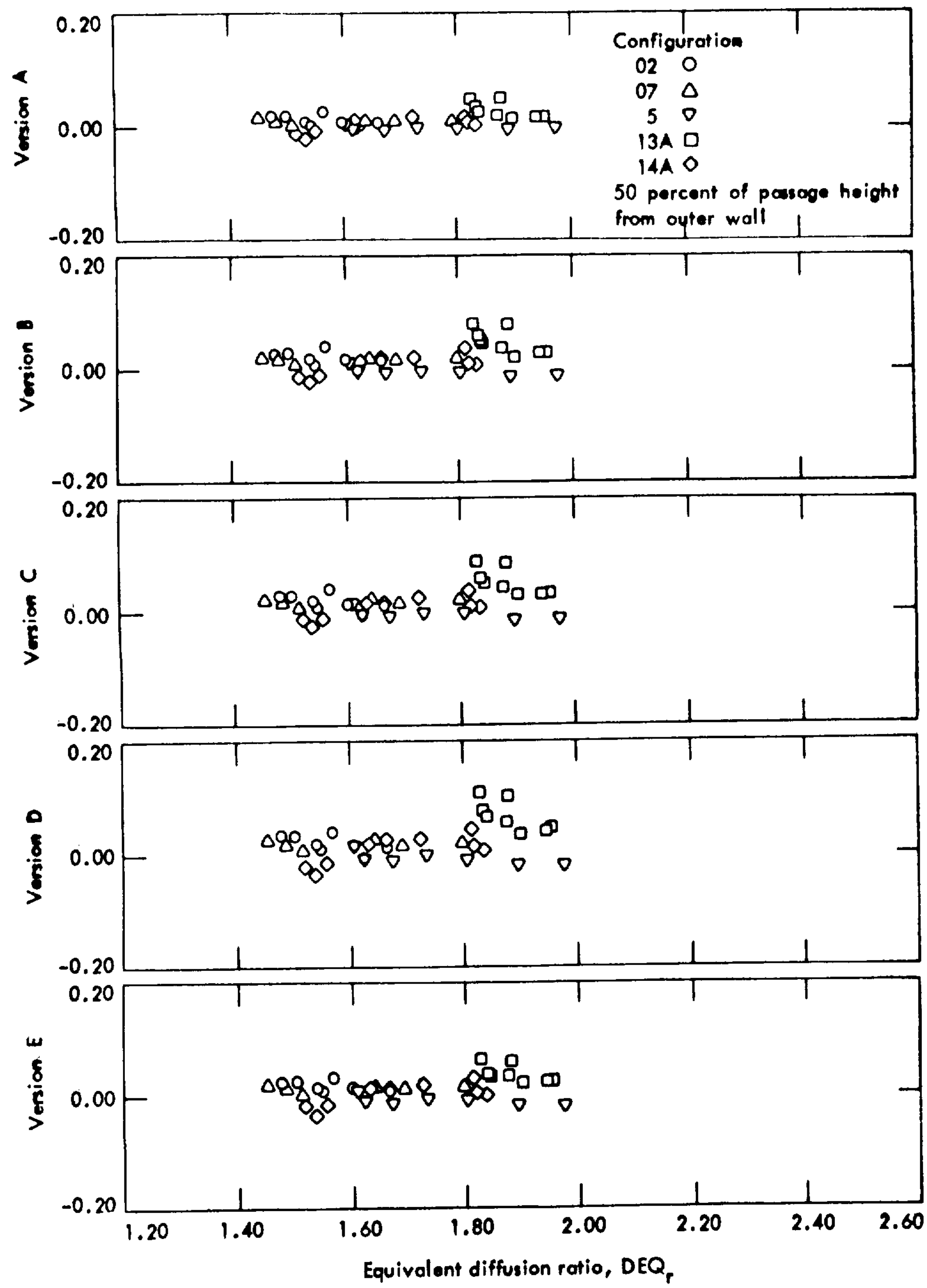

(f) Versions A, B, C, D, and E of the momentum thickness to chord ratio; 50 percent of passage height from the outer wall.

Figure 13. - Continued.

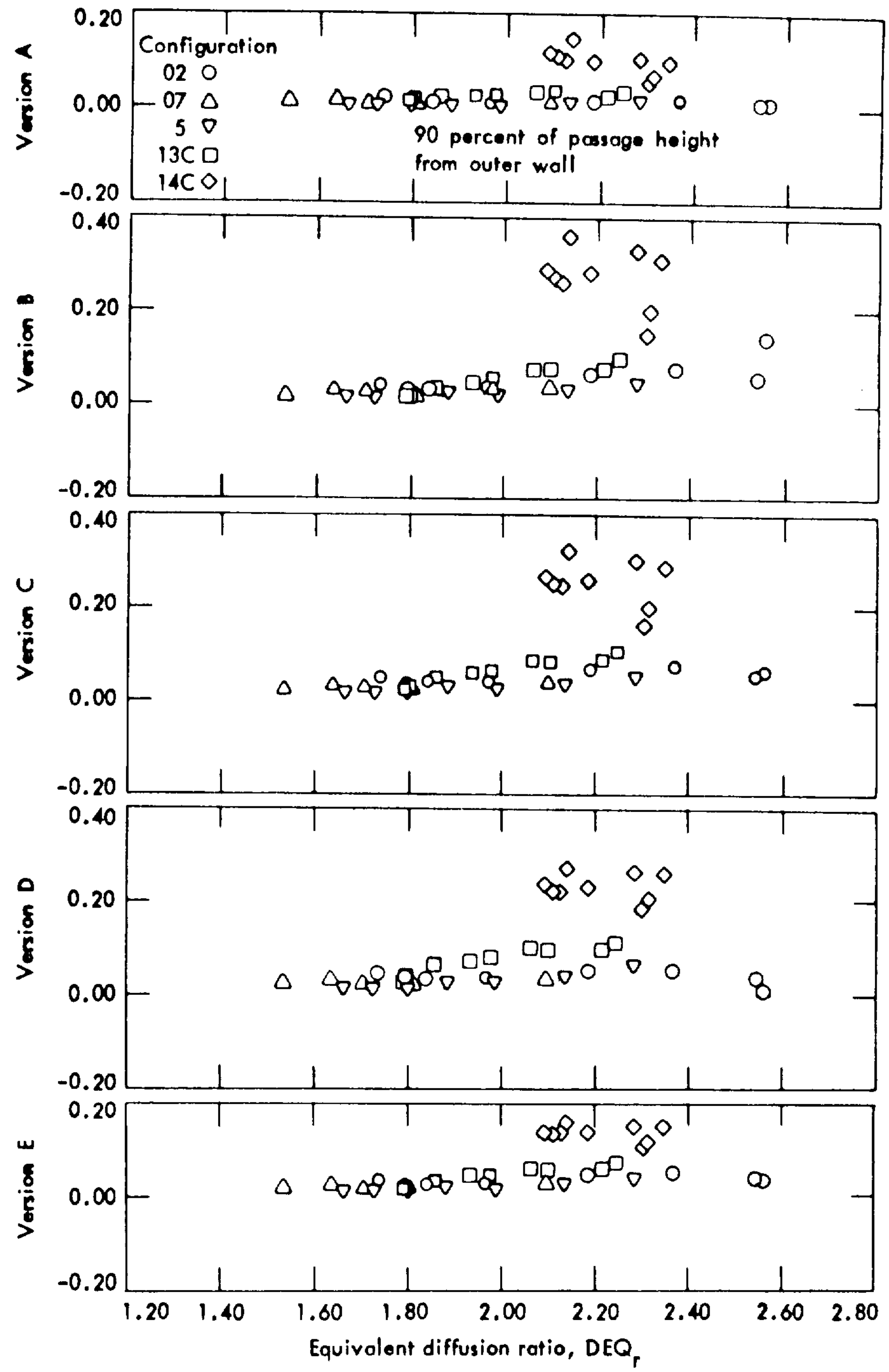

(g) Versions A, B, C, D, and E of the momentum thickness to chord ratio; 90 percent of passage height from the outer wall.

Figure 13. - Concluded.

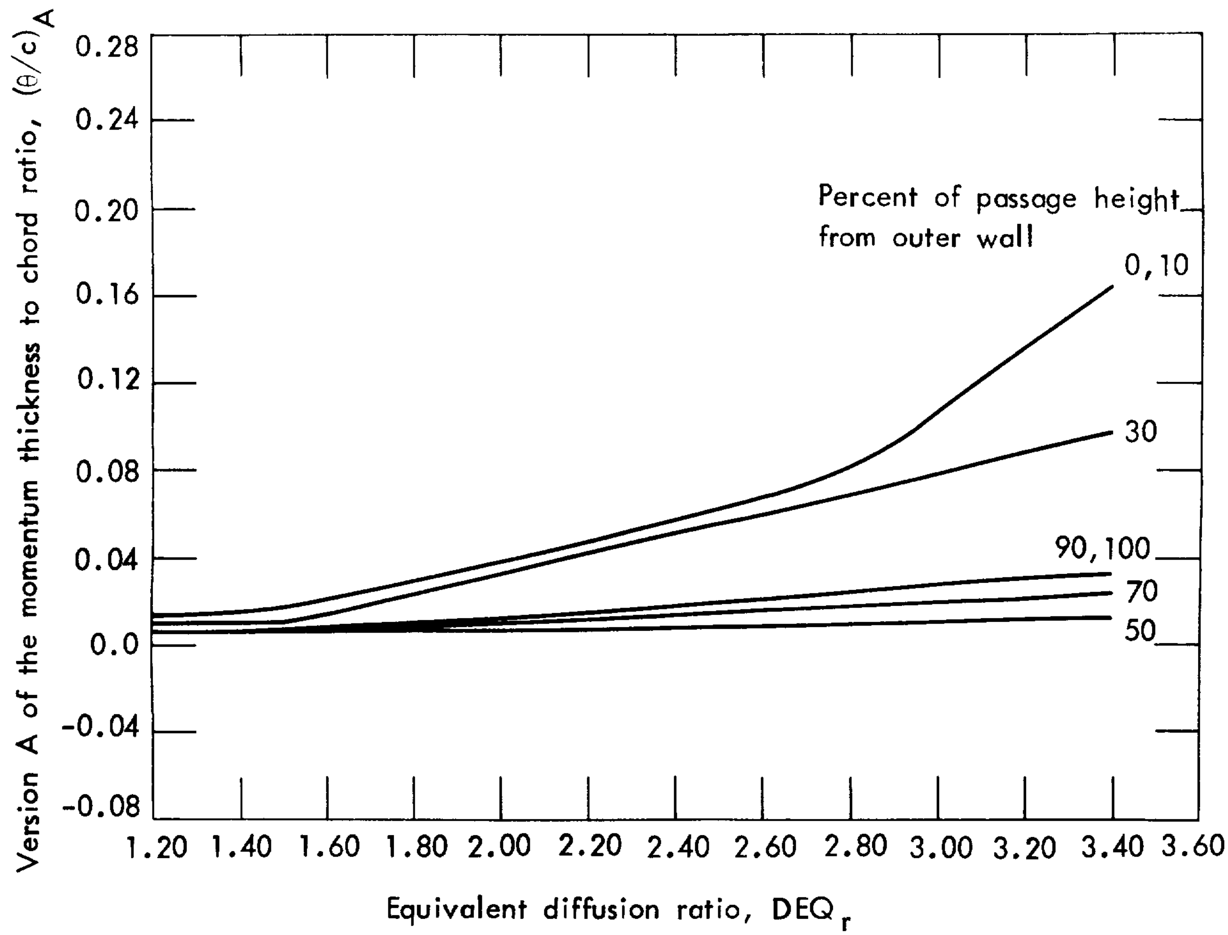

Figure 14. - Loss correlation curves derived from experimental data with Version A of the momentum thickness to chord ratio, equivalent diffusion ratio and percent of passage height from outer wall used as correlating parameters.

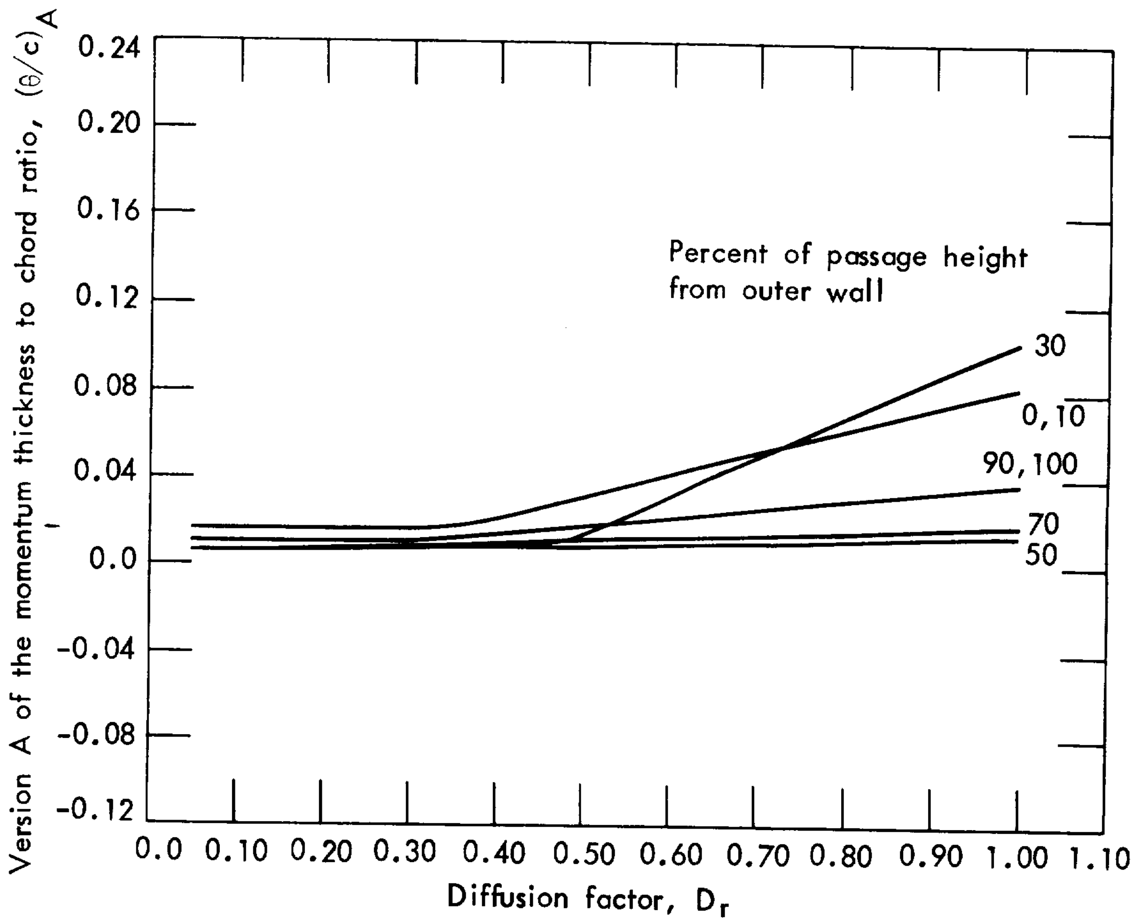

Figure 15.- Loss correlation curves derived from experimental data with Version A of the momentum thickness to chord ratio, diffusion factor and percent of passage height from outer wall used as correlating parameters.

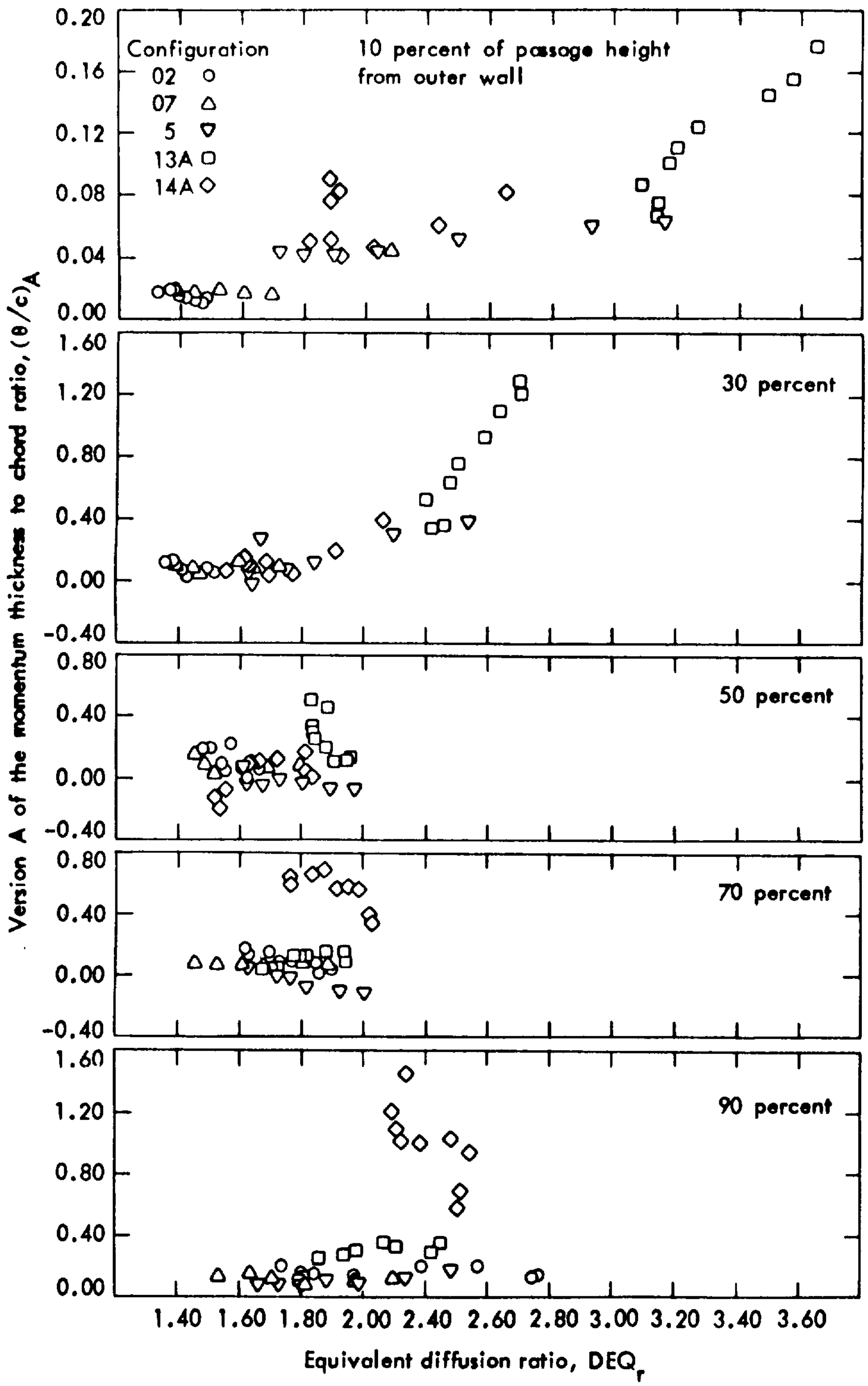

Figure 16. - Variation of Version A of the momentum thickness to chord ratio with equivalent diffusion ratio at different radii.

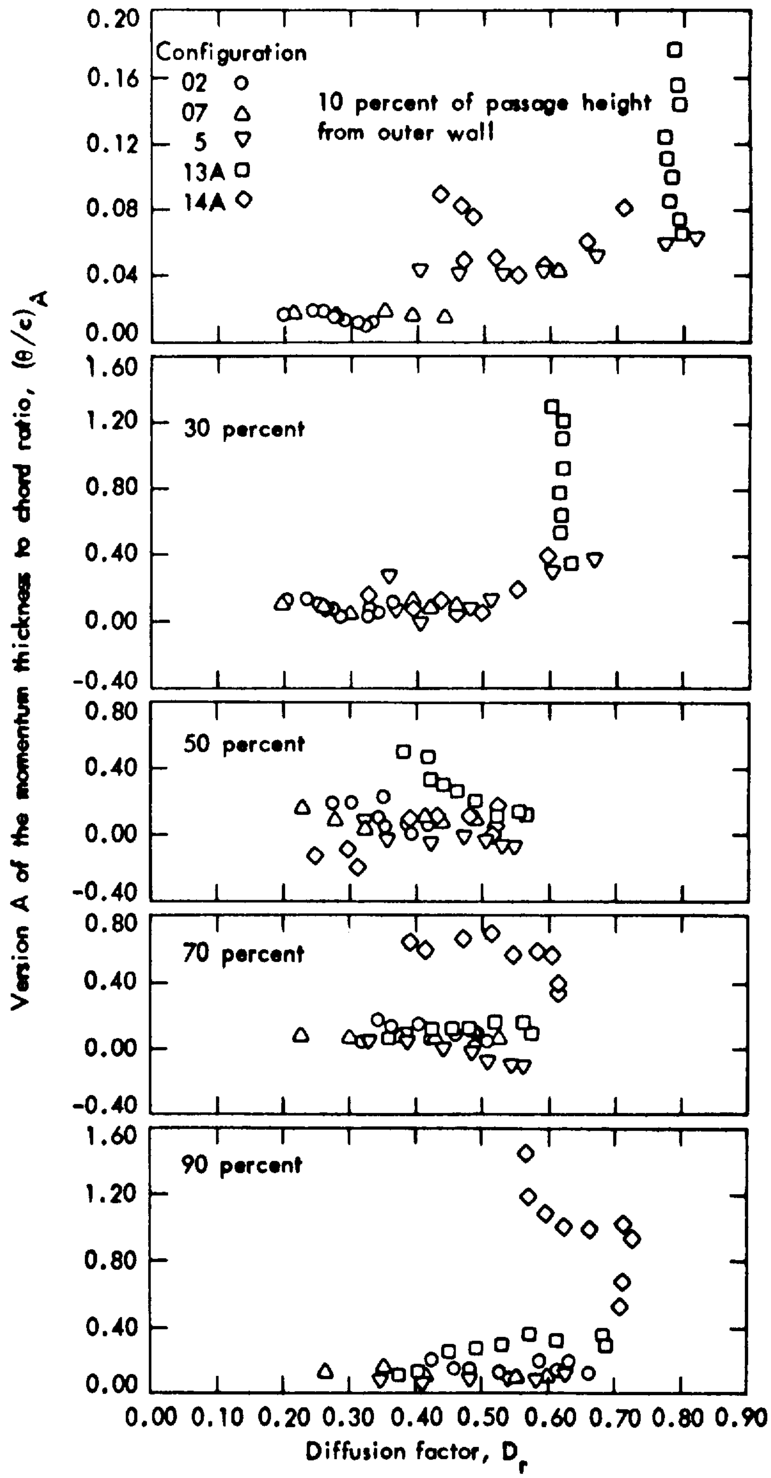

Figure 17. - Variation of Version A of the momentum thickness to chord ratio with diffusion factor at different radii.

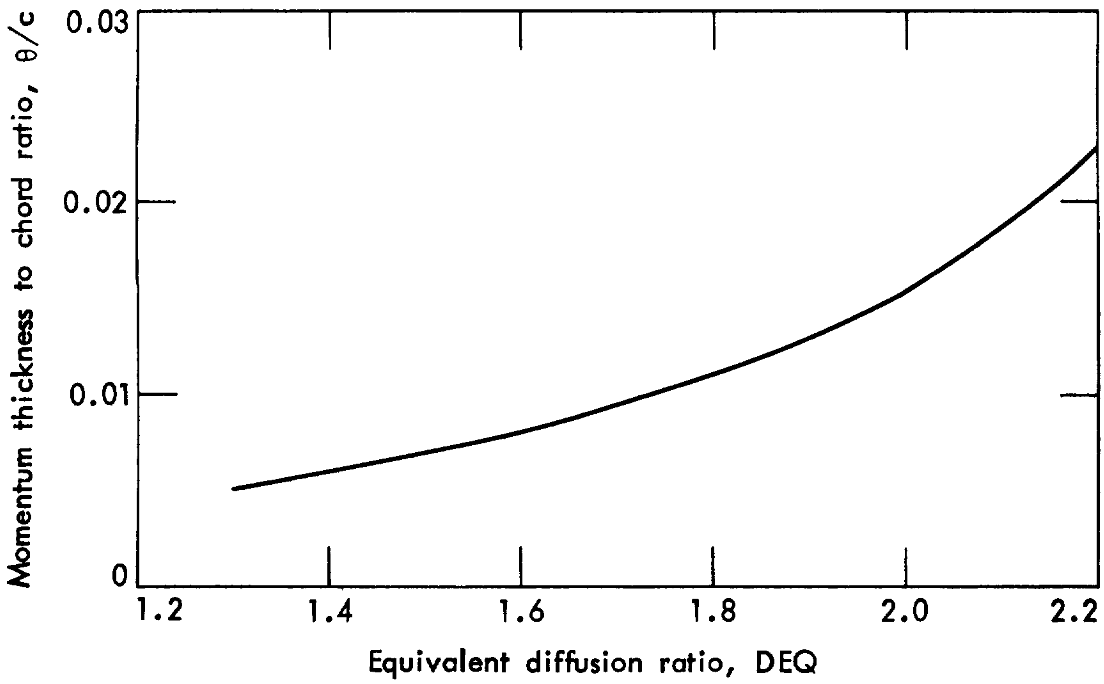

Figure 18. - Two-dimensional cascade loss correlation (ref. 34).

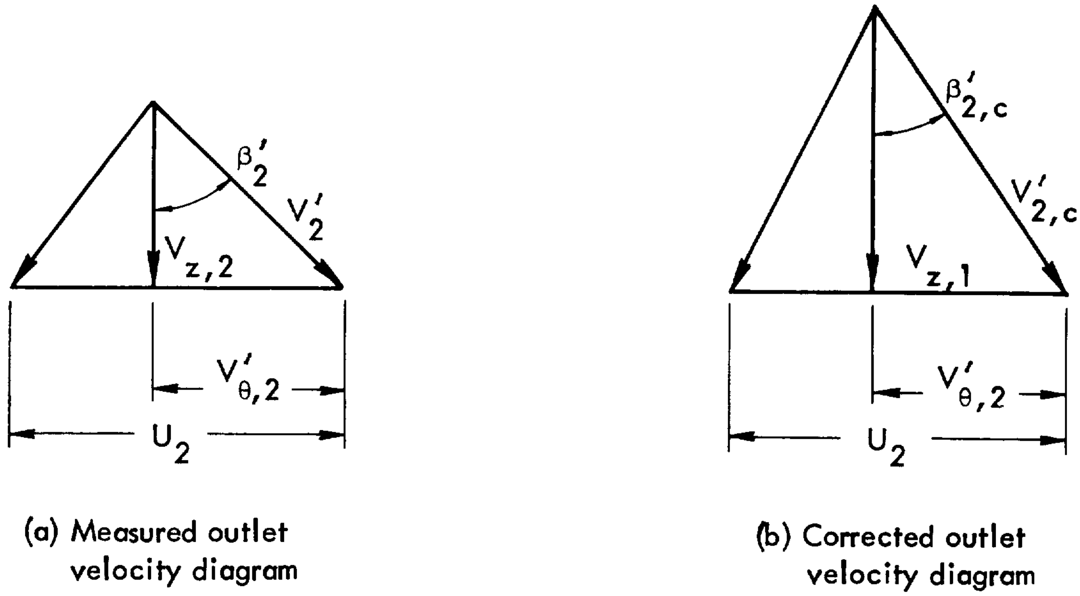

Figure 19. - Velocity diagrams used in the axial velocity ratio correction of reference 51.

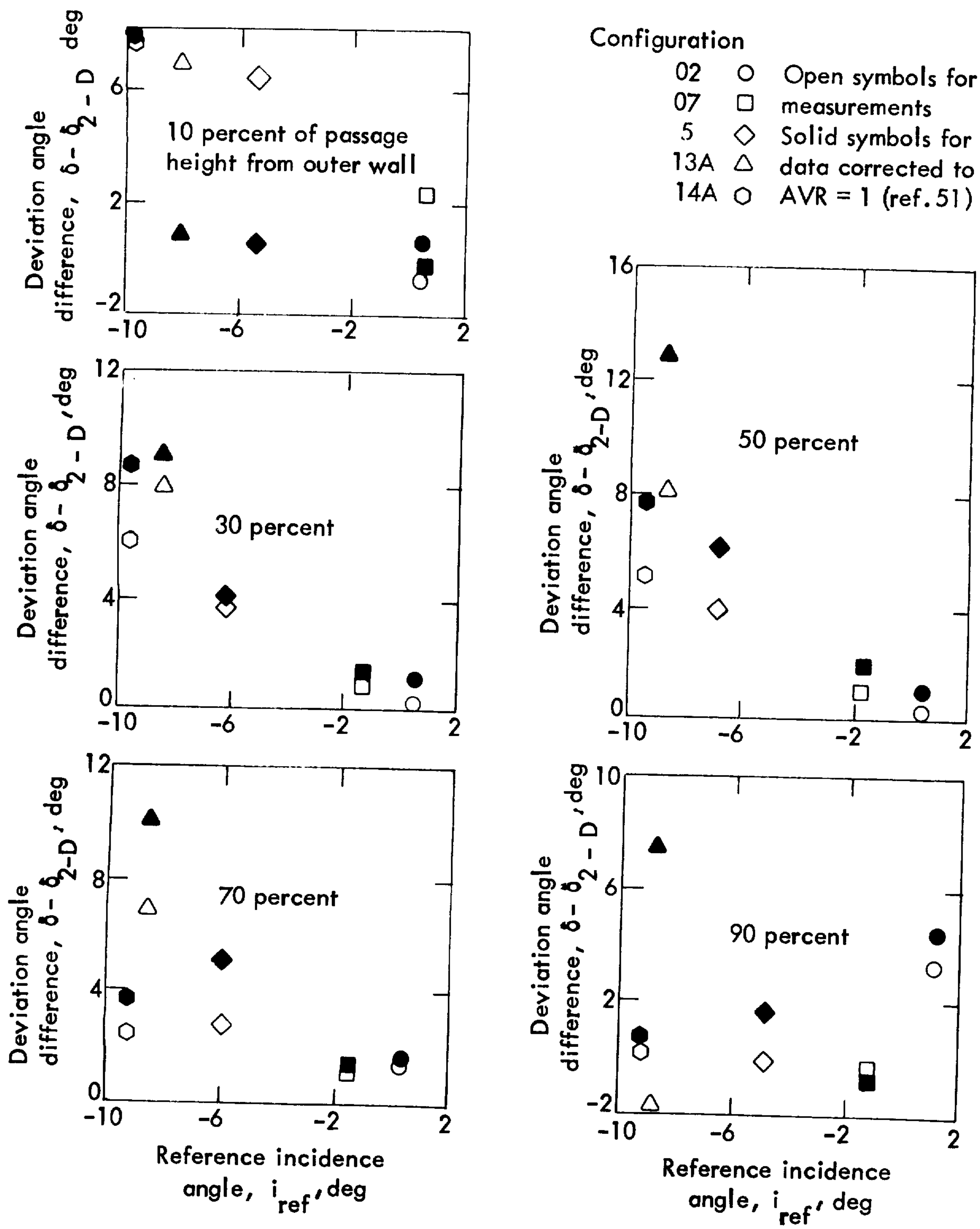

Figure 20. - Results of using the axial velocity ratio correction of reference 51 at reference incidence angle conditions.

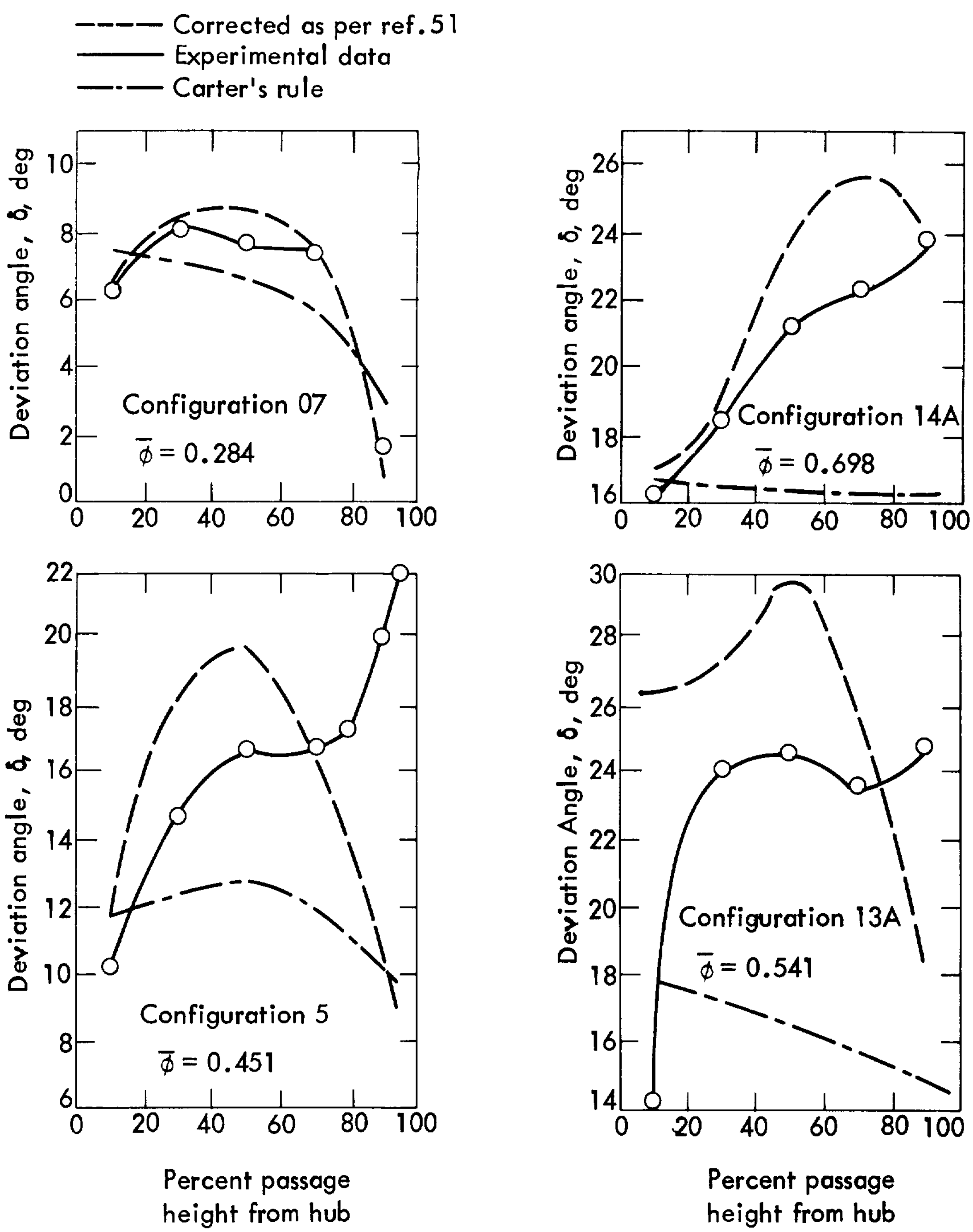

Figure 21. - Results of using the axial velocity ratio correction of reference 51 at design flow coefficient.

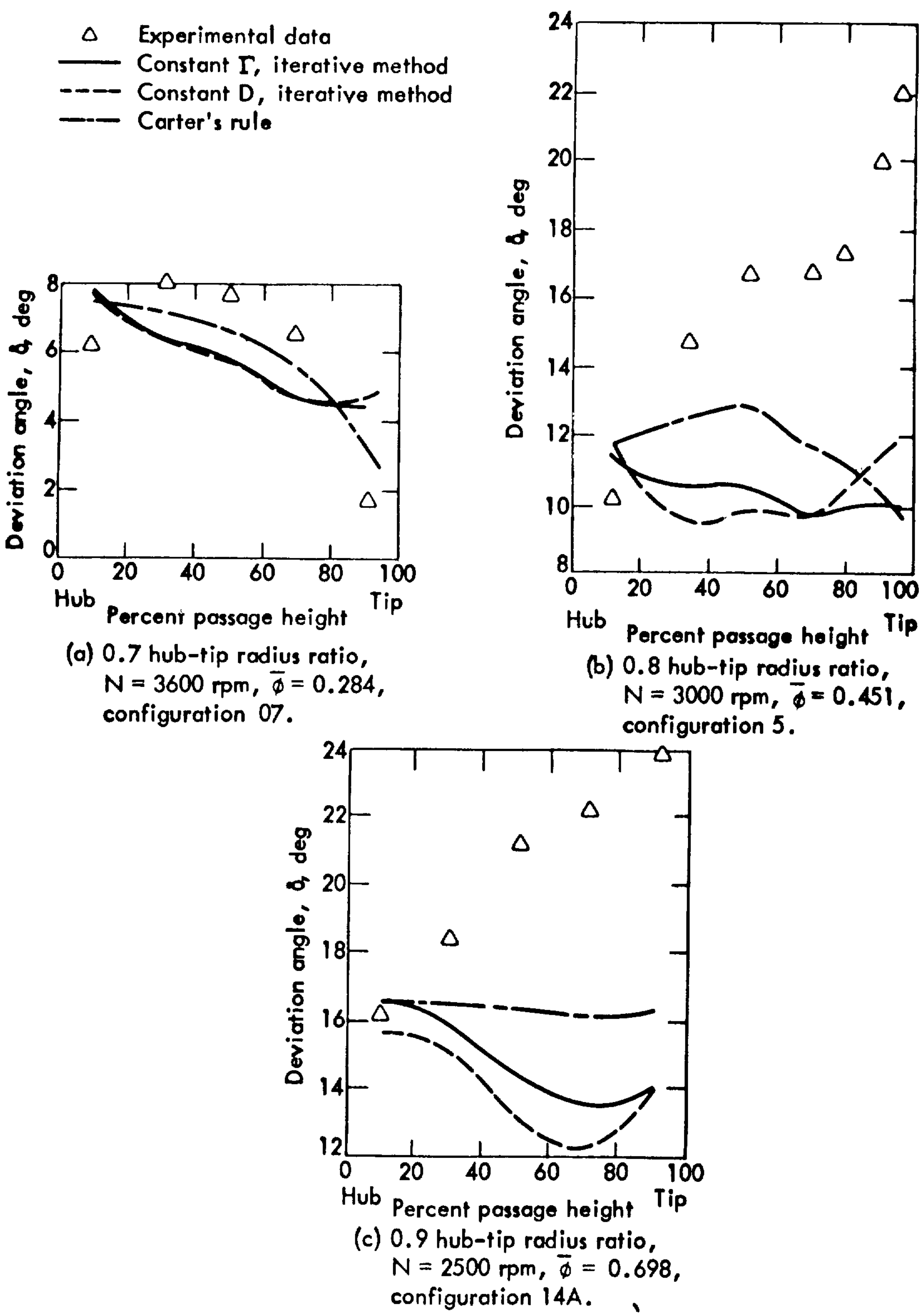

(a) 0.7 hub-tip radius ratio, N = 3600 rpm, $\bar{\phi}$ = 0.284, configuration 07.

(b) 0.8 hub-tip radius ratio, N = 3000 rpm, $\bar{\phi}$ = 0.451, configuration 5.

(c) 0.9 hub-tip radius ratio, N = 2500 rpm, $\bar{\phi}$ = 0.698, configuration 14A.

Figure 22. - Deviation angle radial distribution comparisons.

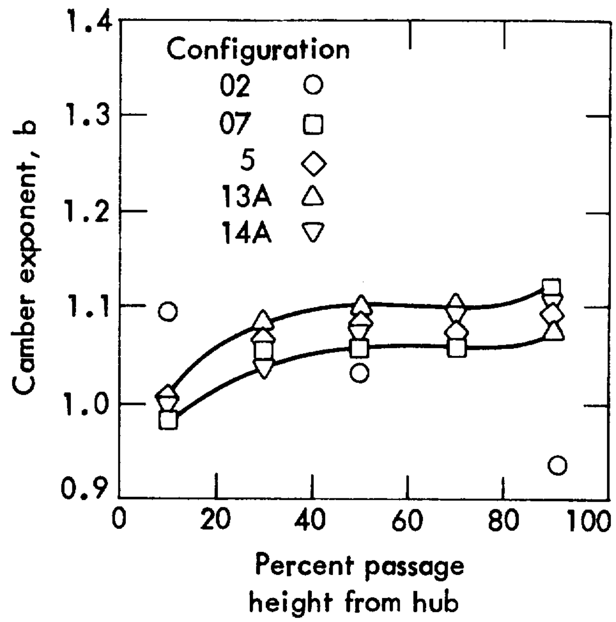

Figure 23. - Camber exponents for reference incidence angle conditions using the corrected camber concept.

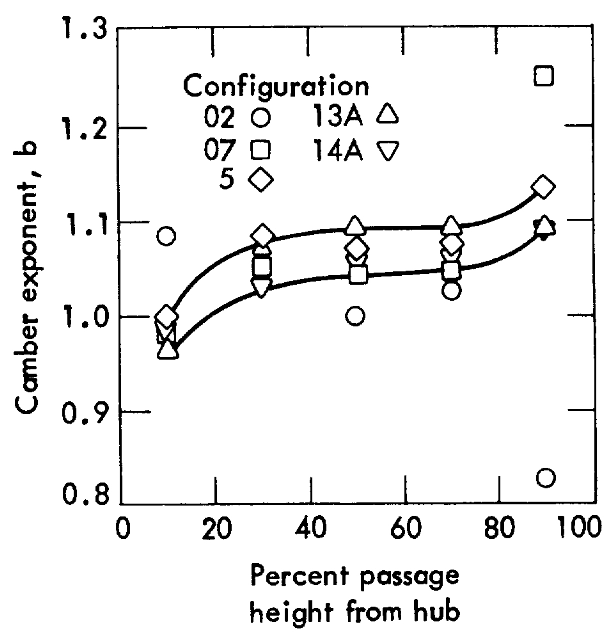

Figure 24. - Camber exponents for reference incidence angle conditions using actual blade camber.

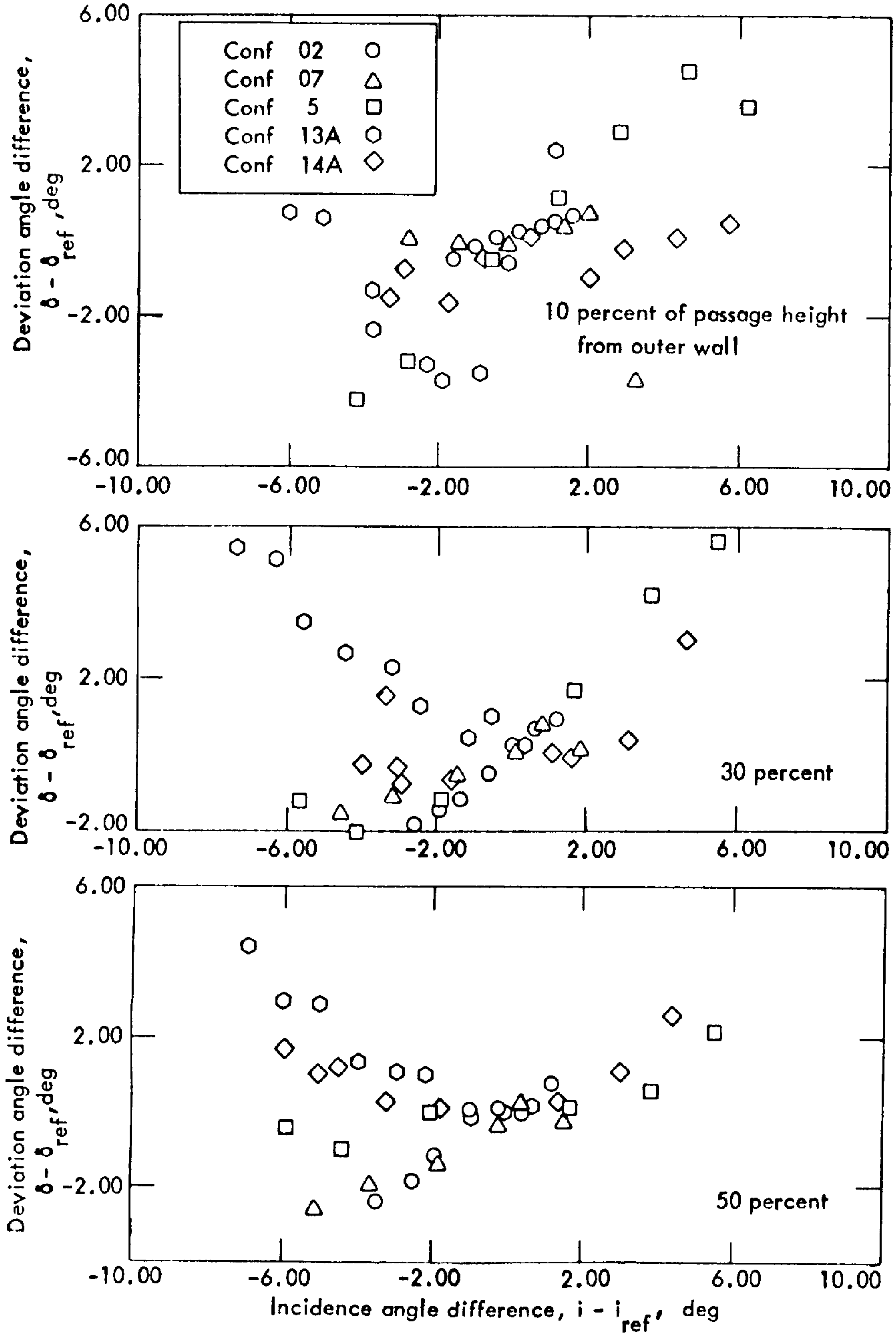

Figure 25. - Measured deviation angle as a function of incidence angle.

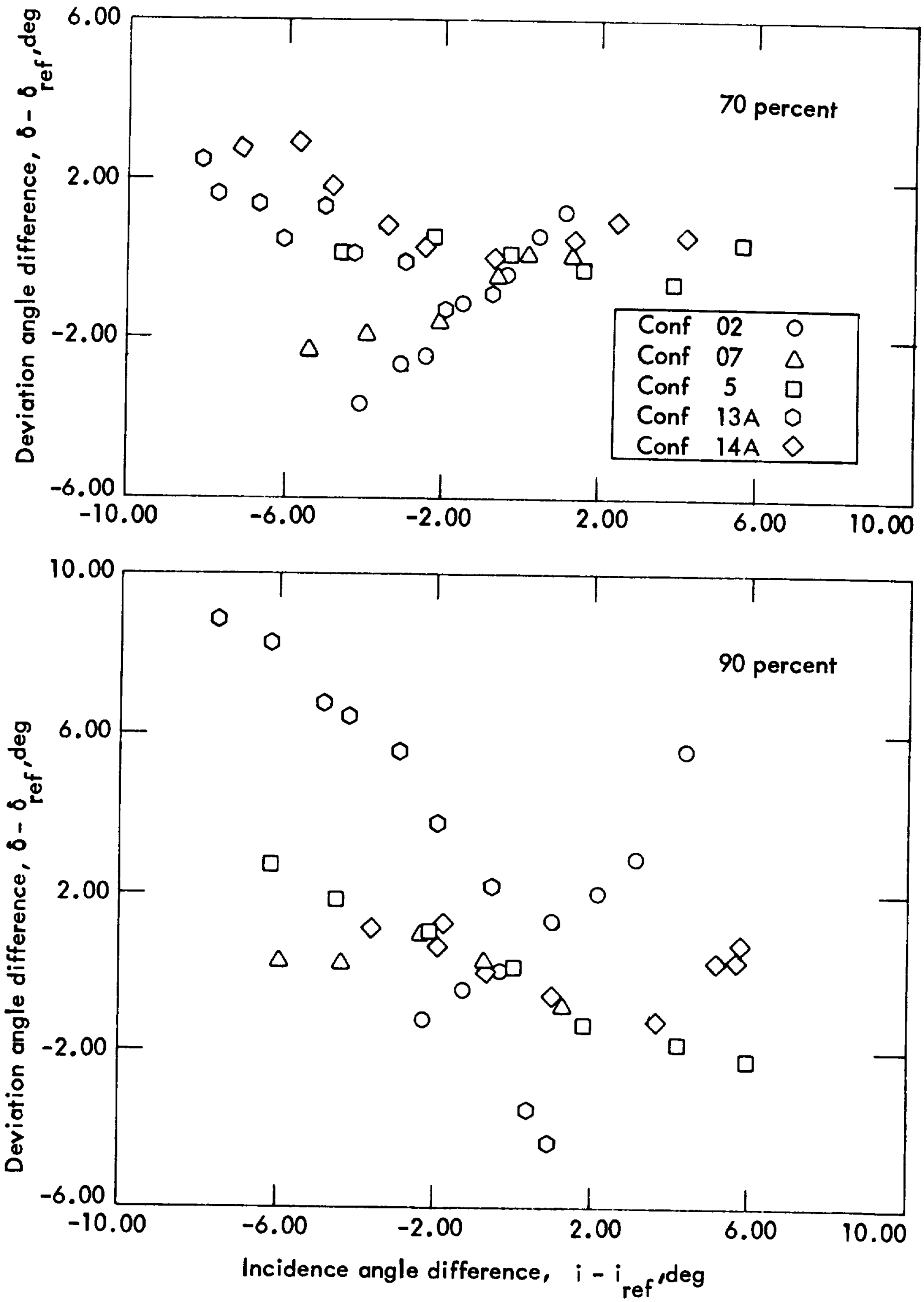

Figure 25. - Concluded.

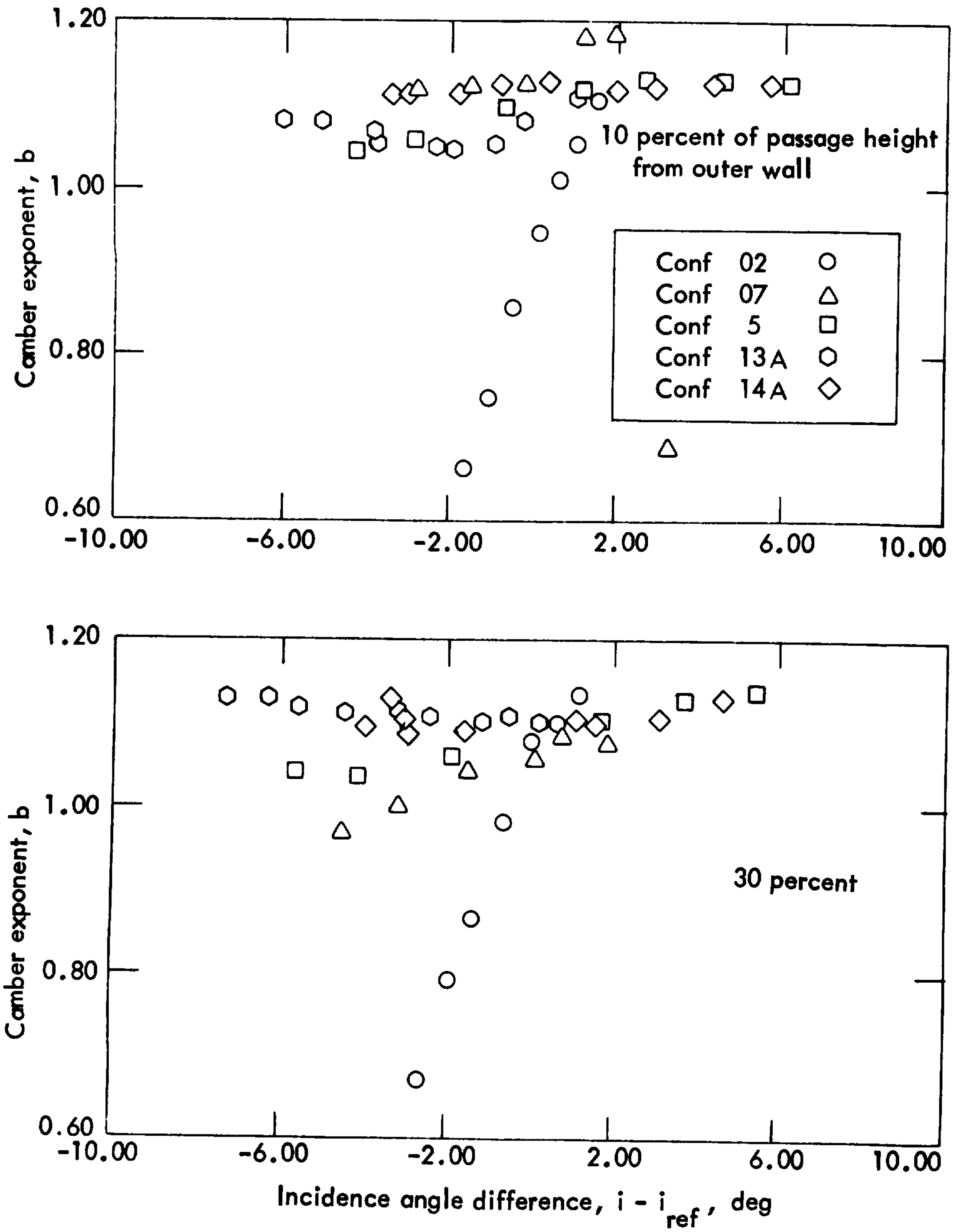

Figure 26. - Camber exponents for entire operating range using equivalent camber concept.

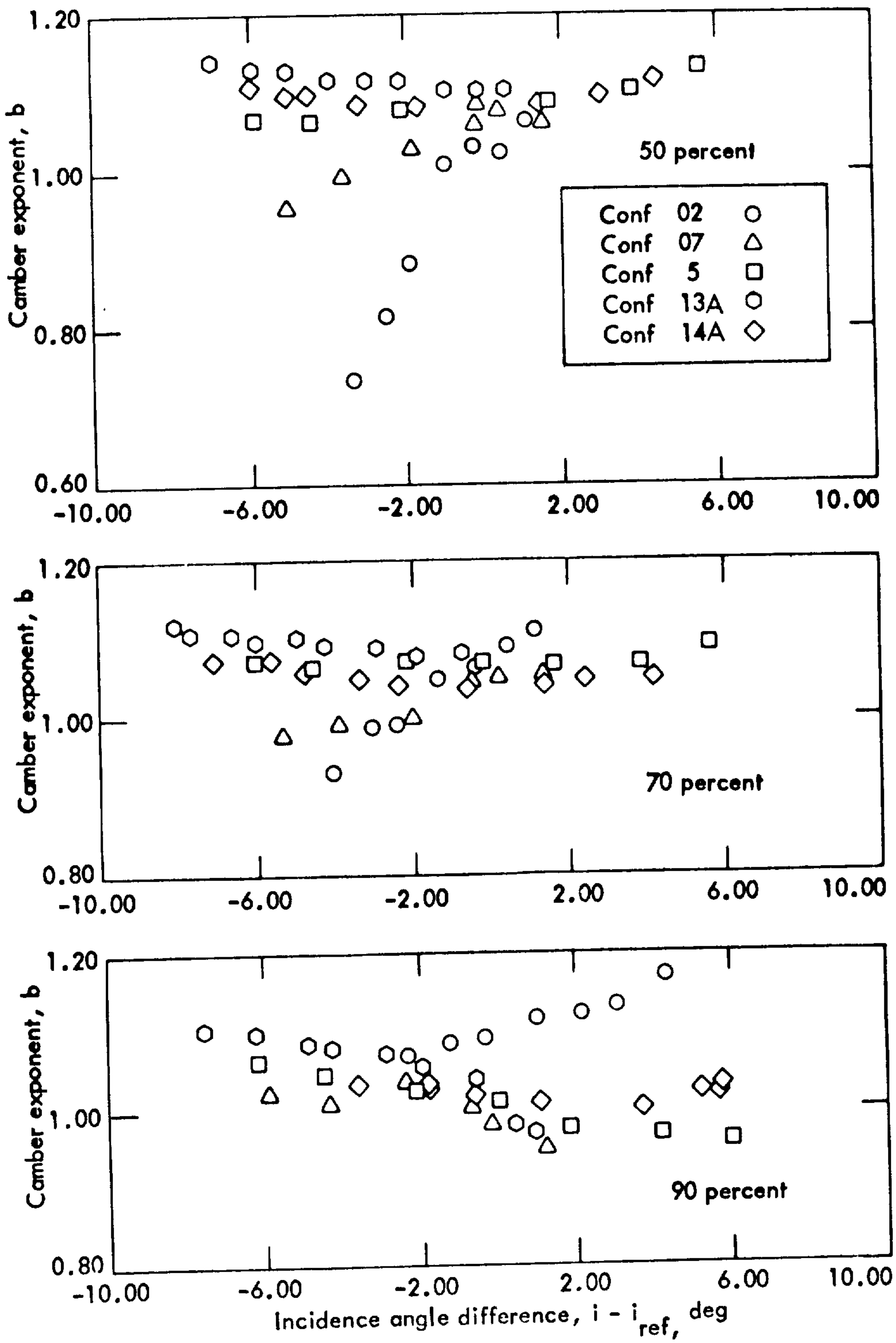

Figure 26. - Concluded.

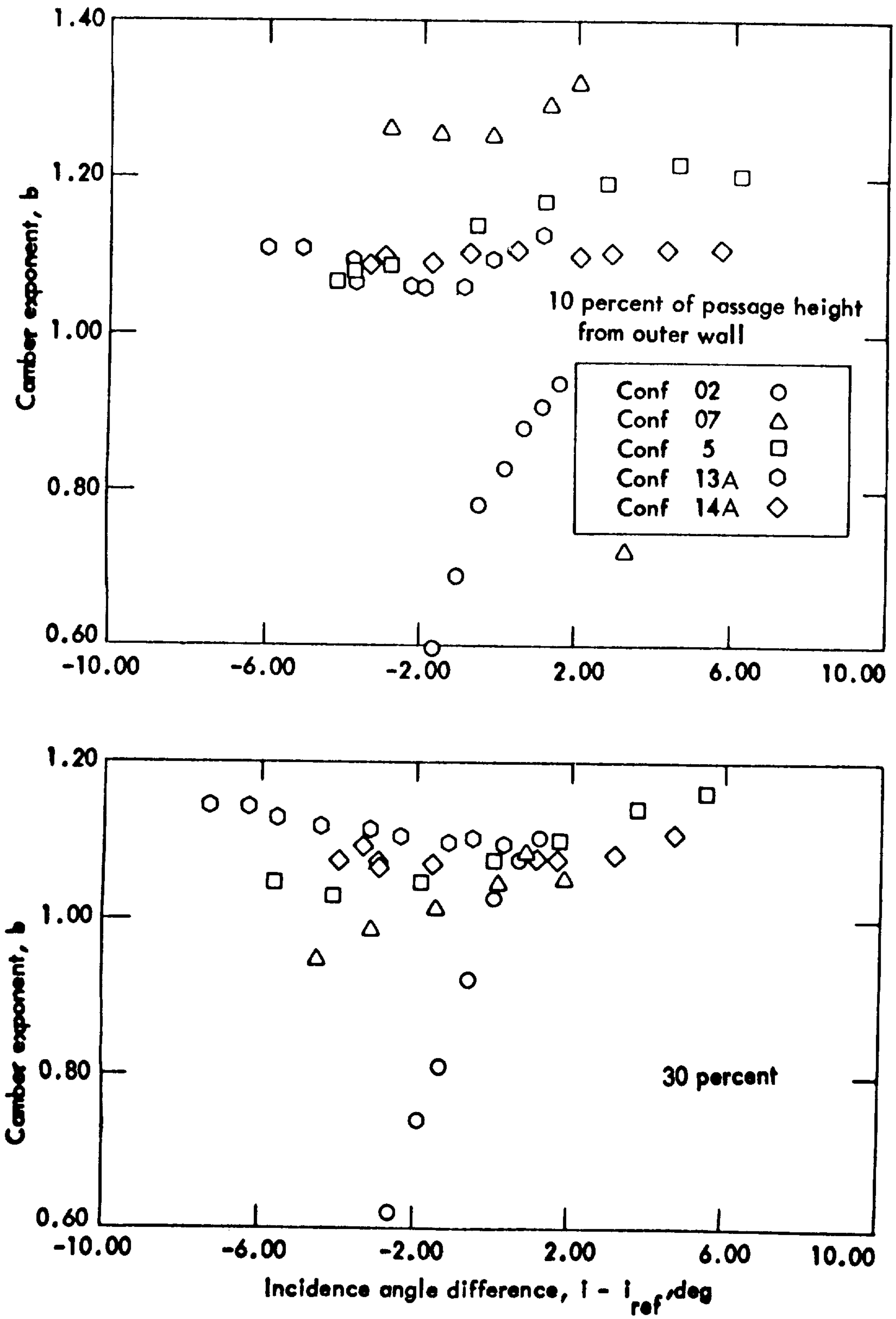

Figure 27. - Camber exponents for entire operating range using actual blade camber.

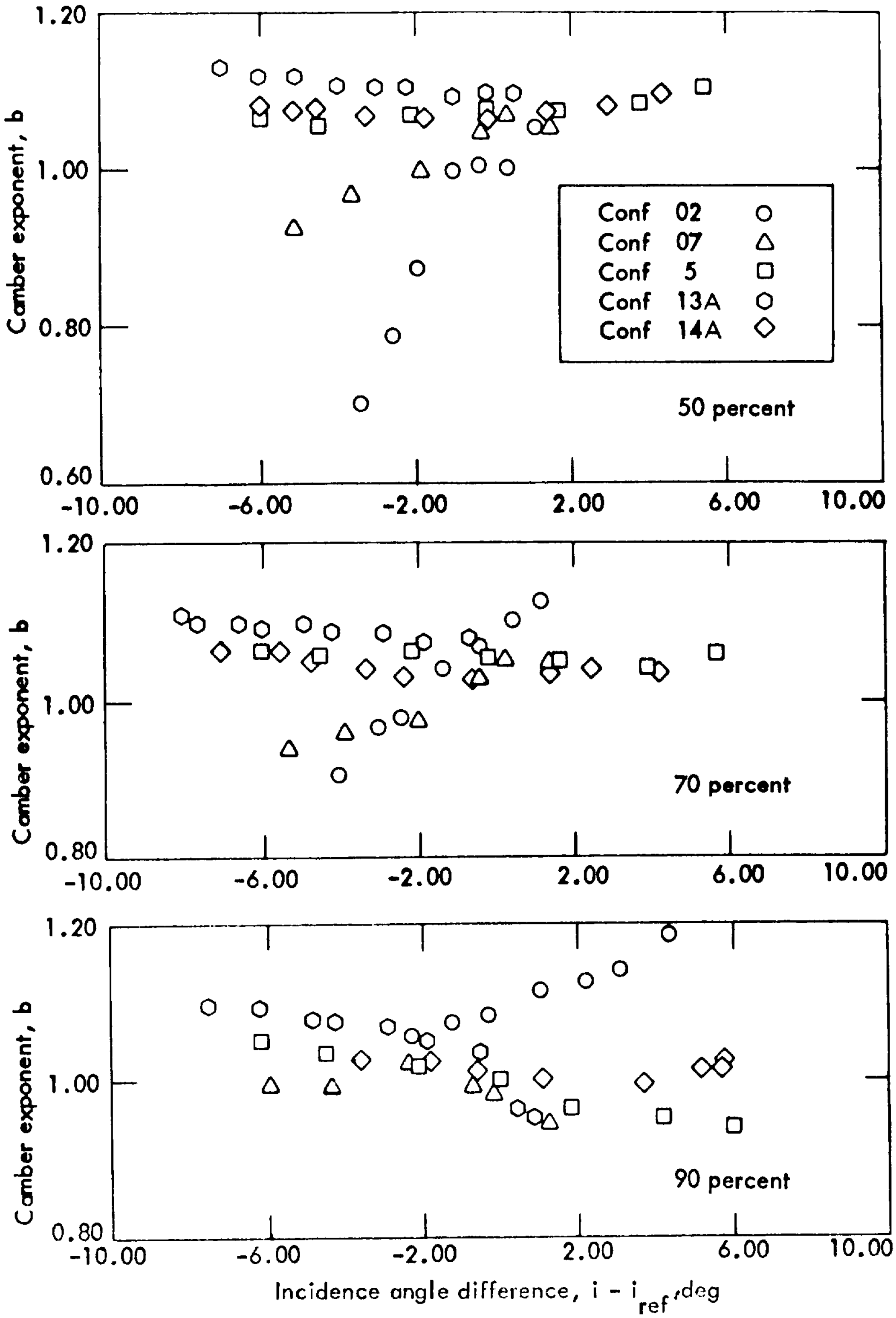

Figure 27. - Concluded.

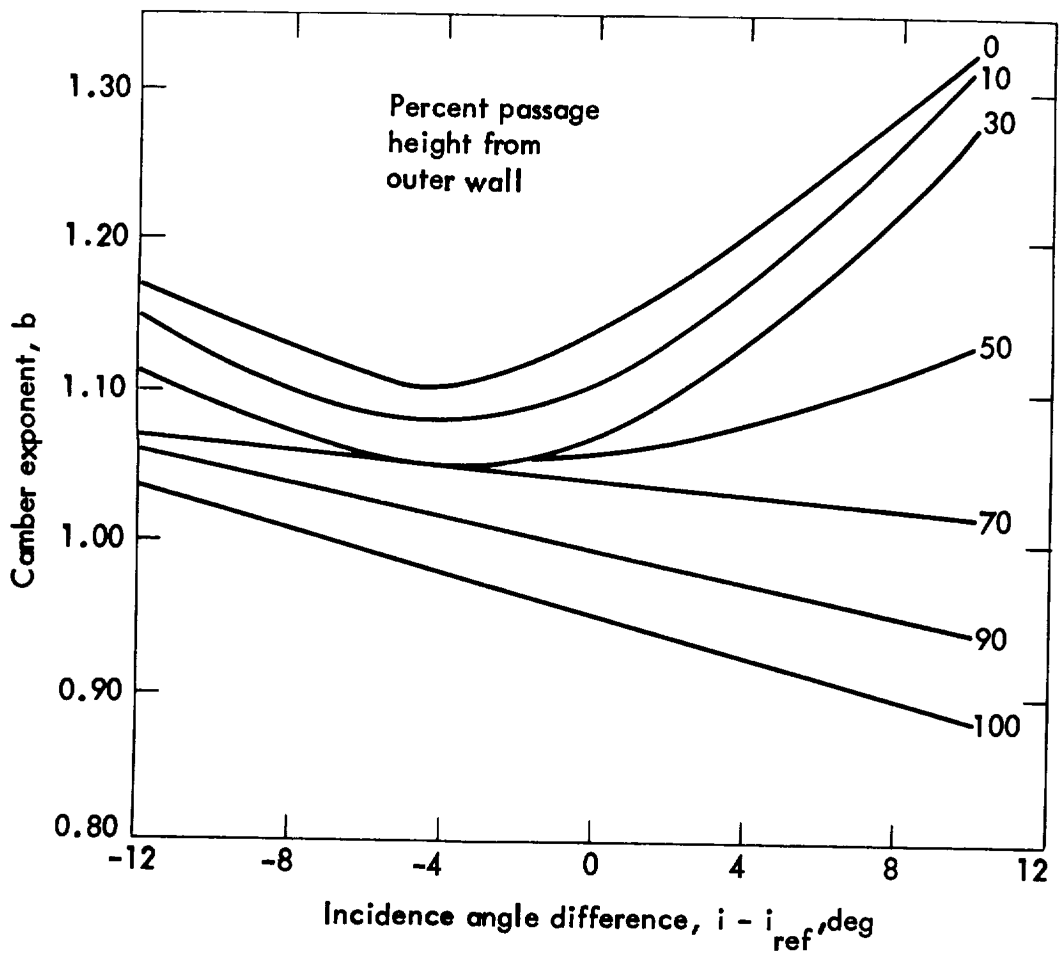

Figure 28. - Curves of camber exponent derived from data of figure 27.

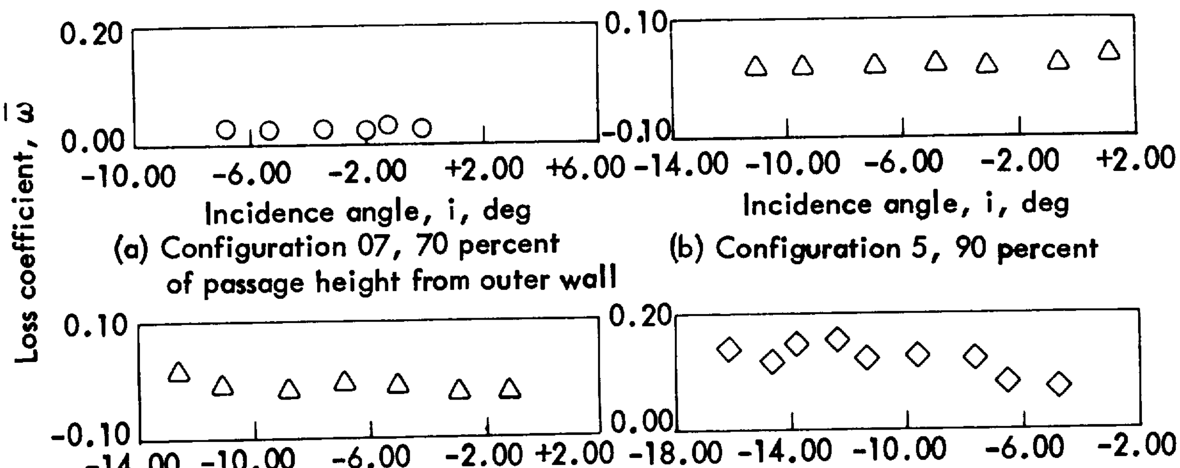

(a) Configuration 07, 70 percent of passage height from outer wall

(b) Configuration 5, 90 percent

(c) Configuration 5, 50 percent

(d) Configuration 14A, 70 percent

Figure 29. - Typical plot of rotor loss coefficients which show little dependence on incidence angle at 50, 70 and 90 percent of passage height from the outer wall.

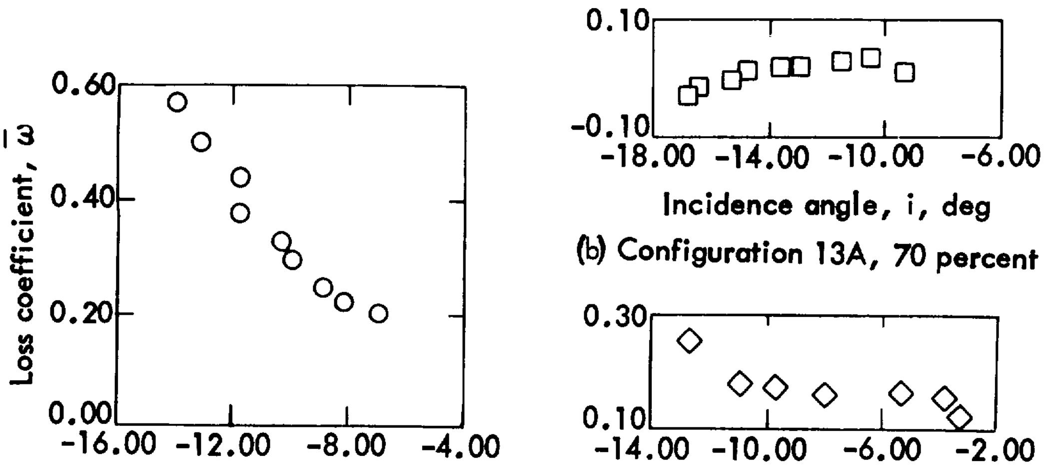

(a) Configuration 13A, 10 percent

(b) Configuration 13A, 70 percent

(c) Configuration 14A, 90 percent

Figure 30. - Examples of loss coefficient variations with no minimum loss incidence angle defined.

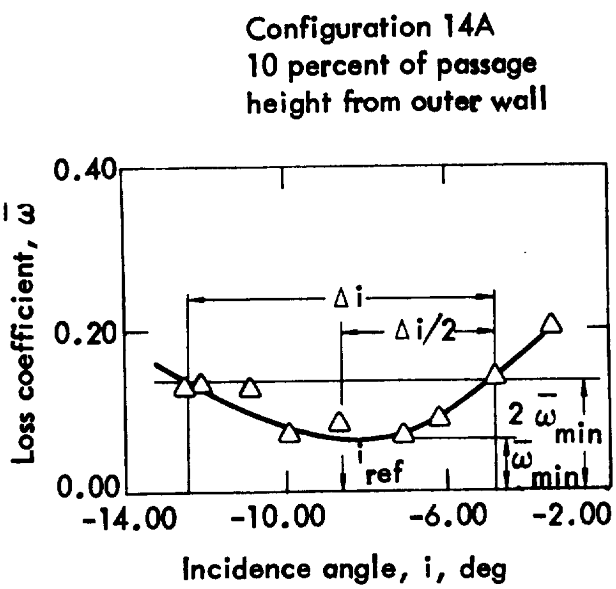

Figure 31. - Example of loss coefficient curve for which a reference incidence angle may be determined.

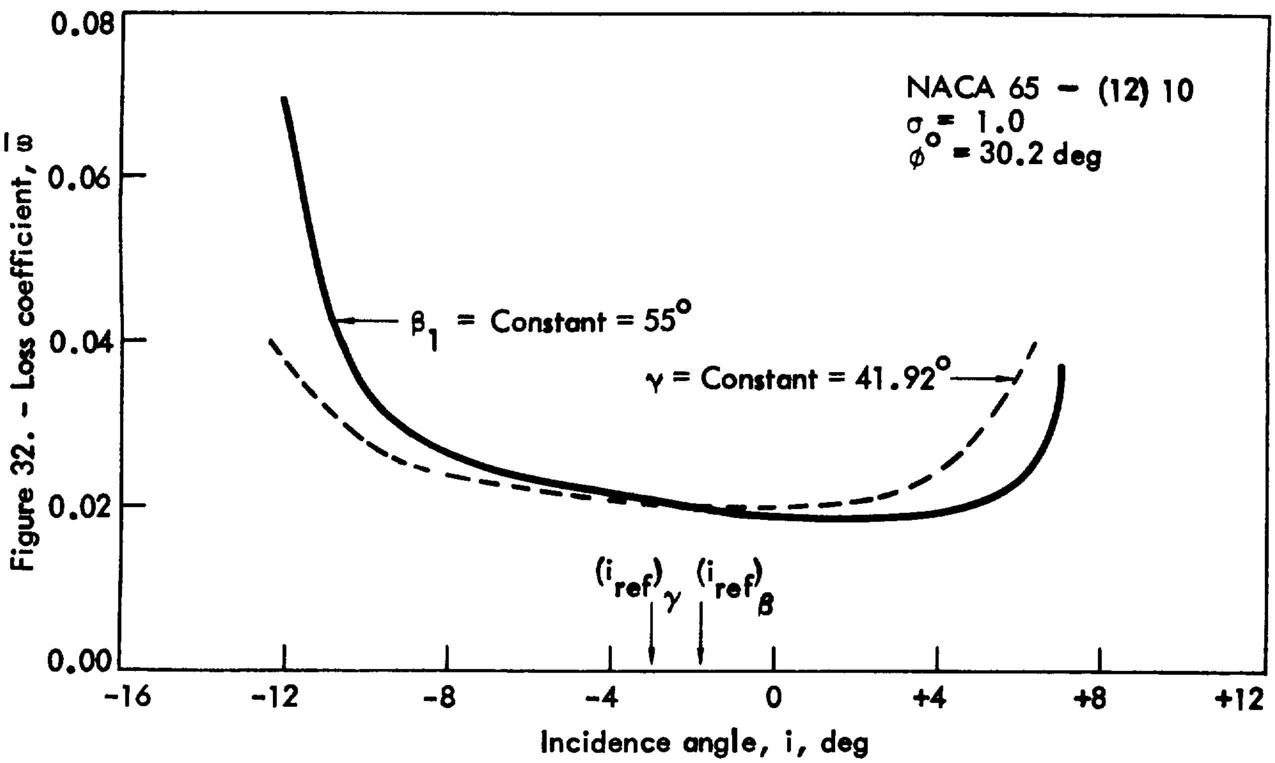

Figure 32. - Variation of loss coefficient with incidence angle at constant inlet flow angle and constant blade setting angle.

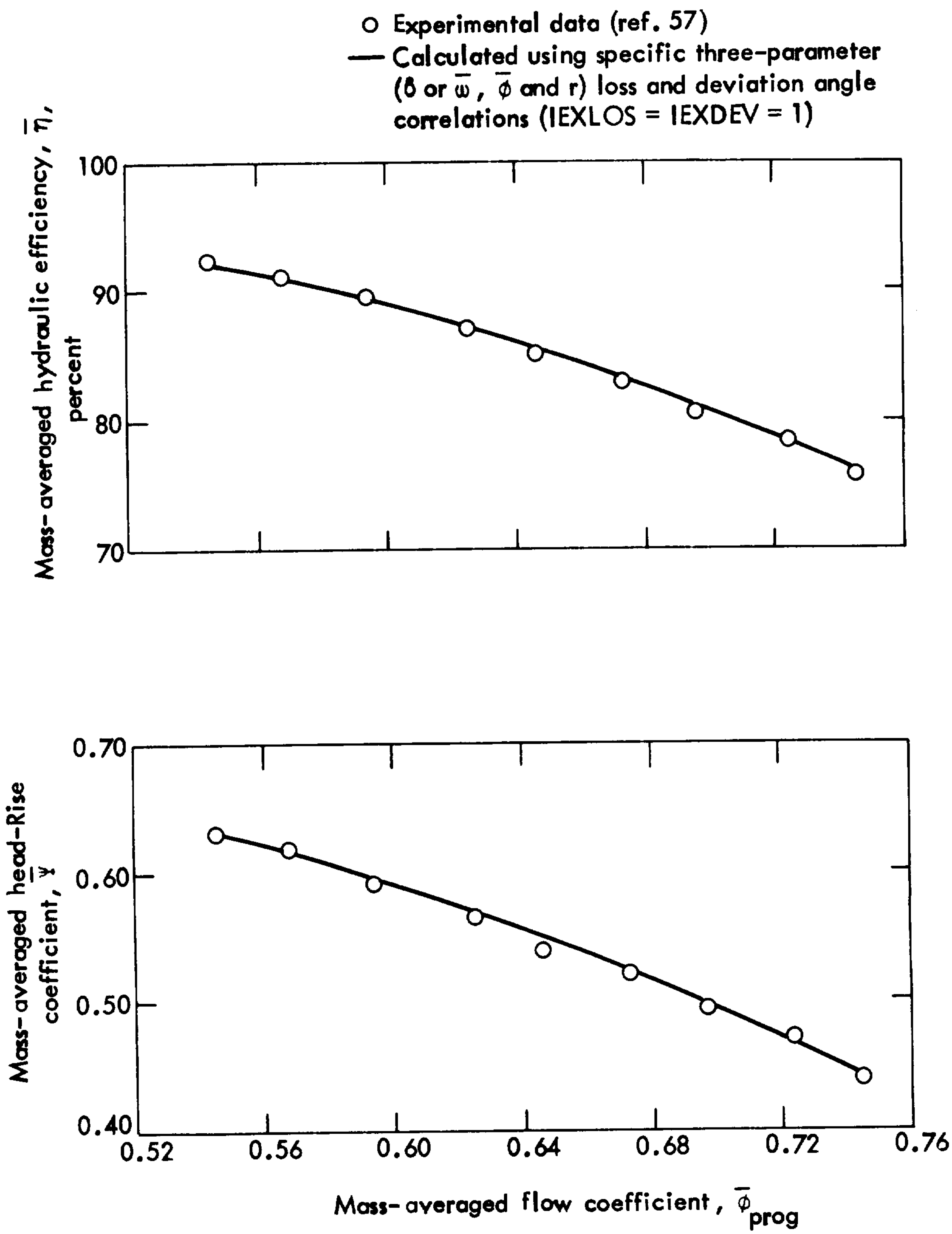

Figure 33. - Rotor overall performance, 9-inch tip diameter, 33 blades, 0.85 hub-tip radius ratio, N = 2420 rpm (configuration 13A).

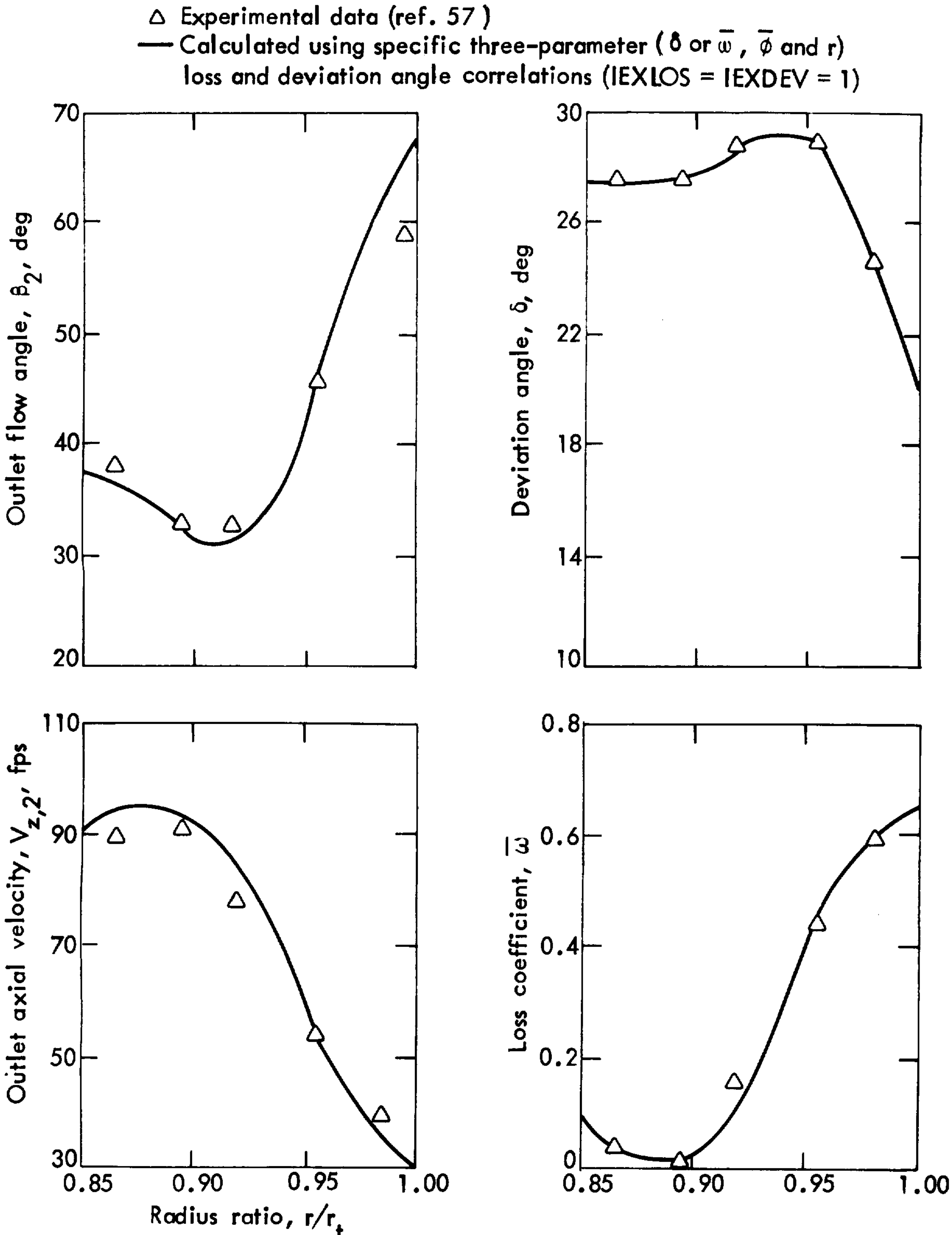

(a) $\bar{\phi}_{prog} = 0.745$

Figure 34. - Rotor blade-element performance, 9-inch tip diameter, 33 blades, 0.85 hub-tip radius ratio, N = 2420 rpm (configuration 13A).

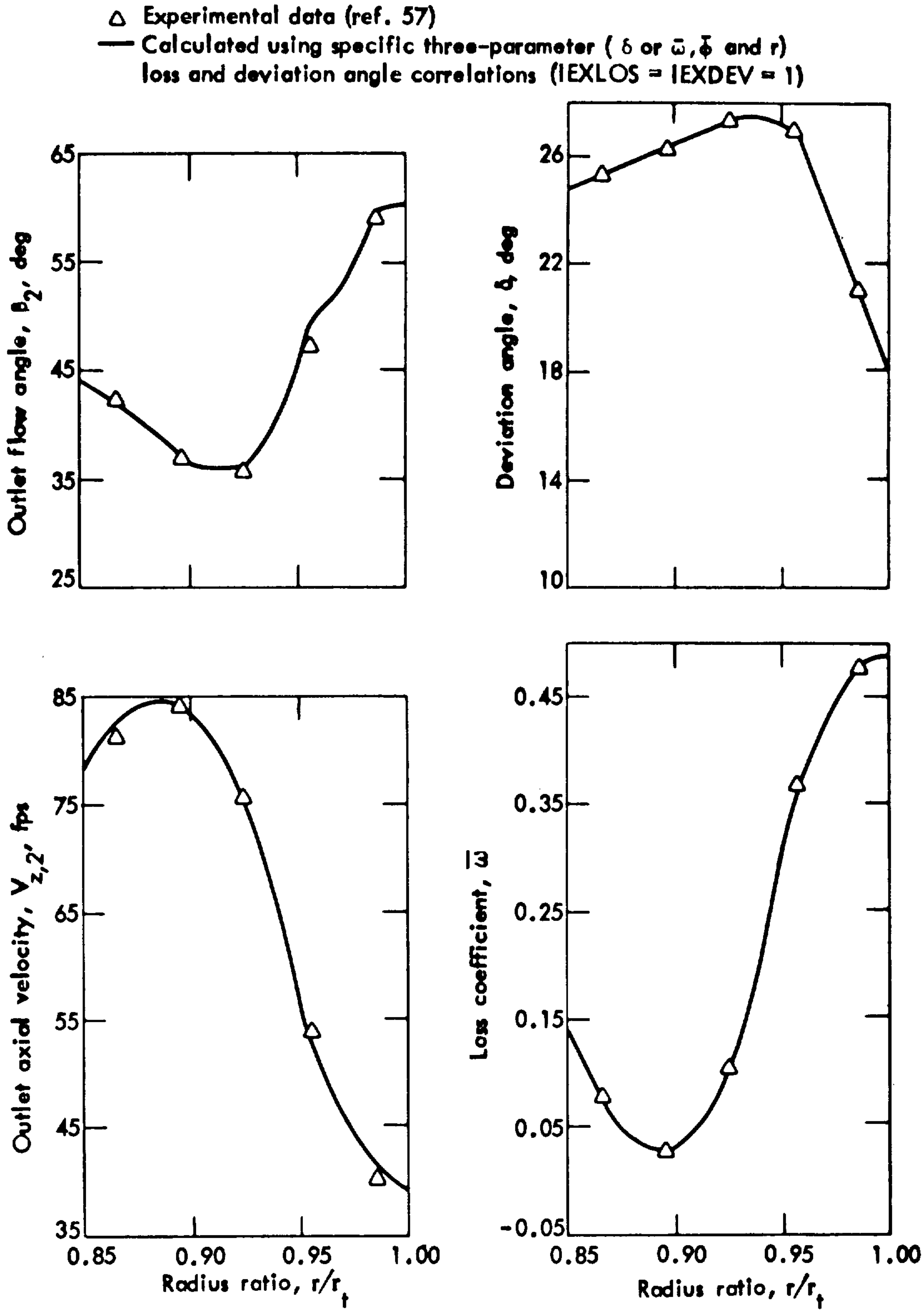

(b) $\bar{\phi}_{prog} = 0.695$

Figure 34. - Continued.

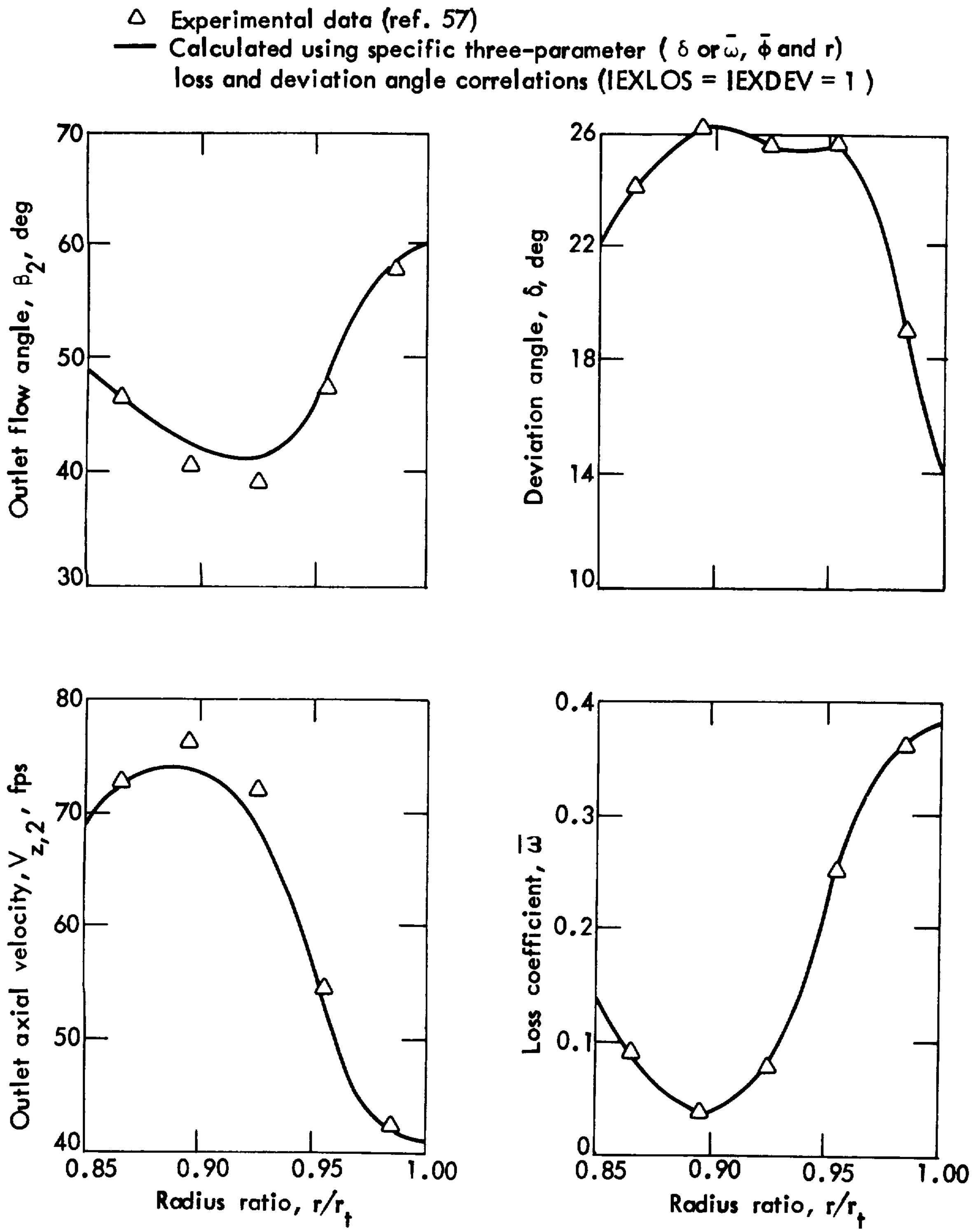

(c) $\bar{\phi}_{prog} = 0.646$

Figure 34. - Continued.

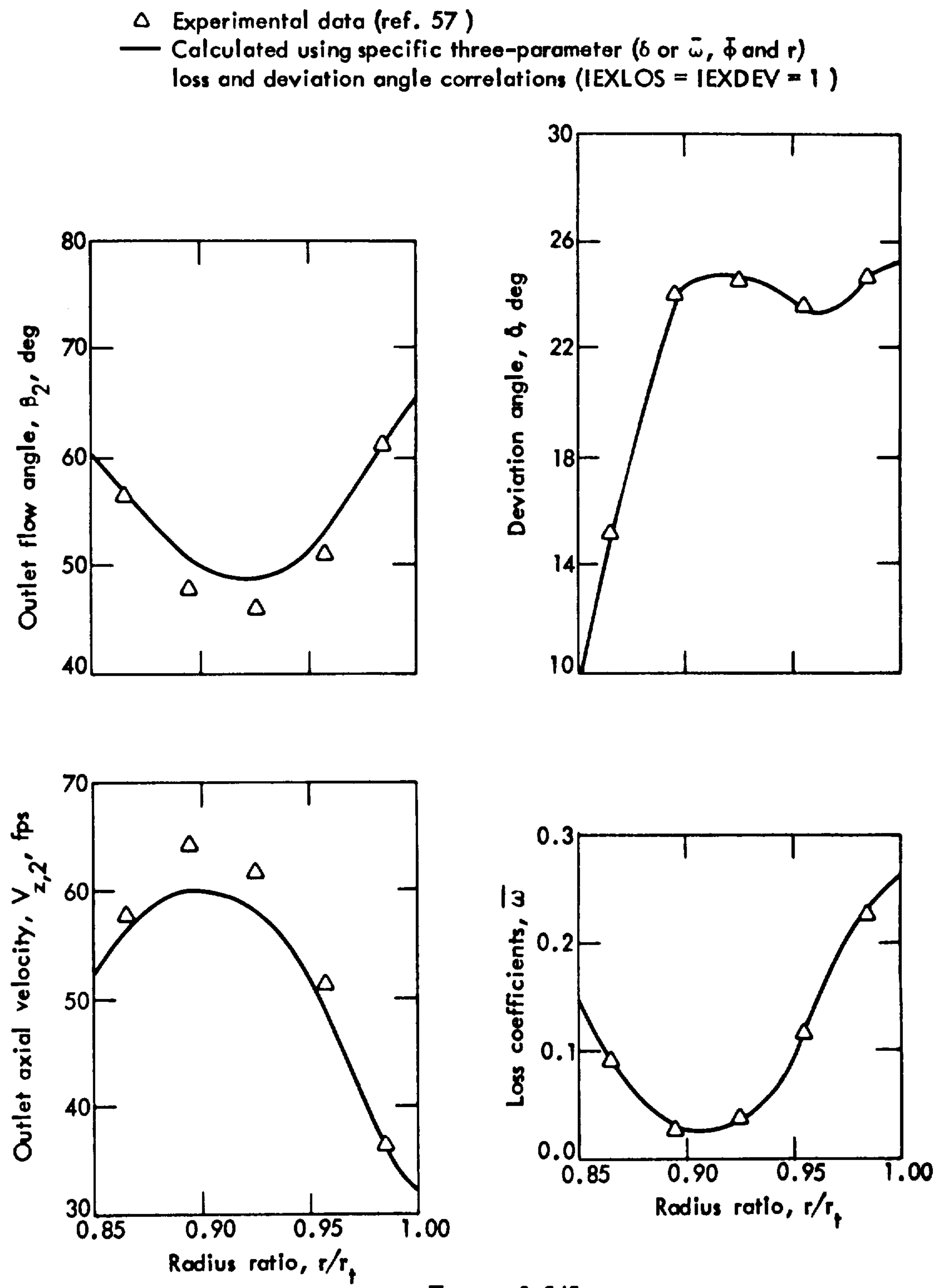

(d) $\bar{\phi}_{prog} = 0.545$

Figure 34. - Concluded

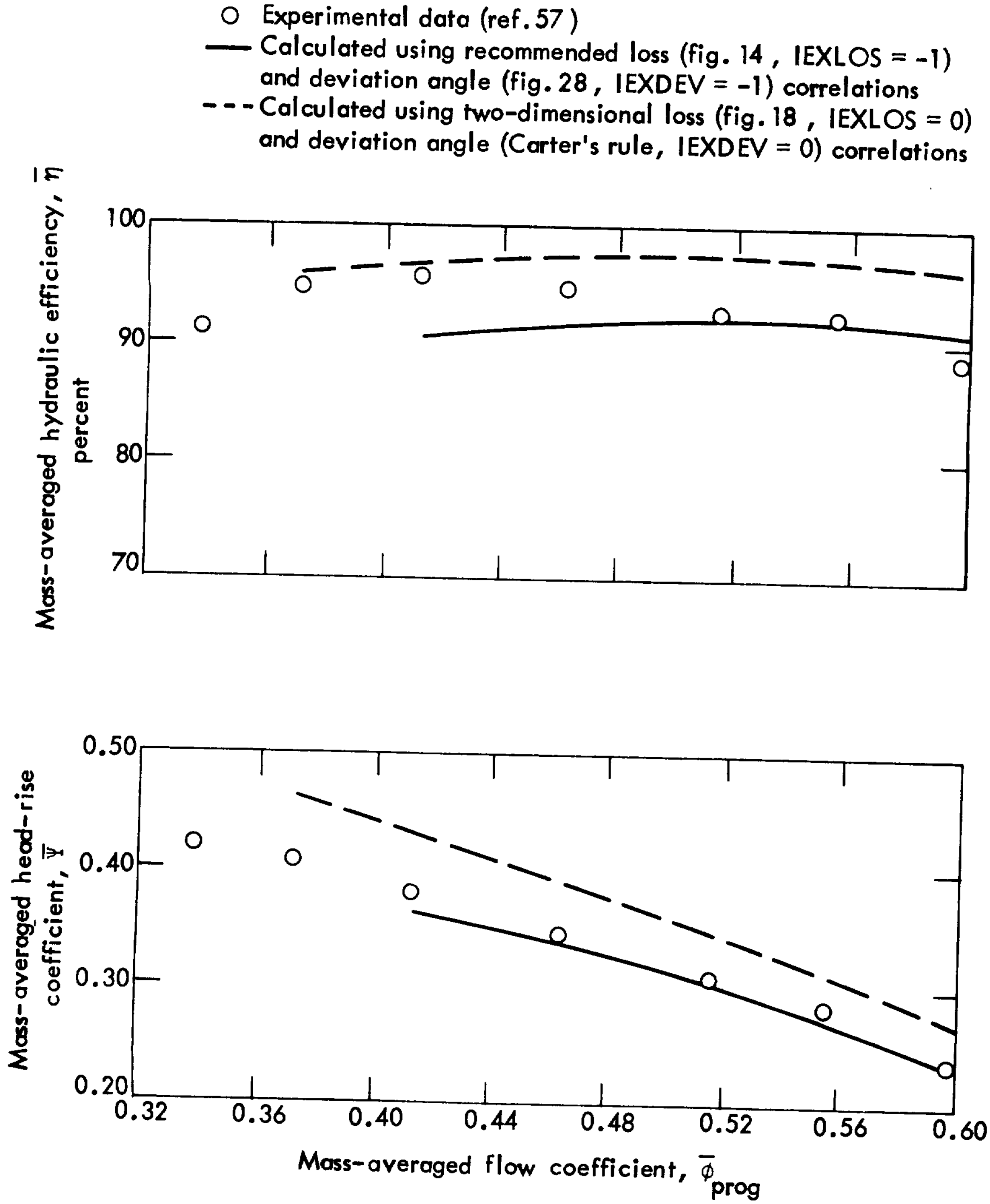

Figure 35. - Rotor overall performance, 9-inch, 19 blades, 0.8 hub-tip radius ratio, N = 3000 rpm (configuration 15).

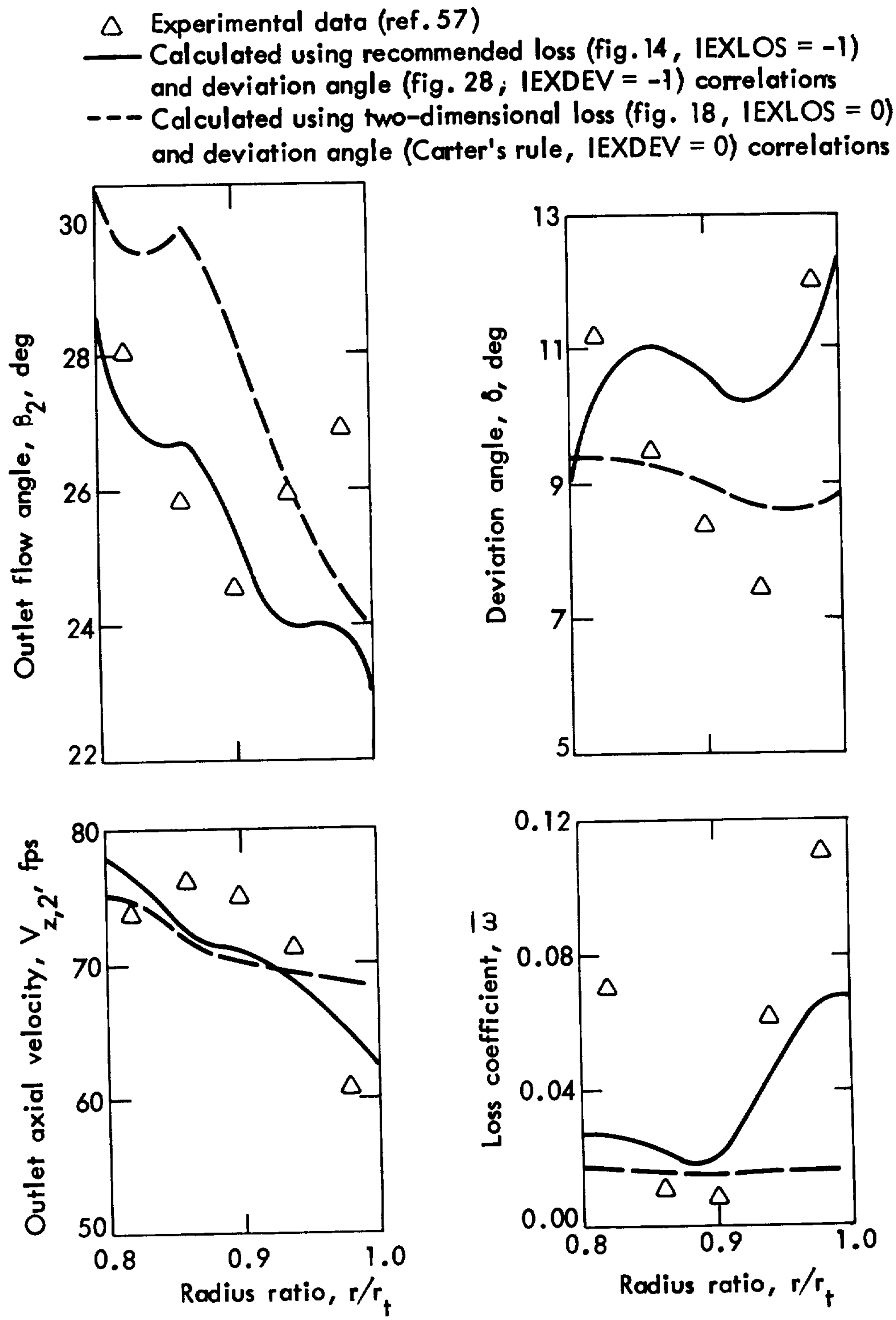

(a) $\bar{\phi}_{prog} = 0.598$

Figure 36. - Rotor blade-element performance, 9-inch tip diameter, 19 blades, 0.8 hub-tip radius ratio, N = 3010 rpm (configuration 15).

△ Experimental data (ref. 57)
— Calculated using recommended loss (fig. 14, IEXLOS = 1) and deviation angle (fig. 28, IEXDEV= = -1) correlations
- - - Calculated using two-dimentional loss (fig. 18, IEXLOS = 0) and deviation angle (Carter's rule, IEXDEV = 0) correlations

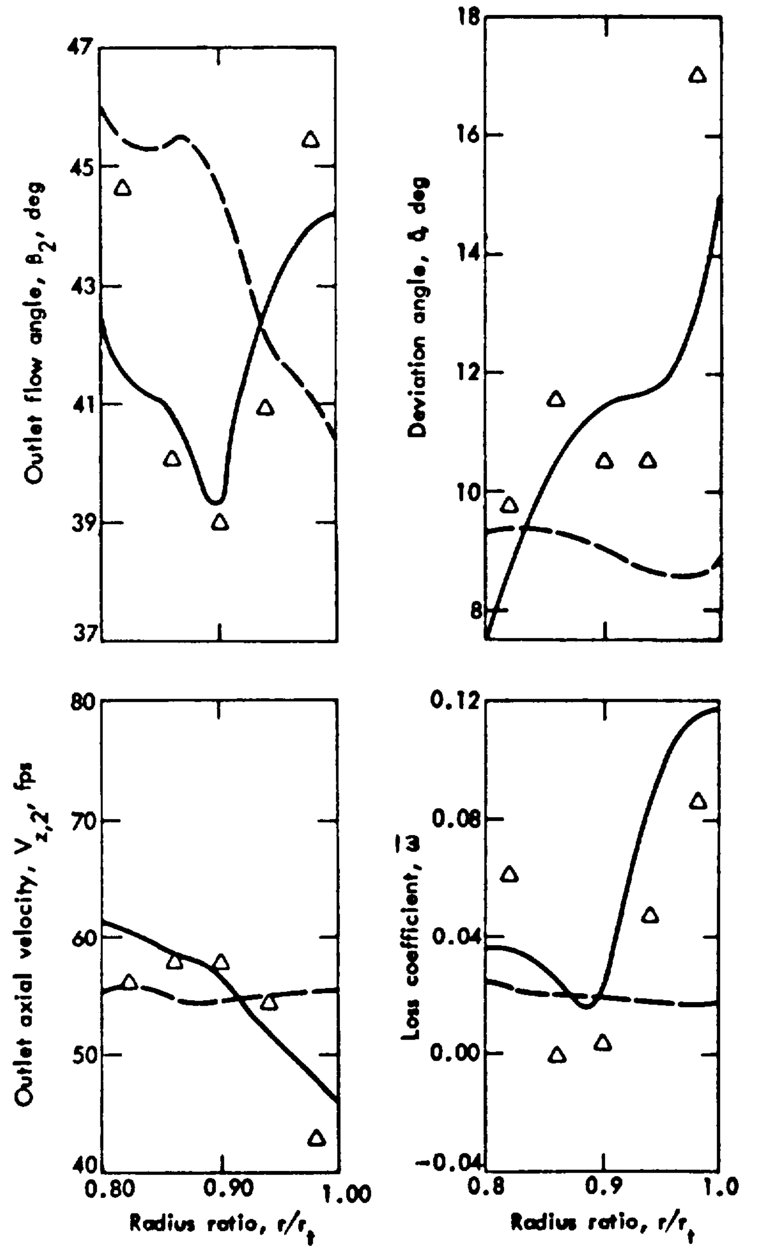

(b) $\bar{\phi}_{prog} = 0.463$

Figure 36. - Concluded.

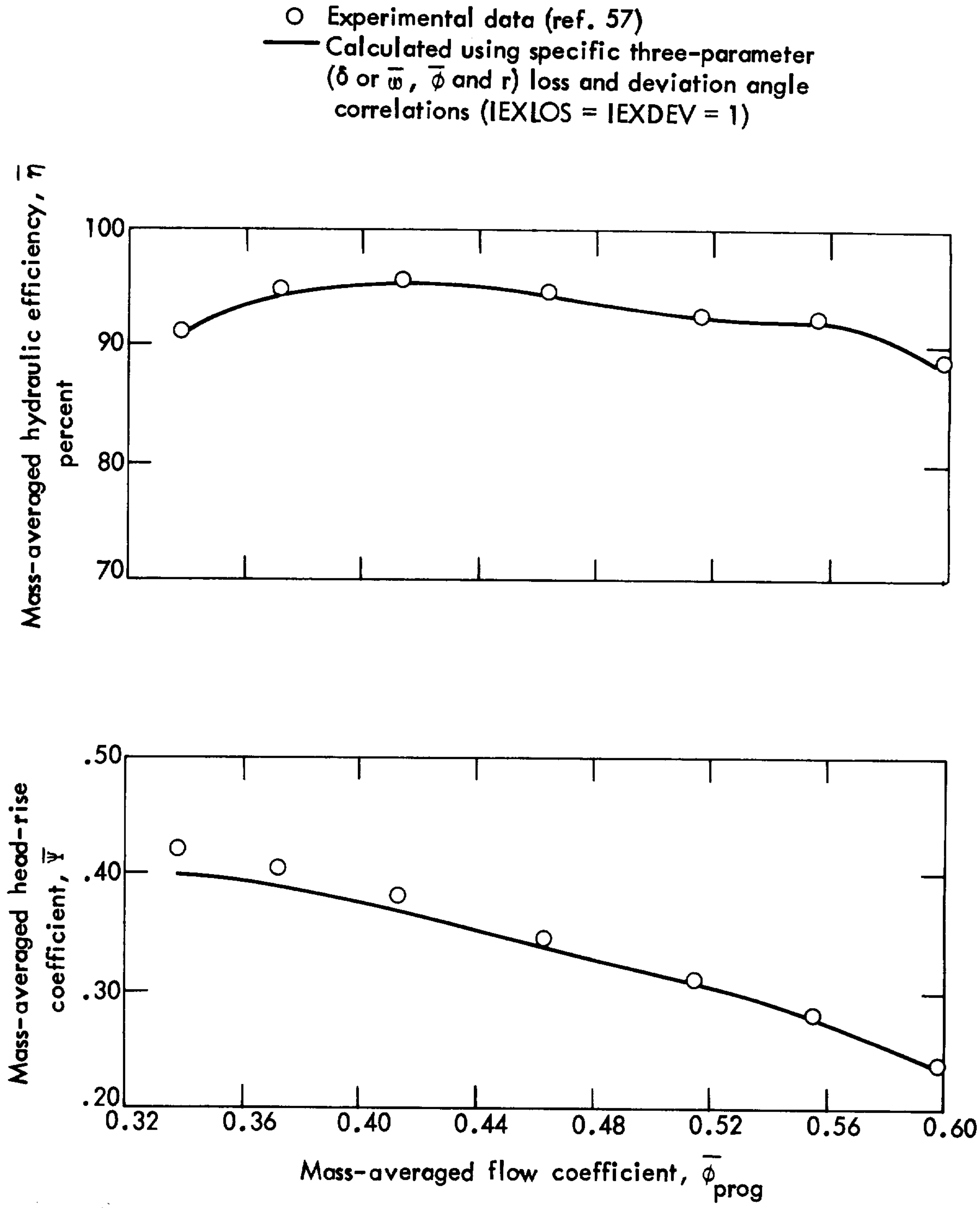

Figure 37. - Rotor overall performance, 9-inch tip diameter, 19 blades, 0.8 hub-tip radius ratio, N = 3010 rpm (configuration 15).

△ Experimental data (ref. 57)
—— Calculated using specific three-parameter (δ or $\overline{\omega}$, $\overline{\phi}$ and r) loss and deviation angle correlations (IEXLOS = IEXDEV = 1)

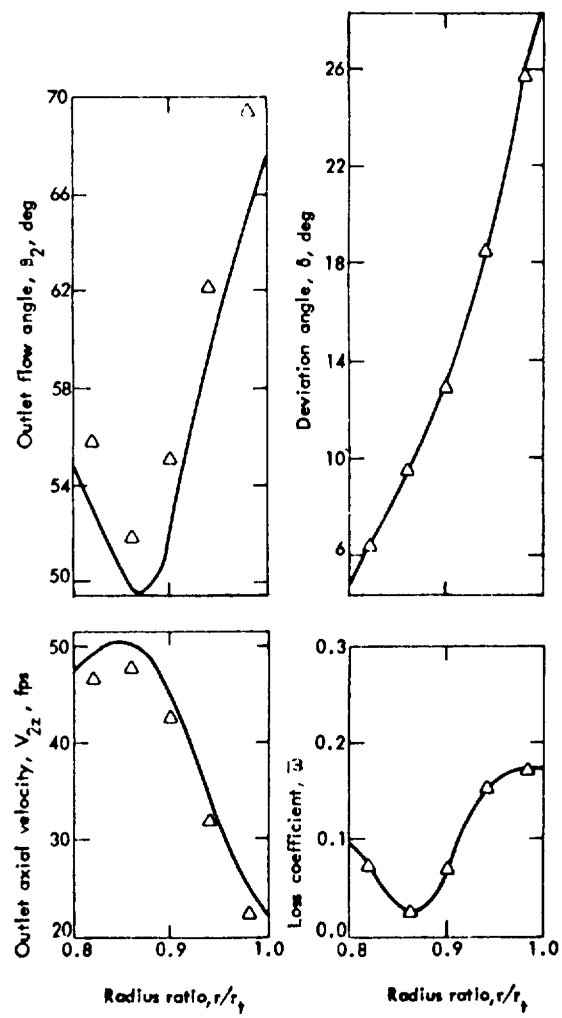

Figure 38. - Rotor blade-element performance, 9-inch tip diameter, 19 blades, 0.8 hub-tip radius ratio, N = 3010 rpm, $\overline{\phi}_{prog} = 0.338$ (configuration 15).

△ Experimental data (ref. 57)

Calculated values associated with each of three iterations before solution failure when using the recommended (figs. 14 and 28, IEXLOS = IEXDEV = -1) loss and deviation angle correlations.

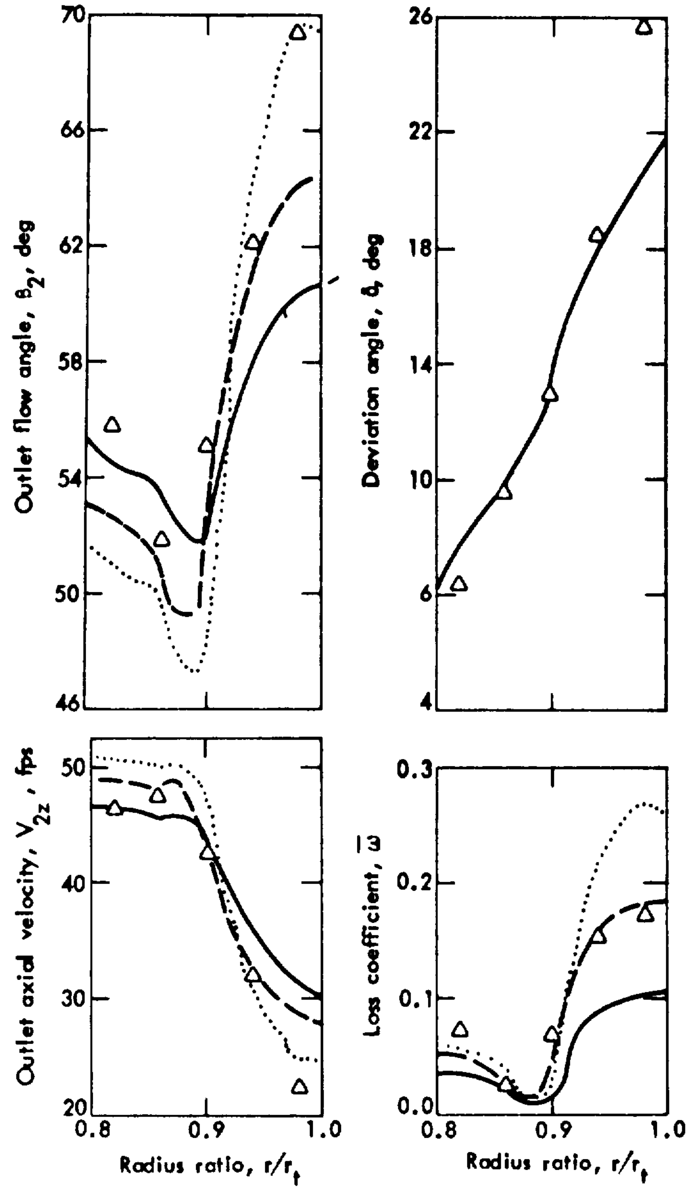

Figure 39. - Rotor blade-element performance, 9-inch tip diameter, 19 blades, 0.8 hub-tip radius ratio, N = 3010 rpm, $\bar{\phi}_{prog} = 0.338$ (configuration 15).

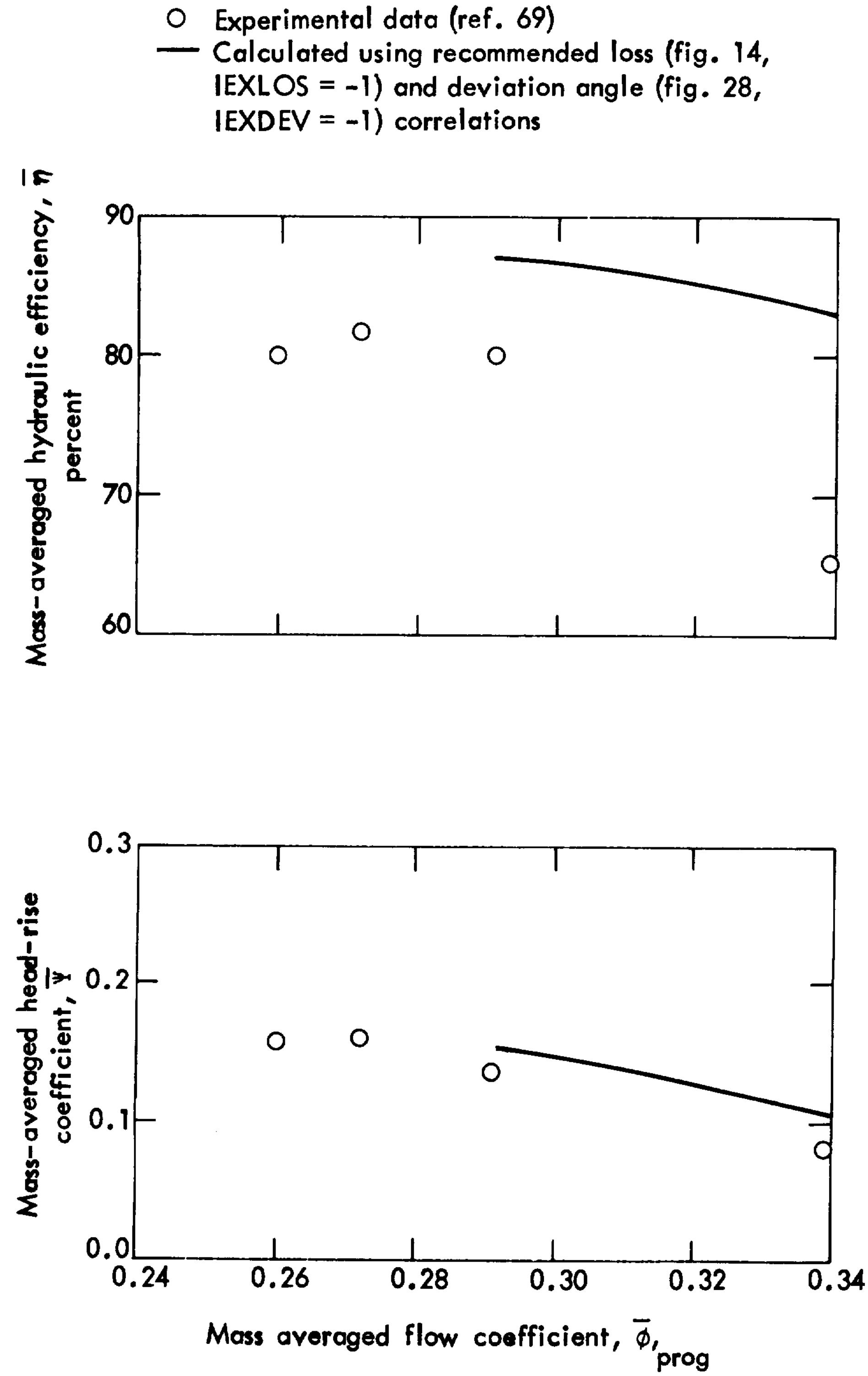

Figure 40. - Stage overall performance; rotor - 9-inch tip diameter, 19 blades, 0.4 hub-tip radius ratio, N = 3910 rpm; stator - 9-inch tip diameter, 18 blades, 0.4 hub-tip radius ratio (configuration 01).

○ Experimental data (ref. 70)

—— Calculated using recommended loss (fig. 14, IEXLOS = -1) and deviation angle (fig. 28, IEXDEV = -1) correlations.

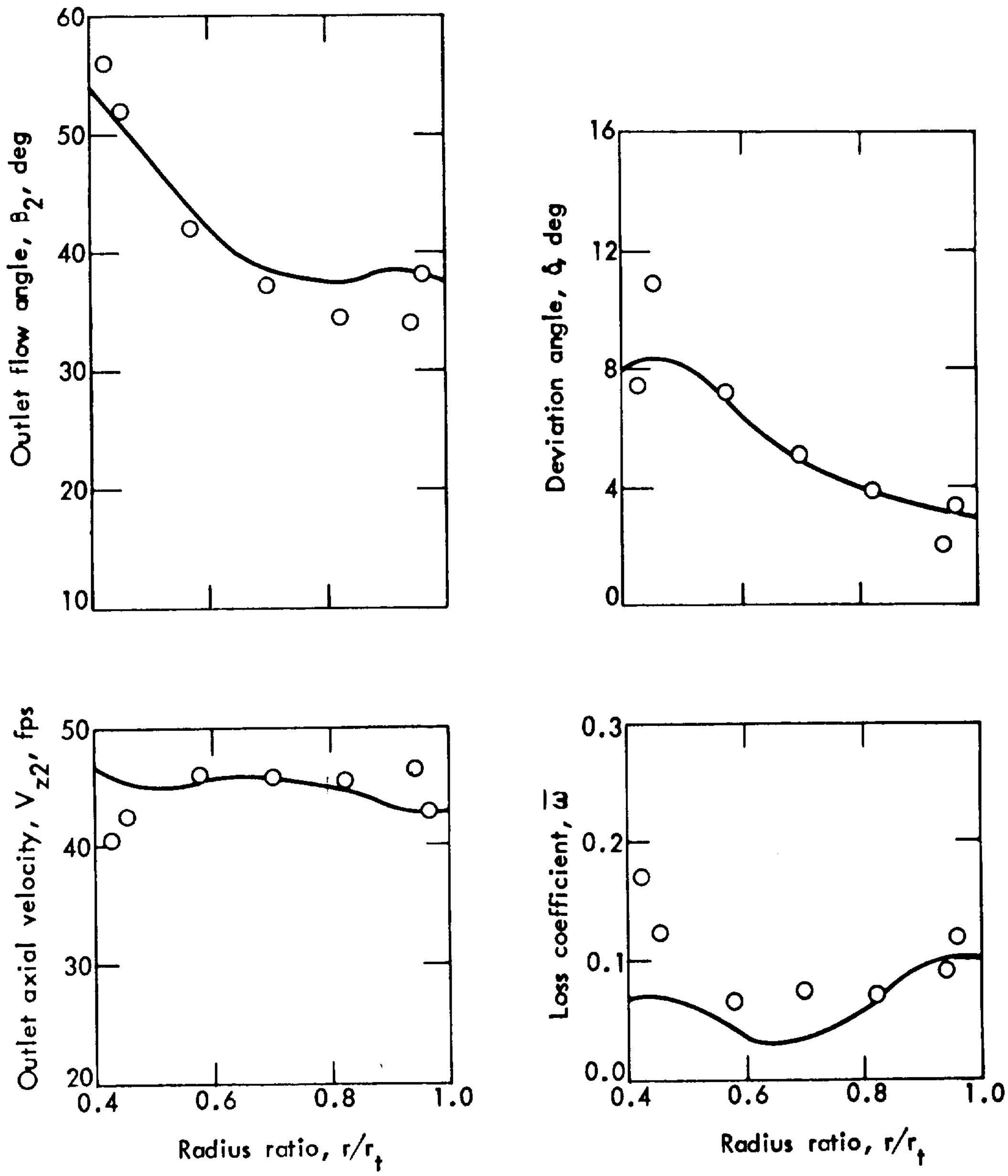

Figure 41. - Rotor blade-element performance; 9-inch tip diameter, 19 blades, 0.4 hub-tip radius ratio, N = 3910 rpm, $\bar{\phi}_{prog}$ = 0.291 (rotor of configuration 01 stage).

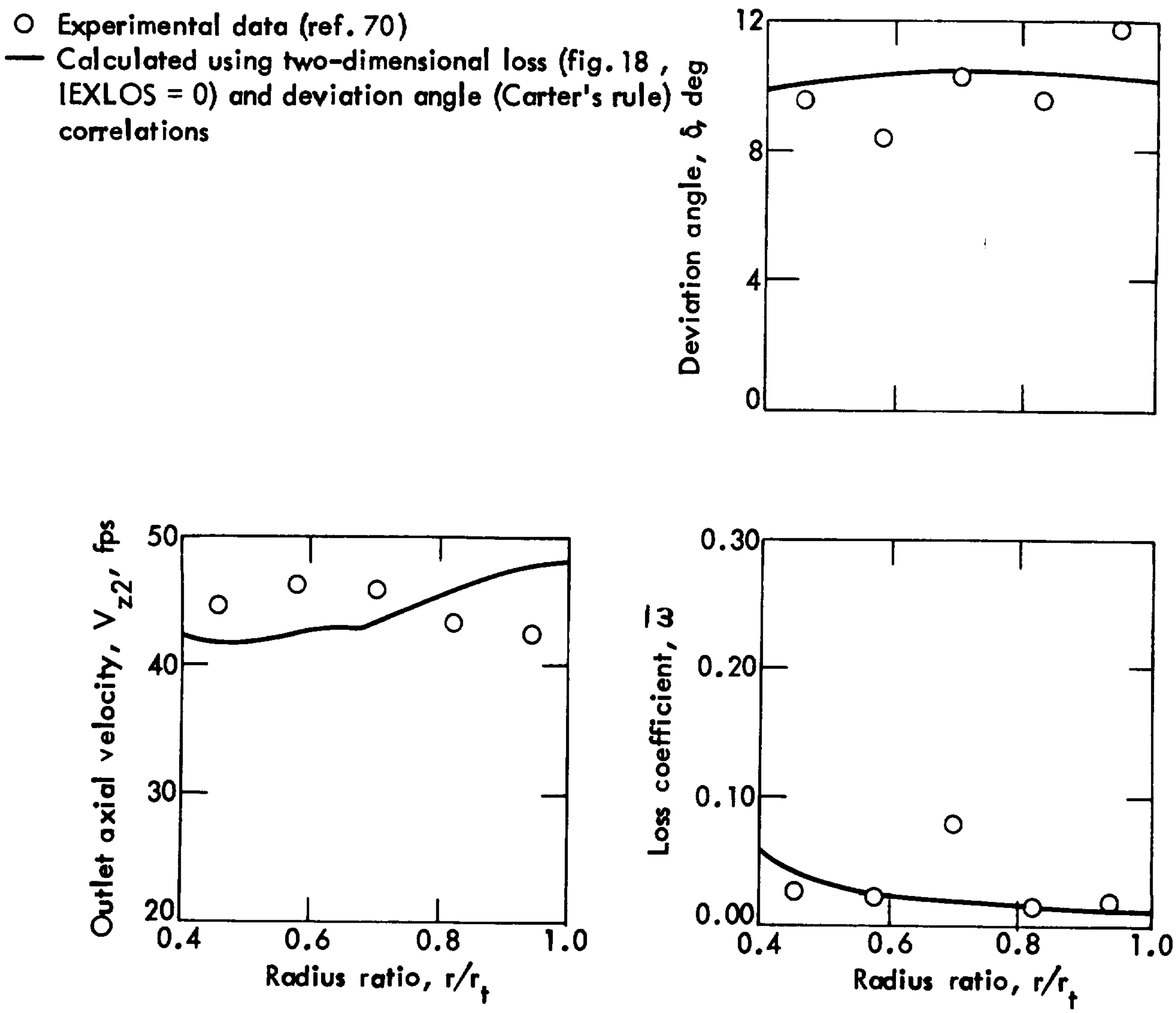

Figure 42. - Stator blade-element performance; 9-inch tip diameter, 18 blades, 0.4 hub-tip radius ratio, $\bar{\phi}_{prog} = 0.291$ (stator of configuration 01 stage).

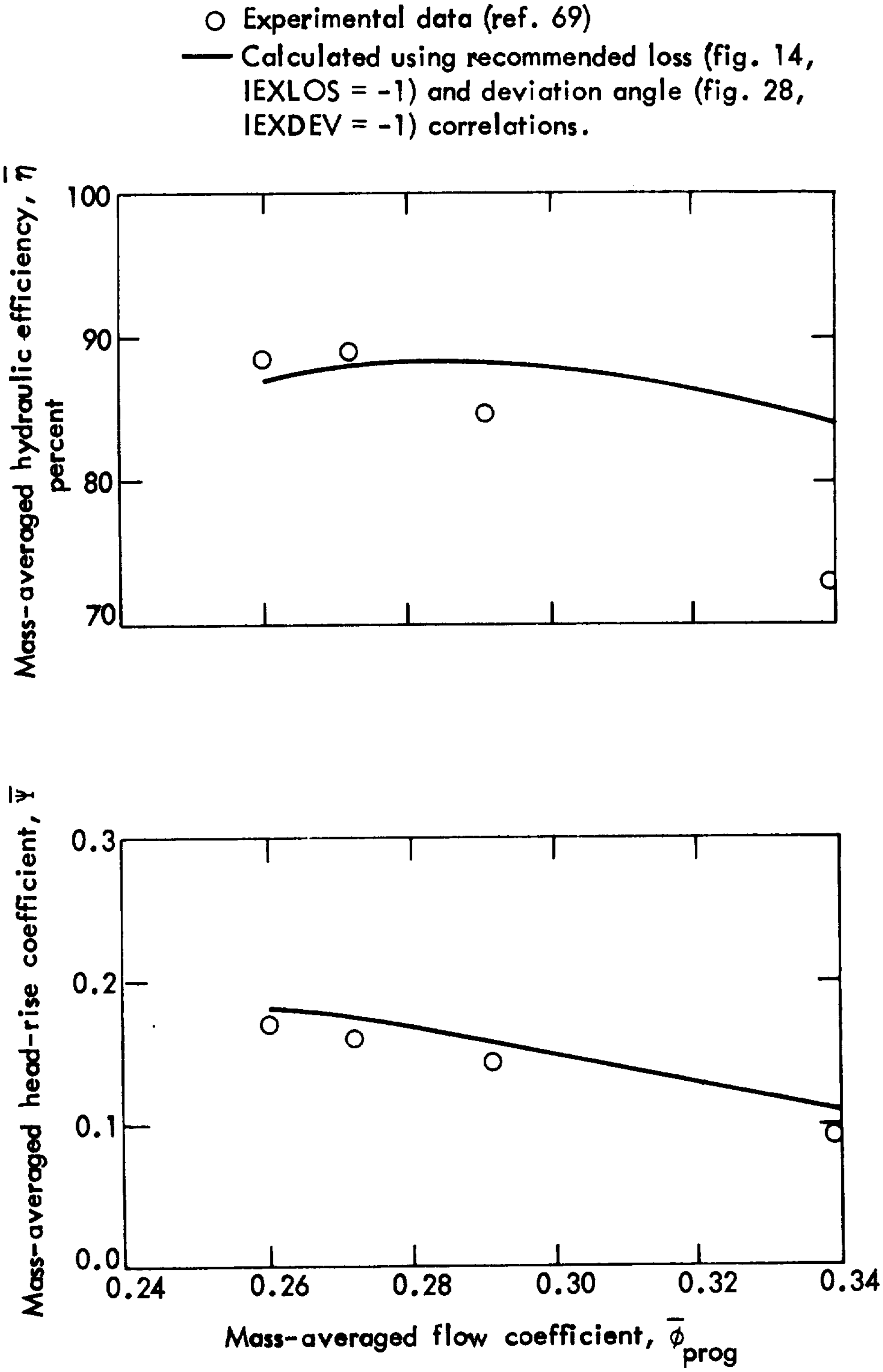

Figure 43. - Rotor overall performance; 9-inch tip diameter, 19 blades, 0.4 hub-tip ratio, N = 3910 rpm (rotor of configuration 01 stage)

○ Experimental data (ref. 70)
—— Calculated using recommended loss (fig. 14, IEXLOS = -1) and deviation angle (fig. 28, IEXDEV = -1) correlations

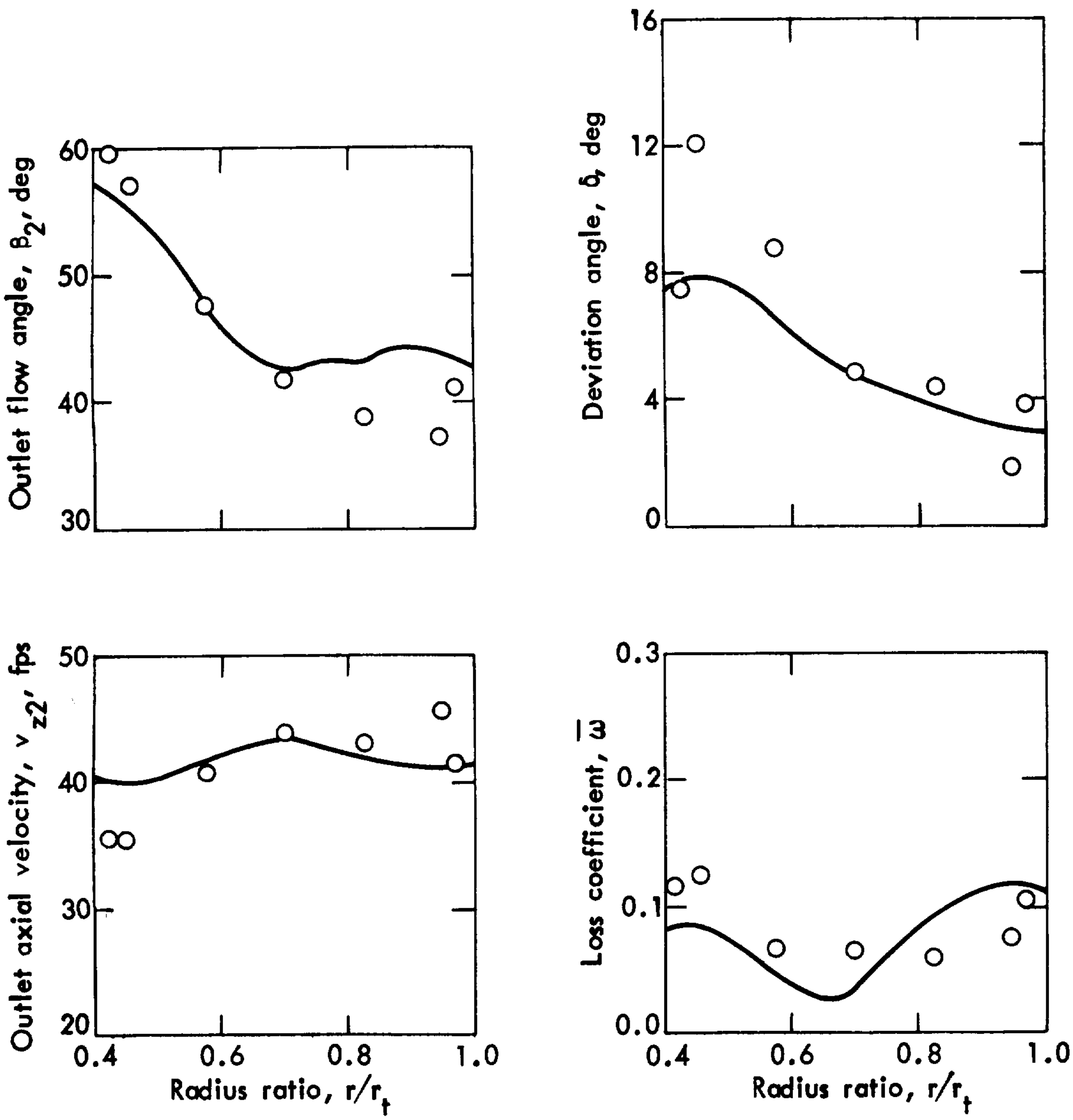

Figure 44. - Rotor blade-element performance; 9-inch tip diameter, 19 blades, 0.4 hub-tip radius ratio, N = 3910 rpm, $\bar{\phi}_{prog}$ = 0.272 (rotor of configuration 01 stage)